Understanding the changes in the ecological functioning of foraminifera during the Palaeocene-Eocene thermal maximum using biological trait analysis

Thesis submitted in accordance with the requirements for the University of Liverpool for the degree of Doctor in Philosophy

Celestine Nwojiji Nwite

Department: Earth Ocean and Ecological Sciences, School of Environmental Sciences

Faculty of Science & Engineering

July, 2018

Abstract

Understanding the changes in the ecological functioning of foraminifera during the Palaeocene-Eocene Thermal Maximum using Biological Trait Analysis

Biological Trait Analysis (BTA) has been used to examine the changes in foraminiferal taxa and traits composition during the Palaeocene -Eocene Thermal Maximum (PETM), 56 million years ago. BTA is a multivariate ordination method used in describing the biological characteristics/behaviour of species and how they are related to the functioning of their ecosystem. It uses a series of life history, morphological and behavioural characteristics of species present in assemblages to indicate their role in ecological functioning (defined as the maintenance and regulation of ecosystem processes).

This study investigated benthic and planktonic foraminifera taxa and trait composition from the Pacific Ocean (ODP Sites 1209, 1212B, 1215A), Atlantic Ocean (ODP Site1265A) and Alamedilla section in Southern, Spain.

Thirteen (13) foraminiferal traits and over 60 trait categories were perceived to be crucial for the foraminiferal ecological functioning in the marine environment. However, BTA recognised test composition, chamber arrangement/ shape, ornamentation, primary aperture position, perforations and living/feeding habit as the most important foraminiferal trait in the benthic ecosystem. Also, bi/tri-serial, planispiral and trochospiral test; spherical/oval and triangular/trapezoid chamber shapes; depressed/ raised sutures or taxa with no ornament were highlighted as the most resilient traits during the period of ecological disturbance.

The results from this study demonstrated for the first time that BTA could detect changes/disturbance in microfossil (foraminifera) ecology. The technique produced a more integrated and quantitative picture of palaeoecological changes across a wide range of locations when compared to the conventional faunal assemblage approach.

The mapping of foraminiferal traits to ecological functions indicated that test composition is related to carbon sequestration and ocean acidification. Test shape and chamber arrangement are linked to productivity, ecological disturbance and oxygen concentration. Ornamentation is also related to ecological disturbance and ocean acidification. Perforation, aperture position and accessories in foraminifera are associated with nutrient/food utilisation, productivity and oxygen concentration. In addition, the living habit can provide a clue to ocean acidification, productivity, oxygen concentration, competition, nutrient/food utilisation in the marine ecosystem.

Our data showed that foraminiferal taxonomic composition experienced extreme biotic turnover that resulted in extensive mortalities and extinction of both planktonic and benthic fauna during the PETM. The faunal assemblage is predominantly made of cosmopolitan taxa indicating ecological disturbance during the PETM. The taxa composition and non-metric multi-dimensional scaling (nmMDS) suggested that the foraminiferal communities in the Atlantic Ocean experienced ecological perturbation before and during the CIE but stabilised during the recovery period. Evidence of disturbance in bottom waters before the CIE supports the theory that the source of the light carbon that caused the PETM may have originated in the Atlantic Ocean causing benthic ecological disturbance and progressively reaching the surface of the ocean. In the Pacific and Tethys Oceans, ecological disturbance was only recorded at the CIE interval.

The scanning electron microscope (SEM) image of some recovered foraminifera revealed evidence of dissolution/etching, extreme recrystallization/neomorphism and secondary calcite cementation on the test. The amount of coccoliths incorporated in the test of some deep infauna species requires further investigation to understand if some foraminiferal taxa construct their test in the dual process of secreting hyaline calcite and incorporation of coccolith plates by agglutinated processes in the later stage of their life history.

Acknowledgements

I want to express profound gratitude to my supervisors, Dr Fabienne Marret-Davies, Dr Bryony Caswell and Dr Alessandro Tagliabue, for their relentless support, encouragement and guidance throughout my research. Your advice and feedback has improved not only my academic and scientific skills but has helped to prepare me for future endeavours. In a special way, I wish to thank Bryony for those days she came to Liverpool all the way from Australia to help with my research. Your visits have always taken my project a step further.

My special thanks also go Drs. Tracy Aze and Charlotte Jeffery for taking the time to read the thesis and making very useful suggestions.

I would like to acknowledge Ebonyi State Government, Nigeria who gave me the initial opportunity to come to the UK for my PhD and paid my first-year fees. I also appreciate the School of Environmental Sciences, University Of Liverpool who paid the rest of my tuition fees after I lost the scholarship from my previous sponsor. Thank you for your help.

I owe many thanks to the members of my family: Daniel, Justina, Celestina, Lucy, Kimberly, Michelle, and Martina for their love, patience, encouragement and support during my time in Liverpool.

Throughout the time I sent in the School of Environmental Sciences, I received many favours from the staff of the School, and I would like to thank Prof. Doug Mair, Prof. Andy Plater, Paula Houghton and Christina Hurst for their intervention when I had difficulty with my funding. I attribute the successful completion of my studies to the school support. I am also grateful to other teaching and non-teaching staff in the school for their support with my laboratory and data analyses especially, Prof. John Boyle, Prof. Jim Marshall, Mike O'Connor and Mrs Jenny Bradley.

I also wish to thank the International Ocean Drilling Program (IODP) for providing the sediment cores for this study.

Finally, I would also like to acknowledge all the postgraduate students and friends in the School of Environmental Sciences especially, Dr Onema Adojoh, Dr Rachel Lem, Karen Halsall, Tafida-Isa Maulud, Yolanda Caballero, Fiona Russell and Thea Wingfield. Thank you for your support and friendship.

Table of Contents

Abstract.....ii

Acknowledgements.....iii

Table of contents.....iv

List of figures..... ix

List of tables.....xiv

List of plates.....xvi

List of appendices.....xvi

CHAPTER ONE: General Introduction..... 1

1.1 Introduction..... 1

1.2 Palaeocene – Eocene thermal maximum (PETM)…….....3

1.2.1 Causes and duration of the PETM.....3

1.3 Abiotic changes during the Palaeocene-Eocene Thermal Maximum.....7

1.3.1 Palaeotemperature changes.....7

1.3.2 Changes in hydrology….....9

1.3.3 Ocean acidification during the PETM….....10

1.4 Biotic changes during the PETM.....13

1.4.1 Changes in deep-sea marine microbenthos.....14

1.4.2 Impact of the PETM on planktonic foraminifera….....15

1.4.3 Effect of PETM on the phytoplankton 17

1.5 Continental configuration and ocean circulation during the PETM.....18

1.6 Foraminifera.....21

1.6.1 Benthic foraminifera.....22

1.6.1.1 Classification.....23

1.6.1.2 Ecology of benthic foraminifera.....25

1.6.2 Planktonic foraminifera.....28

1.6.2.1 Classification.....29

1.6.2.2 Ecology of planktonic foraminifera 31

1.7 Use of Foraminiferal assemblage technique in interpreting palaeoecological and palaeoceanographic conditions.....34

1.8 Geochemical analyses from foraminifera test 37

1.9 Ecological functioning of foraminifera and the biological carbon pump.....38

1.10 Biological Trait Analysis: Can it improve the understanding of the ecological functioning of microfossils in deep time? 40

1.11 Thesis objectives.....43

CHAPTER TWO: Materials, Methods and Taphonomic Considerations 45

2.1 Materials.....45

2.2 ODP Site 1215A.....46

2.3 ODP Site 1265A.....49

2.4 ODP Site 1209B.....51

2.5 ODP Site 1212B.....53

2.6 Alamedilla.....53

2.7 Summary of published micropalaeontological and geochemical studies.....54

2.7.1 ODP Site 1215A.....54

2.7.2 ODP Site 1265A.....55

2.8. Methodology.....56

2.8.1 Sample preparations.....56

2.8.2 Foraminiferal preparation protocols.....56

2.9 Methods of trait coding for Biological Trait Analysis.....57

2.10 Taphonomical considerations.....68

CHAPTER THREE: The PETM extreme climate impact on the benthic foraminiferal traits and ecological functioning in the tropical Pacific and Tethys Oceans.....71

3.1 Introduction.....71

3.2 Results.....71

3.2.1 Age model for sites 1209B and 1212B.....71

3.2.2 Changes in taxonomic composition at ODP Site 1209B. 72

3.2.3 Changes in foraminiferal trait composition.....77

3.2.4 Changes in taxonomic composition at ODP Site 1212B..... 82

3.2.5 Changes in foraminiferal trait composition at ODP Site 1212B.....86

3.2.6 Alamedilla age model.....90

3.2.7 Changes in taxonomic composition at Alamedilla section.....91

3.2.8 Changes in foraminiferal trait composition at Alamedilla section.....95

3.3 Discussion.....100

3.3.1 Similarities in trait compositions across the tropical Pacific Ocean and Tethys Sea.....101

3.3.2 Interpreting ecological function base on changes in foraminiferal fauna and traits.....107

3.3.2.1 Nutrient supply in the Pacific Ocean during the PETM.....107

3.3.2.2 Nutrient supply to the Tethys Sea during the PETM as interpreted from Alamedilla section.....110

3.3.3 Productivity/global carbon cycle.....112

3.3.3.1 Palaeoproductivity/global carbon cycle in the Pacific Ocean.....112

3.3.3.2 Palaeoproductivity/global carbon cycle in the Tethys Ocean as interpreted from fauna and trait composition from Alamedilla section ……....115

3.3.4 Oxygen concentration in the seafloor.....116

3.3.4.1 Pacific Ocean.....116

3.3.4.2 Tethys Ocean.....118

3.4 Conclusions.....118

CHAPTER FOUR: The impact of high palaeoproductivity on the test and ecological function of foraminifera in the equatorial Pacific Ocean during the PETM.....122

4.1 Introduction..... 122

4. 2 Results.....125

4.2.1 Core description 125

4.2.2 Chronology.....128

4.2.3 Benthic foraminiferal composition and changes through time in site 1215A 130

4.2.4 Benthic foraminiferal traits composition in the equatorial Pacific Ocean.....138

4.3 Discussion 144

4.3.1 Interpreting the ecological functioning of the seafloor from the fauna and trait composition of benthic foraminifera 144

4.3.2 Preservation of foraminiferal test in the equatorial Pacific during the PETM 147

4.4 Conclusions.....154

CHAPTER FIVE: Biological trait composition and ecological functioning of foraminifera in the SE Atlantic Ocean during the PETM..... 157

5.1 Introduction.....157

5.2 Results.....160

5.2.1 Core description.....160

5.2.2 Chronology ….....161

5.2.3 Planktonic foraminiferal distribution 163

5.2.3.1 Taxa composition and changes through time 163

5.2.3.2 Trait composition and changes through time 169

5.2.4 Benthic Foraminifera.....174

5.2.4.1 Taxa composition and changes through time.....174

5.2.4.2 Trait composition and changes through time.....183

5. 3 Discussion….....188

5.3.1 Changes in pelagic ecology as indicated by planktonic foraminifera 188

5.3.2 Benthic foraminiferal markers indicating ecological changes in the seafloor during the PETM at Walvis Ridge.....190

5.3.3 Trait indices in ecological function and community interaction in the Surface Ocean and Seafloor….....193

5.4 Conclusions….....197

CHAPTER SIX.....200

General Discussion 200

6.1 The similarities in foraminiferal composition across the PETM intervals in all the studied sites 200

6.1.1 Pre-CIE fauna.....201

6.1.2 CIE fauna….....203

6.1.3 Post CIE (Recovery) fauna.....206

6.2 Mapping foraminiferal traits to their ecological functioning.....208

6.2.1 Test shape.....208

6.2.2 Test composition.....209

6.2.3. Chamber arrangement.....209

6.2.4 Ornamentation.....210

6.2.5 Apertures.....210

6.2.6 Perforation.....211

6.2.7 Life habit.....211

6.2.8 Foraminiferal trait sensitivity/selectivity during the PETM across the studied sites...212

6.3 The past as the key to the future.....215

CHAPTER SEVEN.....218

General Conclusions.....218

Future work..... 222

References.....224

List of Figures

Figure 1. 1: The detailed PETM architecture showing the four main CIE interval and plotted with a combination of δ13C and δ18O values from planktonic and benthic foraminifera as well as bulk carbonates from ODP site 690 on Maud Rise in the Weddell Sea ……...5

Figure 1. 2: Carbon speciation in the Ocean: When CO2 is dissolved in the seawater, the product is bicarbonate ion which produces free radicals to cause ocean acidification….....11

Figure 1. 3: Digital photos and CaCO3 (weight %) content showing layers of carbonate dissolution (as indicated by sharp declines in CaCO3) for five cores from at ODP Leg 208-Walvis Ridge, Atlantic Ocean.....12

Figure 1. 4: Inferred flow paths of global deep water during the PETM based on benthic foraminifera and bulk sediment carbon isotopes.....19

Figure 1. 5: Late Palaeocene-Early Eocene palaeogeography showing the main landmasses and marginal seas, and the Turgay Strait connecting the Arctic and Tethyan oceans.....20

Figure 1.6: Cross section of benthic foraminiferal cell.....22

Figure 1.7: A generalised order of foraminiferal evolution with the oldest at the base and youngest at the top 25

Figure1. 8: Schematic representation of foraminiferal niches in the marine environment. The cartoon represents a hypothetical foraminiferal ecology from sea surface to deep sediments.....27

Figure 1.9: The TROX model indicating the critical limit for oxygen and nutrient supply in foraminiferal microhabitat. 28

Figure 1. 10: Foraminifera classification based on the test morphology.....31

Figure 1.11: The distribution of planktic foraminifer species across the global ocean based on mean annual temperature. 32

Figure 1.12: Schematic representation of planktic foraminifer vertical depths habitats.....33

Figure 1. 13: Foraminifera morphotypes, their inferred microhabitat depth and critical oxygen threshold.....35

Figure 1.14. Cartoon of ocean biological carbon pump indicating how carbon dioxide is recycled between the atmosphere, oceans, marine organisms and the sediment.....39

Figure 2. 1: Location of the studied sites. 1215A, 1265A, 1209B, and 1212B are ODP site while outcrop data came from Alamedilla in Spain.....45

Figure 2.2: Stratigraphic sections and sample points for Alamedilla section, Sites 1265A, 1215A, 1209B and 1212B. 47

Figure 2.3: Topography of Shatsky Rise showing the location and present depth of all the sites in ODP Leg 198.....52

Figure 2.4: Combined litho and biostratigraphy as well as PETM events in Alamedilla section. 54

Figure 2.5. Micrographic representation of test shape, test composition, chamber arrangement, chamber shape, test macro-ornamentation of foraminifera and their modalities. 61

Figure 2.6. Micrographic representation of test micro-ornamentation, aperture form, aperture accessory structures, primary aperture position of foraminifera and their modalities.....62

Figure 2.7. Micrographic representation of test perforation, life habits of foraminifera and their modalities 63

Figure 3.1: Integrated age model for site 1209B (a) and site 1212B. Also shown is the CIE sections interpreted from δ13C isotope data.....72

Figure 3. 2: Benthic foraminiferal distributions across the PETM section at ODP Site 1209B.....74

Figure 3. 3: Non-Metric Multidimensional Scaling ordination of foraminiferal taxonomic composition (transformed with log x+1) of Bray-Curtis similarity from Site 1209B on the Shatsky Rise, Pacific Ocean.....75

Figure 3. 4: Non-metric Multidimensional Scaling ordination of foraminiferal traits composition (transformed with log x+1) of Bray-Curtis similarity from Site 1209B on the Shatsky Rise, Pacific Ocean.....78

Figure 3. 5: Similarity percentage (SIMPER) showing traits that cumulatively contributed ~50% to the differences in benthic foraminiferal trait composition across the CIE events at Site 1209B.....80

Figure 3.6: Changes in the traits of benthic foraminifera across the PETM events at Site 1209B in the Shatsky Rise, Pacific Ocean.....81

Figure 3.7: Benthic foraminiferal distribution across the PETM at ODP Site 1212B.....83

Figure 3.8: Non-Metric Multidimensional Scaling ordination of foraminiferal taxonomic composition (transformed with log x+1) of Bray-Curtis similarity from Site 1212B on the Shatsky Rise, Pacific Ocean.....84

Figure 3.9: Non-metric Multidimensional Scaling ordination of foraminiferal traits composition (transformed with log x+1) of Bray-Curtis similarity from Site 1212B on the Shatsky Rise, Pacific Ocean.....86

Figure 3.10: SIMPER result of the most significant trait (at 50% cut off) that contributed to the differences in benthic foraminiferal trait composition across the CIE events at Site 1212B. 88

Figure 3.11: Benthic foraminiferal trait composition and distribution of the CIE events at Site 1212B….....89

Figure 3.12: Age model for Alamedilla outcrop based on the integration of biostratigraphy, isotope stratigraphy derived from ODP site 690 and Leg 208.....90

Figure 3.13: Non-metric Multi-dimensional Scaling of foraminiferal traits composition of Bray-Curtis similarity from the Alamedilla outcrop, Spain.....93

Figure 3.14: Non-metric Multidimensional Scaling ordination of foraminiferal traits composition from Alamedilla (transformed with total resemblance) of Bray-Curtis similarity indicating the grouping of samples across the CIE events.....95

Figure 3.15: Similarity percentage (SIMPER) showing traits that cumulatively contributed ~50% to the differences in benthic foraminiferal trait composition across the CIE events at Alamedilla section, Spain.....96

Figure 3.16: Benthic foraminiferal trait composition and distribution across the CIE events at Alamedilla section..... 99

Figure 3.17: Composite trait composition from the Tethys Sea and the tropical Pacific Ocean to show some trait similarities across the studied sites. 105

Figure 3.18: Litho, bio and geochemical stratigraphy of PETM section in core 1209B-22H-1.....108

Figure 3.19: Litho, bio and geochemical stratigraphy of PETM section in core 1212B-9H-5. 109

Figure 3.20: Stratigraphic profile of Alamedilla section.....111

Figure 3.21: Records of benthic and planktonic foraminiferal abundance and $\delta^{13}C$ record from Site 1209B indicating changes in litho, bio and isotope stratigraphy during the PETM. 113

Figure 4. 1: Digital core photograph of Core H8, ODP Site 1215A. 124

Figure 4.2: A section of core 8H-03 showing sediment diapir and soft sediment deformation 125

Figure 4.3: A section of core 8H-02 showing a fracture across the core.....126

Figure 4.4: A section on core 6H-03 showing sediment mixing within the core. 127

Figure 4.5: Chronology and stratigraphy of the studied section of ODP Site 1215, cores 6H - 8H.....129

Figure 4.6 Age – depth model and sedimentation rate for Site 1215A 130

Figure 4.7: Non-metric Multidimensional Scaling ordination of benthic foraminifera taxa composition (transformed with total resemblance) of Bray-Curtis similarity from site 1215A ODP Leg 199, Central equatorial Pacific Ocean. 132

Figure 4.8: Benthic foraminiferal events in ODP Site 1215A.....135

Figure 4.9: Distribution of cosmopolitan benthic foraminifera in ODP Site 1215A.....137

Figure 4.10: Non-metric Multidimensional Scaling ordination of foraminiferal traits composition (transformed with total resemblance) of Bray-Curtis similarity from Site 1215A ODP Leg 199, Central equatorial Pacific Ocean. 138

Figure 4.11: SIMPER result of the most significant trait (at 50% cut off) that contributed to the differences in benthic foraminiferal trait composition across the CIE events at ODP Site 1215A 140

Figure 4.12: Benthic foraminiferal traits distribution in ODP Site 1215A 142

Figure 5. 1: Three-dimensional diagram of the Leg 208 drill sites showing the location of Site 1265A and its associates with corresponding bathymetry. 159

Figure 5.2: Chronostratigraphy of the studied section of Site 1265A 162

Figure 5.3. Linear sedimentation rate and Age – depth curve of Site 1265A.....162

Figure 5.4: Non-Metric Multidimensional Scaling ordination of planktonic foraminiferal taxonomic composition (transformed with log x+1) of Bray-Curtis similarity from Site 1265A.....164

Figure 5.5: The distribution of planktonic foraminiferal species in the PETM section of Site 1265A.....168

Figure 5.6: Non-metric Multidimensional Scaling ordination of planktonic foraminiferal traits composition from site 1265A (transformed with total resemblance) of Bray-Curtis similarity indicating sample ordination across the CIE events. 170

Figure 5.7: Mean abundance of planktonic foraminiferal traits driving the main differences in distribution across the PETM interval at Site 1265A (Data cut off 50%).....171

Figure 5. 8: Planktonic foraminiferal traits distribution across the three intervals of PETM at ODP Site 1265A-South Atlantic Ocean shown with core depths (mbsf) on the left, bulk $\delta^{13}C$ record. 173

Figure 5. 9: nmMDS ordination of benthic foraminifera abundance in ODP Site 1265A 175

Figure 5. 10: Benthic foraminiferal taxa present before and during the CIE at ODP Site 1265A….....180

Figure 5. 11: Faunal distribution of benthic foraminiferal taxa that remarkably increased and/ or originated after the PETM.....181

Figure 5. 12: Other cosmopolitan benthic foraminifera recovered from Site 1265A most of which are resurrection taxa.....182

Figure 5. 13: SIMPER result of the most significant trait (at 50% cut off) that contributed to the differences in benthic foraminiferal trait composition across the CIE events at Site 1265A …….....185

Figure 5. 14: Changes in the traits of benthic foraminifera across the PETM at Site 1265A shown with core depths (mbsf) on the left, $\delta^{13}C$ record (extracted from Zachos et al., 2005) and age (Ma) on the far right.....186

Figure 5. 15: nmMDS ordination of benthic foraminiferal traits composition (transformed with log x+1) of Bray-Curtis similarity from Site 1265A.....187

Figure 5. 16: Summarised depth profile and life strategies of major Palaeocene – Eocene planktonic foraminifera.....188

List of Tables

Table 1. 1: Agglutinated foraminiferal morphotypes indicating their relationship with the environment and their living habits based on Nagy (1995).....36

Table 1. 2: Palaeoceanographic parameters and the geochemical proxies for their determination.....37

Table 2. 1: Summary of sites and data sources.....46

Table 2. 2: Sample levels from cores 6H and 8H, Site 1215A with the corresponding metre below seafloor (mbsf) and metres composite depth (mcd).....48

Table 2. 3: Cores depth of the section analysed from Site 1265A with their corresponding metre below seafloor (mbsf) and metres composite depth (mcd).....49

Table 2. 4: Biological traits and associated modalities used in this study.....59

Table 2. 5: Example list of eight foraminiferal taxa from Site 1209B with the fuzzy trait coding for two (test shape and chamber arrangement) out of the 13 traits used for this study. See supplementary data in appendix for the complete table.....64

Table 2. 6: An example list of the product of taxonomic composition and fuzzy coding using matrix multiplication.....66

Table 3. 1: Site 1209B Similarity percentage (SIMPER) result of the average taxonomic abundance and their respective percentage contribution within the pre-CIE and the main CIE intervals.....76

Table 3. 2: Site 1209B SIMPER results of the average abundance and their respective percentage contribution within the main CIE and recovery intervals.....76

Table 3. 3: Site 1209B SIMPER result of the average taxonomic abundance of benthic foraminifera and their respective percentage contribution within the pre-CIE and the recovery intervals.....77

Table 3. 4: Mean abundance of taxa contributing to the most dissimilarity between the recovery and the CIE intervals (56% cut off) at Site 1212B.....85

Table 3. 5: Mean abundance of species contributing to the most dissimilarity between the Recovery and the pre-CIE intervals at Site 1212B (54% cut off).....85

Table 3. 6: Mean abundance of species contributing to the most dissimilarity between the CIE and the pre-CIE intervals at Site 1212B. 86

Table 3. 7: Mean abundance of species making a cumulative contribution to the dissimilarity between the CIE and the recovery intervals at Alamedilla section.....93

Table 3. 8: Mean abundance of species making a cumulative contribution of ~50% to the dissimilarity between the pre-CIE and recovery intervals at Alamedilla section.....94

Table 3. 9: Mean abundance of species making a cumulative contribution of ~50% to the dissimilarity between the CIE and pre-CIE PETM intervals at Alamedilla.....94

Table 3. 10: Summary of trait occurrence across the PETM events in the tropical Pacific and Tethys Oceans.....120

Table 4. 1: Mean abundance of taxa that contributed the most dissimilarities observed in faunal distribution across the CIE intervals at ODP Site 1215A.....133

Table 5. 1: Mean abundance of species contributing to the most dissimilarity between the Recovery and the CIE intervals at Site 1265A.....165

Table 5. 2: Mean abundance of species contributing to the most dissimilarity between the Recovery and the pre-CIE intervals at Site 1265A. Data cut off at 50% cumulative similarity. 165

Table 5. 3: Mean abundance of species contributing to the most dissimilarity between the CIE and pre-CIE intervals at Site 1265A.....166

Table 5. 4: Site 1265A SIMPER results of the average abundance of benthic foraminiferal taxa and their respective percentage contribution within the recovery and pre-CIE intervals. 176

Table 5. 5: Site 1265A SIMPER results of the average abundance of benthic foraminiferal taxa and their respective percentage contribution within the CIE and pre CIE intervals.....177

Table 5. 6: Site 1265A SIMPER results of the average abundance of benthic foraminiferal taxa and their respective percentage contribution within the recovery and CIE intervals. (Data cut off 50%).....178

Table 6. 1: Benthic foraminiferal assemblage that dominated the pre-CIE interval but became extinct after the CIE.....203

Table 6. 2: Benthic foraminiferal assemblages that originated after the CIE in all the studied sites.....207

Table 7.1: Foraminifera traits and related ecological parameter.....219

List of plates

Plate 4.1: Foraminiferal test from sample 1215A_8H-03_60-62 showing evidence of early stage of diagenesis ……148

Plate 4.2: Foraminiferal test at an advanced stage of dissolution. ……150

Plate 4. 3: Evidence of nannofossil incorporation in foraminifera test from sample 1215A_8H-03_130-132 ……152

List of appendices

Appendix 1: Benthic foraminiferal abundance and associated trait coding from ODP Site 1209B

Appendix 2: Benthic foraminiferal abundance and associated trait coding from ODP Site 1212B

Appendix 3: Benthic foraminiferal abundance and associated trait coding from Alamedilla

Appendix 4: Benthic foraminiferal abundance and associated trait coding from ODP Site 1215A

Appendix 5.1: Benthic foraminiferal abundance and associated trait coding from ODP Site 1265A

Appendix 5.2: Planktonic foraminiferal abundance and associated trait coding from ODP Site 1265A

CHAPTER ONE

General Introduction

1.1 Introduction

It is a generally accepted knowledge among contemporary and deep time ecologists that marine ecosystems are currently deteriorating due to recent climate change (Aze *et al*., 2014a; Foster *et al.,* 2018; IPCC 2018). The change in climate is caused by natural and anthropogenically driven activities such as emission of CO_2, variation in orbital cyclicity/ solar radiation, tectonic events, El Niño-Southern Oscillation (ENSO), over-exploitation of resources, change in land use and environmental pollution (IPCC, 2013). The impact of the changing climate on marine ecosystems has raised concerns about the future of global biodiversity (Laffoley and Baxter, 2016). The rate at which species are disappearing in the biosphere has made the scientific community propose that if mitigating circumstances are not put in place, the Earth will be approaching the sixth mass extinction before the end of the century (Barnosky *et al.*, 2011). The loss of biodiversity in the oceans will not only have a severe impact on the marine food chain that directly affects global food supply, economic and social wellbeing of humans, but will also enhance positive feedback on a climate system that is already perturbed (Ceballos and Ehrlich, 2018). The understanding of the impact of extreme climate on marine biodiversity resulting from increased greenhouse gas input into the oceans is critical to the understanding of how the Earth systems will function in the near future (IPCC, 2018, Caswell *et al.,* 2017; Zebee and Zachos 2013; Frid *et al.,* 2015). The primary driver of current climate change is the emission of carbon dioxide (CO_2). The estimated CO_2 concentration of the ocean-atmosphere for the next 100 – 500 years, based on the assessments of fossil fuel reserves and other resources is 5000 petagrams of carbon (Rogner, 1997; Zeebe *et al.,* 2016; Foster *et al*., 2018).

To understand the impact this enormous volume of greenhouse gas will have on the marine ecosystems in the future, marine ecologists are inspired to look back in the geologic archive to investigate periods that recorded an equivalent amount of greenhouse gas in the past. This is because it takes several millennia for the ocean to revert to stability after perturbation due to its volume and heat capacity (IPCC, 2013). Also because, the available evidence indicates that CO_2 concentration did not exceed 1000 ppm in the last 35 million years of Earth history (Bijl, 2011), and in most of this period CO_2 concentrations were less than 500 ppm (Beerling and Royer, 2011) which is far below the forecasted figure of 2000 ppm (Bijl, 2011; Zeebe and Zachos, 2013) for the near future. This means that contemporary data cannot be used in

isolation to successfully predict the impact of the current climate on the global ecosystem. The earliest climate event in the geologic record associated with the magnitude of CO_2 concentration speculated for the future is the Palaeocene – Eocene Thermal Maximum (PETM) which occurred 56 million years ago (Kennett and Stott, 1991; Kelly *et al*., 1996; Zachos *et al.* 2005, 2008; Zeebe *et al.,* 2016). Understanding the biotic turn over during this event will provide useful clues to the current climate impact on global biodiversity.

Most of the deep time studies used in understanding the impact of extreme climate on biotic turnover have been based on faunal assemblage, marker species and geochemical data (e.g. Thomas, 1998; 2003; 2007; Alegret *et al.,* 2009; D'haenens *et al.,* 2012; Aze *et al.,* 2014b); Giusberti *et al.,* 2016 and Luciani *et al.,* 2017). However, faunal assemblage data are prone to error due to poor preservation that may result from the taphonomic processes (Twitchett, 2006). To minimise the impact of poor preservation on the fossil record in understanding biotic changes in palaeorecords, this study has adopted a technique known as Biological Trait Analysis (BTA) to investigate the effect of the extreme climatic conditions on the biological traits of microfossils in the ocean. The technique is widely applied in contemporary ecology to understand the impact of anthropogenic practices on fluvial and marine ecosystems (McClanahan *et al*., 1999; Lotze *et al.,* 2000; Törnroos *et al.,* 2015) and has assisted palaeoecologists in the interpretation of large-scale changes in biodiversity (i.e the total number of organism living in an ecosystem as well as their genetic, and trait composition) by linking the trait (well defined and measurable attribute of an organism) composition of the species to their abundance and distribution (Bremner *et al*., 2006; Tyler *et al.,* 2012; Caswell and Frid 2017). Generally, biological attributes rather than the taxonomic composition of species control an organism's interaction within their ecological community (Tyler *et al.,* 2012).

A large body of research comprising sophisticated computer models and proxy records have been conducted and are still ongoing to understand the impact of the current climate change on marine ecosystems (e.g. Thomas *et al*., 2007; Zeebe *et al*., 2016; Foster *et al*., 2018;). The fundamental challenge with contemporary data is that they are restricted regarding how far they can go in time because the available climate data only started in the past few centuries. More so, volume, topography and accessibility, limit the amount of data collected from the ocean. To get a better understanding of past changes in the climate, palaeo-records preserved in sedimentary deposits are very useful archive (Williams *et al.,* 2007). Both the contemporary data and palaeo-records play a complementary role because “the present is the key to the past”.

The palaeo-record also has its weakness ranging from selective/non-preservation of species that existed when the sediment under investigation was deposited, the limited understanding of the past ecologies and changes in life strategies and ecology over the geological time. Nevertheless, the palaeo-record is quite useful in the understanding of events that take many years to occur because the impact of the event will be recorded on the organism that existed throughout the period and will be preserved in the sediment while contemporary data can only show the impact on the environment at the time it was collected.

1.2 Palaeocene – Eocene Thermal Maximum (PETM)

The PETM was characterised by a sudden and extreme global warming event, linked to the massive injections of ^{13}C-depleted carbon into the global ocean-atmosphere carbon reservoir (Zeebe and Zachos, 2013). The average rise in temperature during the PETM was estimated to be 6°C (Dunkley-Jones *et al.,* 2013). The reconstruction of mid to high latitude temperatures indicate that they attained 24°C–29°C (Frieling *et al.,* 2017) while tropical temperature exceeded 30°C (Aze *et al.,* 2014b) in the continental margins of East Africa. In addition, the event resulted in severe environmental impacts, including ocean acidification and the global expansion of oxygen minimum zones (Penman *et al*., 2014), photic zone euxinia (Sluijs *et al.* 2007), sea-level rise (Deprez *et al.,* 2017), a prominent shoaling of the global ocean carbonate compensation depth (CCD; Thomas, 2007), and an accelerated hydrological cycle (Frieling *et al*., 2017). In this discussion, we will only consider changes in temperature, hydrology and ocean acidification as reflected on the data collected for this thesis.

1.2.1 Causes and duration of the PETM

One of the most popular causes of the PETM among the palaeoclimate research community is that of the massive injection of $\delta^{13}C$ depleted carbon from methane clathrates into the global exogenic carbon reservoir (Zachos *et al*., 2005). Other sources of light carbon that is believed to have caused the hyperthermal include; decaying terrigenous organic matter, lithospheric gas explosions (William *et al.,* 2007), thermogenic methane, deep sea permafrost gas release (Panchuk *et al.,* 2008), carbon dioxide released by volcanism during the opening of the North Atlantic in the late Palaeocene (Winguth, 2011) and tectonically induced uplift/ desiccation of epicontinental seas (Cramer *et al.,* 2005; Higgins *et al.,* 2006; Frieling *et al.,* 2016). Of all the above-listed causes no single hypothesis has been able to account for the entire amount of carbon associated with the magnitude of the negative CIE recorded during the PETM. Hence, the event may have been caused by a combination of two or more of the listed hypothesis, and

in some location, the cause may have been localised resulting to different authors coming up with a different hypothesis depending on the region they are working at.

During the PETM, about 3,000 Pg to 10,000 Pg of isotopically light carbon were released into the ocean-atmosphere system (Gutjahr *et al.,* 2017), which triggered profound changes in the carbon cycle, global climate, and ocean chemistry (see Babila *et al.,* 2018). The rate of the carbon release during the PETM was believed to be rapid (in geological terms) and the greenhouse gas release lasted for about ~20,000 years (excluding the feedbacks; Sluijs *et al*., 2007). In turn, this affected both marine and terrestrial ecosystems (Stassen *et al.,* 2015; Schmidt *et al.,* 2018).

The negative carbon isotopic excursion (CIE; Figure 1.1) is thought to reflect the injection and subsequent sequestration of huge amounts of ^{13}C-depleted carbon into the ocean-atmosphere system (Dickens *et al.,* 1995). The onset of the CIE has been defined as starting from the last sample before the first shift in the CIE until the sample with the lowest CIE value (Figure 1.1).

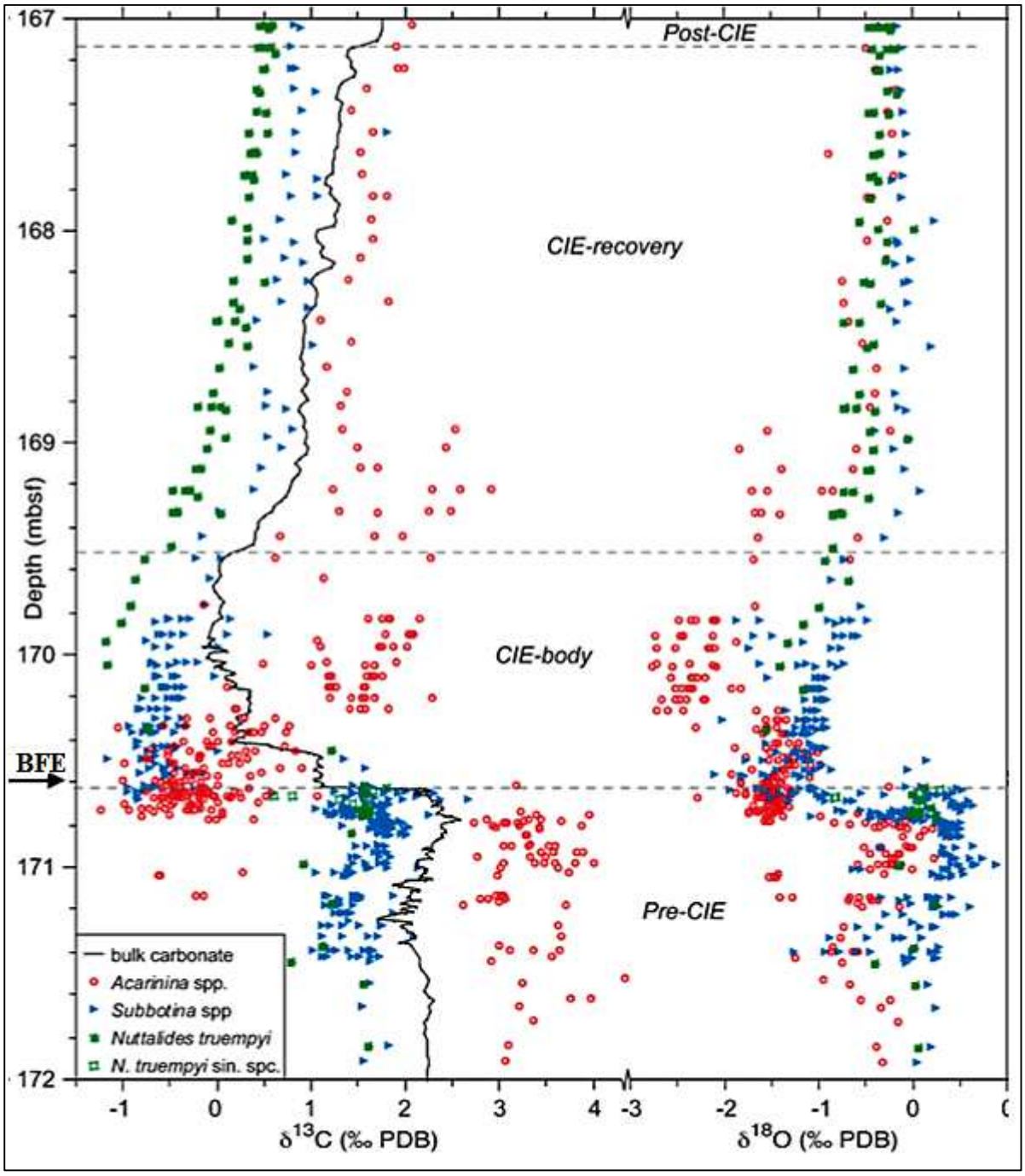

Figure 1.1: The detailed PETM architecture showing the four main CIE interval and plotted with a combination of $\delta^{13}C$ and $\delta^{18}O$ values from planktonic and benthic foraminifera as well as bulk carbonates from ODP site 690 on Maud Rise in the Weddell Sea. Each colour reflects the isotope values from a particular foraminifera specimen, and the legend is given at the bottom left of the figure. PDB = PeeDee Belemnite standard. BFE = Benthic Foraminiferal Extinction horizon. The general shape of the CIE has been interpreted to reflect a pulsed and geologically rapid input of ^{13}C-depleted carbon into the Earth system (CIE body) followed by the gradual sequestration of excess carbon through negative climate feedbacks, taken from Sluijs et al. (2007)

The onset of the CIE is marked by an abrupt, negative shift in $\delta^{13}C$, lasting for about 10,000 years (Sluijs *et al*., 2007). This is followed by a phase of relatively stable low values, which has been termed the body/core of the CIE and subsequent recovery to higher $\delta\ ^{13}C$ values that

follows a parabolic trend (Figure 1.1; Sluijs *et al*., 2007). The absolute age of the PETM has been estimated from radiometric dating of volcanic ash layers as well as orbital tuning of deep marine cores to range from 55.8 to 56.2 Myr (Rohl *et al.,* 2007; McInerney and Wing, 2011). Palaeomagnetic age models for the PETM/CIE indicated that the whole event lasted between 100 Kya to 250 Kya (Bains *et al.,* 1999; Thomas *et al.,* 2002; Kelly *et al.,* 2005; Sluijs *et al*., 2007; Turner, 2018). The duration of the main CIE interval was established from continental PETM sections which were not affected by carbonate dissolution and ranged from 10 Kya–23 Kya (McInerney and Wing, 2011). The time it took for the carbon isotopes to return to the pre-CIE values (the Recovery period, Figure 1.1) was estimated using the astronomically tuned age model from well-preserved PETM sections at Maud Rise- ODP site 690 and Walvis Ridge (Site 1266) and is suggested to have lasted for 112 Kya (Rohl, *et al.,* 2007).

The principal evidence for the PETM in the geological record is a massive and rapid negative carbon isotopic excursion (CIE), shoaling of lysocline/calcium carbonate compensation depth (CCD), benthic foraminiferal extinctions in the deep ocean (Dunkley-Jones *et al*., 2013) as well as speciation and migrations of pelagic fauna from low – high latitude oceans (Speijer *et al.,* 2012). Evidence from palaeotemperature proxies and climate model simulations indicate that global temperatures rose between 5–8 $^{\circ}$C on the continents (Thomas *et al.*, 2003; Sluijs *et al.* 2007) and 3–5 $^{\circ}$C in the deep sea (Gehler, 2016). The temperature differential between the equatorial regions and the poles decreased, and this led to the migration of organisms that originally thrived in the warm tropics into the Polar Regions (Pross *et al.* 2012). Evidence of temperate species such as palms and the dinoflagellate (e.g. *Apectodinium*) have been reported in the fossil record of Greenland (Bijl *et al.,* 2013).

The most widely accepted cause of PETM is the methane hydrate /greenhouse gas release theory which suggests that PETM was caused by the dissociation of about 3000-10,000 Pg of isotopically light carbon from methane clathrate reservoirs in the continental margin (McInerney and Wing, 2011). The release of this quantity of greenhouse gas into the marine environment will result in widespread anoxia, dissolution of calcium carbonate and ocean acidification. Other hypotheses which have been published include: impact from huge comet (Kent *et al.,* 2003), orbital forcing/eccentricity cycles (Lauren 2005; Sluijs *et al.,* 2007), biomass combustion (Manner *et al.,* 2013), volcanic/igneous activities resulting from the opening of the North Atlantic Ocean or possibly associated with mantle plume outgassing (Gutjahr *et al.* 2017; Thomas, 2007) and drying of the epicontinental seas (Higgins and Schrag 2006).

The recovery of the PETM came about from increases in carbonate burial and consumption of CO_2 due to enhanced silicate weathering (Winguth, 2010). The surge in terrestrial inputs also increased the nutrient supply to the oceans, by promoting the production of biogenic $CaCO_3$ by marine calcareous plankton and their subsequent burial in seafloor sediments that would have sequestered the excess carbon (Shaffer *et al*., 2016). Fluctuations in the carbonate compensation depth (CCD) during the CIE and PETM recovery reflect the self-stabilising system of the Earth's climate, which has ensured the continual maintenance of a habitable Earth throughout recent history. The recovery of PETM seems to have been a gradual process and was estimated to have lasted for 83 Ka (Murphy *et al.,* 2010). The event had an enduring effect on the benthic foraminifera ecosystem that never fully recovered to the pre-PETM conditions as most of the Mesozoic fauna that survived the K-Pg extinction were wiped away (Speijer *et al.,* 2012). This suggests that the current climate changes may also totally change the ecosystem in the future.

Climate scientists (e.g. Zeebe and Zachos, 2013) have speculated that the current anthropogenic and natural greenhouse gas emission into the Earth system would add more than 2000 ppm of carbon into the Ocean-atmospheric system if not checked. A scenario that could increase the atmospheric pressure (pCO_2) to more than what was experienced during the late Palaeocene – early Eocene climatic warming (IPCC, 2013). With the increase in CO_2, the mean global temperature will commensurately increase by more than 8°C, and the pH of the surface ocean may decline to about 0.7 units (Zeebe and Zachos, 2013; Zeebe *et al.,* 2016). The impact of excessive input of CO_2 in the Earth system may be more devastating in the marine environment hence, more studies on the PETM (like ours) are needed to better understand climate sensitivity and the impact on the marine biota because the PETM offers an ample opportunity for understanding the future climate.

1.3 Abiotic changes in the environment during the Palaeocene-Eocene Thermal Maximum

1.3.1 Palaeotemperature changes

There are many palaeotemperature proxies used in estimating the temperature changes during the PETM. These include the stable isotopes of oxygen (Kennett and Stott, 1991; Zachos *et al.,* 2007) and Mg/Ca ratio (Dunkley-Jones *et al.,* 2013) of the planktonic near-surface dwelling and deep-dwelling benthic foraminifera, biomarkers derived from organic materials such as TEX_{86} (Sluijs *et al.* 2007 and Frieling *et al*., 2017), UK^{37} derived from the alkenones of haptophyte algae (Bijl, 2011), Methylation of Branched Tetraethers and the Cyclisation of

Branched Tetraethers (MBT-CBT) index from membrane lipids of soil bacteria (Peterse *et al*., 2012; Tierney, 2010) as well as minerals with temperature-dependent formation (Dunkley-Jones *et al.,* 2013).

The average global temperature values from Mg/Ca ratios from foraminifera suggest 6-10°C warming from low–mid-latitudes (Dunkley-Jones *et al.,* 2013). Poor test preservation and vital effects rather than seawater salinity have been identified as the main causes of variation between the $\delta^{18}O$ and Mg/Ca-derived temperatures (Zachos *et al*., 2003; Tripati and Elderfield 2004; Birch *et al.,* 2016). The biomarker TEX_{86} has been reported to give higher and more consistent palaeotemperature values, unlike calcite and other mineral-based proxies whose availability is environmentally controlled (Bijl, 2013). Calcite for instance forms in the ocean and can be influenced by dissolution and recrystallisation whereas organic matter based TEX_{86} does not degrade and can be found in abundance in both marine and terrestrial environments (Frieling *et al*., 2017). This could explain why the temperature estimates based on TEX_{86} are higher across the PETM compared with the other proxies (Frieling *et al.,* 2017). Nevertheless, Bijl (2013) has argued that TEX_{86} could be recording summer temperatures instead of mean annual values, but this could also apply to all proxies. Other materials that have been used for palaeotemperature reconstruction during the PETM include; soil nodules (McInerney and Wing 2011), the shapes of fossilised leaf margins (Fricke and Wing 2004), the tooth enamel of mammals (Wagner 2013) and $\delta^{18}O$ composition fish scales (Bowen *et al*., 2001).

Climate model simulations of the amount of warming based on the magnitude of the CIE usually produce a maximum increase of 5°C in sea-surface temperature (SST) and much cooler polar regions (Shellito and Sloan, 2006; Inglis *et al.,* 2017). This was also the case even when the atmospheric CO_2 was increased 16 times that of the pre-industrial values (Dunkley-Jones *et al.,* 2013). Comparisons of proxy derived SSTs, and modelled values tend to both show consistent first-order spatial patterns of warming. However, proxy derived SSTs indicate there was a weak meridional temperature gradient during the PETM and this has been difficult to replicate in the models (Lunt *et al*., 2017). The modelled estimates of the mean global warming may appear comparatively small (Huber *et al*., 2003) in relation to some of the larger temperature anomalies recorded in the proxy data, but it actually represents the true average of the overall global temperature rise during the period (McInerney and Wing 2011). Two major sources of error in deep time climate models and proxy comparisons have been identified. Firstly, palaeoclimate models depend on the proxy data; thus errors may result from palaeogeographical reconstructions of continental margins and ocean gateways or inferred water depth could affect model outputs. Secondly, not all the parameters in the physical

environment can be simulated to run concurrently in the model configuration (Lunt *et al*., 2017).

1.3.2 Changes in hydrology

The effects of increased temperatures and high atmospheric CO_2 concentrations on the hydrological cycle tend to show complex regional responses across the globe (Handley *et al.,* 2012). In some places, the PETM is associated with increased atmospheric humidity that led to high precipitation (Baczynski *et al*. 2017); while in other locations, evidence of increased aridity has been documented (Handley *et al.,* 2012). Increases in kaolinite deposition recorded in marginal marine sections of late Palaeocene–early Eocene age in North America, Asia, Antarctica and Africa indicated that there was enhanced weathering of adjacent continental rocks instigated by an increase in precipitation during the warm, humid climate (Handley *et al.,* 2012). There is also evidence of increased precipitation and terrestrial run off with significant increases in non-marine palynomorphs and an *Apectodinium (*dinocyst) population explosion in the PETM marine sections (Sluijs *et al.*, 2008; Frieling *et al.,* 2017). Also, the PETM fluvial systems in the Pyrenees in Spain has a conglomeritic base (Schmitz and Pujalte, 2007) which indicates that there was increased and violent rainfall due to climate perturbation.

Kraus and Riggins (2007) reported that palaeosol horizons in Bighorn Basin (Wyoming, USA) revealed some evidence for decreased chemical weathering during the PETM and changes in ichnofossil assemblages corresponded with drier and well-drained soils. Other studies from the same location (Bowen *et al.,* 2004; Wing *et al.,* 2005) reported a reduction in the morphology (size) of leaf margins from early Eocene flora indicating an increase in water stress. General circulation models (GCM) parameterised based on the climate of the western interior of the USA showed an increase in convective atmospheric circulation off the palaeo-Gulf of Mexico leading to enhanced monsoons (Handley *et al.,* 2012). These model predictions have been substantiated with recognition of vast braided plains or mega fan (conglomerate) deposits at the onset of PETM in northern Spain which shared a similar palaeolatitude/palaeoclimate with western parts of the USA (Handley *et al.,* 2012). Hydrogen isotope records from the PETM core from the Arctic Ocean indicated a spike in deuterium isotopes signalling enhanced precipitation and greater water transport to the poles (Pagani *et al.,* 2006). At low latitude sections in Tanzania, Handley *et al.* (2012) observed seasonal precipitation punctuated by hot and arid conditions comparable to those existing today.

In summary, proxy data and model simulations tend to agree that there was an increase in seasonal rainfall and more severe storms rather than there being a persistent wet climate

(Baczynski *et al*. 2017). The return to cooler conditions during the Palaeogene is believed to have begun with increases in precipitation that led to enhanced silicate weathering on the continent which in turn resulted in major negative climate feedbacks that caused a long-term drawdown of CO_2 (Bowen and Zachos, 2010).

1.3.3 Ocean acidification during the PETM

One of the most significant environmental feedbacks from the massive injection of greenhouse gases and the coeval increase in temperature that occurred during the PETM was ocean acidification (Babila *et al.,* 2018). In essence, the oxidation and absorption of this excess carbon lowered ocean pH particularly in the deep sea because the free radicals (molecules that contain at least one unpaired electron) generated by the dissolution of CO_2 in seawater leads to the acidification of the ocean (See Figure 1.2) and thereby triggered a rapid and upward shoaling of the lysocline and calcite compensation depth (CCD; Zachos *et al.,* 2005). This led to sea floor carbonate dissolution and reductions in the amount and rates of carbonate burial (Winguth, 2010). The extent of ocean carbonate ion dilution, as well as the global shallowing of the CCD, is related to the amounts of carbon dioxide injected into the ocean-atmosphere system (Sluijs *et al*., 2014; Palike *et al*., 2014). When CO_2 dissolves in seawater, it reacts with water to form carbonic acid, which dissociates to bicarbonate, carbonate, and hydrogen ions. The higher concentration of hydrogen ions changes pH making seawater acidic, but this process is buffered over long time scales by the interplay of seawater, seafloor carbonate sediments, and weathering of the continents (Zebebe and Wolf-Gladrow, 2001; Aze *et al*., 2014a). Several trace element and stable isotope proxies have been used to establish a change in carbonate chemistry of seawater during the PETM. For example, the Manganese (Mn) and Uranium enrichment factors in deep-sea cores from Atlantic, Pacific and Sothern Oceans were used by Palike *et al*. (2014) to constrain the paleoredox changes in these oceans during the PETM. The result from this study went as far as identifying the source of greenhouse gas that causes the ocean acidification during the PETM in the Atlantic Ocean (Palike *et al*., 2014).

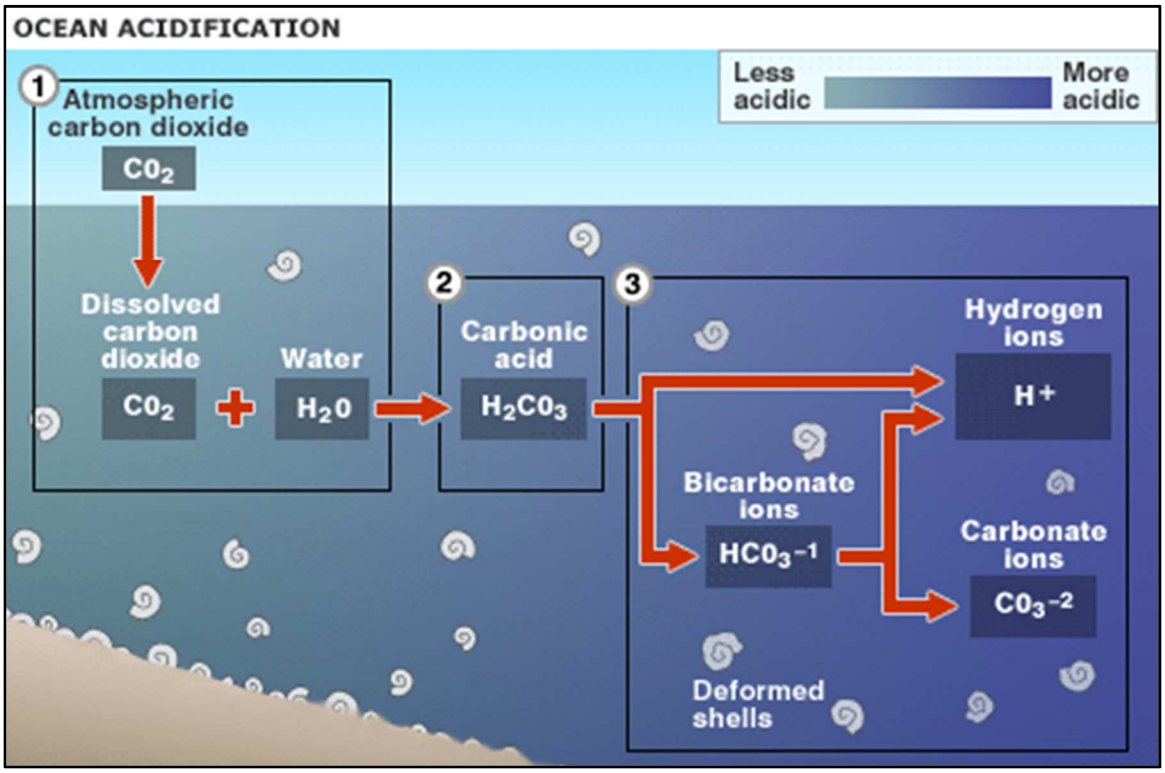

Figure 1.2. Carbon speciation in the Ocean: When CO_2 is dissolved in the seawater; the product is bicarbonate ion, which produces free radicals to cause ocean acidification, taken from Strain (2015)

Direct geochemical evidence for changes in past ocean acidity (including the PETM) are still relatively scarce (Gutjahr *et al.,* 2017), and past ocean acidification is often extrapolated from decreases in calcium carbonate accumulation and preservation in marine sediments. This may be represented by the existence of clay-rich layer between calcite beds and high-level dissolution or fragmentation of foraminiferal shells (Coadic *et al*., 2013)

Carbonate dissolution near the sea floor during the PETM is widely documented across the globe (Babila *et al.,* 2018). At Walvis Ridge in the southeast Atlantic Ocean where one of the cores used in the present study was recovered, carbonate dissolution occurred to the magnitude of 2km at palaeodepth of 1500 – 3600m along a transect (Figure 1.3; Zachos *et al.*, 2005). Using the data from Walvis ridge Zachos *et al.* (2005) estimated that 4500 gigatons of carbon were released during the PETM. It was proposed that the amount of calcite dissolution at the Walvis Ridge represents the global ocean average and that the geometry of the ocean basins, as well as the seawater alkalinity, were comparable to those of the modern ocean (Sluijs *et al.,* 2007). However, there is uncertainty (Thomas, 1998) in the estimated value of carbon released because the site is located in the subtropics near a tectonically active hydrothermal vent. Cores from ODP site 690 in the Southern Ocean recovered at palaeodepth of 1900m showed a slight

decrease in carbonate content of between 85% and 60% (Bralower *et al.,* 2004). At Shastky Rise (ODP site 1209) in the central Pacific Ocean, the deepest site studied for PETM, carbonate content decreased by about 10% (Colosimo *et al.,* 2005). Whilst at the continental slope section in Mead stream New Zealand and coastal sections in Tanzania decreased carbonate content was interpreted to reflect dilution by increased terrigenous influx rather than dissolution (Hollis *et al*., 2005; Hardley *et al.,* 2008). Thus, the data from Walvis Ridge show that there was more severe dissolution in the Atlantic Ocean compared with the Pacific than predicted by models that assume late Palaeocene ocean circulation patterns were similar to those in the present day (Sluijs *et al.,* 2007). The increased carbonate dissolution in the Atlantic Ocean could be attributed to its proximity to the main source of carbon injection (Zachos *et al.,* 2005).

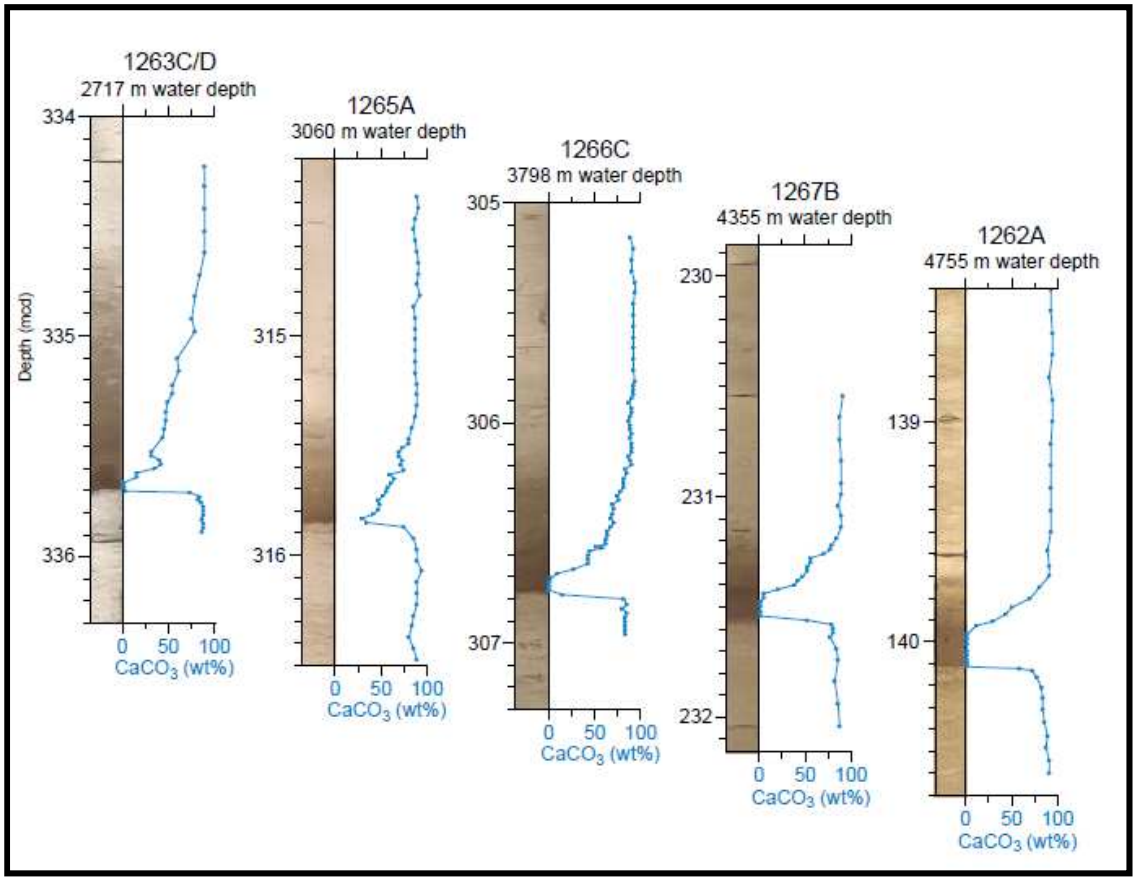

Figure 1.3: Digital photos and $CaCO_3$ (weight %) content showing layers of carbonate dissolution (as indicated by sharp declines in $CaCO_3$) for five cores from at ODP Leg 208-Walvis Ridge, Atlantic Ocean. Each core represents different palaeowater depths. Mcd =metre composite depth (Adapted from Zachos et al., 2005).

Severe dissolution has also been observed in many present-day marginal basins, such as the North Sea (e.g. Gradstein *et al.,* 1994), the Gubio Basin, and the marginal Tethys (Schmitz *et al.,* 2004). From the above discussion it can be seen that the major controls on carbonate

dissolution in the ocean during the PETM included; increased CO_2 concentration, the changing rate of clastic and organic matter flux as well as terrestrial runoff and post-depositional dissolution in the deep sea.

1.4 Biotic changes in the marine environment during the PETM

The extreme climatic perturbation that occurred during the PETM affected both terrestrial and marine ecosystems, notably causing extinction of marine benthic microfauna. As the main focus of this thesis is on the impact of PETM on foraminifera and the marine ecosystem, the discussion in this section will be limited to the impact of the event on foraminifera. PETM resulted in origination and migration of planktonic foraminifera as well as some local extinctions. The pattern of faunal changes in the pelagic and benthic ecosystem are well documented across the globe (Thomas 2007; Speijer *et al*., 2012; Arreguin-Rodriguez *et al.,* 2018). The most significant foraminiferal turnover during the PETM is the extinction of 40-60% of benthic foraminifera (Thomas, 2007; Algret *et al.,* 2009; Speijer *et al.,* 2012). The taxa recognised to have disappeared globally worldwide during the PETM is *Gavelinella beccarriformis,* while the extinction of other taxa is believed to be local or regional (Thomas, 1998). The cause of this massive extinction include; 1) ocean anoxia, 2) highly corrosive and acidified ocean resulting from methane and other greenhouse gas oxidation, 3) increased temperature that altered the productivity and metabolism of the organisms and, 4) a combination of these factors. The listed factors have been identified in different PETM sections but not all the parameters exist globally in all the sections studied (Speijer *et al.,* 2012). The post CIE fauna is characterised by small, thin-walled calcareous taxa with low diversity and the emergence of 'modern' Eocene taxa such as *N. truempyi, O. umbonatus, T. selmensis, B. tuxpamensis and* Abyssaminids*,* which replaced the 'older' Cretaceous taxa that became extinct.

The PETM also resulted in a major biological turn-over in pelagic planktonic foraminifera leading the morphological innovations in *Acarinina* and *Morozovella* taxa. Most significantly is the diversification and migration of most planktonic foraminifera as well as the latitudinal expansion of their distribution from low to high latitudes (Kelly *et al.,* 1996). *Acarinina sibaiyaensis, A. africana, A. multicamerata and Morozovella allionensis* are reported to have originated as excursion taxa during the PETM (Kelly *et al.,* 1996; Petrizzo *et al*., 2006; Speijer *et al.,* 2012; Aze *et al.,* 2014a). Warming of the pelagic zone and the resulting changes in the surface currents have been suggested as the major cause of speciation, migration and morphological changes in planktonic foraminifera during the PETM. The warming of high

latitude regions as a result of increased temperature resulted in species migrating from low to high latitudes and the changing surface current facilitated their movement.

1.4.1 Changes in deep-sea marine microbenthos

The benthic foraminiferal extinction event (BEE) during the PETM was the most severe in over 90 Ma of Earth history and is crucial to the identification of the hyperthermal in deep-sea marine sections (Kennett and Stott, 1991; Thomas and Shackleton, 1996; Thomas, 1998). During the BEE, 40-60% of species of benthic foraminifera disappeared from the fossil record. It marks the swift transition from a Cretaceous Valasco-type fauna to a more ("modern") Eocene benthic foraminiferal fauna (Arreguin-Rodiguez *et al.,* 2018). The BEE is usually found before the onset of the CIE or at the peak of the PETM warming (Thomas, 2007). Contemporaneously, shallower water fauna also underwent rapid changes in composition as well as undergoing several extinctions (Alegret *et al.* 2009a, b; Aref and Youssef 2004; Thomas 1998; Littler *et al*., 2014; Giusberti *et al.,* 2016). It has been shown to be most severe at middle bathyal and greater ocean depths but was much less severe on the continental shelves (Gibson *et al.,* 1993; Speijer *et al.,* 2012; Stassen *et al.,* 2015). Throughout the CIE, the benthic foraminiferal fauna at all depths showed lower species richness and diversity and was composed mainly of small, thin-walled or agglutinated (non-calcareous) species (Thomas 2007). Detailed studies of the benthic foraminiferal extinction at the Alamedilla and Zumaia sections in Spain show that the extinction was rapid, but not ecologically instantaneous (Alegret *et al.,* 2009a, 2009b).

The cause of this global extinction of benthic foraminifera is not yet fully understood, but as stated above, increases in the corrosiveness of deep bottom water due to ocean acidification, increases in water temperature, ocean anoxia, and the associated changes in food supply, as well as ocean circulation, may have combined to cause these extinctions (McInerney and Wing, 2011). Some studies have shown that neither anoxia, higher or lower productivity, nor carbonate dissolution is recorded in all the PETM sections across the globe (e.g., Thomas, 2003, 2007; Alegret *et al*., 2010), and in the modern oceans, benthic foraminifera have been reported to be tolerant of some of these conditions (Alve and Goldstein, 2003, Giusberti *et al.,* 2016). It is most likely that the 5–8°C warming of the ocean is the cause of the extinction (Alegret *et al.,* 2009; Sluijs *et al.* 2007; Thomas 2007; Aze *et al.,* 2014; Frieling *et al.,* 2017). But how warming caused the extinctions is still under debate and another likely cause maybe fluctuation in organic matter supply to the ocean. Increased nutrient supply into the surface waters during PETM would increase the accumulation and degradation of organic matter on the sea floor,

causing depletion of pore water oxygenation and upward movements of the redox boundary (Thomas, 2007). Concentration of organic matter in the shallow sediment surface layers could have caused deoxygenation and localised anoxia, and could have caused the disappearance of deep trace makers, while those living in shallower substrates, close to the surface of the seafloor, with plentiful food available and in contact with oxic bottom waters, could have survived (Takeda and Kaiho, 2007). However, this seems to be inconsistent with the extinction of *G. becarriformis* which is an epifaunal species; its extinction could be related to the possession of bigger pores within the test and thus greater susceptibility to a reduced oxygen supply and carbonate dissolution (Giusberti *et al.,* 2016).

The composition of the benthic foraminiferal assemblages that survived were dominated by infaunal taxa, which survived the increased delivery of organic matter and other stresses at the seafloor (Alegret *et al.,* 2009). During carbonate dissolution in the water column, sediment pore waters may become highly saturated in carbonate (Ilyina and Zeebe, 2012), and the infaunal benthic foraminifera residing in the sediments can be shielded from these corrosive waters (Foster *et al.,* 2013), whereas epifaunal taxa are directly exposed to this dissolution, and so their tests may become damaged, and thus they are unable to calcify and survive under these conditions. Contrary to the significant extinction of benthic foraminifera, there is little or no extinction associated with other microbenthos such as ostracods on the sea floor during the PETM. Ostracods are another group of deep-sea benthic organisms studied across the PETM, though not in at the same level of detail as the foraminifera (Steineck and Thomas, 1996). The records of other microbenthos feedback to the PETM warming ranges from decreased diversity and abundance (Steineck and Thomas, 1996) to little or no significant change in the general occurrence (Webb *et al.,* 2009). More studies are needed to make the ostracod record across the PETM more robust, but so far, no extinctions within this fossil group have been reported. The study of ichnofacies at the Forada section in Italy have established that there was a decrease in ichnodiversity and ichnofossil abundance across the PETM (Guisberti *et al.,* 2016). This suggests that a deterioration of the environmental conditions for microbenthic communities occurred across the event at this section.

1.4.2 Impact of the PETM on planktonic foraminifera

The most common feature among the planktonic foraminifera across the PETM in both low and high latitude sections is the significant decrease in the relative abundance of the deep (thermocline) dwelling *Subbotina* and the conspicuous increase in *Acarinina* and *Morozovella* at the onset of the event (Lu and Keller, 1995b; Berggren and Ouda 2003; Berggren and

Pearson, 2005). During this period, planktonic foraminifera expanded their original territory. For instance, some tropical species of *Morozovella* were reported to have migrated to high latitudes just before and during the early part of the PETM (McInerney and Wing, 2011).

In general, the abundance of symbiont-bearing genera (*Acarinina* and *Morozovella*) and the reduction in populations of the non-symbiotic *Subbotina* genus from the PETM assemblage is evidence for persistent warming of the surface ocean and a nutrient depleted mixed layer. The abundance of heavily calcified symbiotic *Acarininids* shows that the surface water was highly productive and well foraged while the sudden appearance of tropical *Morozovella* at the onset of CIE in the subpolar region is evidence of high latitude warming that enabled warm water taxa initially restricted to the tropics to extend their biogeographic ranges into the polar oceans (Dunkley Jones *et al.,* 2013).

Changes in water column structure is another remarkable impact of the PETM in the oceans. The result from planktonic foraminiferal records has been used to interpret stratification of the water column in the pelagic zone. For instance, the stable isotope composition of *Morozovella* and *Acarinina* recovered from ODP site 690 (Maud Rise) indicate a shift into deeper water habitats due to the warming resulting from the PETM (Kelly, 2002). The Winguth *et al.* (2012) models of PETM ocean circulation support the changes in water column structure during this period. Also during greenhouse climates such as those of the early Eocene, when the SSTs were high, intense hurricane activity drives strong mixing in the upper layers of the tropical oceans (Korty *et al.,* 2008).

Other significant evolutionary changes were more or less localised, with each region reacting according to the prevailing conditions. Some of these changes include; increase in the body size of planktonic foraminifera due to an increase in nutrient supply (Kaiho *et al.,* 1996; Petrizzo, 2007). Increases in the test size of planktonic foraminifera could reflect the dominance of larger foraminifera with a greater capacity for photosymbionts over the less competitive asymbiotic species in well-grazed oligotrophic surface waters. Dwarfing of benthic foraminifera may have resulted from the effects of temperature, bottom water oxygenation and the low quality of organic matter reaching the ocean floor (Thomas, 2003). Alternatively, they may represent physiological changes as they adapted to the anoxic condition in bottom waters. Higher temperatures may also have increased food consumption and resulted in a food scarcity (Grigoratou *et al.,* 2018; Algret *et al.,* 2010). More so, increases in the rate of fragmentation and dissolution of planktonic foraminifera were reported in the Pacific Ocean

suggesting that ocean acidification may have been more severe in the region than it was in the Atlantic (Petrizzo, 2007).

Rapid diversification and morphological evolution of planktonic foraminifera have been observed across many PETM sections (Petrizzo *et al.,* 2017). These major morphological diversification are exhibited by *Acarinina africana, Acarinina sibiyaensis* and *Morozovella allisonensis* which are known as the 'excursion taxa' because they made their first and only appearance within the body of the CIE at the Pacific, Alamedilla (Spain) and Tanzanian (Africa) basins (Kelly, 2002; Pearson *et al.,* 2006; Aze *et al.,* 2014a). It is believed that these excursion taxa originated suddenly due to the extreme environmental changes within peripherally isolated populations ((Kelly, 2002)

1.4.3 Effect of PETM on the phytoplankton

Analyses of calcareous nannofossil community changes across the PETM showed that water temperature, nutrient availability and competition were the major factors that controlled phytoplankton distribution during the event (Schneider *et al.,* 2013). Some significant transformations occurred in the calcareous nannoplankton community including a change from ecologically restricted taxa to a more cosmopolitan community. For instance, before the PETM at Maud Rise (Southern Ocean), the calcareous nannofossil community was dominated by cool water taxa (*Chiasmolithus*), but with the increases in temperature during the PETM, warm water species (*Fasciculithus* and *Zygrhblitus*) migrated to high latitudes and subjugated the existing communities (Bralower, 2002). Perturbations of calcareous nannoplankton communities were reported to be most severe in the marginal seas, at coastal and high-latitudes sites compared with the open ocean, and the relative influence of water temperature and nutrient availability on the assemblage varies regionally (Gibbs *et al.,* 2006b). Calcareous nannoplankton that were more adaptable to oligotrophic conditions became more abundant at open ocean sites such as Shatsky Rise and Walvis Ridge (Bralower 2002, Gibbs *et al.,* 2006b; Tremolada and Bralower 2004). Only the nannoplankton taxa adapted to the warming conditions and their associated ecological modifications during these hyperthermals enabled them to survive beyond the CIE, whereas the less resilient taxa were reported to have disappeared (Schneider *et al.,* 2013). In the mid-latitudes, nutrient supply played a greater role in shaping the community structure than water temperatures because the major changes recorded were the increases in *Sphenolithus* which is associated with warm oligotrophic environments (Schneider *et al.,* 2013). Some local extinctions of calcareous nannofossil species have been reported to occur at the onset of the CIE and the high abundance occurring at the

peak of the event, however, these changes have not been documented globally (Ma *et al.,* 2014). The impact of the PETM on calcareous nannoplankton shows that even though some species were able to adapt to the environmental changes, the community structure remained completely altered after the conditions returned to the pre-CIE state. The changes caused by PETM persisted for about 500 kyr into the Eocene, and this suggests that the phytoplankton community in the modern ocean may be permanently altered with the current change in climate (Gibbs *et al.,* 2006).

Another significant biotic signature during the PETM was the global dominance of the dinoflagellate taxa *Apectodinium* (Sluijs *et al.* 2014). This taxon was largely restricted to low latitudes during the late Paleocene but migrated to the polar latitudes in both hemispheres during the PETM (Sluijs 2007). Dinoflagellates are sensitive to physiochemical variations in the surface waters such as salinity, temperature, nutrient availability and stratification (Fensome *et al.,* 1996; Sluijs 2007, 2014). The *Apectodinium* acme appears to be associated with both increased temperatures and nutrients; hence, in many samples from across the PETM, their relative abundances exceeded 40% of the total dinocysts recovered. It is believed that *Apectodinium* was able to spread to higher latitudes because of the changing temperatures and higher nutrient levels produced by the PETM climate feedbacks (Sluijs *et al*., 2007; McInerney and Wing, 2011).

1.5 Continental configuration and ocean circulation during the PETM

Continental arrangement in the late Paleocene-early Eocene was to modern day configuration, with some notable exceptions, such as India and Australia being further south than they are now (Figure 1.5) and there was also a transcontinental seaway from central Asia through to the Arctic Ocean called the Tethys Ocean. The Tethys Ocean comprised the current Atlantic and Indian Oceans the Mediterranean and the Middle East (Figure 1.5). Tectonic upheaval driven by the igneous activity in the North Atlantic region resulted in changes in the ocean circulation and the global climate. Evidence of marine transgressions during the PETM (Sluijs *et al*., 2008; Handley *et al*., 2011; Winguth, 2011) have been linked to changes in the rate of seafloor spreading, volcanism, regional perturbations as well as changes in ocean circulation. Increase in precipitation resulting from rises in surface temperatures triggered: the freshening of the sea surface, changes in vertical ocean density gradients and stratification of the deep sea (Handley *et al.,* 2012).

Zeebe and Zachos (2007) inferred that ocean circulation changed based on the concentration of deep-sea carbonate ions [$CO^2_3{}^-$] measured from bulk sediment during the PETM. They

compared this proxy data with the results from the Ocean Earth System Model to show that carbonate ion dissolution intervals increased from the Atlantic through the Southern Ocean into the Pacific. This suggests there was a significant reversal relative to the current thermohaline circulation of the modern ocean. Abrupt changes in deep water circulation from a mostly Southern Hemisphere to Northern Hemisphere overturning (Figure 1.4) is believed to have pushed warmer waters into the deep sea which triggered further warming. This change in deep water circulation is estimated to have lasted for more than 40,000 years before returning to the original circulation pattern (Nunes and Noris, 2006). The distribution of carbonate ions in the modern ocean is mostly controlled by deep water circulation and vertical fluxes of carbon and alkalinity due to the biological pump. The release of greenhouse gases that caused the PETM may have contributed to the reversal of this biological-carbon cycle gradient. Dickens (2000) box model showed that the dissociation and oxidation of methane hydrates in the deep Atlantic Ocean would lead to greater shoaling of the lysocline and CCD in the Atlantic, as was the case at the Walvis Ridge (Zachos, 2008), compared to the Pacific. This implies that the location of the source of the PETM carbon in the Atlantic Ocean was the major cause of the reversal as indicated by Zeebe and Zachos (2007).

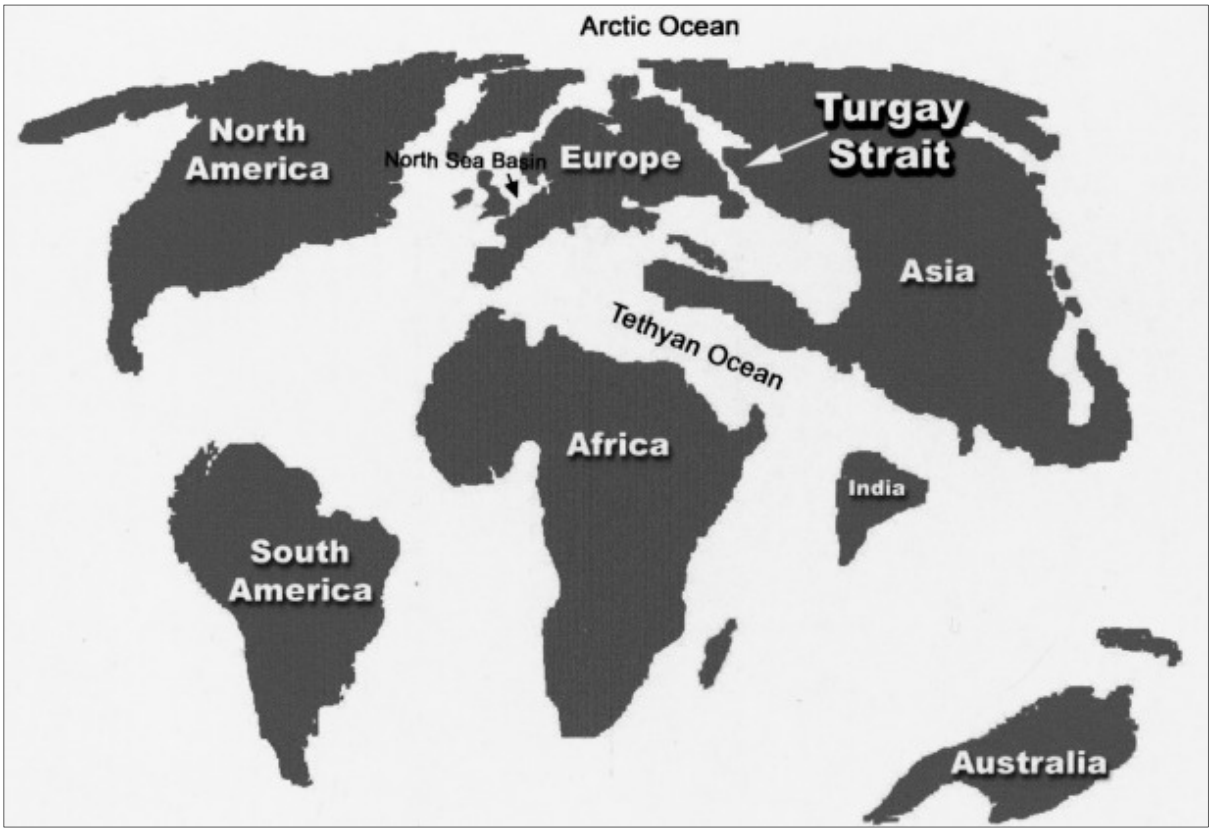

Figure 1.4: Late Palaeocene-Early Eocene palaeogeography showing the main landmasses and marginal seas, and the Turgay Strait connecting the Arctic and Tethyan oceans (Taken from Iakovleva et al., 2001)

Feedbacks from the increased carbon dioxide forcing in the ocean reduced the ventilation of the deep sea and increased significantly, especially at high latitudes, the age of water masses at intermediate depth (Abbott *et al.,* 2016). This intermediate and deep water mass warming resulted in positive feedbacks on ocean circulation (Bice and Marotzke, 2002). The feedback loop associated with the rise in global temperatures and sea level would have also led to an enhanced influx of fresh water from the Arctic Ocean enhancing the changes in global circulation patterns (Winguth, 2011). Evidence from dinoflagellate cysts (Iakovleva *et al.,* 2001) confirms this increase in freshwater inflow through the Turgay Strait - the passage between the Arctic and Tethyan Oceans in the late Palaeocene (Figure 1.5). Also, Nd-Sr isotopes in fish fossils (Gleason *et al.,* 2000; Abbott *et al.,* 2016) suggest that the higher sea levels might have allowed a connection between the Fram and Bering Straits. Consequently, the influx of fresh water from the Arctic Ocean into the North Pacific would have produced an increase in vertical density gradients by reducing the density of the North Pacific intermediate water masses by 2.5Sv at 30°N and would have corresponded to an increase in the Pacific deep-sea circulation (Winguth, 2011).

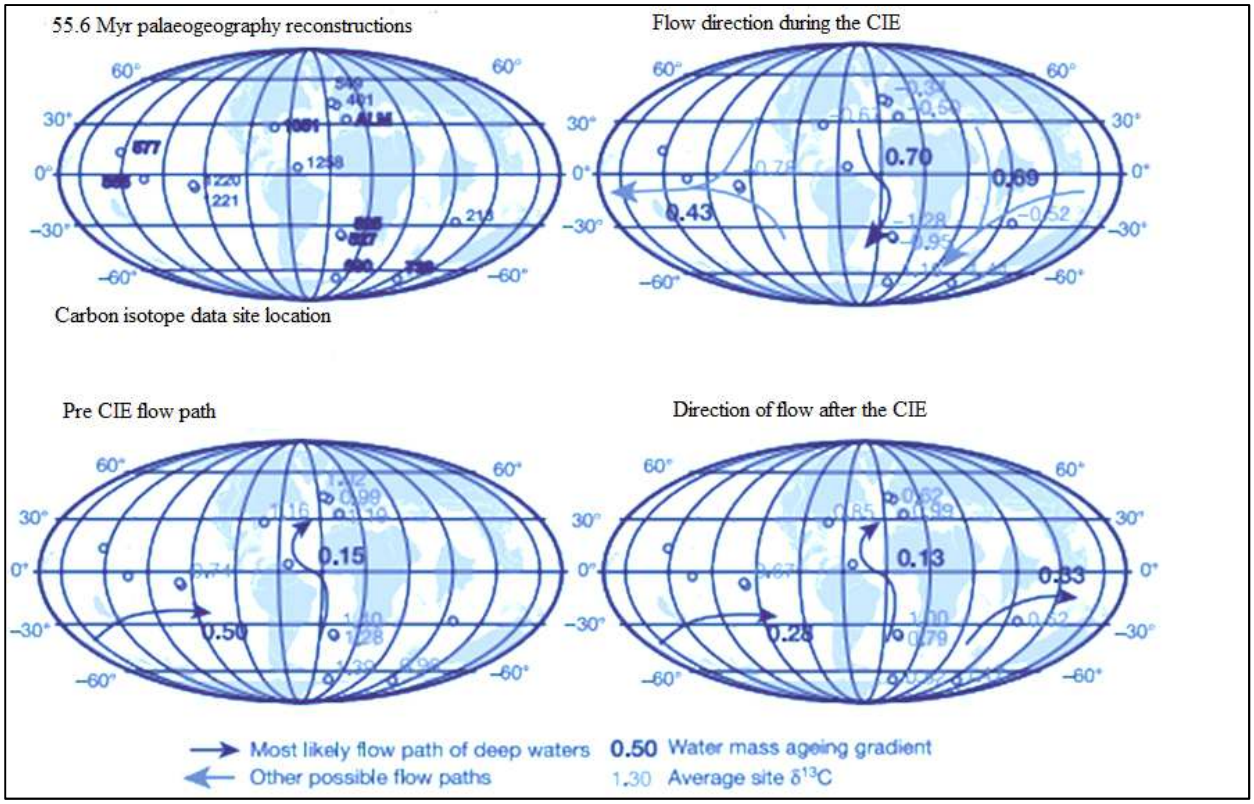

Figure 1.5: Inferred flow paths of global deep water during the PETM based on benthic foraminifera and bulk sediment carbon isotopes. The flow directions of deep water during different intervals of the PETM are represented by arrows. Deepwater originated from the Southern Ocean during both the pre and post-CIE period while the source changed to the Northern hemisphere during the core period of the CIE (Source: Nunes and Noris, 2006).

1.6 Foraminifera

Foraminifera are unicellular marine protozoans with calcareous shells usually subdivided into chambers. They are classified as eukaryotes, i.e. organisms whose cytoplasm is organised into a complex structure with internal membranes containing a nucleus, mitochondria, ribosomes and Golgi bodies (Figure 1.6). Benthic foraminifera appeared in the geologic record in the Cambrian (524 million years ago) while it is suggested that their planktonic counterparts evolved from a benthic ancestor during the Early-Middle Jurassic (170 Ma; Schiebel *et al*., 2018).

Foraminifera usually produce a shell, also known as a test, which can have one or more chambers. The test could be made of organic matter, mineral substances, or agglutinated particles. The chambers increase in number during growth and may have one or several apertures/foramina (a term from which the name of the group is derived), that allow the chambers to communicate within the organism as well as the surrounding environment (Bellier *et al.,* 2010).

When alive, foraminifera are endowed with extraskeletal (organic) projection known as pseudopodia and rhizopodial which is a web-like granular filament formed into network or a filapodia. The cytoplasm emerges from these outer orifices, covers more or less the test, and emits fine and reticulated pseudopodia with which the microorganism fixes itself on the substratum, moves, and captures its food. Naked forms –i.e. foraminifera without hard parts have been previously reported, (Pawlowski, 2000) but such forms are absent in the fossil record due to their inability to be preserved in the sediment.

A fully developed foraminiferal test ranges from 100 micrometres to almost 20 centimetres long in diameter (Henehan *et al.,* 2017). Both the microscopic and exceptionally large foraminifera are single-celled irrespective of their sizes. Because foraminifera could be large with only one cell, they could face the problem of sustaining the surface/volume ratio. And this is where the reticulopodia, an extremely efficient and multifunctional organelle, come into play. The reticulopodia not only provide the surface for respiration but also perform critical functions like feeding, locomotion, test building and metabolite release (Hottinger, 2006). The thickness of these cytoplasmic threads (reticulopodia) ranges from less than 1µm across to more than 25 times the diameter of the entire test.

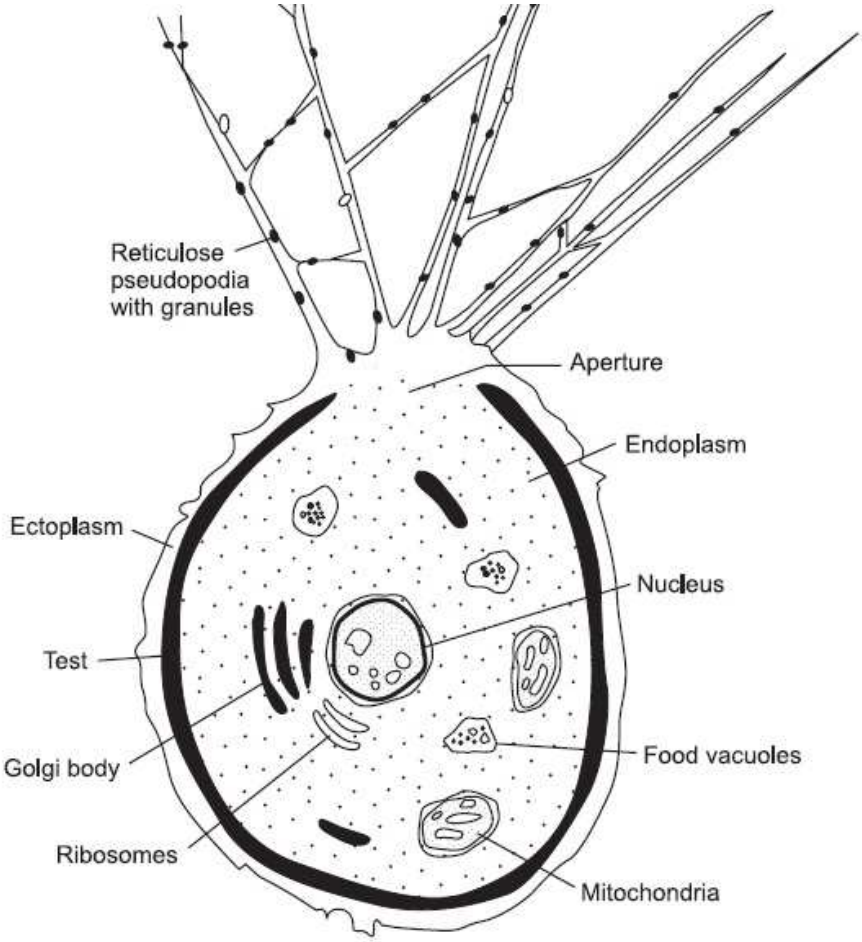

Figure 1.6. Cross section of the benthic foraminiferal cell (Taken from https://paleonerdish.wordpress.com)

1.6.1 Benthic foraminifera

Benthic foraminifera dwell in all benthic marine environments, living either above, at or below the sediment-water interface in water depths ranging from the intertidal zone to the deep ocean (Holbourn *et al.,* 2013). In the deep sea, benthic foraminifera represent the most important contributors to the micro-faunal biomass, and their distribution is intricately linked to the flux of particulate organic matter from the upper ocean to the sea floor (Jorissen *et al.,* 2007). Even though foraminifera predominantly live in the marine environment, few benthic species have been reported in terrestrial environments such as lagoon, freshwater ponds, rivers and groundwater (e.g. Murray, 1991; Goldstein, 1999; Bellier *et al.,* 2010 and Kitazato and Bernhard, 2014).

1.6.1.1 Classification

Foraminiferal classification has been heavily investigated and continued to evolve from the first description of *Ammonia* in 1772 to present as new information is gathered (Murray, 2006). The widely used classification of foraminifera is that of Loeblich and Tappan (1992) for the calcareous taxa and Kamiski (2004) for the agglutinated taxa. Pawlowski *et al.* (2013) invested some time updating the classification based on the genetic composition. In general, benthic foraminifera is classified as follows (Adl *et al.,* 2005)

Domain: Eukaryota

Kingdom: Protista

Subphylum: Sarcodina

Superclass: Rhizopoda

Class: Granuloreticulosea

Order: Foraminiferida

There are 14 orders, four suborders, 84 superfamilies, 315 families, 326 subfamilies, 213 genera (Loeblich and Tappan, 1992) and thousands of species which cannot be completely elucidated because scientists keep describing new species every day. The basis for foraminiferal classification is hinged on the diverse and well-known features of the test (Murray, 2006). Evolutionary trends in foraminifera are represented as the modification of the most basic feature of the test, its chemical composition, ultrastructure and mode of formation. Test shape could be elongate, spiral, globose, tubular, arborescent, lenticular, conical, flabelliform, fusiform or discoidal (Loeblich and Tappan, 1992).

Features such as agglutinated or secreted hyaline tests and perforate or imperforate walls are the major characteristics used in the classification of foraminifera over the years (Murray, 2006). Other important attributes used for classification include the genetic composition (Pawlowski *et al*. 2013), nature of the cement in agglutinated tests (Loeblich and Tappan, 1992), mode of wall formation for test enlargement (Loeblich and Tappan, 1992), percentage calcitic or aragonitic composition of hyaline tests and the orientation of their crystals (Loeblich and Tappan, 1992). Features like the type of inter-and-intra-cameral partitions and intercameral (a single or multiple opening in a chamber wall that allow the communication of a main chamber lumen with the ambient environment) sutures could also play some roles in the classification (Hottinger, 2006).

As stated earlier in section 1.6 above, a foraminiferal test can be agglutinated, porcellanous, secreted hyaline, microgranular or made entirely of organic matter. The agglutinated test are made of foreign materials (quartz grains, sponge spicules, broken test from other foraminifers, etc.) picked on the sea floor and glued to the chitinous or calcareous cement secreted by the organism (Holbourn *et al.,* 2013). The porcellanous test is common in Milolida order and is composed of calcite secreted by the organism. The surface of the test under the light microscope is imperforate, smooth and homogeneous with a sparkling white or amber appearance similar to porcelain (Murray, 2006). The hyaline test composition is also made up of radially symmetric secreted calcite or aragonite. The tests are lamellar, layered with compound wall structure and generally perforate (Holbourn *et al.,* 2013). Most of the wall microstructure described above was identified using a thin section or scanning electron microscopy; however, it could be difficult to differentiate all these test structures under light or stereomicroscope used in the laboratory.

Foraminiferal wall structure appears to have evolutionary and adaptive significance. The first foraminiferal hard part that appeared in the fossil record was the agglutinated test (Figure 1.7; Ohtsuka *et al.*, 2015). The adaptive success of this type of wall structure is shown by their abundance at all depths. Notably, non-calcareous members of this group dominate extreme environments such as the abyssal plain below the calcium carbonate compensation depth (CCD), in silled basins and marginal marine environments with lowered oxygen and salinity (Sen Gupta, 1999). Foraminifera found in normal marine environments are characterised by lighter secreted calcite and a more anatomically complex shell (Kitazato and Bernhard, 2014). The evolution of this type of wall was clearly a factor in the development of broad floating chambers and the invasion of the pelagic realm by the planktonic species later in the geologic record (Ohtsuka *et al.*, 2015).

The hyaline wall with radial structures has an adaptive advantage towards the depth limit of the phototrophic zone, and it is significant that the large Rotaliids and planktonic foraminifera are all radial (Sen Gupta, 1999). Some families such as Cassidulinidae, Chilostmellidae, Nonionidae, and Pleurostomellidae are reported to thrive in cool deep water (Haynes, 1982).

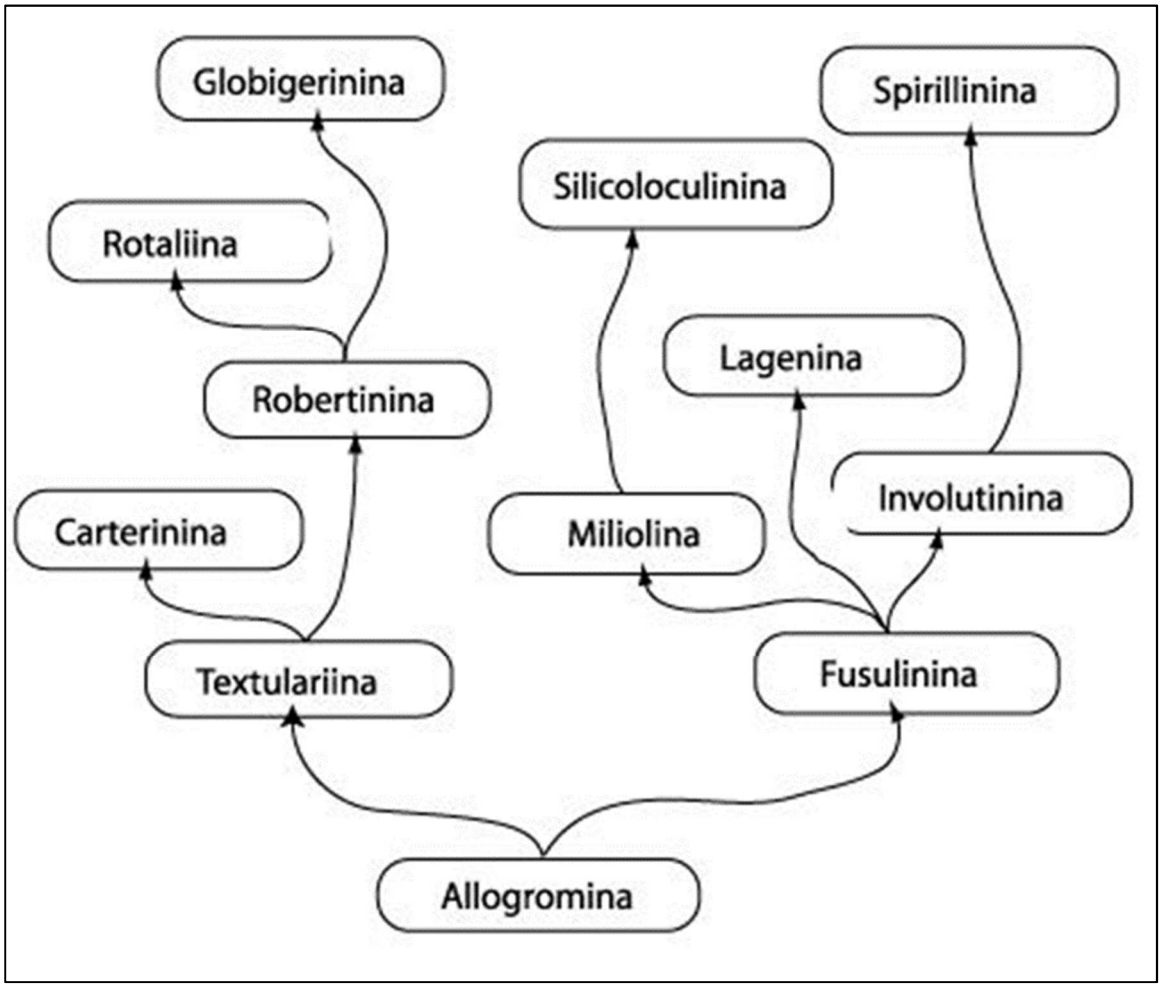

Figure 1.7: A generalised order of foraminiferal evolution with the oldest at the base and youngest at the top. Taken from (http://www.ucl.ac.uk/GeolSci/micropal/foram.html)

Nevertheless, groups with the porcellanous test are particularly abundant in shallow water, especially on the inner shelf of the tropical waters, open bays and lagoons (Murray, 1991). These distributions suggest that porcellanous structure may give a protective advantage and the crystal arrangement is helpful to scatter short wavelength and ultraviolet (UV) light in the upper water column (Murray, 1991).

1.6.1.2 Ecology of benthic foraminifera

The ecology of benthic foraminifera is dependent on the physiochemical conditions of their environment. It encompasses the interaction between individuals and their environment, the interaction between species as well as the interaction between other members of the community in the ecosystem (Murray, 1991). The environmental conditions, such as water depth, temperature, dissolved oxygen availability, salinity; *pH*, quality and quantity of food materials, nature of the substrate, total organic matter, competition, predation as well as the calcium carbonate concentration are major factors in the distribution of benthic foraminifera

Foraminiferal niche is a bit difficult to conceptualise, this is because despite the amount of research done on the topic, very little is known about the real niche of any group of foraminifera from any locality in the world (Murray, 2006). Each species has its unique niche; however, many foraminifera are opportunistic and great survivors; they exist in small numbers for long periods when conditions are far from optimal, but they rapidly increase their numbers when conditions change in their favour (Gooday, 1992). There is a need to differentiate the ecospace where a species could potentially exist and where the species does. In as much as it is convenient to think of niche operating at the scale of species distribution, in reality, it operates on very local patches and even at the scale of the individual (Murray, 2000) where they may be small but significant differences in the values of factors associated with patch scale variability in the environment.

Benthic foraminiferal niches range from taxa living within the upper 15cm of the sediment, those living on the sediment surface and others clinging to the substrate such as grass, rocks or the body of larger organisms. This has led to the classification of foraminiferal microhabitat in the ocean as epifaunal, shallow infaunal and deep infaunal (Figure 1.8).

Epifaunal species are those that live on or above the sediment surface. They are mostly suspension feeders and are good indicators of bottom water current transporting the suspended organic carbon. Shallow infaunal species live partly below and relatively above the sediment surface and are mostly deposit feeders (Murray, 1991). Most of the shallow infaunal species are opportunistic and are over-represented in the faunal record (Jorissen *et al.,* 2007). They are hugely influenced by pore water chemistry and are deposit feeders that tolerate low-quality organic matter as well as low oxygen concentration. The deep infaunal species live inside the sediment within the zone of maximum nitrate concentration.

Jorissen *et al.* (1995) have proposed trophic conditions and oxygen concentrations (TROX) Model of benthic foraminifera ecology, where they considered critical oxygen level and quantity/nature of available food particles as the major factors that determined foraminiferal microenvironment (Figure 1.9).

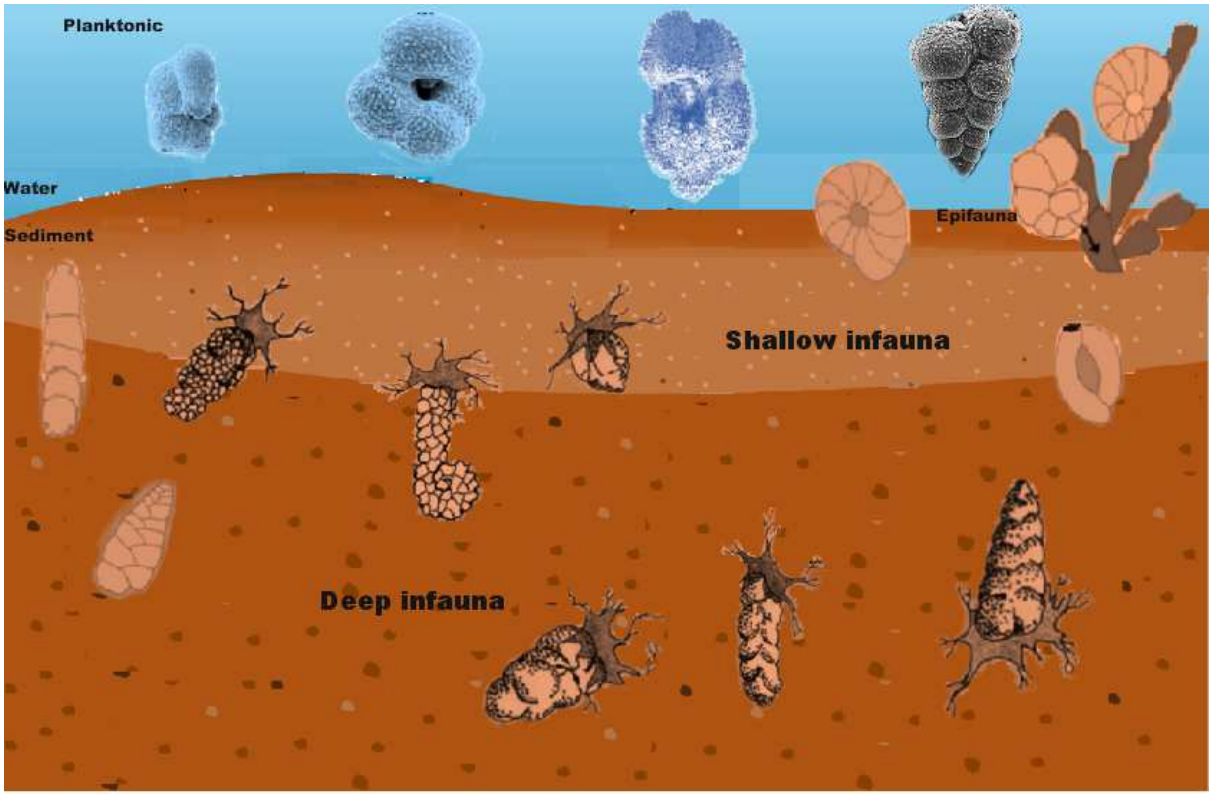

Figure1. 8: Schematic representation of foraminiferal niches in the marine environment. The cartoon represents a hypothetical foraminiferal ecology from the sea surface to deep sediments.

The model indicates that the depth of foraminiferal microhabitat in an oligotrophic ecosystem is restricted by the availability of the required nutrient within the sediment, whereas in eutrophic systems, a critical oxygen level decides what depth down the sediment most species can survive. Therefore, the quality of organic carbon reaching the niche is a major controlling ecological parameter. For instance, in the area where there is an input of large quality of organic matter, deep infaunal species abundance supersedes epifaunal species (Fontanier *et al.,* 2005). Some foraminifera are believed to adopt anaerobic pathways in organic matter remineralisation and as well respire nitrogen dioxide in the absence of oxygen (Keating-Bitonti and Payne, 2017).

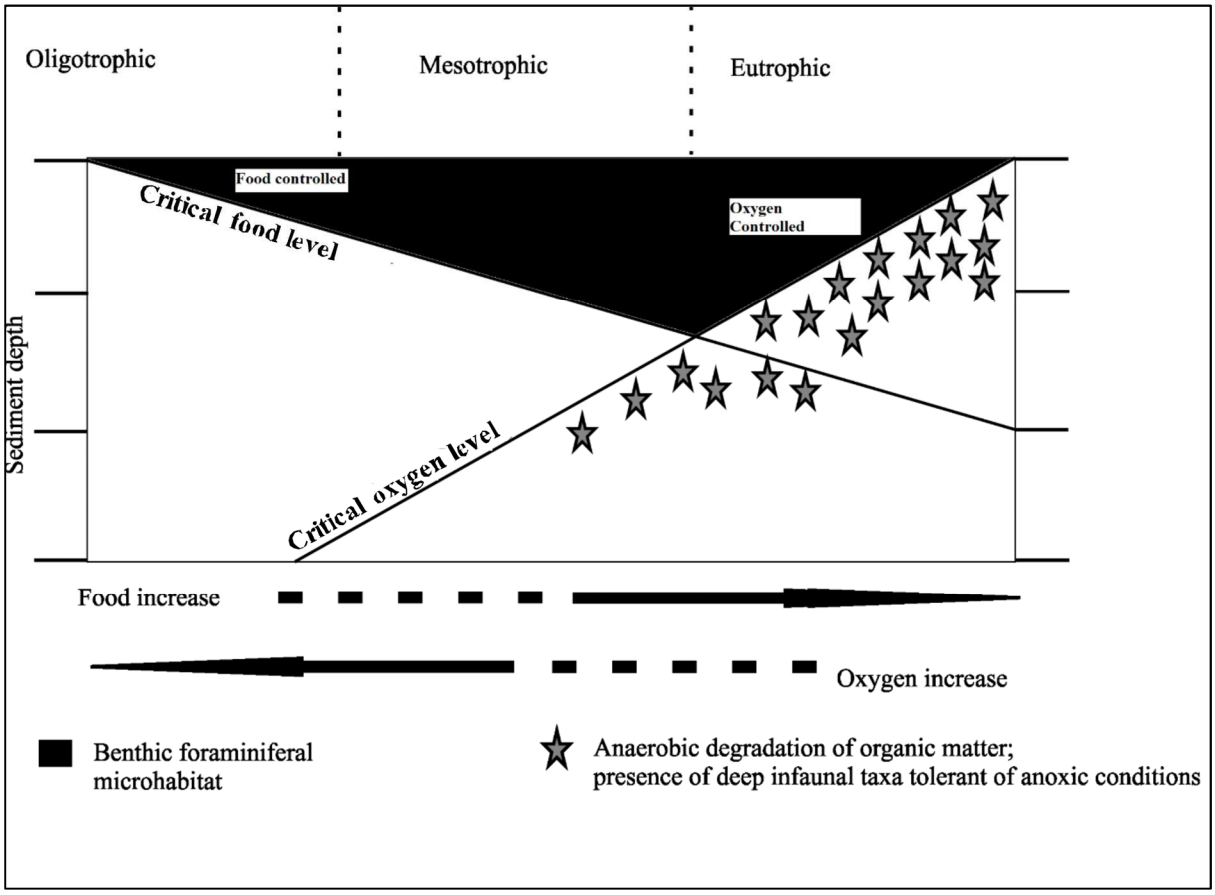

Figure 1.9: The TROX model indicating the critical limit for oxygen and nutrient supply in foraminiferal microhabitat. Living depth of foraminifera is controlled by the quality of food material in the bottom sediment during the oligotrophic condition. However, oxygen is the main factor in eutrophic ecosystems. The amount of oxygen available within the deep infauna microhabitat is believed to not be a limiting factor in this model because foraminifera adopt anaerobic pathways in organic matter remineralisation and respiration (redrawn from Jorissen et al., 1995)

The ecology of foraminifera is well studied, but it is still relatively complex because field data of living foraminifera is limited to where current technology can access and monitor, and laboratories studies are limited to few controlling factors that differ from the prevailing condition in the natural world. Some of the species believed to be totally infaunal may migrate to the surface sediment when the conditions deep down the sediment become unfavourable (Jorissen *et al*., 2007).

1.6.2 Planktonic foraminifera

Planktonic foraminifera live in the euphotic zone of the ocean during lifetime and some live deeper down to approximately 2km (Schiebel and Hemleben, 2017). Their tests that are made of relatively globular chambers (though some families like Chiloguembelinidae, Globanomalidae and others have different chamber arrangement) are essential to buoyancy, and this enables them to float freely with the water column (Schiebel and Hemleben, 2017). Some species are spinose while others are not. Planktonic foraminifera especially the spinose

taxa are known to harbour algae such as dinoflagellate and chrysophycophyte as symbionts. Modern species such as *G. sacculifer* sometimes show remarkable yellowish-brown colouration due to the presence of numerous dinoflagellates within the rhizopodial system and in the internal cytoplasm. Non-spinose species such as *Globigerinita glutinata*, *Neogloboquadrina dutertrei, Pulleniatina obliquiloculata, Globorotalia inflata,* and *Globorotalia menardii* are believed to have symbionts which are capable of photosynthesising (Hemleben *et al*., 1989). The symbionts play a significant role in gas exchange, metabolism and calcification in planktonic foraminifera and also affect the carbon stable isotope composition of the test.

The majority of planktonic foraminifers are omnivorous. The feed on varieties of food including animal, organic matter, and plant materials (Hemleben *et al.,* 1989). Spinose species are reported to show preference to animal prey such as phytoplankton and zooplankton as well as other larger metazoans such as copepods, pteropods, and ostracods (Rhumbler 1911; Caron and Bé 1984; Spindler *et al.,* 1984). Non-spinose are predominantly herbivores but are also known to prey on smaller animals like diatoms, dinoflagellates, thecate algae (Schiebel and Hemleben, 2017). Deeper dwelling taxa widely depend on sinking organic matter for food and are good indicators of vertical flux of particulate organic matter especially in tropical to sub-tropical oceans (Itou *et al.,* 2001). Cannibalism in planktonic foraminifera has been reported, but little is known about this feeding mode.

The global and local abundance and diversity of planktonic foraminifera across the water column reflect the temporal and spatial distribution of food/nutrient material in the ocean because nutrient availability is directly related to growth and development of the organism. Taxa capable of feeding on a wide range of food material and effectively assimilating them are more likely to survive in different climatic conditions and during environmental change. The highest diversity of planktonic foraminifera are found in the oligotrophic subtropical gyres where ecological and biological factors are most conducive (Schiebel and Hemleben, 2017).

1.6.2.1 Classification

The most recent classification of planktonic foraminifera (Schiebel and Hemleben, 2017) shows that the organism belongs to

Kingdom: Protozoa

Subkingdom: Biciliata

Infrakingdom: Rhizaria

Phylum: Sarcomastigophora

Subphylum: Sarcodina

Superclass: Rhizopodea

Class: Granuloreticulosa

Order: Foraminiferida

Suborder: Globigerinina

The classification of planktonic foraminifera is based on the morphological concept of species. The genealogy of planktonic foraminifera show that they evolved with a simple trochospiral morphology and microperforate structure from benthic species in the early Jurassic (Schiebel and Hemleben, 2017) and have continued to develop until the present day. Test morphology such as test surface structure and ornamentations such as spinose, non-spinose, normal perforate and microperforate are very important in the planktonic foraminifera classification. Other features used for classification include pore size, and position of the primary, and secondary apertures, mode of coiling, the shape of test and chambers, position and shape of apertures (e.g., lip and rim), and shell texture (e.g., spines and pustules)

About 48 morphological groups of planktonic foraminifera are currently described. The morpho-groups are classified into taxonomic groups as follows (a) spinose (all Globigerinoidea), (b) non-spinose normal perforate or macroperforate (all Globorotaloidea and their ancestors), (c) non-spinose microperforate (Heterohelicoidea), (d) monolamellar Hastigerinidaespecies, (e) all microperforate species including Tenuitellids and Heterohelicoidea. Three superfamilies are reported to be extant; these include Heterohelicoiddea, Globigerinoidea and Globorotaliodea. The detailed foraminifera classification based on the test morphology is shown in figure 1.10

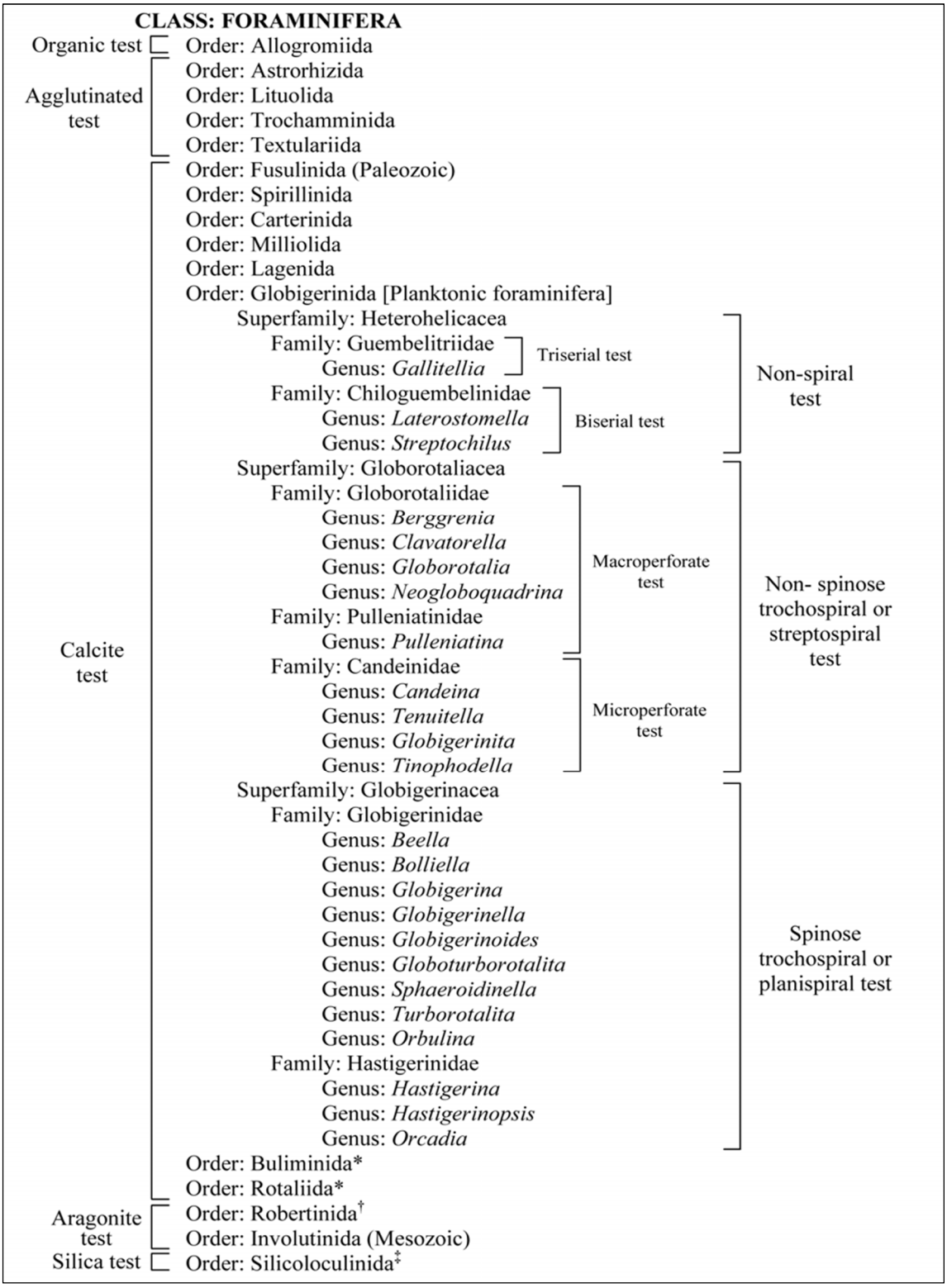

Figure 1. 10: Foraminifera classification based on the test morphology. Taken from Seears (2011)

1.6.2.2 Ecology of planktonic foraminifera

The ecology of planktonic foraminifera is not as distinct or definitive as the benthic foraminifera because of the dynamics of the pelagic environment caused by changes in the

physical and biotic condition of the ocean. The spatial and temporal distribution of planktonic foraminifera in the water column is controlled by hydrology, nutrient availability, primary production, turbidity, temperature and salinity. Planktonic foraminifera occur in highest abundance and diversity in the subtropical and temperate oceans as well as in the marginal upwelling zones (Peters *et al.,* 2013). The abundance of planktonic foraminifera is equally high in the Polar Regions (Figure 1.11) but are limited to very few major species.

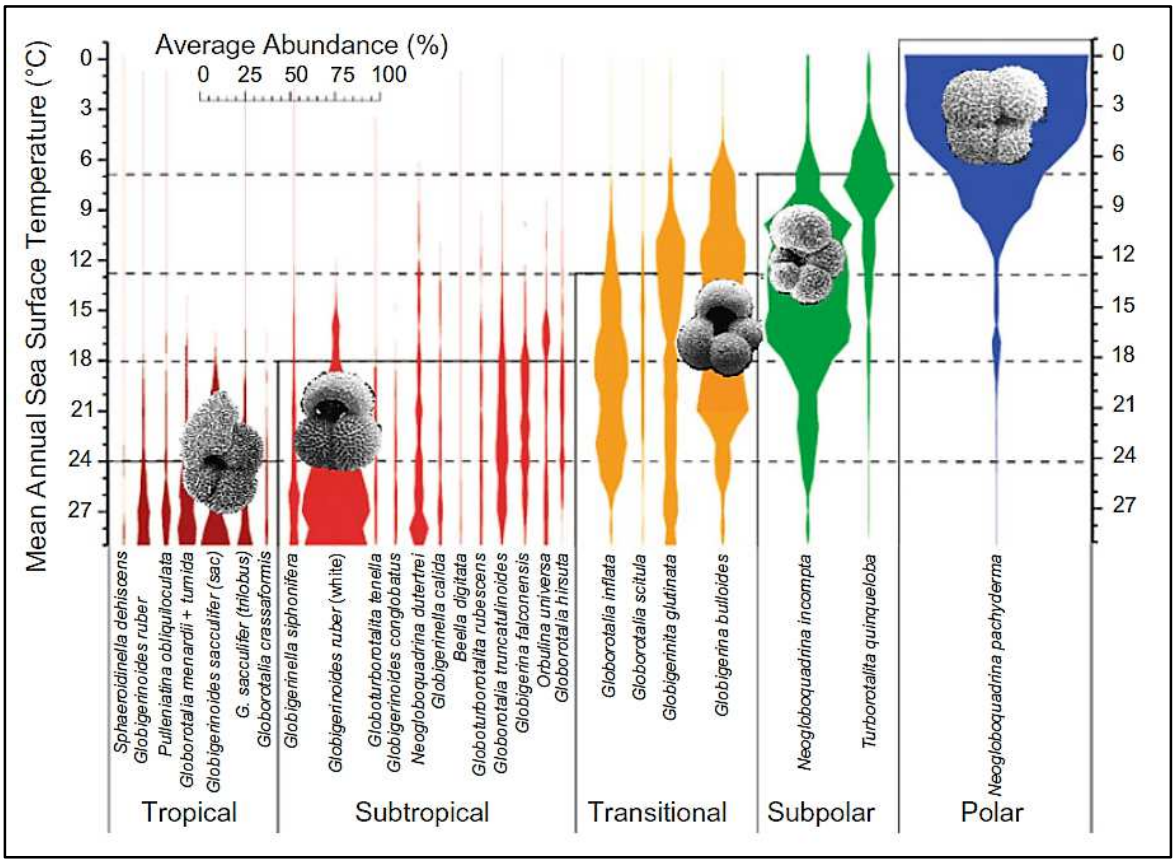

Figure 1.11: The distribution of planktonic foraminifer species across the global ocean based on mean annual temperature. The bar above represents the proportions of major species found in each region from plankton tow and surface-sediment data. Taken from Schiebel and Hemleben (2017)

The symbiont bearing species thrive better in lower latitudes and clear oligotrophic water especially in subtropical gyres where their prey (such as copepods and other zooplankton) predominate (Hemleben *et al.,* 1989). In contrast, non-spinose and symbiont barren species are more prevalent in turbid eutrophic waters such as upwelling regions where they feed on large quantities of phytoplankton (Schiebel and Hemleben, 2017).

The distribution of the intermediate and deep dwelling planktonic foraminifera are not clearly understood as those of the shallow dwelling species.

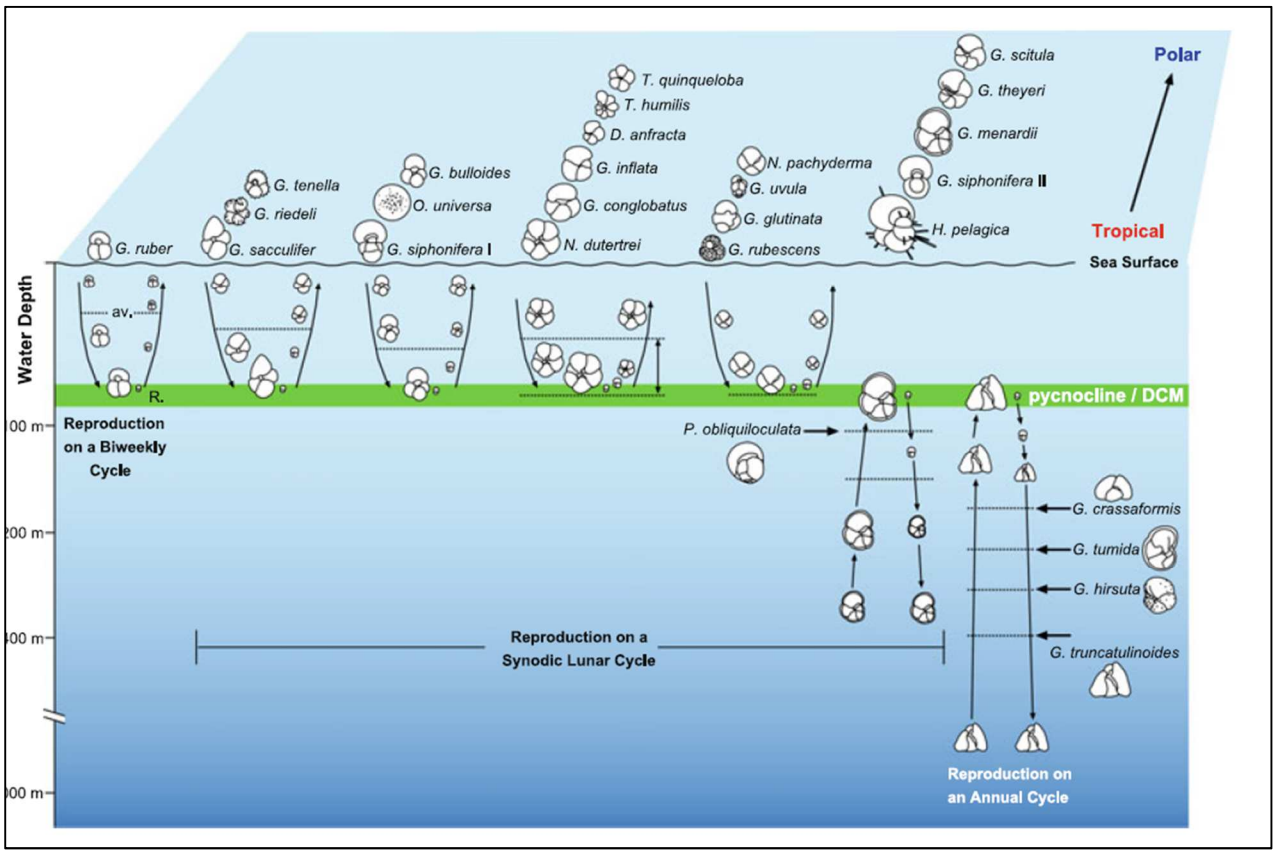

Figure 1.12: Schematic representation of planktonic foraminifera vertical depths habitats. The grey line separates the species that live on top of the water column until the pycnocline while the green line separate the species that live in the intermediate – deeper depths. The species arranged at the top of the figure represent their distribution across latitudes, tropics at the base and Polar Regions on top. Also shown are the reproduction depths (biweekly and synodic lunar cycles) of species as they move down the water column during ontogeny. Taken from Schiebel and Hemleben (2017)

The intermediate and deeper water habitat are more ecologically uniform than the surface waters, though robust planktonic foraminifers' data are not available. The major driver of planktonic foraminiferal distribution in the intermediate -deep water is quality and quantity of food. Nevertheless, due to their slow reaction to changing ecological conditions, deep-water dwellers are good indicator of changes in water masses (e.g. Berger 1970b).

The distribution of planktonic foraminifera in the water column is hypothetical, as it is believed to be controlled by various factors such as the need for sunlight, ontogenetic and reproduction

stages, food distribution and water mixing (Schiebel and Hemleben, 2017). The vertical distribution of modern planktonic foraminifera show that species such as *Globigerinoides ruber, Globoturborotalita tenella, Globigerina bulloides, Globorotalia inflata, Neogloboquadrina pachyderma* and *Hastigerina pelagica* live in the upper water column above the pycnocline while *Globorotalia truncatulinoides, Globorotalia hirsute, Globorotalia tumida* live deeper below the pycnocline (Figure 1.12)

In the Eocene, symbiont bearing planktonic foraminifera such as *Morozovella, Igorina*, and *Acarinina* lived in the warm surface waters. *Chiguembelina, Zeauvigerina* and *Pseudohastigerina* presumably lived in the intermediate zone while non-spinose and symbiont barren species like *Subbottina, parasubbotina, Globanomalia*, *Globorotaloide* and *planorotalites* lived in the deeper cold water (Luciani *et al.,* 2007). The understanding of the depth habitat and distribution of planktonic foraminifera in the water column is critical for the reconstruction of palaeoceanographic parameters such as temperature and productivity.

1.7 Use of foraminiferal assemblage technique in interpreting palaeoecological and palaeoceanographic conditions

Foraminifera are very useful to palaeontologists and palaeoclimatologists in academia and industry as powerful tools in relative age determination (biostratigraphy and chronostratigraphy), correlation of strata from one location to another and for palaeoenvironmental reconstruction. Because planktonic species are free floating in the upper water column and benthic foraminifera live in the bottom sediments, they are very useful for reconstructing simultaneously, the character of the upper water column and conditions at the seafloor. Information from foraminiferal assemblages studied as palaeobiological communities are very useful in understanding the ancient ocean-climate system, depositional environment, biotic response to global change, as well as patterns of evolution (e.g. Petrizzo, 2007; Luciani *et al*., 2010; Thomas, 2007; Gooday and Jorissen, 2012; Schmidt *et al.,* 2018). In addition, the geochemical content of their shells can be analysed to provide different types of proxies (indirect evidence) of palaeoceanographic conditions (Katz *et al.,* 2010; Schiebel *et al*., 2018). The use of foraminiferal assemblage for palaeoceanographic parameters varies from their application to interpreting depth stratification, palaeo-oxygenation and palaeo-productivity (Jorissen *et al.,* 2007).

Foraminiferal assemblage attributes have also been used to reconstruct bottom water temperatures and salinity in the open ocean environment based on the distribution patterns of marker species. It is very efficient in the shallow and coastal waters where strong temperature

and salinity gradients exist. For example, productivity and oxygen concentration can be inferred based on the assemblage composition of foraminifera (Figure 1.13). Low oxygen environments are dominated by Bolivinids, Buliminids, and some other biserial taxa (D'haenens *et al.* 2012; Frenzel, 2000) while environments with high oxygen content are dominated by taxa such *as Cibicidoides, Gyroidinoides, Oridorsalis, Anomalinoides* etc. (Schmiedl *et al.,* 2003; Kuhnt *et al.,* 2007; Gupta and Thomas, 2003)

Also, the number of foraminiferal traits has been combined with assemblage information to interpret palaeoecology. For instance, a close relationship between morphology in planktonic foraminiferal and environmental parameters has repeatedly been demonstrated both in the fossil record and in the modern ocean (Schiebel and Hemleben, 2017). Vertical habitat separation is reflected in the morphological stratification of the planktonic foraminiferal ecosystem within the top hundreds of metres of the water column (Hemleben *et al.,* 1989).

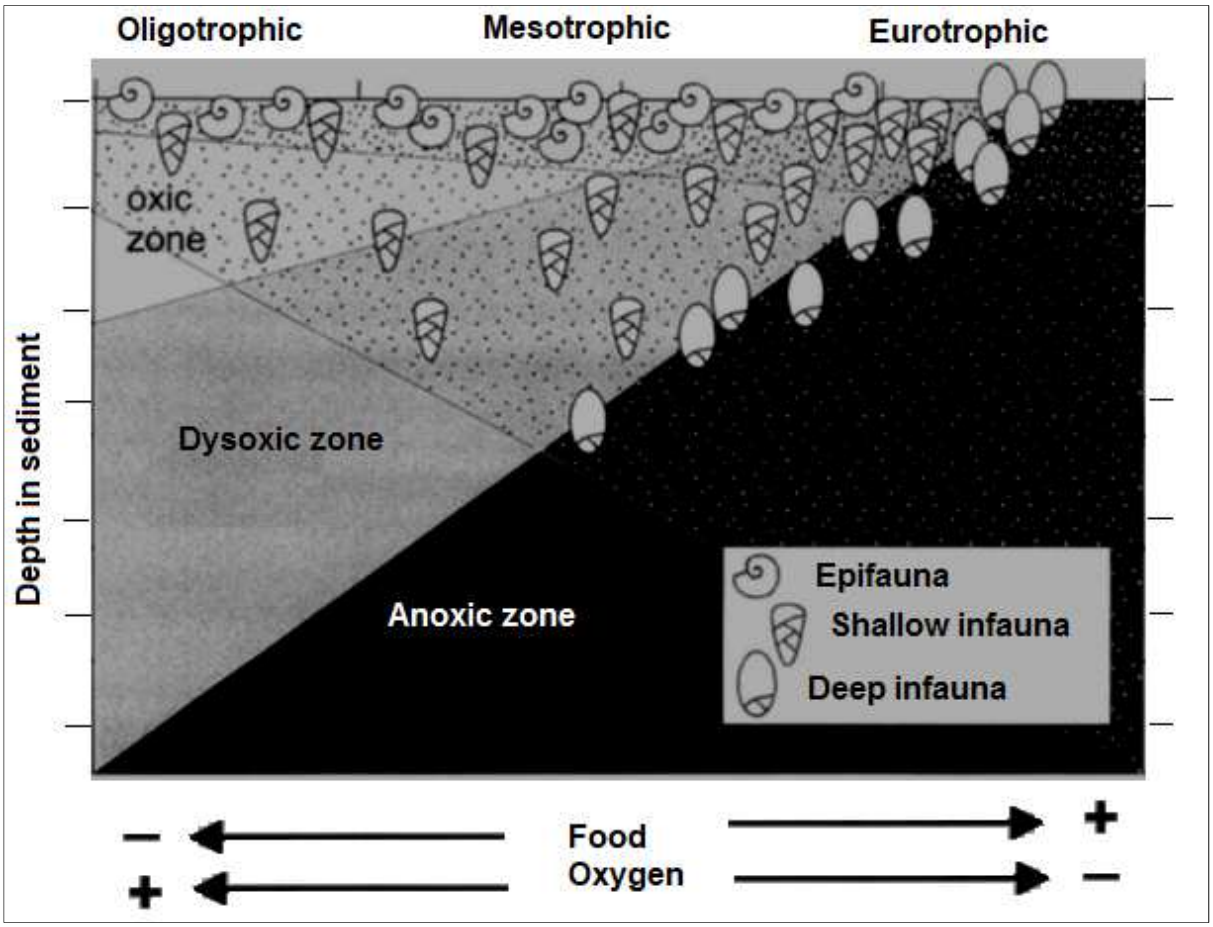

Figure 1. 13: Foraminifera morphotypes, their inferred microhabitat, depth and critical oxygen threshold. The food availability increases from left to right while oxygen concentration decreases from left to right. (Taken from Jorissen, 1999)

In the modern ocean, mixed layer species tend to have a rounded globular test, such as in the Globigerinids. They often carry symbionts and have a carnivorous feeding habit. The flattened discoidal, or conical forms, representing Globorotaliid morphologies, generally live at or below the thermocline and are predominantly herbivorous (Schiebel and Hemleben, 2017). In benthic foraminifera, morphological features such as test shapes (Table 1.1) and other traits have been linked to their preferred ecology. Infaunal morphotypes are dominated by species with globular, elongate, tapered cylindrical ovoid and spherical shapes. Taxa with these test shapes also occur in highly productive zones (Table 1.1). Epifauna are usually trochospiral, planispiral, streptospiral or milioline. Depending on the prevailing condition, some taxa move across different habitats (Jorissen *et al.*, 2007), and some infaunal species may migrate to the sediment surface to feed or respire and move back into the sediment while some epifauna taxa may move deep into to sediment during extreme condition (Jorissen *et al.*, 2007).

Table 1.1: Agglutinated foraminiferal morphotypes indicating their relationship with the environment and their living habits based on Nagy et al. (1995)

Test shape	**Life position**	**Feeding Habit**	**Environment**
Tubular	Erect epifauna	Suspension Feeding	Tranquil bathyal and abyssal with low organic matter flux
Globular	Shallow Infauna	Suspension Feeding	Bathyal and abyssal
Rounded trochospiral and Streptospiral	Surficial epifauna	Active deposit feeding	Shelf to marginal marine
Planconvex trochospiral			
Elongate Keeled	Surficial epifauna	Active deposit feeding	Shelf to marginal marine
Flattened trochospiral	surficial epifauna	Active and passive deposit feeding	High energy lagoon and estuary
Flattened planispiral and Streptospiral			
Flattened irregular	Surficial epifauna	Passive deposit feeding	Upper bathyal to abyssal
Rounded planispiral	Surficial epifauna - Shallow infauna	Active deposit feeding	Inner shelf to upper bathyal
Elongate subcylindrical	Deep infauna	Active deposit feeding	Inner shelf to upper bathyal with increased organic matter
Elongate tapered			

Foraminiferal assemblage composition is widely used in the study of ecological changes during the PETM and other hyperthermal induced ocean anoxic events (e.g. Schmidt *et al.,* 2018; Thomas *et al.,* 2018). In fact, the recognition of the extinction of benthic foraminifera such as *Stensoina beccariiformis* and *Neoflabellina sp*. in the foraminiferal assemblage in the Antarctic waters (Kennett and Stott, 1991) was responsible for the identification of the Palaeocene – Eocene boundary and eventually the PETM.

1.8 Geochemical analyses from foraminifera test

Geochemical analyses of foraminifera tests have been used over many decades to reconstruct past climatic and oceanographic conditions of the Earth (Emiliani, 1954; Shackleton *et al.,* 1985; Zachos *et al.,* 2008; Katz *et al.,* 2010). The results from the geochemical reconstruction of the carbonate test of foraminifera are used in the understanding of past changes in temperature (Zachos *et al.,* 2005); salinity (Katz *et al.,* 2010), carbon cycle (Zachos *et al.,* 2008), productivity (Pälike *et al.,* 2014), circulation patterns (eg. Kennett and Stott, 1991), oxygen concentration, changes in nutrient and ice volume of the ocean (Thomas, and Shackleton, 1996) provided that the tests are not seriously affected by post mortem recrystallization or diagenesis. Because foraminifera can retain the chemical composition of the seawater in which they calcified, measurement of the isotopic and trace element variation in the test across time slice is used as a proxy for changes in the palaeoclimatic/ecological condition of the period they lived (Katz *et al.,* 2010). The major proxies used in the geochemical analyses of foraminifera in palaeoceanography are the variation in the isotopic composition of oxygen ($\delta^{18}O$), carbon ($\delta^{13}C$), boron ($\delta^{11}B$), nitrogen ($\delta^{15}N$), and strontium ($^{87}Sr/^{86}Sr$). Other proxies include the ratio of some trace elements such as (Mg, Cd, Ba, Zn, B, U) and calcium in the foraminifera test (Katz *et al*., 2010; Groeneveld and Filipsson, 2013). Some of the isotopic/trace element ratios are still at the early stage of development for the palaeoclimatic studies, but the well-established and frequently used ones are presented in table 1.2 below. Only the $\delta^{13}C$ data previously published from the sites we studied was used to constrain the occurrence of negative carbon isotopic excursion (CIE).

Table 1.2: Palaeoceanographic parameters and the geochemical proxies for their determination

Parameters	Sea Surface Temperature	Productivity	Carbon cycle	Salinity	pH	Nutrient Availability	Stratification	Oxygen condition
Isotopic/trace element ratios	Mg/Ca; $\delta^{18}O$	Sr/Ca; $\delta^{13}C$	$\delta^{13}C$	$\delta^{18}O$	$\delta^{11}B$	$\delta^{15}N$; $\delta^{13}C$	$\delta^{18}O$	Mn/Ca

The geochemical proxies discussed above are for both the planktonic and benthic foraminifera; results from planktonic foraminifera provide information on the surface and upper water column while the deep water conditions are recorded in the geochemical composition of benthic foraminifera.

1.9 Ecological functioning of foraminifera and the biological carbon pump

Ecological function is a term used to define the structural elements in an ecosystem (in this case marine) and how they interact with the organisms living in them, as well as the role provided by these organisms in the maintenance of the whole system (Bremner *et al.,* 2006). Ecosystem functions are made up of biological, chemical and physical processes operating within the ecosystem. Physiology, living habit and the anatomy of the biological component are emphasised in the role they play in the ecological processes. Maintaining ecological processes is pivotal to sustaining biodiversity and equilibrium within an ecosystem for the overall benefits of the components (Bremner, 2008). The interplay between taxa and their physical or chemical environment largely depend on their traits, and any alteration in the biodiversity of these taxa will have serious implications for ecological functioning (Barnosky *et al.*, 2011). In general, understanding of ecological functioning involves total evaluation of taxonomic composition in a community, the biological attributes they express, their roles in maintenance and regulation of ecosystem processes as well as their response to disturbance within the community. The ecological functional analysis provides useful information on the factors controlling the change in communities and is capable of elucidating links between taxa and other ecosystem components. They are helpful for monitoring of changes in ecology in a system with a large number of species because they reduce complexity to a manageable size and can trace variations in longer time scales (Padilla and Allen, 2000).

The ocean is made up of vast and highly interconnected environments composing of a wide variety of specialised ecosystems ranging from littoral, pelagic to benthic and host numerous faunal communities (Cavan *et al*., 2017). More than 50% of the Earth's primary production takes place in the ocean (Pettit *et al.* 2013) and foraminifera which are the primary focus of this study play a vital role in biological carbon pump/ecological function in the ocean (Birch *et al.,* 2016). Foraminifera play this role by making their shell from carbonates formed from dissolved inorganic carbon thereby regulating the carbon content of the ocean (Cavan *et al*., 2017) and contributing remarkably to the global carbon cycle. Carbon is recycled between reservoirs in the oceans, on land and in the atmosphere principally as carbon dioxide and carbonate rocks. In the ocean, carbon dioxide dissolves in seawater forming carbonic acid and

is eventually removed from the marine system through processes such as the formation of calcium carbonate and the creation of limestone (Chisholm, 2000; Zebebe and Wolf-Gladrow, 2001).

Carbon also occurs in many forms in the ocean, predominantly as dissolved inorganic carbon (DIC), and as organic carbon in the form of marine creatures and their remains (Figure 1.14; Chisholm 2000). The amount of carbon occurring in the oceans makes it the largest reservoir of carbon on Earth with an estimated 40,000 gigatons (www.pmsp.org.uk). The exchange of carbon between the ocean and other Earth systems such as atmosphere, biosphere and lithosphere takes several hundred years, and carbon dioxide quantity is a major factor that controls the ocean-atmospheric system (Zeebe *et al.,* 2008).

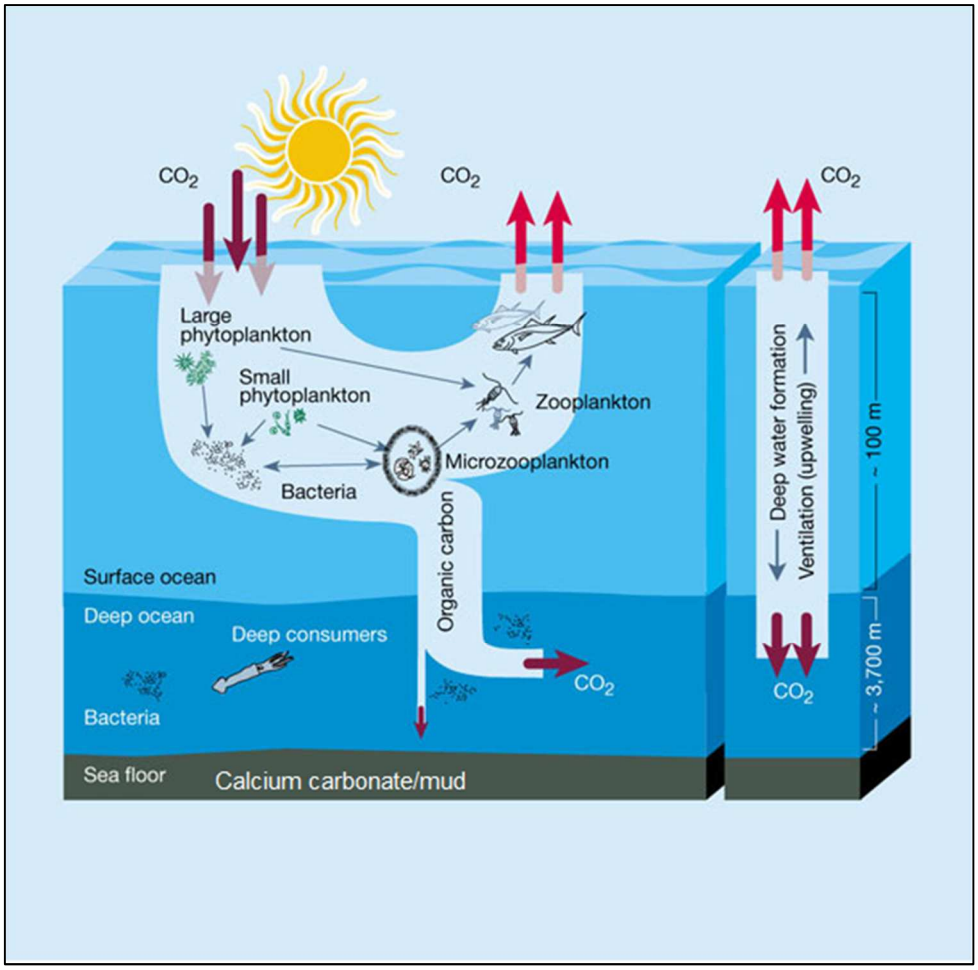

Figure 1.14. Cartoon of ocean biological carbon pump indicating how carbon dioxide is recycled between the atmosphere, oceans, marine organisms and the sediment. The phytoplankton manufactures their food and test from the atmospheric CO_2, zooplankton (e.g. foraminifera) feed on the smaller phytoplankton and use the carbonate formed from dissolved CO_2 to make their body parts while larger sea animals feed on the plankton and respire CO_2. When the organisms die, they accumulate to form sediment on the sea floor. Foraminifera are found within the circled group. (Taken from Chisholm, 2000)

Foraminifera belong to marine zooplankton, which comprises of two major types: holoplankton and meroplankton. Holoplankton live and spend their whole lives as zooplankton, examples include: radiolarians, foraminifera, amphipods, krill, copepods and salps, while the meroplankton spend the early part of their life cycle as zooplankton and develop to higher organisms later in life (www.pmsp.org.uk).

Zooplankton play an indispensable role in the functioning of marine ecosystems and ocean biogeochemical cycles such as organic carbon export because they are critical components of the trophodynamics of benthopelagic ecosystems (Cavan *et al*., 2017). They link the primary production from phytoplankton to the higher trophic levels - fish, mammals and seabirds. Zooplankton transform particulate organic matter (POM) into dissolved organic carbon through grazing and the process of metabolism (Keister and Bonnet, 2012). Grazing affects the population of primary producers, and within the water, column grazing contributes to remineralisation as well as the export of particles to the deeper ocean floor (Cavan *et al*., 2017).

The role of zooplankton in controlling the effectiveness of biological carbon pump (BCP) in the ocean also includes fragmentation of large particulate organic matter sinking from the upper water column into smaller digestible sizes as well as the active transfer of the particles to depth through vertical migration (Chisholm 2000; Cavan *et al*., 2017). The understanding of the ecosystem services provided by zooplankton is crucial to understanding the impact of current climate change in the ocean and the best group for doing this is foraminifera, hence their use in this study.

1.10 Biological Trait Analysis: Can it improve the understanding of the ecological functioning of microfossils in deep time?

Over the years, contemporary ecologists, as well as palaeoecologists have been confronted with which technique is the best to study species assemblages and how their lifestyle is related to the role, they provide in their communities. There is enormous data from field and laboratory experiments on the taxonomic assemblage and possible lifestyles (Bremner *et al*., 2005; Beauchard *et al.,* 2017) but they are rarely enough to make robust conclusions due to the limited access to various species niches and the challenge of simulating all the biotic and abiotic parameters in the laboratory (Cardinale *et al.,* 2012). To contribute towards a resolution of this problem, ecologists have been devising different statistical approaches to analyse field data to generate wider and spatially variable predictions/analyses across longer time frames to make up for the conundrums in the physical data. One of the approaches proposed for the solution of this challenge is biological trait analysis (Statzner *et al.,* 1994).

Biological trait analysis (hereafter referred to as BTA) is a statistical approach used by ecologists to study species distribution, the biological characteristics they exhibit, and how these attributes relate to the functioning of their ecosystem (e.g. Bremner *et al.,* 2006, Charvet *et al.,* 2000; Elena *et al.,* 2010; Paganelli *et al.,* 2012; Caswell and Frid, 2017).

BTA was initially designed to study terrestrial and freshwater biological communities but has been recently modified and can be applied in all ecosystems including the marine. The approach creates a meaningful connection between species and environments, as well as processes within the trophic level. Biological trait analysis uses a series of life history, morphological and behavioural characteristics of species present in assemblages to indicate aspects of their ecological functioning (defined by Naeem *et al.* (1999) as the maintenance and regulation of ecosystem processes). It has been successfully used to investigate anthropogenic influence in the marine benthic ecosystem (Frid *et al.,* 2000). BTA is applied widely in studying anthropogenic influence in modern ocean macrobenthic communities and has successfully discriminated environmental disturbance (Bremner et al., 2005). Due to the successes recorded on using the tool to study the functional ecology of marine benthos during the late Jurassic ocean anoxic event (see Caswell and Frid, 2013), we have deemed it appropriate to deploy this approach in studying the trait changes fossil foraminifera across the Palaeocene-Eocene thermal maximum in order to infer their ecological functions.

BTA differs from transfer function and other statistical approaches because it comprehensively integrates information on all members of the assemblages, how they are related to each other, the interaction with individual species and their physical, biogeochemical environment as well as their perceived responses to stress and disturbance in the environment (Edwards *et al.,* 2004). BTA has the ability to integrate intraspecific variation in trait expression (Chevenet *et al.,* 1994) thereby overcoming the challenges encountered in the trophic and functional group analyses when taxa fit into more than one functional category. Previous applications of BTA (see Charvet *et al.,* 2000; Statzner *et al.,* 2001; Bremner *et al.,* 2005; Bremner 2008; Paganelli *et al.,* 2012; Caswell and Frid 2013; Shojaei *et al.,* 2015 and Costello *et al.,* 2015) have demonstrated that the tool has the ability to detect large-scale geographic changes provided that the biological trait composition remains stable over regional and continental scales.

The selection of biological traits for BTA is critically essential for the quality of the result that will be produced. There is a wide range of existing traits which can be used for describing ecological functioning; however, not all these are useful or available in all the species. The choice of any trait to be selected must be informed by their importance to the ecological

functioning examined and the amount of information retrievable for the organism under consideration (Gayraund *et al.,* 2003). Mode of feeding and living habit, for instance, is very crucial for analysing functioning because they provide useful indications for resource utilisation and energy transfer in an ecosystem. The size and thickness of the test can be used as evidence of the amount of carbon dioxide sequestration and palaeoproductivity during the time of their existence (Bremner *et al.,* 2006). The chamber arrangement and the nature of the apertures could be linked to the organism position in the water column (Boltovkoy *et al*., 1991), hence their role in organic carbon export that plays a critical role in nutrient cycling across the whole water column (Cavan *et al*., 2017). In addition to this, traits like ornamentation can be used to interpret resilience by organisms during extreme conditions. Species with a smooth body surface and no perforation are associated with the well-lit and oxygenated environments, while complex sutures are an indication of harsh conditions (Dubicka *et al.,* 2015). Different traits can describe various aspects of ecological functioning, and some are intimately linked to particular functions, whereas others serve only as indirect indicators (Lavorel and Garnier, 2002). Therefore, the number and type of trait selected for biological trait analysis have the potential to sway the result.

1.11 Thesis objectives

The main aim of this thesis is to test the applicability of biological trait analysis in detecting the impact of the extreme environmental conditions on foraminifera and as well as using the tool to understand their ecological functioning in deep time. The study has examined the link between trait changes in foraminifera and their ecosystem functioning during the Palaeocene – Eocene Thermal Maximum (PETM) that occurred 56 million years ago. Conventional biostratigraphic/faunal assemblage analysis techniques and other paleoecological proxies have also been examined to constrain the outcome of biological trait analysis.

Since the identification of PETM in the 1990s, significant effort has been invested in the understanding of the hyperthermal event because it is believed to be a potential 'partial' analogue for our future planet if the current release of carbon dioxide into the ocean-atmospheric system is not reversed (Zeebe *et al.,* 2013). Despite enormous information gathered on this extreme climate event, no consensus has been reached by the scientific community on the cause of extinction recorded in the microbenthic community and other biotic changes. This study aims to use trait-based approach to investigate the ecological functioning provided by the foraminifera during this event by conscientiously analysing how the traits exhibited by different species of foraminifera could be correlated to environmental changes

across the PETM. Assessing the variability in the biological traits of both the benthic and planktonic foraminiferal assemblages over a range of environmental conditions will provide a useful understanding on the impact of the PETM on the marine biota, the attributes that enabled most of them to survive and, which led to some species becoming extinct.

Our study is novel because BTA has not been previously applied in the study of microfossils, either in the continental and marine environment. However, the results from previous studies (Charvet *et al.,* 1998; Bremner *et al.,* 2006; 2008; Tyler *et al.* 2012; Frid *et al*., 2009; Caswell and Frid, 2013; Beauchard *et al.,* 2017) have motivated the use of such techniques in investigating the impact of the PETM on the trait changes and ecological functioning of foraminifera (microfossil). The foraminiferal turnover during the PETM is well documented (Foster *et al.* 2013, Jennions, *et al.* 2015, Giusberti, *et al.* 2016) based on faunal assemblage and geochemical data. However, because foraminiferal community interaction with the environment and with other marine fauna is driven by biological traits instead of taxonomic composition (McGill *et al.,* 2006; Tyler *et al.,* 2012) and literal counting of fauna composition could lead to overestimation of biotic turn over (Twitchett, 2006), it is necessary to use the BTA to assess the impact of the hyperthermal on the ecological functioning of foraminifera in the marine ecosystem.

The study aims to identify which traits are more resilient to extreme environmental conditions and which are not. It will also seek to understand the traits that supported ecological functioning during the extreme environmental event. The result will also help in recognition of species with such traits and improve the understanding of the major drivers of faunal turn over during the PETM. Biological trait analysis has been used to examine the tenacity of functional traits of marine macrobenthos during the Early Jurassic ocean anoxic event by Caswell and Frid (2016), but only changes in life habit were highlighted, with epifauna being more resilient than the infauna. In this study, more traits shall be considered across a larger time scale and geographies.

This study will examine the foraminiferal assemblages from sites 1209B, 1212B and 1215A in the Pacific Ocean, site 1265A in the South East Atlantic and the Tethyan section of Alamedilla. These sites will be used to compare the ecological disturbance from these oceans during the PETM using BTA. These sites were chosen because of their location in equatorial latitudes and the scarcity of data on the impact of the PETM on the tropical climate. The results from this work will provide more insight on the impact of the event on the subtropical ecosystem.

Specifically, this thesis aims to achieve the following objectives:

1. Evaluate the similarities/differences in the degree of ecological disturbance in the Tethys, Atlantic and Pacific oceans and improve the understanding of biotic changes during the PETM
2. Analyse the benthic and planktonic foraminiferal assemblages from ODP Site 1265A to understand changes in the ecological functioning across the water column from the pelagic to the benthic ecosystem during the PETM
3. Examine the benthic foraminiferal composition from ODP Site 1215A and evaluate the impact of ocean acidification on the preservation of benthic foraminifera test.
4. Explore the usefulness of biological trait analyses (BTA) in investigating the impact of extreme climate on the ecosystem functions of fossil foraminifera.
5. Investigate the tenacity of the identified traits in the face of the extreme ecological condition.

CHAPTER TWO

Materials, Methods and Taphonomic considerations

2.1 Materials

The material for the primary data used in this study was sampled from Ocean Drilling Program (ODP) expedition: Leg 199, Site 1215A Cores 6H and 8H (Lyle *et al.,* 2002); Leg 208 Site 1265A Cores 29H and 30H (Zachos *et al.,* 2004). While secondary data were extracted from published foraminifera census data from Leg 198 Site 1209B, Core 22H (Takeda and Kaiho, 2007), Site 1212B core 13H (Takeda and Kaiho, 2007) and outcrop samples from Alamedilla in Southern Spain (Alegret *et al.* (2009); Figure 2.1; Table 2.1). These sites were selected because of their location in the subtropics. Most of the PETM studies are focussed in high latitudes where there are pronounced changes during the event (Kennett and Stott, 1991; Koch *et al.,*1992; Dickens *et al.,* 1995; Kelly *et al.,* 1996; Thomas and Shackleton, 1996) and very little is published on the impact of event in the subtropics (Frieling *et al*., 2016).

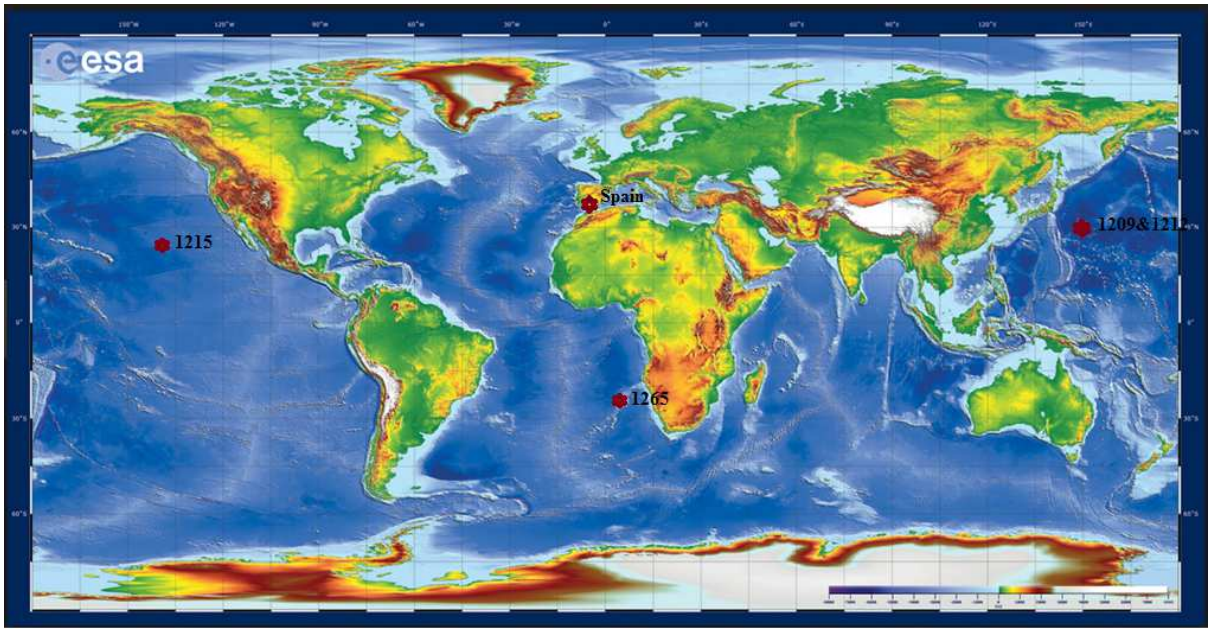

Figure 2.1: Location of the studied sites. 1215A, 1265A, 1209B, and 1212B are ODP site while outcrop data came from Alamedilla in Spain (modified from The European Space Agency map retrieved at http://www.esa.int/ESA).

Table 2.1: Summary of study sites, location, palaeowater depth, new data and previously published data

Sites	Latitude	Longitude	Water depth (m)	Primary data	Secondary data	References
ODP 189 Site 1215	26.0296	-147.9332	5396	Foraminifera census & traits	$\delta^{13}C$	Leon-Rodriguez & Dickens (2010)
ODP 208 Site 1265	-28.835	2.6389	3060	Foraminifera Census & traits	$\delta^{13}C$	Zachos *et al.,* 2005
ODP 198 Site 1209	32.6517	158.5059	2387	Foraminifera traits	$\delta^{13}C$ & Foraminifera census	Takeda & Kaiho (2007)
ODP198 Site 1212	32.4483	157.7117	2681	Foraminiferal traits	$\delta^{13}C$ & Foraminifera census	Takeda & Kaiho (2007)
Outcrops	37.5816	-3.2439	2000	Foraminiferal traits	$\delta^{13}C$ Foraminifera census	Alegret *et al.,* (2009)

2.2 ODP Site 1215A

Thirty- eight (38) samples were selected across 15.62 metres of core (6 and 8H) from ODP Leg 199, Site 1215A (Figure 2.2 and Table 2.2), and analysed for foraminiferal abundance and trait composition. The two holes (A and B) cored at Site 1215 were drilled at 5396 metres below sea level (mbsl) at 26°01.77'N, 147°55.99'W (Lyle *et al.,* 2002). The summarised stratigraphy of Site 1215 (see Figure 2.2; Lyle *et al*., 2002; Leon-Rodriguez & Dickens 2010) indicated pelagic clay and clayey nannofossil ooze as the dominant lithology. The stratigraphy of the holes is subdivided into units I, II III and IV based on the characteristic sedimentary facies (Lyle *et al.,* 2002). Unit I is composed of red clay intercalated with zeolites. Unit II from where the samples for this study were collected consists of brown – dark brown, clayey, calcareous ooze with some cherts sandwiched within the sediment. Unit III is a metalliferous dark – brown ooze with little clay and no ash nor fossil, it is unconformably overlying the basaltic igneous rock of unit IV.

Site 1215A is located in the abyssal hill north of Molokai fracture northeast in the central Pacific Ocean. The core was taken in an area with typical abyssal hill topography but continuous sediment cover. Molokai Fracture is characterised by an extensional tectonic setting and with hydrothermal vents around it.

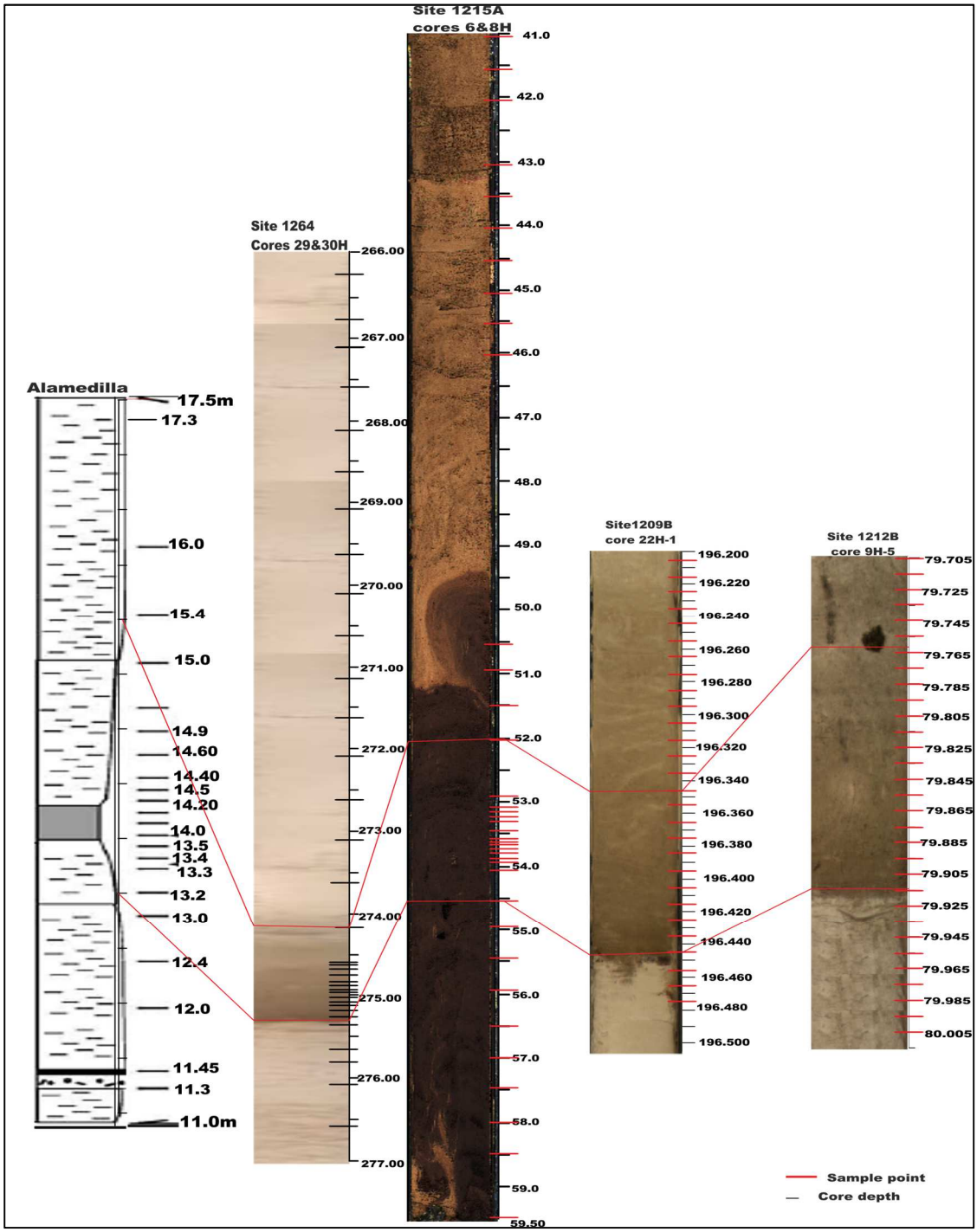

Figure 2.2: Stratigraphic sections and sample points for Alamedilla section, Sites 1265A, 1215A, 1209B and 1212B. The area correlated with the red line marks the CIE section as interpreted from the carbon isotope and sedimentological changes. The cores for the primary data were sampled at a slightly lower resolution to capture long timeframe in order to understand reasonable changes across the PETM.

Table 2.2: Sample levels from cores 6H and 8H, Site 1215A with the corresponding metre below seafloor (mbsf[1]) and metres composite depth (mcd)

Sample code	mbsf	mcd
1215_6H-02_30-32	41.01	44.85
1215_6H-02_80-82	41.51	45.35
1215A_6H-02_130-132	42.01	45.85
1215A_6H-03_80-82	43.01	46.85
1215A_6H-03_130-132	43.51	47.35
1215A_6H-04_30-32	44.01	47.85
1215A_6H-04_80-82	44.51	48.35
1215A_6H-04_130-132	45.01	48.85
1215A_6H-05_30-32	45.51	49.35
1215A_6H-05_80-82	46.01	49.85
1215A_8H-01_30-32	50.51	54.35
1215A_8H-01_78-80	50.99	54.83
1215A_8H-01_130-132	51.51	55.35
1215A_8H-02-30-32	52.01	55.85
1215A_8H-03_28-29	53.485	57.325
1215A_8H-03_30-32	53.51	57.35
1215A_8H-03_33-34	53.535	57.375
1215A_8H-03_35-36	53.555	57.395
1215A_8H-03_37-38	53.575	57.415
1215A_8H-03_39-40	53.595	57.435
1215A_8H-03_41-42	53.615	57.455
1215A_8H-03_46-47	53.665	57.505
1215A_8H-03_48-49	53.685	57.525
1215A_8H-03_60-62	53.81	57.65
1215A_8H-03_63-64	53.835	57.675
1215A_8H-03_64-65	53.845	57.685
1215A_8H-03_65-67	53.86	57.7
1215A_8H-03_80-82	54.01	57.85
1215A_8H-03_130-132	54.51	58.35
1215A_8H-04_28-30	54.99	58.83
1215A_8H-04_78-80	55.49	59.33
1215A_8H-04_128-130	55.99	59.83
1215A_8H-05_30-32	56.5	60.35
1215A_8H-05_80-82	57	60.85
1215A_8H-05_128-130	57.48	61.33
1215A_8H-06_30-32	57.96	61.85
1215A_8H-06_80-82	58.46	62.35
1215A_8H-07_30-32	59.46	63.35

There were three key palaeoceanographic objectives for drilling Site 1215.

1. To core the Palaeocene – Eocene boundary for the first time in the Central Pacific Ocean.
2. To define the North equatorial current and North Pacific subequatorial gyre processes
3. To trace the Intertropical convergence zone during the Palaeogene by following the variation in the Aeolian – dust composition and flux through time.

[1] [1] mbsf- metres below seafloor

This study will seek to understand the impact of extreme climatic change on the benthic foraminiferal communities and the effect of high organic flux on foraminifera preservation.

2.3. ODP Site 1265A

Thirty-four (34) sediment samples were collected and analysed across 11m of the core from Site 1265A (Figure 2.2; Table 2.3). The lithologic composition of the recovered cores on this site includes; nannofossil ooze, foraminifer-bearing nannofossil ooze, foraminifer-nannofossil ooze, nannofossil-foraminifer ooze, clay-bearing nannofossil ooze, and foraminifer- and clay-bearing nannofossil ooze. Smear slide result also revealed minor and accessory lithologies such as ash-bearing nannofossil ooze, ashy nannofossil ooze, clay-bearing volcanic glass, zeolite- and nannofossil-bearing clay, clay, calcareous dinoflagellate cyst–bearing nannofossil ooze, and hematite-bearing nannofossil ooze.

Table 2.3: Cores depth of the section analysed from Site 1265A with their corresponding metre below seafloor (mbsf) and metres composite depth (mcd).

Sample depth/ code	mbsf	mcd
29H1-30-32	266.31	307.09
29H1-80-82	266.81	307.59
29 H2-80-82	267.62	308.48
29 H2-130-132	268.12	308.98
29 H3-30-32	268.62	309.48
29 H3-78-80	269.1	309.96
29 H3-130-132	269.62	310.48
29 H4-30-32	270.12	310.98
29 H4-80-82	270.62	311.48
29 H4-130-132	271.12	311.98
29 H5-80-82	272.12	312.98
29 H5-130-132	272.62	313.48
29 H6-30-32	273.12	313.98
29 H6-78-80	273.68	314.46
29 H6-128-130	274.18	314.96
29H7-20-22	274.58	315.36
29H7-25-26	274.63	315.41
29H7-30-32	274.68	315.46
29H7-35-36	274.74	315.52
29H7-40-42	274.78	315.56
29H7-45-46	274.84	315.62
29H7-50-53	274.88	315.66
29H7-60-62	274.98	315.76
29H7-65-66	275.04	315.82
29H7-70-71	275.08	315.86
29H7-75-76	275.13	315.91
29H7-78-80	275.16	315.95
29H7-80-83	275.19	315.97
29H7-130-132	275.68	316.46
29HCC-22-24	275.88	316.66
30 H1-29-31	276.18	317.92
30 H1-80-82	276.66	318.42

The whole section of the recovered core is divided into two units based on magnetic susceptibility measurement and sedimentary facies composition. The samples for this study was collected from unit II, particularly within the subunit IIC. The average percentage carbonate content for the subunit II section is 93 ± 2 wt% except in the clay – enriched horizon of the PETM (Zachos *et al*., 2004). The P/E boundary interval was encountered in Hole 1265A at ~275.09 mbsf (315.87 mcd). However, the lowermost Eocene was not recovered due to drilling disturbance. The P/E boundary interval occurred at the contact between underlying Palaeocene nannofossil ooze and a reddish brown nannofossil clay of the lowermost Eocene (Figure 2.2). The sediment sequence was marked by a red clay layer, which varies in thickness from 20 to 50 cm from site to site, within a thick and uniform sequence of upper Palaeocene and lower Eocene foraminifer-bearing nannofossil ooze.

Site 1265A is located at latitude 28°50.10´S and longitude: 02°38.35´E in the Water depth of 3060 m as part of the Leg 208 Early Cenozoic Extreme climate: The Walvis Ridge Transact. This site is situated at a couple of metres under the peak of the seamount in the north-western flank of the Walvis Ridge. It was drilled at the shallowest sea depth of the Leg 208 depth transect. Walvis Ridge is located in the eastern part of the South Atlantic Ocean (Figure 2.3). This site has been identified from the seismic survey as one of the best-known locations where it is possible to recover Paleogene sediments from the late Cretaceous to Recent over a broad range of depths. The ridge has been the target of previous drilling by Deep Sea Drilling Project (DSDP) Leg 74, which is designated as sites 525–529 on the northern flank of the ridge across the depths of 2.5 and 4.2 km (Moore *et al.,* 1984).

Brief tectonic history of Walvis Ridge by Sager *et al.* (2015) shows that Walvis Ridge (WR) is one of the Cretaceous-Cenozoic large igneous provinces (LIPs) formed by the Tristan-Gough hotspot interacting with the Mid-Atlantic Ridge (MAR). Plate tectonic reconstructions indicate that the main Rio Grande Rise (RGR) plateau and large N-S plateau in the eastern Walvis Ridge erupted at the same point at ~90 Ma. After about ~8Ma of continuous eruption, these juxtaposed igneous provinces formed a "V" shape with a basin in between them (Sager *et al*., 2015). Walvis Ridge is a northeast-southwest–trending aseismic ridge that divides the eastern South Atlantic Ocean into two basins, the Angola Basin to the north and the Cape Basin to the south (Zachos 2004). The ridge is composed of a number of concatenated crustal blocks declining down the slope towards the northwest and ascending more steeply towards the southeast. Previous data from magnetic and gravity survey indicate that Walvis Ridge was formed by hotspot volcanism near the spreading ridge during the process of Atlantic basin expansion (Rabinowitz and Simpson, 1984) and later in the latest Cretaceous, a 1.1 km basin was formed

as a result of thermal subsidence (Moore *et al.,* 1984). The ridge was covered with thick pelagic sediment that significantly prograde in thickness toward the continental margin (Moore *et al.,* 1984). The sediment thickness varies from ~ 300m at the deepest part of the seafloor adjacent the ridge to about 600m near the summit in the southeastern portion. This was interpreted from a pattern expressed in seismic sequences acquired before the drilling (Zachos *et al.,* 2004)

The primary objective of Leg 208 expedition was to recover sedimentary sections with sufficient resolution to characterise high-frequency changes in bottom water chemistry and circulation at shallow bathyal depths during several of the key climatic events of the Paleogene including the Eocene–Oligocene transition, the Early Eocene Climatic Optimum (EECO) and the PETM. This is because most of the sites cored before Leg 208 to constrain major geologic events during the Paleogene suffered from poor recovery and drilling disturbance (Zachos *et al.* 2004). Advances in coring technology and drilling strategies (i.e., multiple-hole composite sections) allowed for almost 100% recovery of sequences that were only partially recovered during previous drilling campaign

2.4 ODP Site 1209B

Sampling at Site 1209B was at a higher resolution (Takeda and Kaiho, 2007) compared to Sites 1215A and 1265A. Thirty sediment samples were analysed across a 30cm of core 22H-1 in Site 1209B, Leg 198. ODP 198 is located at the southern high of the Shatsky Rise along a depth transact (Figure 2.3; Table 2.1). The sites are spread along a prograding depth of 500m. The position of Shastky Rise in the Pacific Ocean during the PETM was reconstructed to be latitude 32.6517 and longitude 158.5059 and palaeowater depth of 1900-2200m indicating that Site 1209B (Table 2.1) was the shallowest depth in the ODP Leg 198 (Figure 2.3; Bralower *et al.,* 2002). The Lithology of the analysed core consists largely of nannofossil ooze and nannofossil ooze with clay. The core contained a distinct dark brown clay-rich interval that marks the core of the PETM and the P/E boundary. Inorganic calcite noodles have been reported just above the clay-rich layer by the shipboard report (Bralower *et al.,* 2002)

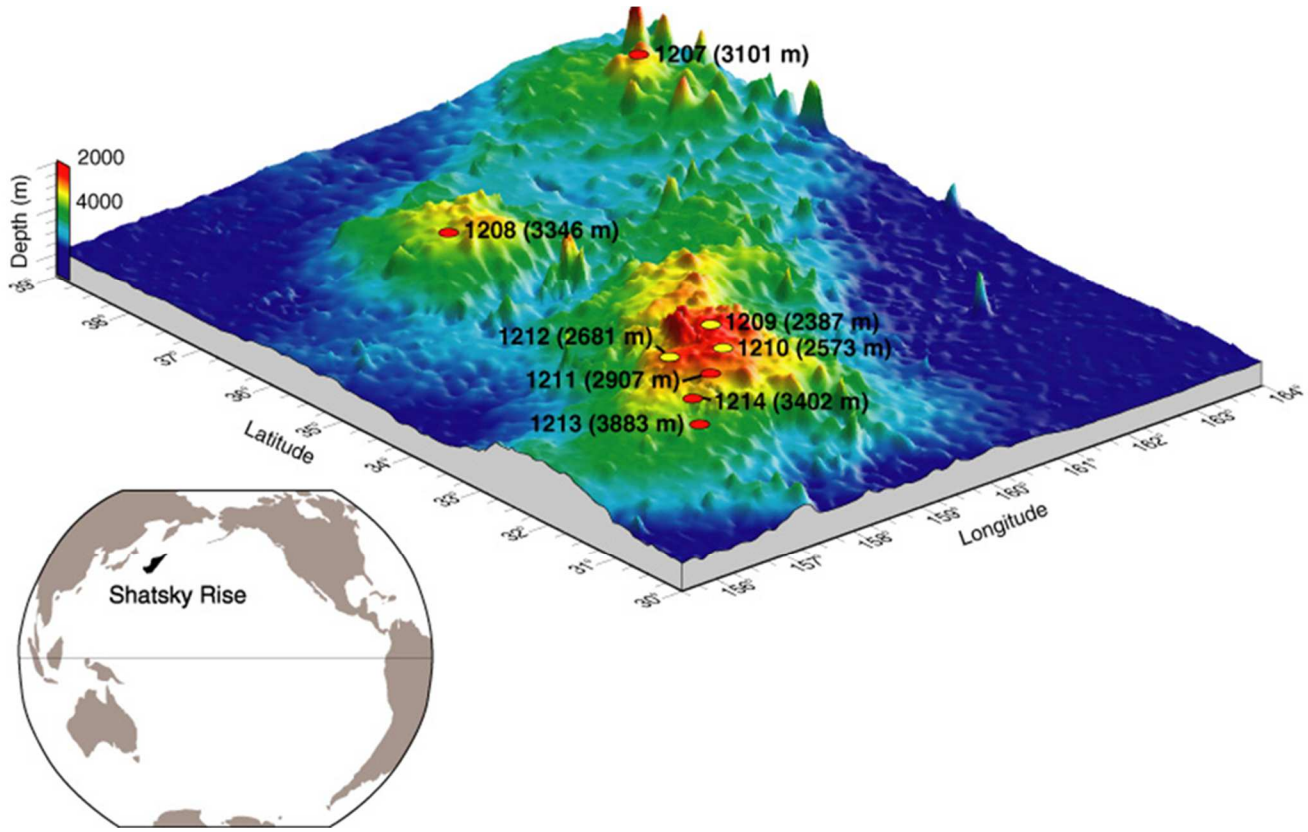

Figure 2.3: Topography of Shatsky Rise showing the location and present depth of all the sites in ODP Leg 198 (source http://www-odp.tamu.edu/publications/198_SR/synth/syn_f1.htm).

Results from the preliminary biostratigraphic analysis of cores recovered from the site were used to constrain the onset of the PETM at the top of the P5 planktonic foraminiferal zone and CP8 of calcareous nannoplankton zone. The PETM section is represented by an abrupt change from light brown nannofossil oozes to a dark brown clay horizon (see Figure 2.3) that grades upward into a more carbonate-rich sediment. At Site 1209B the PETM occurred at core 198-1209B-22H-1_132-110. The clay layer at the onset of the event was bioturbated indicating exposure of the seafloor and well aerated benthic environment. The last down-hole occurrence of *Morozovella valescoensis* is the biostratigraphic event that marks the peak of the CIE, at Site 1209B it was located just above the clay enrichment. The sharp lithologic contact and a 6cm section (Petrizzo, 2007) indicated that the PETM section at Shatsky Rise was more condensed compared to the length recorded at the Atlantic and Tethys sea (Takeda and Kaiho 2007).

2.5 ODP Site 1212B

Site 1212 is located on the southern flank of Shatsky Rise at a water depth of 2681m (middle bathyal). The site is ~300 m deeper than Site 1209B (2387 m). Thirty-two (32) sediment samples were collected from a 30cm length of core across the PETM interval at Site 1212B. The PETM section was composed of pale yellowish-brown nannofossil oozes interbedded with clayey pale-orange brown ooze (Takeda and Kaiho 2007). A number of minor diastems occurred in the clay-rich interval indicated by thin, darker horizons. Volcanic glass, iron oxide and pyrite were also reported within the PETM interval in the shipboard visual core description (VCD) record (more details on Bralower *et al.,* 2002). P/E boundary occurred within core 198-1212B-9H-5_72-50cm i.e. 80.08-79.705 mbsf. The analysed part of the core is located in the unit II section of the hole.

2.6 Alamedilla

The Alamedilla section is located in Granada Province, Southern Spain. The upper Palaeocene-early Eocene section exposed at Alamedilla is composed of pelagic sediments consisting of grey marls, with a 15-cm thick turbidite at the base (Algret *et al.,* 2009). The section consists of a continuous sediment cover from the late Cretaceous to early Eocene, and it represents a very important location for understanding the Palaeocene - Eocene (P/E) boundary (Algret *et al.,* 2009). Twenty four outcrop samples were collected across 17.40m at 10-20 cm interval within the CIE section and 40 cm apart at the pre-CIE and recovery sections respectively. A transition from pink marl at 13.50-13.80 m into a thick red clay horizon marks the beginning of the PETM in Alamedilla.

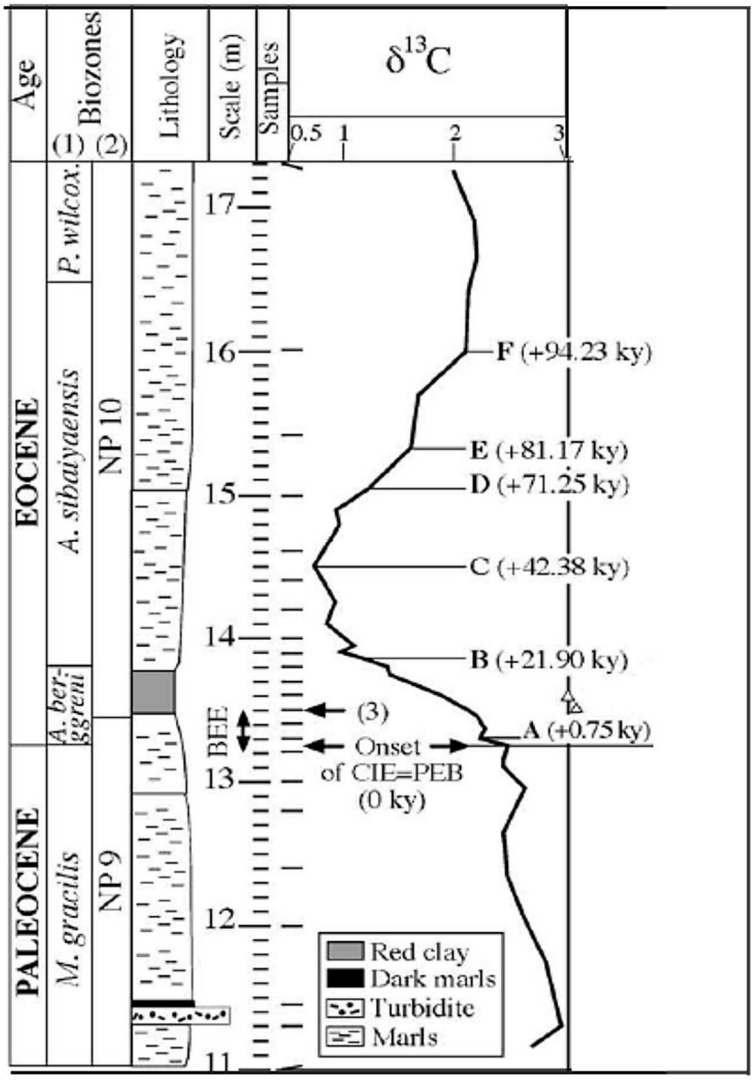

Figure 2.4: Combined litho and biostratigraphy as well as PETM events in Alamedilla section (Adapted Algret et al., 2009). Column (1) is the planktonic foraminifera zone, (2) is Nannofossil zone. BEE = Benthic foraminifera extinction, PEB = PEB = Paleocene/Eocene boundary. Point A is the record of the first evidence of negative carbon isotopic excursion (CIE) and the duration from the PEB. It represents the first oxidation of methane in the section during the PETM. B. record of further reduction in the CIE. C. peak of the PETM warming and the CIE. D. Evidence of initial sign of CIE recovery. E. Further sign of recovery and F. return of the CIE to the pre CIE values

2.7 Summary of published micropalaeontological and geochemical studies

2.7.1 ODP Site 1215A

The micropalaeontological composition of the analysed section of Site 1215A has been earlier published as part of ODP Leg 199 -Palaeogene Equatorial transect scientific report (Nomura and Takata, 2005). The report presented a comprehensive catalogue of benthic foraminiferal assemblage from Sites 1215A, 1220B, and 1221C. However, no detailed interpretation and discussion of the foraminiferal assemblage were given. Nomura and Takata (2005) also reported poor recovery and very few foraminifera from the section, and I believe that apart from the high dissolution associated with this section, the quantity of the foraminifera

recovered would have been hugely affected by the preparation method. They adopted the traditional method of washing under the tap and picking with the brush, instead of the more effective washing with shower head tap. Washing with shower head tap involves using mild pressure tap fitted with the shower head to flush all the mud leaving the residue with foraminifera only.

In another study, Leon-Rodriguez and Dickens adopted integrated biostratigraphic and geochemical approaches to constrain the amount of carbon injected in the Pacific Ocean during the Late Palaeocene – late early Eocene hyperthermal (PETM (~55.5 Ma), H1/ETM-2[2] (~53.7 Ma), I1[3] (~53.2 Ma), and K/X[4] (~52.5 Ma) events. They analysed core sections of about 42m in length transcending 56 – 52Ma, focusing mainly on planktonic foraminifera, calcareous nannofossil and stable isotope compositions of carbon and oxygen from bulk carbonate. The result was used to derive the age model, carbon fluxes, temperature changes and the impact of ocean acidification on the sediment. They noted that the CCD was 200m below the depositional environment during the PETM in already corrosive water as indicated by high-level dissolution of foraminifera test. The general trend in carbonate preservation in Site 1215A indicated an increase from late Palaeocene to the early Eocene with a punctuated but significant decrease during the CIEs. The $\delta^{13}C$ isotope data for this study was extracted from Leon-Rodriguez and Dickens (2010) supplementary data. New benthic foraminiferal census data was acquired from this site and analysed for both taxa and trait changes.

2.7.2 ODP Site 1265A

Onshore micropalaeontological studies have not been conducted on the core section analysed from Site 1265A except for the general shipboard biostratigraphy report published as part of the initial report of the Leg 208 –Early Eocene Cenozoic Extreme Climates: The Walvis Ridge Transact. This study has provided a detailed understanding of changes in benthic and planktonic foraminiferal composition across the late Palaeocene – early Eocene of Core 29H and part of 30H and identified some climate signals using the trait changes in the recovered foraminifera. Some geochemical (stable isotope) studies have been published from Leg 208 (Thomas Westerhold *et al*., 2017; 2007; McCarren *et al*., 2008 and Zachos *et al.*, 2005). The $\delta^{13}C$ isotope used to constrain the CIE in this study was sourced from the supplementary data

[2] Second early Eocene thermal maximum
[3] Lighter hyperthemal after ETM-2
[4] Last early Eocene hyperthemal

from Zachos *et al.* (2005), nevertheless, the isotope data did not cover the whole core section studied.

2.8. Methodology

2.8.1. Sample preparations

Wet and dry weight, as well as the volume of samples, were measured prior to the micropalaeontological preparation. This allows for accurate calculation of microfossil concentration, mass accumulation rate and other statistical analysis that requires specimen absolute abundance. Materials used for weighing the samples include XS204 DeltaRange METTLER TOLEDO precision balance, 250ml glass beaker, 50ml centrifuge tube, wash bottle with double distilled water, funnels, filter paper and spatula. Sediment samples were divided into two, one part for foraminiferal analysis and the other for palynological analysis.

During the measurement, a 50ml centrifuge tube was filled with 20 cm^3 of double distilled water, placed in the glass beaker and then on the precision balance. The balance was then tared (make the value equal to 0.0 g) with the beaker and centrifuge tube. The sediment was then transferred to the tared centrifuge tube in the beaker, and volume change and wet weight were recorded. The wet sediment is poured onto a conical folded filter paper (pre-labelled with the same sample number as the sediment) and placed in the funnel supported on a rack. New centrifuge tube and filter paper were used for each sample.

All the measured samples were dried in the laboratory oven at 20°C overnight, and the dry weight is measured the next day.

2.8.2. Foraminiferal preparation protocols

Weighed sediment samples were transferred into the 250ml glass beaker and soaked with water and 2-3 drops of sodium hypochlorite solution overnight in a fume cupboard. This allows enough time for the sediment to disaggregate. The disaggregated sediment samples were washed with Endecotts stainless steel 63µm sieve under running tap water. The recovered residues were transferred to a labelled filter paper placed in a funnel and dried in the oven. The dried residue was stored in vials for identification and counting.

Before the counting, the recovered microfauna were sieved into three fractions, >63-125 µm (fine), >125-250 µm (medium) and >250 µm (coarse). Each size fraction was counted separately to avoid the larger microfossil from obstructing the smaller ones. Counting was done by sparingly spraying the microfossils on the observation tray. The observation tray is divided into forty –two equal sized squares and 2-3 microfossil filled trays were counted for each

sample by following systematically a particular transect. Because the number of planktonic foraminifera was high (e.g. some species exceeding 1000 in one fraction) in Site 1265A, only counted one tray was counted for each size fraction. However, for the benthic group that was less abundant more than one tray was counted to get sufficient data. Many species (e.g. *Chiloguembellina, Globanomalia, Abyssamina, and Pleurostomellids*) which were scarce in the larger fraction were abundant in the fine fraction. This is in contrast with the proposition that sizes <250 µm should be neglected because they contain mainly juvenile species (Kaiho *et al*., 2006; Luciani *et al*., 2007). Extreme environmental conditions can cause dwarfism in foraminifera (Alegret and Thomas 2009; D'haenens *et al*., 2012), hence the fine fraction may contain some important species not found in the coarse fraction. Nevertheless, it was difficult to identify some species of *Subbotina, Acarinina* and *Morozovella* in the fine fraction due to their small size, and so for these taxa identification was made to the genus level only. Most of the taxa were identified to the species level using the systematic description and micrographs from Holbourn *et al.* (2013), Pearson et al. (2006), Olsson *et al.*(1999), Widmark (1997), Bolli *et al.* (1994), Speijer (1994), Nomura (1991), Loeblich and Tappan (1987), Tjalsma and Lohmann (1983), Cushman (1951) and other peer-reviewed publications.

2.9. Methods of trait coding for Biological Trait Analysis

Biological Trait Analysis utilises multivariate ordination method in describing the patterns of biological trait composition across the entire assemblages (i.e. the types of trait present in assemblages and the relative frequency with which they occur). Three main ordination methods are fit for this technique; they include the Fuzzy correspondence analysis (FCA), co-inertia analysis (CoI) and non-metric multi-dimensional scaling (nmMDS). Fuzzy correspondence analysis is a parametric linear ordination method that uses eigenanalysis to investigate differences between samples, based on the biological traits exhibited by species present in the assemblages, weighted by their abundance or biomass (Bremner *et al.,* 2006). Co-inertia on the same vein is also based on eigenanalysis. However, it differs from FCA in that it investigates patterns in species' distributions and their biological traits separately, as well searching for covariation between them (Doledec and Chessel, 1994). Both FCA and CoI allow the traits that contribute most to differences in functioning between assemblages to be identified and visualised. Non-metric Multi-dimensional scaling (nmMDS) is an indirect gradient analysis approach which produces an ordination based on a distance or dissimilarity matrix and is frequently used in the analysis of marine assemblage composition (Clarke, 1993). Unlike FCA and CoI, which utilise absolute distance between samples as a measure of the difference

between them, nmMDS is based on the rank similarities of samples and produces an ordination plot showing relative differences in biological trait composition.

For this work, we shall be using non-metric multi-dimensional scaling (nmMDS) and Similarity percentage analysis (SIMPER) because they are easier to visualise and interpret. The SIMPER analysis produces the percentage of similarity and dissimilarity of the factor of interest (in this case traits or species composition), the percentage of similarity and dissimilarity between the hierarchy of the elements and for specific levels of each factor. It shows which variables in the data explain the similarities or dissimilarity, the percentage of contribution (Contrib %) of variables that describe these similarities as well as the cumulative percentage. The result of variables is classified from the highest to the lowest contribution.

The number of traits selected for this study and analyses is based on the perceived role they play in ecological functioning. These traits were those considered to reference core ecosystem functions or processes in the ocean that may be provided by foraminifera. Important traits that can provide an index for some of these ecosystem functions include essential aspects of foraminiferal morphology and behaviour such as the shape of the test, test composition, chamber arrangement, chamber shape, ornamentation, nature of aperture (form, accessory, structure and position), test perforation, life habit, feeding habit and mobility.

Data on traits like life habit, feeding habit and mobility that cannot be directly observed in under the light microscope were obtained from databases and literatures. For a couple of species, some traits like mobility or feeding habit could not be directly established because they are already extinct with no record of the life history in the literature. In such cases, the missing traits were extrapolated from the closest relative (at the genera or family level) or from the functional morphology of a known taxa. For instance, if the chamber form of a species was rounded trochospiral, Nagy *et al. (*1995) functional morphology principles were applied to indicate that the species was a superficial epifauna and must have been a deposit feeder (see Table 1.1; http://nhm2.uio.no/norges/full/atlas/pecol_text.htm), though this was in very rare cases.

All the traits were each classified into subcategories referred as modalities (Table 2.4; Figures 2.5-2.7), for instance, test shape was classified into spiral, elongate, globose, tubular, subquadrate, and others. This categorisation is not exhaustive but highlighted the modalities that are quantifiable, common in the recovered species or those available in the accessed literature and databases.

Table 2.4: Biological traits of benthic foraminifera and associated modalities used in this study (See appendix 5.2 for planktonic traits)

Traits	**Modalities**
A. Test Shape	A1. Spiral
	A2. Elongate
	A3. Globose
	A4. Tubular
	A5.Subquadrate
	A6. Others
B. Test Composition	B1. Agglutinated
	B2. Secreted: microgranular
	B3. Secreted: Hyaline calcite
	B4. Secreted: Hyaline aragonite
	B5. Secreted: Porcellanous
C. Chamber arrangement	C1. Unilocular
	C2. Uniserial
	C3. Bi/Tri-serial
	C4. Planispiral
	C5. Trochospiral
	C6. Other
D. Chamber shape	D1. Spherical/Oval
	D2. Tubular
	D3. Triangular or trapezoidal
	D4. Semi-circular
	D5. Others
E. Test macro-ornamentation	E1. Depressed/incised sutures
	E2. Raised sutures
	E3. Cancellate/ponticuli
	E4. Muricae
	E5. Keeled
	E6. Others/none
F. Test Micro-ornamentation	F1. No ornament
	F2. Spinose
	F3. Hispid
	F4. Striate
	F5. Others
G. Aperture form	G 1. Oval/reniform
	G2. Arcuate
	G3. Radiate
	G4. Slit-like
	G5. others
H. Aperture accessory structures	H1. Lips
	H2. Bifid teeth

	H3. Umbilical teeth
	H4. Neck
	H5. None
I. Primary aperture position	I1. Terminal
	I2. Basal interiomarginal
	I3. Umbilical
	I4 Extra-umbilical
	I5. Areal
J. Test perforation	J1. Micro-perforation (<1um)
	J2. Fine perforation (1-3 um)
	J3. Macro-perforation (>3um)
	J4. No perforation
K. Life habit	K1. Benthic epifaunal
	K2. Benthic shallow-infaunal
	K3. Benthic deep- infaunal
	K4. Planktonic
L. Feeding habit	L1. Deposit feeder
	L2. Grazer
	L3. Suspension feeder
	L4. Symbiosis
	L5. Denitrification
M. Mobility	M1. Sessile
	M2. Clinging
	M3. Free-living benthic
	M4. Planktonic

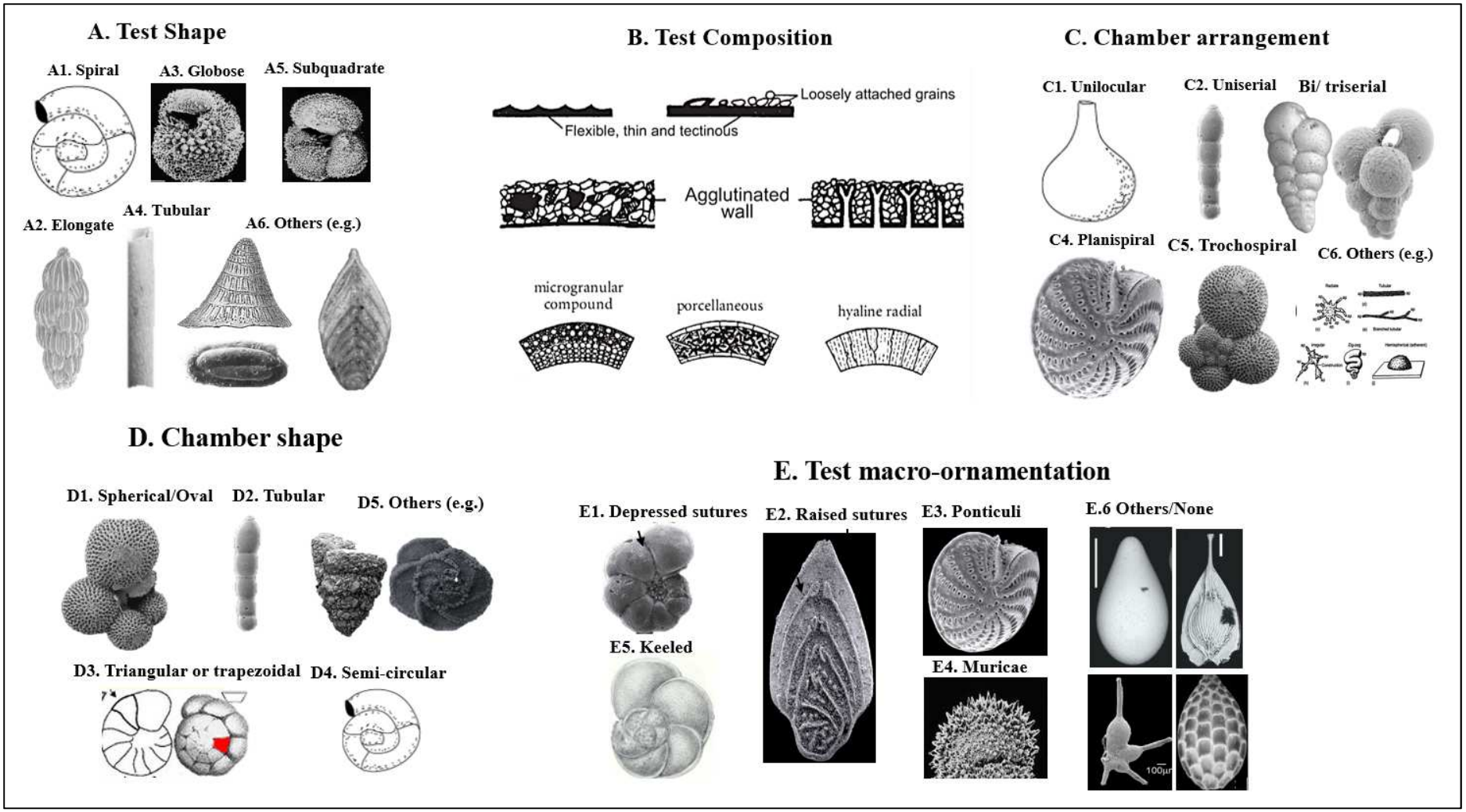

Figure 2.5. Micrographic representation of test shape, test composition, chamber arrangement, chamber shape, test macro-ornamentation of foraminifera and their modalities. Not all the species in the micrographs were identified in this study. The best images to represent the traits were prioritised.

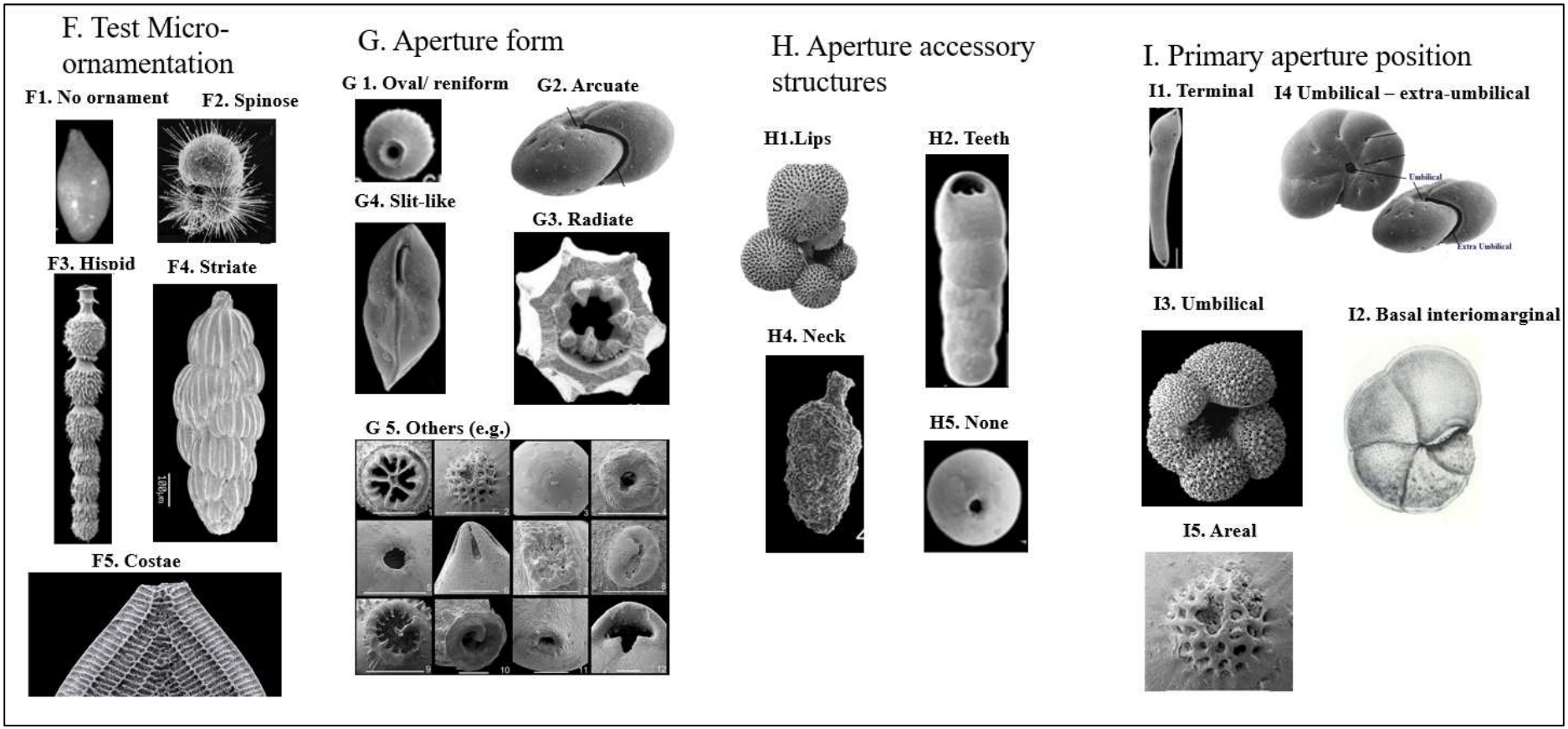

Figure 2.6. Micrographic representation of test micro-ornamentation, aperture form, aperture accessory structures, primary aperture position of foraminifera and their modalities

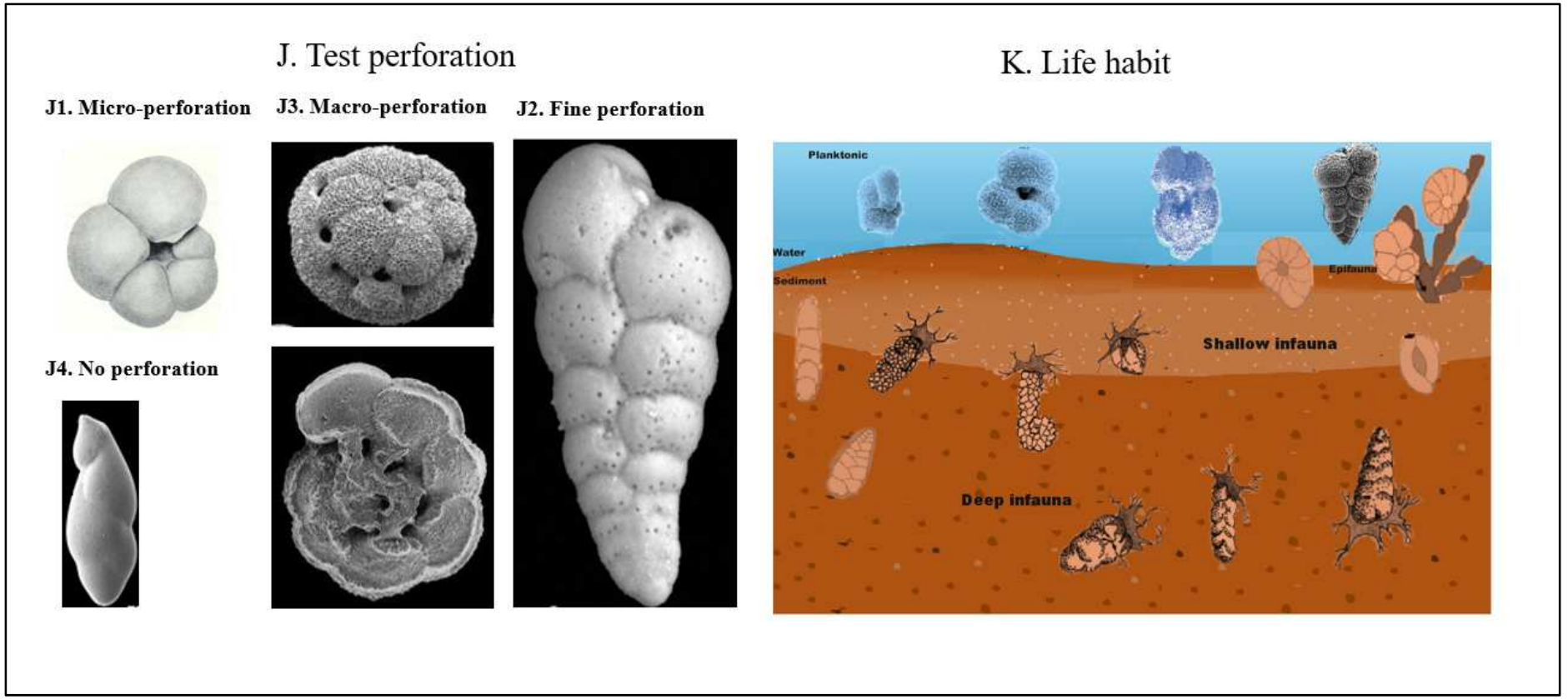

Figure 2.7. Micrographic representation of test perforation, life habits of foraminifera and their modalities

Table 2. 5: Example list of eight foraminiferal taxa from Site 1209B with the fuzzy trait coding for two (test shape and chamber arrangement) out of the 13 traits used for this study. See supplementary data in the appendix for the complete table.

Trait	A. Test Shape					C. Chamber arrangement					
Modality	A1. Spiral	A2. Elongate	A3. Globose	A4. Tubular	A5. Others	C1. Unilocular	C2. Uniserial	C3. Bi/Tri-serial	C4. Planispiral	C5. Trochospiral	C6. Others
Anomalinoides trinitatensis	1	0	0	0	0	0	0	0	0	1	0
Bolivina inconspicua	0	1	0	0	0	0	0	1	0	0	0
Quadrimorphina profunda	1	0	0	0	0	0	0	0	1	0	0
Oridorsalis umbonatus	1	0	0	0	0	0	0	0	0	1	0
Nuttallides truempyi	1	0	0	0	0	0	0	0	0	1	0
Gyroidinoides spp.	1	0	0	0	0	0	0	0	0	0.5	0.5
Laevidentalina spp.	0	0	0	1	0	0	1	0	0	0	0
Aragonia spp.	0	1	0	0	0	0	0	1	0	0	0

A fuzzy coding technique was used to express the affinity of different species to the associated traits modalities using a scale of 0.0–1.0 (Chevenet *et al*., 1994). The absence of an affinity of a particular trait was denoted with 0 whereas 1 was used to code a species that exhibited a high affinity to a trait (Table 2.5). This coding technique allows species that exhibited more than one modalities to be categorised according to their affinity (e.g. Table 2.5), however, all the categories must sum to one (Caswell and Frid 2013; 2015; 2016).

The information on the biological traits were sourced from the biological database such as WORMS – World Register of Marine Species: http://www.marinespecies.org, The Palaeobiology database http://palaeodb.org; Fossilworks http://fossilworks.org/ Pangaea https://www.pangaea.de/and Atlas of Paleogene Cosmopolitan Deep-Water Agglutinated Foraminifera http://nhm2.uio.no/norges/full/atlas/pecol_text.htmp and published literature (e.g. Holbourn *et al.,* 2013; Bolli *et al.,* 1994; Pearson *et al.,* 2006; Olsson *et al.,* 1999).The review of these data resources as well as morphometric measurements of specimens under the light microscope, and personal communications with experts on a range of taxa informed the coding of traits selected for this analysis based on extant analogues, their functional morphology, and occurrences within marine ecosystems.

The frequency of each traits' modality in the dataset was determined by multiplying the trait modality scores (e.g. Table 2.5) by the relative abundance of each species (see the foraminifera

abundance in the appendix) exhibiting those modalities in each sample. This was achieved by matrix multiplication (Charvent *et al*., 1998; Caswell and Frid, 2016). The product of the matrix multiplication was then used for statistical analysis (table 2.6; see the complete data in the appendix).

All the statistical analyses of both taxonomic abundance and trait composition were performed with PRIMER v.6 (PRIMER-e, Plymouth, UK). Prior to the statistical analysis, data were factorised into three to reflect the stages in the PETM (pre-CIE, CIE, Recovery) event. The pre-analysis treatment of the samples required standardisation of the species data which was transformed with Log (x+1) to reduce the influence of dominant species on the overall result. The similarities of both species and biological traits between samples were calculated using the Bray-Curtis index to create resemblance matrices. Non-metric multidimensional scaling (nmMDS) was used to visualise the similarities/differences in species and trait composition between the different stages of PETM. Species/taxa composition and biological trait composition were compared using Analysis of Similarity (ANOSIM), and subsequently, the similarity percentages (SIMPER) routine was used to identify which taxa or traits contributed the most to differences identified from the ANOSIM across the PETM. We used 50% data cut off for SIMPER result (as is the norm) in this study as any result higher than 50% does not make any significant difference (Clarke, 1993).

In reality, linking foraminifera traits to their ecological function is not as straight forward as it is in macrofauna (Bremner, 2008), nevertheless, traits such as test function as a protective tool and is known to reduce biological, physical and chemical stress in their environment (Armstrong and Brasier 2005). The test shape could indicate ecological adaptation and preference by foraminifera. Spiral tests have been associated with epifaunal habitats (Corliss and Chen, 1998), they are characterised by plano-convex – bi-convex trochospirally coiled tests with large pores (e.g. *Gavelinella beccarriformis*). The shallow infauna taxa (Figure 2.7) are usually elongate, uniserial to triserial chambered or planispirally coiled (e.g. Dentalinids or Buliminids) while the deep infauna are usually ovate (globose) to triserial and are dominated by imperforate taxa such as *Oolina globosa* and *Tappanina selmensis*.

Table. 2.6. An example list of the product of taxonomic composition and fuzzy coding using matrix multiplication

Depth Sample	A1. Spiral	A2. Elongate	A3. Globose	A4. Tubular	A5. Others	B1. Agglutinated	B2. Secreted: microgranular	B3. Secreted: Hyaline calcite	B4. Secreted: Hyaline aragonite	B5. Secreted: Porcellanous
110-111	55	58	0	2	0	2	2	62	14	36
111-112	40	89	0	0	0	0	1	94	18	16
112-113	50	62	0	3	0	3	0	69	21	22
113-114	41	89	0	0	0	0	2	94	12	22
114-115	43	84	0	1	0	1	0	89	15	23
115-116	46	82	0	1	0	1	1	88	17	22
116-117	43	89	0	0	0	0	1	90	16	25
117-118	47	81	0	0	0	0	0	88	25	16
118-119	48	82	0	1	0	1	0	83	19	28
119-120	46	74	0	0	0	0	0	81	23	15
120-121	49	70	0	2	0	2	0	72	21	25
121-122	42	86	0	1	0	1	1	95	18	14
122-123	55	65	0	0	0	0	1	72	33	15
123-124	48	72	0	1	0	1	2	82	25	12
124-125	63	48	0	2	0	2	1	54	49	6
125-126	58	56	0	1	0	1	3	64	37	11
126-127	60	49	0	0	0	0	2	59	39	8
127-128	59	47	0	0	0	0	2	63	41	0
128-129	48	72	0	0	0	0	3	75	38	4

Foraminifera test composition which varies from agglutinated materials to secreted calcite could indicate changes in the ambient environmental chemistry and composition (Holbourn *et al.,* 2013). The arrangement of the test chambers and their shape could also indicate ecological stress, for instance, change from sinistral to dextral or evolute to involute coiling in trochospiral test has been related to change in water temperature and bathymetry (Boltovskoy *et al*., 1991). Elements of test microstructure such as the macro-ornamentation (e.g. spines or muricae) could also reflect the mode of living and adaptation to surrounding water condition. Spinose species of living foraminifera are known to be symbiotic, harbouring photosynthetic alga-like dinoflagellates within their spines and gaining sufficient nutrient from them (Schiebel and Hemleben, 2017). The spinose species have wide dispersal capability and can spread across ocean basins. This particularly has made planktonic foraminifera a good tool for correlation and age dating across geological records.

More so, ornamentation in foraminifera play a huge role in feeding, adaptation to extreme environmental condition, movement as well as prey -predation relationship. A study by Dubicka *et al.*, (2015) demonstrated that foraminifera (*Haynesina germanica)* use body ornamentation to sort food particles into a different shape and sizes thereby removing harmful substances as well as disaggregating larger particles into smaller pieces before ingestion. The form of apertures, the presence of accessory structures and their primary position vary with changes in prevailing environmental conditions. For instance, at ambient water chemistry, *Haynesina germanica* had a well developed apertural face, teeth, tubercle and umbilical area but these features were difficult to identify in species found in extreme CO_2 and *p*H levels (Dubicka *et al.,* 2015).

The perforation of foraminiferal tests is a critical functional feature of the organism; they could be coarse (Figure 2.6) exceeding 10µm or fine ranging from 1µm to a few tenths of micro-millimetres (Dubicka *et al.,* 2015). Pores in foraminifera are used for gas exchange, osmoregulation, intake and release of nutrient and ecosymbiosis. Large pores are possessed by species in a well-oxygenated environment while species found in the low oxygen environment have smaller pores (Jorissen *et al.,* 2007). They allow the organism to attach to the hard substrate by secreting some organic adhesives through them.

Foraminiferal behavioural traits such as their life habit (whether they live infaunally or planktonically), feeding habit and mobility may indicate their level of tolerant to prevailing water chemistry, nutrient and oxygen concentration and other hydrodynamic conditions.

2.10. Taphonomical considerations

Most of the foraminiferal specimen especially in the CIE section indicated evidence of poor preservation. In the fossil record, original foraminifera tests are frequently found to be altered by test wall dissolution, fragmentation or diagenetic recrystallization. Foraminifera dissolution has been used as an evidence of lysocline/CCD shoaling during the PETM (Nguyen *et al.,* 2009; Petrizoo *et al.,* 2008). Some planktonic taxa such Acarinina was reported to relatively increase in abundance within the dissolution interval compared to Subbotina suggesting that Acrainina is more resistant to ocean acidification than Subbotina (Petrizoo *et al.,* 2008).

When foraminifera test is modified by taphonomic processes, the calcareous ones lose the original smooth and reflective surfaces which is responsible for the frosty and glassy appearance used in the qualitative characterisation of foraminifera test preservation under a light microscope. Previous studies showed that only a fraction (19%) of foraminifera test produced in the water column gets to the seafloor for preservation because of carbonate dissolution occurring within the undersaturated deep sea area (Berger, 1970; Schiebel et al., 2007). It is therefore important to set some background on the taphonomic processes that affected foraminifera during sedimentation, burial and preservation which is very crucial to the understanding of the organism's ecology.

After the death of foraminifera, they pass through series for test preservation issues such as abrasion, bioerosion, breakage, encrustation, and dissolution and cement degradation on transit through the water column to the final resting place, the sea floor. The chemical composition of the sea/pore water, test composition, size, perforations play a major role in the postmortem preservation of foraminifera (Nguyen *et al.,* 2009). The degradation of foraminifera test is primarily controlled by the nature of organic carbon mineralisation in the water column, other factors include, temperature, sedimentation rate and post-depositional diagenesis (Berkerley *et al.,* 2007).

Carbonate ion concentration in the sea water is the major factor that controls the preservation or degradation of foraminifera test in the ocean. The differences between the concentration of

Calcium (Ca^{2+}) carbonate (CO_3^{2-}) ions with the equilibrium value determines whether calcareous test will be precipitated or dissolved [$Ca^{2+}{}_{(aq)} + CO_3^{2-}{}_{(aq)} = CaCO_{3(s)}$.] Carbonate occurs in different forms in the ocean due to the continual dissolution of carbon dioxide and dissociation of hydrogen ions. Carbonic acid (H_2CO_3) dominates the seawater at pH values <6.0, bicarbonate (HCO_3^-) occurs within the pH range of 6.0-9.1 and carbonate (CO_3^{2-}) dominates at pH > 9.1(Krauskopf and Bird, 1995; Martin, 1999a) So any condition that increases the concentration of carbonic acid will favour the dissolution of calcium carbonate and foraminifera test [$CaCO_3 + H_2CO_3 = Ca_2 + HCO_3^-$]

In the sediment, the onset of taphonomic degradation of foraminifera starts with the continuous deposition of organic matter on the surface of the sediment (Berkerley *et al.,* 2007). The organic matter provides a chemical solution within the sediment that drives early diagenesis. At this point, the agglutinated foraminifera which make their test with predominantly organic matter and other detrital materials may begin to oxidised (Sexton *et al*., 2006). The new chemical state created by organic matter in the upper surface of the sediment column may also result to the dissolution of the calcareous foraminifera test. The degree of degradation or preservation resulting deposition of organic matter depends on the redox condition of the sediment i.e. oxic, hypoxic or anoxic.

Bacterial activities is another factor that contribute to the degradation of foraminifera after burial (Goldstein and Becker, 1998). The bacteria found on the wall of empty foraminifera test has been associated with thinning and fragmentation of test in the Georgia saltmarsh. In addition, temperature determines the rate of test preservation or degradation. High temperature leads to poor preservation especially in oxic environment while lower temperature results in good test preservation. This explains the nature of foraminifera test preservation found in the tropical Pacific and southern ocean during the PETM.

The sedimentation rate is very critical to the preservation potential of foraminifera. It controls the residence time of foraminifera in the organic layer. Rapid sedimentation in even in the oxic environment results in better quality preservation while slow sedimentation increase the residence time of the test within the organic matter layer hence results in poor preservation. Bioturbation has also been found to influence the preservation of foraminifera. Bioturbation increases control the oxygen concentration within the sediment column and rate of organic matter degradation. High bioturbated environment results in intense mixing and poorer

preservation. Low organism activities within the sediments result to lower sediment oxygenation and enhance better preservation (Sexton *et al*., 2006).

Foraminifera morphology, test size and composition has also been linked to their susceptibility to dissolution (Berger, 1970; Dittert *et al.,* 1999), species with small and thin walls with large pores are more susceptible to dissolution than those with big and thick walls with small pores (Sliter *et al.,* 1975). Also, surface dwellers and warm water-loving spinose taxa were reported to be more delicate and prone to dissolution while the cold- water non-spinose taxa are more resistant (Hemleben *et al.,* 1989). While the factors mentioned above are extrinsic to foraminifera test preservation, some factors which are intrinsic to individual species also play a significant role in the selective dissolution of specific species.

In general, a higher rate of organic matter and carbonate test degradation occurs in the oxic environment compared to anoxic one.

CHAPTER THREE

The PETM extreme climate impact on the benthic foraminiferal traits and ecological functioning in the tropical Pacific and Tethys Oceans

3.1 Introduction

The foraminiferal census data for this chapter has been previously published based on faunal turnover during the PETM from the Northeastern Pacific Ocean (ODP Sites 1209B and 1212B; Takeda and Kaiho, 2007) and pelagic marls exposed at Alamedilla, Spain (Alegret *et al.,* 2009). The census data were used to generate the trait compositions (new data) of all the benthic foraminifera taxa present in both sites. The taxonomic and trait compositions of the benthic foraminiferal assemblages from each site were analysed using biological trait analysis to examine changes in traits and ecological functioning during the PETM.

In this chapter, we present new results from the statistical analysis (BTA) of taxa and trait compositions as well as the age model for each site. We compare the changes in taxa and trait compositions in both basins in other to check for patterns in fauna and trait changes during the PETM.

3.2 Results

3.2.1. Age model for Sites 1209B and 1212B

The age model for sites 1209B and 1212B were based on the paleomag, sedimentation rate high-resolution biostratigraphic data and astronomically calibrated stratigraphic framework for the late Palaeocene-early Eocene period. The age model was developed by Bralower *et al.* (2002) and have been previously published by (Takeda and Kaiho, 2007). Presented in figure 3.1 is the summary of the chronostratigraphy of the studied sections of Sites 1209B and 1212B. The age model of both sites is presented together because they were drilled during the same expedition are close to each other.

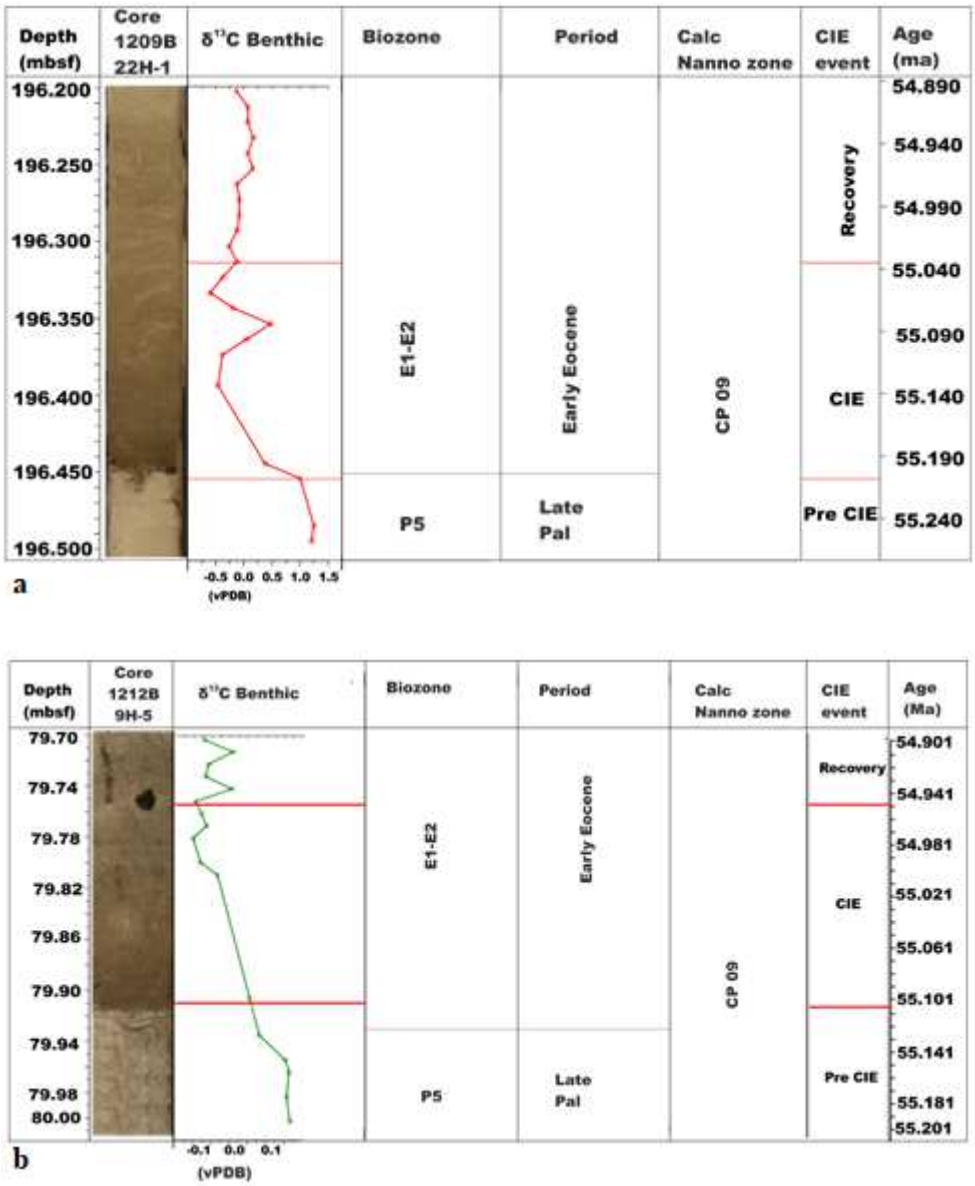

Figure 3.1: Integrated age model for Site 1209B (a) and Site 1212B. Also shown is the CIE sections interpreted from $\delta^{13}C$ isotope data.

3.2.2 Changes in taxonomic composition at ODP Site 1209B

The majority of the benthic foraminiferal assemblages recovered from Site 1209B are dominated by calcareous taxa and very few agglutinated forms such as *Bathysiphon* spp., *Spiroplectammina* spp., and *Tritaxia* spp. (Takedo and Kaiho, 2007). Epifauna taxa accounted for only 14% of the total faunal abundance and are characterised by *Anomalinoides, Cibicidoides, Oridosalis*, *Gavelinella and Gyroidinoides* taxa. Infauna morphogroup constituted over 80% of the total abundance and was dominated by the Buliminds with 50% of

the total abundance (Figure 3.2). The pre-CIE interval of the PETM in this location was characterised by a predominance of *Bolivina inconspicua*, *Bulimina kugleri, Paralabamina* spp., *Gavelinella* spp., *Gyroidinoides* spp., *Lenticulina* spp., *Siphogenerinoides brevispinosa*, *Fursenkoina* sp. and the Stilostomellids. Most of these taxa disappeared at the peak of the CIE (Takedo and Kaiho, 2007; Figure 3.2). The CIE interval was characterised by the acme of *Bolivina gracilis, Anomalinoides trinitatensis, Buliminella* cf. *beaumonti, Globocassidulina subglobosa, Quadrimorphina halli, Q. pacifica, Q. profunda, Quadrimorphina* sp. 1, *Tappanina selmensis* and *Bulimina bradburyi.* The recovery section recorded the highest relative abundance of foraminifera at ODP Site 1209B and was dominated by *Bulimina* spp., *Nuttallides truempyi, Bulimina bradburyi* and Pleurostomellid taxa. The detailed faunal composition has been discussed in Takedo and Kaiho (2007) and the focus here is on describing the changes in taxonomic composition in relation to changes in trait composition.

Non-metric multi-dimensional scaling (nmMDS) ordination of the recovered benthic foraminiferal assemblages (Figure 3.2) showed three clear taxonomic groupings during the pre-CIE, CIE and the recovery (Figure 3.3). ANOSIM values confirmed that the three groups significantly differed (global R= 0.693; $p<0.01$) and pairwise ANOSIM with $p<0.01$ showed that all the three groups significantly differed from each other. However, the faunal assemblages from 196.455, 196.445 and 196.435 mbsf were distinct from the other assemblages present during the CIE, being more similar to those from the pre-CIE interval, the recovery interval or dissimilar from all other assemblages respectively. This suggests that foraminifera assemblage from these depths were highly disturbed and represented the transition stages between the CIE.

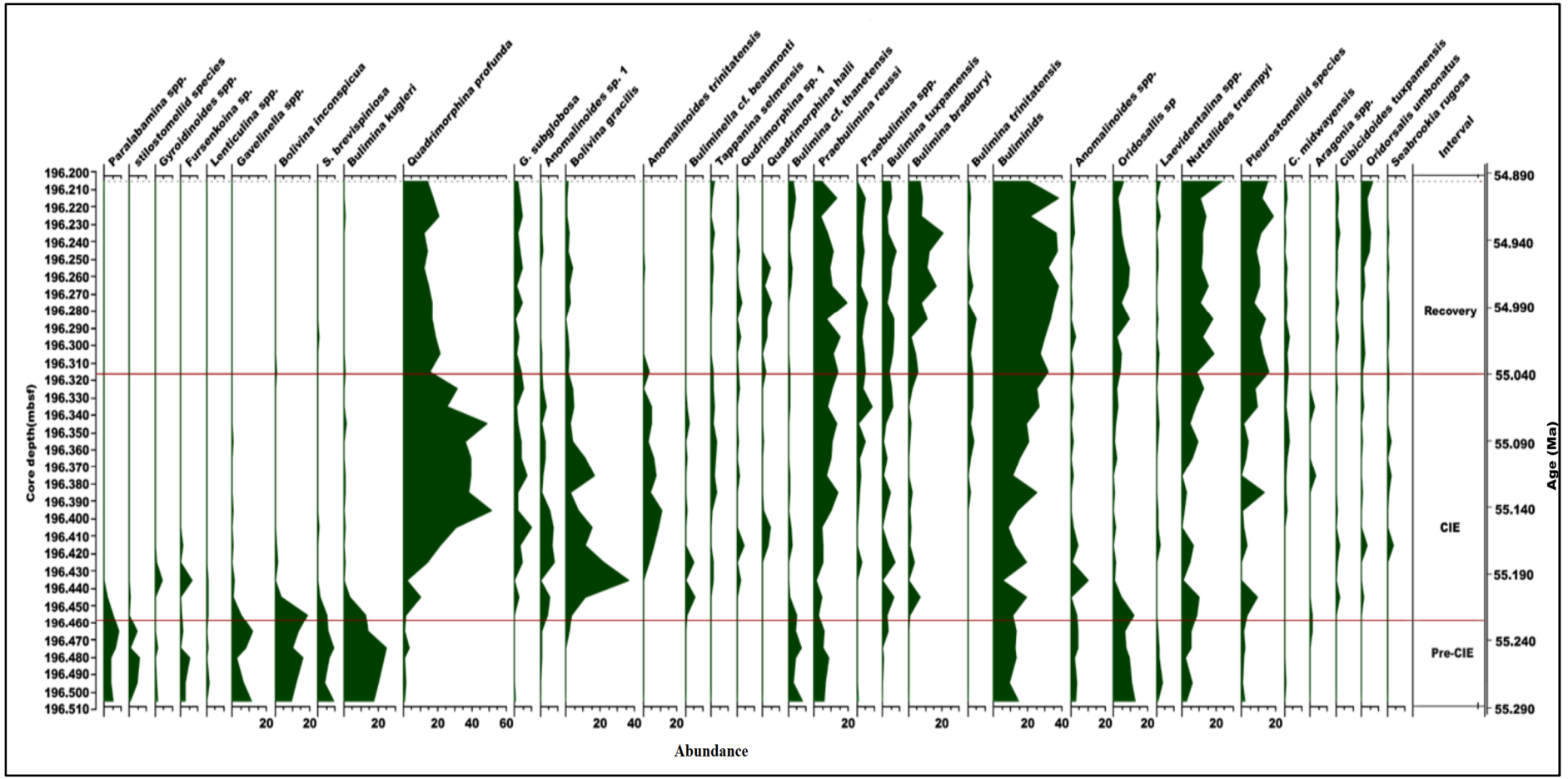

Figure 3.2: Benthic foraminiferal distributions across the PETM section at ODP Site 1209B. Sample depth in mbsf is plotted at the left-hand side while the age is plotted in the right-hand side. Pre-CIE (before the onset of the PETM); CIE (Peak of the PETM warming); Recovery (period of PETM recovery). The foraminiferal abundance data from Takeda and Kaiho (2007) were used to plot this chart.

Examination of the foraminifera census data (Takedo and Kaiho) showed that the sample from 196.435 mbsf yielded less than 100 foraminiferal specimens. The low faunal abundance of this sample could be due to the severe environmental changes that occurred at this point as this sample coincides with the benthic foraminiferal extinction event (BEE; Takeda and Kaiho, 2007).

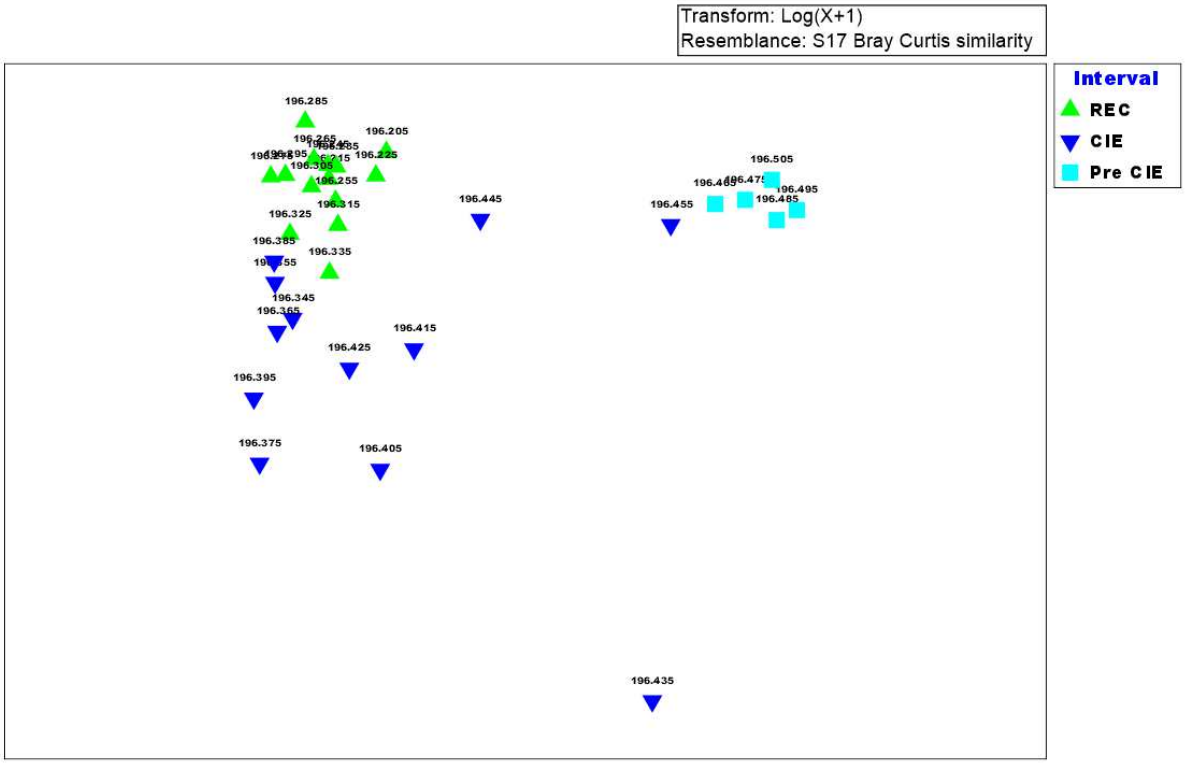

Figure 3.3: Non-Metric Multidimensional Scaling ordination of foraminiferal taxonomic composition (transformed with log x+1) of Bray-Curtis similarity from ODP Site 1209B on the Shatsky Rise, Pacific Ocean. The samples are grouped into three intervals according to the PETM events. Sample 196.435 indicates the position of the BEE.

Similarity percentage (SIMPER) analysis showed that 50% of the dissimilarity between the taxonomic composition of the foraminiferal assemblages present during the pre-CIE and the CIE intervals were attributable to differences in the mean abundance of five taxa only (Table 3.1). The taxa contributing most to the dissimilarity were *Quadrimorphia profunda* and *Bolivinia gracilis* which was 20-fold more during the CIE than at the pre-CIE. *Bulimia kugleri* that was also 20-fold less during the CIE than pre-CIE as well as *Bolivinia inconspicua* and *Oridosalis spp* which significantly decreased in abundance during the CIE (Table 3.2). During the recovery period, half as many *Quadrimorphia profunda* and ten-fold less *Bolivina gracilis*

occurred compared with the CIE period (Table 3.2). Whereas *Buliminids, Nuttalides truempyi* and *Pleurostomellid* spp increased. During the recovery, the assemblage differed from the pre-CIE in having less *B. kugleri* and *B. inconspicua,* Buliminids*, Quadrimorphina profunda*, *Pleurostomellid* spp. and *Nuttallides truempyi* than pre-CIE (Table 3.3).

Table 3.1: Site 1209B Similarity percentage (SIMPER) result of the average taxonomic abundance and their respective percentage contribution within the pre-CIE and the main CIE intervals (Data cut off 50.96 %). Numbers in bold highlight the higher of the two values.

Species	**Mean abundance**		**Contribution to dissimilarity (%)**
	Pre-CIE	**CIE**	
Quadrimorphina profunda	1.45	**27.66**	17.41
Bulimina kugleri	**20.27**	1.79	12.47
Bolivina gracilis	0.33	**11.87**	8.13
Bolivina inconspicua	**12.30**	2.08	7.63
Oridosalis spp.	**9.29**	1.92	5.31

Table 3.2. Site 1209B SIMPER results of the average abundance and their respective percentage contribution within the main CIE and recovery intervals. (Data cut off 52.8%)

Species	**Mean abundance**		**Contribution to dissimilarity (%)**
	CIE	**Recovery**	
Quadrimorphina profunda	**27.66**	17.96	14.58
Buliminids	14.92	**30.79**	13.63
Bolivina gracilis	**11.87**	1.83	9.04
Nuttallides	4.59	**13.39**	7.61
Pleurostomellid spp.	3.10	**11.41**	7.52

Table 3.3: ODP Site 1209B SIMPER result of the average taxonomic abundance of benthic foraminifera and their respective percentage contribution within the pre-CIE and the recovery intervals (Data cut off 53.39 %).

Species	**Mean abundance**		**Contribution to dissimilarity (%)**
	Pre-CIE	**Recovery**	
Bulimina kugleri	**20.27**	0.12	12.42
Buliminids	12.50	**30.79**	11.21
Quadrimorphina profunda	1.45	**17.96**	10.22
Bolivina inconspicua	**12.30**	0.07	7.55
Pleurostomellid spp.	1.14	**11.41**	6.35
Nuttallides truempyi	4.27	**13.39**	5.64

3.2.3 Changes in foraminiferal trait composition at ODP Site 1209B

Similar to the ordination for taxonomic composition, the trait composition (Figure 3.4) differed between the three intervals of the PETM (global R = 0.581, $p<0.01$). Pairwise ANOSIM indicated that the composition present during the recovery period significantly differed ($p<0.01$) from both those preceding it. The trait assemblages present during the pre-CIE significantly differed from those present during the CIE although at lower significance ($p<0.01$). Overall trait composition during the recovery was more similar to the CIE than at the pre-CIE (Figure 3.4) as was the case for taxonomic composition. The trait composition of samples from depth 196.455, 196.435 and 196.445 mbsf were also of distinct trait composition from the other samples from during the CIE just like in taxa. This suggests that the trait composition did not change until after ~390 ka (sample 196.445 mbsf, Figure 3.4; Takeda and Kaiho, 2007) at Site 1209B. This was 100 ka after the benthic foraminiferal extinction event (Takeda and Kaiho, 2007).

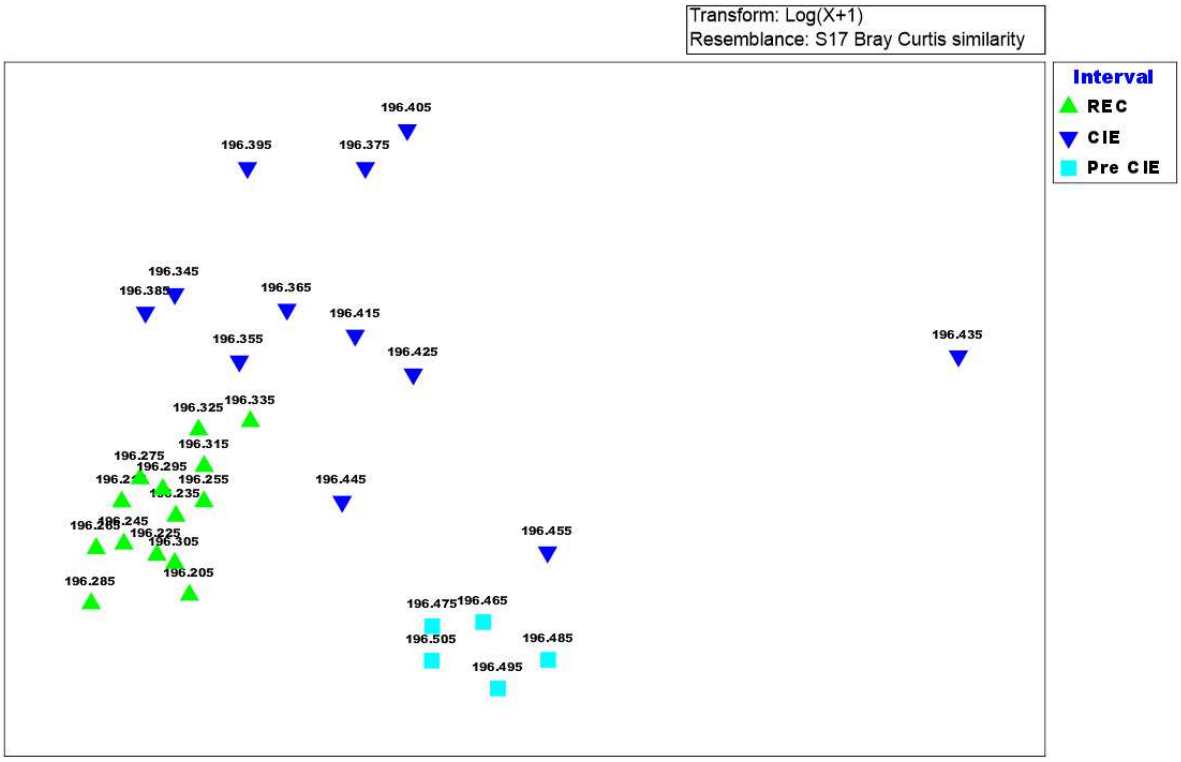

Figure 3.4: Non-metric Multidimensional Scaling ordination of foraminiferal traits composition (transformed with log x+1) of Bray-Curtis similarity from ODP Site 1209B on the Shatsky Rise, Pacific Ocean. The samples are grouped into three intervals according to the CIE events. The outlier 196.435mbsf indicates the position of BEE.

SIMPER results showed that 19 traits contributed to 50% of the dissimilarity between intervals (Figure 3.5) all of which were more abundant during the recovery as opposed to pre-CIE, these included spiral and elongate tests; hyaline calcite and hyaline aragonite tests; bi/triserial and planispiral chamber; spherically shaped chambers, depressed sutures, costae ornamentation, fine perforations and bifid teeth. Foraminifera with apertures at the terminal and umbilical positions that lived a sessile lifestyle, and shallow – deep infauna also contributed significantly to the dissimilarities. The mean abundance of foraminifera with spiral coiling, hyaline aragonite test, planispiral chamber arrangement, no apertural accessories, aperture at the umbilical position and live shallow infauna were higher during the CIE than at any other interval of the PETM.

After the CIE, the benthic communities seem to become more successful than before the CIE, as shown by the high abundance of most of the trait modalities at the recovery (Figure 4.4). The higher abundance of the traits at the recovery interval may be due to the bloom of foraminifera after the hyperthermal. This could be related to the optimum ambient condition and increased nutrient reaching the ocean from enhanced continental weathering. The higher relative abundance of hyaline calcite tests after the CIE could be due to increased carbonate preservation after the event. While the high mean abundance of shallow infauna during the CIE may imply that some deep benthic taxa migrated or changed their habitat to live in the upper sediment column due to low oxygen in the sediment.

Benthic foraminiferal trait distribution from the raw data (Figure 3.6) indicates high variability in the predominant traits across the PETM. The pre-CIE trait composition was dominated by a high relative abundance of globose taxa, tubular shaped chambers, species with apertural necks and uniserial test arrangements (Figure 3.6). Taxa with shallow infaunal habits were more common before compared with during or after the CIE. However, during the main interval of the CIE the relative proportions of species with hyaline aragonite tests, planispiral chamber arrangement, raised sutures, umbilical apertures, shallow infaunal habits, grazing and free-living lifestyle increased. There was a distinct switch from predominantly hyaline calcite (~60% of the assemblage in approximation) and porcellanous tests to hyaline aragonite (the latter of which was markedly absent before the event) tests during the CIE. However, hyaline calcite tests also remained common during the event (Figure 3.6). Taxa with elongate shapes, hyaline calcite tests, costate ornamentation, terminal apertures and suspension feeding habits decreased during the CIE (Figure 3.6). During the recovery interval immediately after the CIE, the trait composition was characterised by blooms of foraminifera with elongate shapes, bi/triserial chamber arrangement, hyaline calcite tests, with fine perforations, apertural teeth, terminal aperture, deep benthic, sessile and suspension feeding habits. Taxa with porcellanous tests increased. Those with hyaline aragonite tests, raised sutures, umbilical teeth, macro-perforation, and shallow infaunal lifestyle also decreased during this interval.

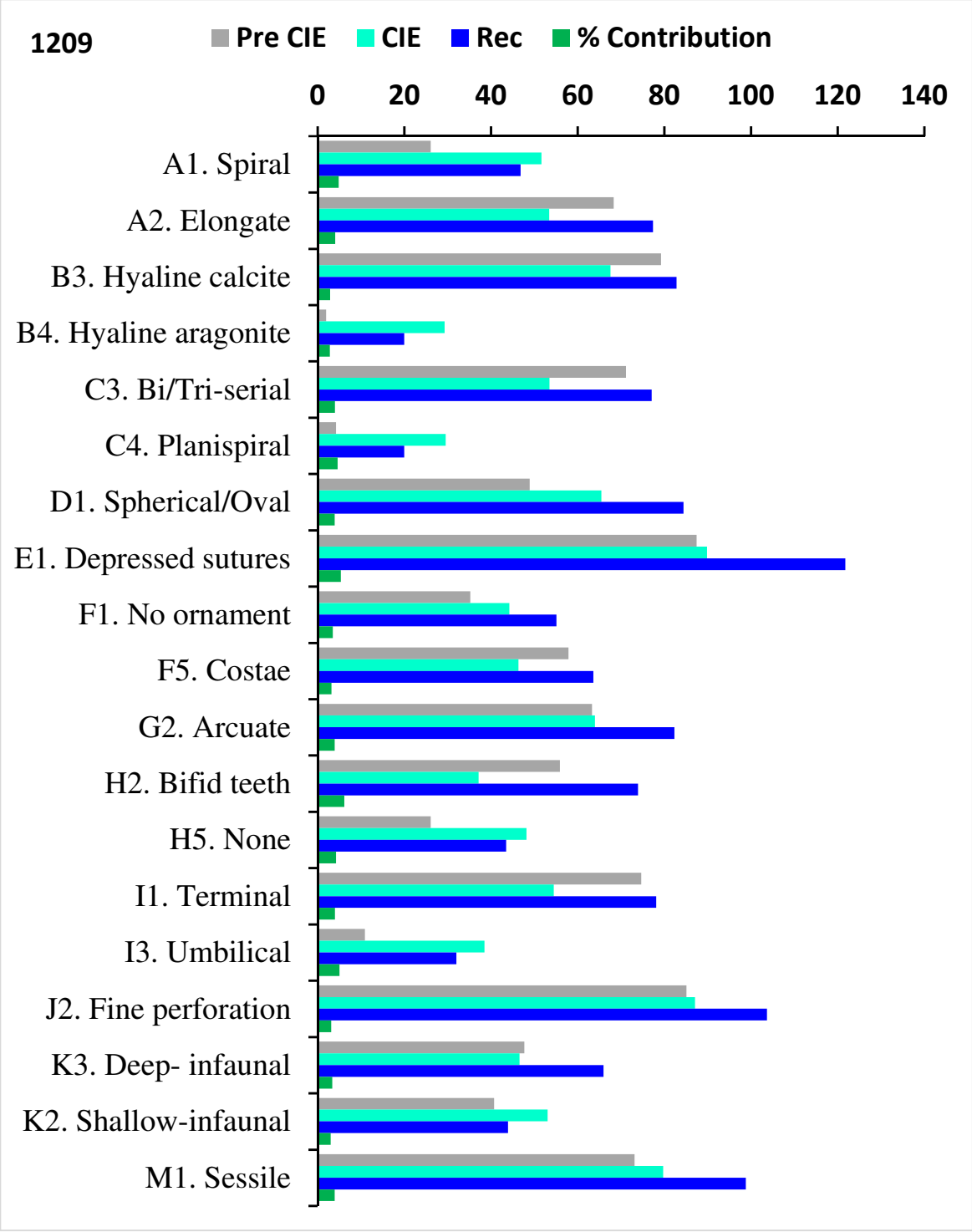

Figure 3.5: Similarity percentage (SIMPER) showing traits that cumulatively contributed ~50% to the differences in benthic foraminiferal trait composition across the CIE events at Site 1209B. Grey bars = Pre-CIE; sky blue bars = CIE core; deep blue bars= Recovery; green bars = % contribution that each trait modality is making to the overall similarity.

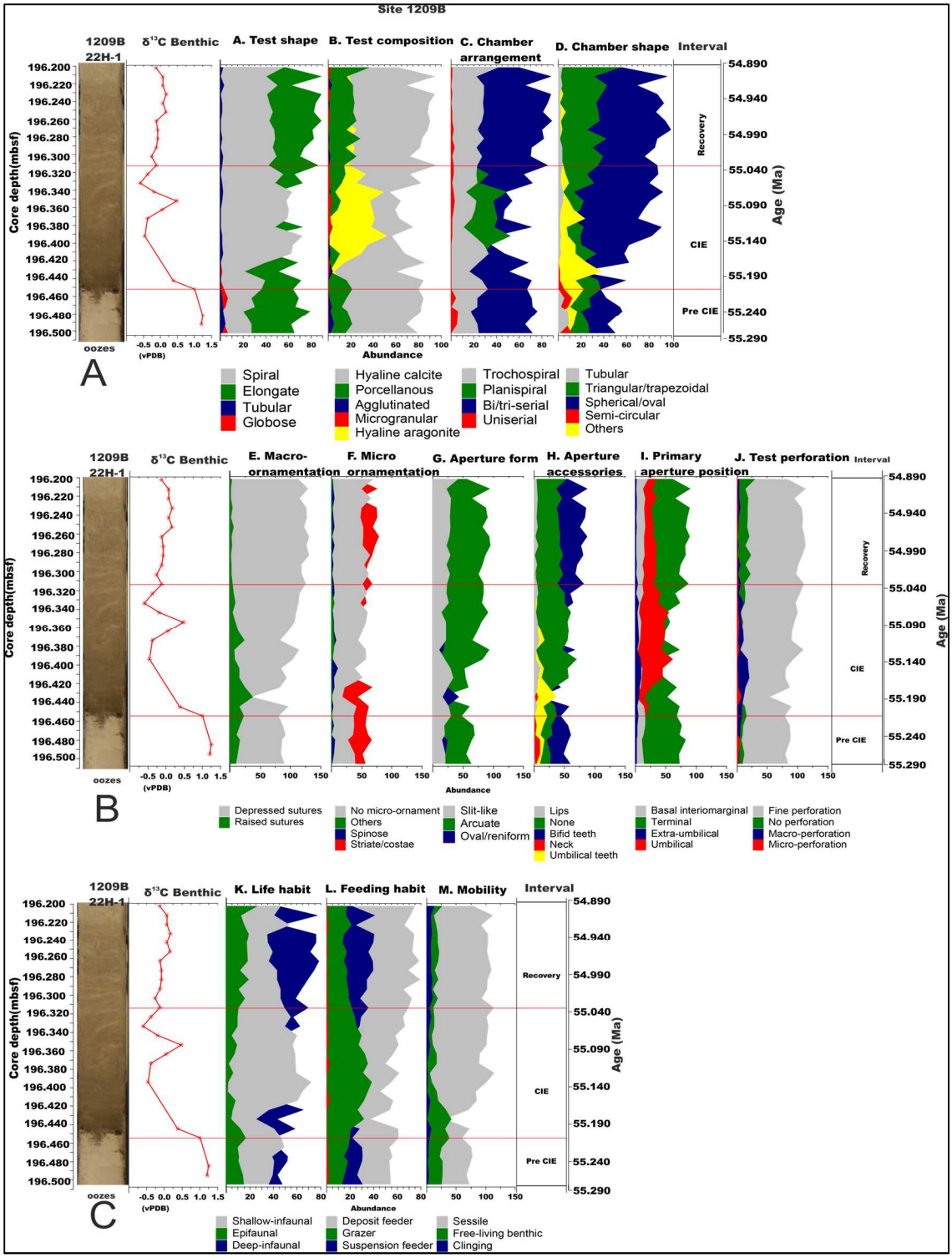

Figure 3.6: Changes in the traits of benthic foraminifera across the PETM events at Site 1209B in the Shatsky Rise, Pacific Ocean. On the left: Core depths, lithology and carbon isotope record (derived from benthic foraminifera; Takeda and Kaiho, 2007). The numerical age is plotted on the right-hand side of the figure. A. Shows traits for test composition and morphology. B. Test ornamentation and aperture traits. C. Traits associated with life habit. The lithostratigraphy is not to scale but was used to indicate the changes in the calcareous oozes coeval to the PETM

3.2.4. Changes in taxonomic composition at ODP Site 1212B

The recovered taxa from Site 1212B were dominated by cosmopolitan foraminifera, mostly of calcareous test wall (Figure 3.7). The foraminiferal census data (Figure 3.7) showed that *Siphogenerinoides brevispinosa,* Stilostomellids*, Bulimina kugleri and Bolivina inconspicua* were present at the pre-CIE section but disappeared during the PETM. However, *Quadrimorphina profunda, Tappanina selmensis, Bolivina gracilis, Anomalinoides trinitatensis* and *Laevidentalina* spp. recorded their highest abundance during the CIE while *Eponides elevata* was a local excursion taxon that appeared towards the end of CIE. The details of faunal distribution as retrieved from the supplementary data of Takedo and Kaiho, (2007) is plotted on the distribution chart shown in figure 3.7 below.

The ordination of samples from Site 1212B in the nmMDS (Figure 3.8) showed three distinct groupings with global R =0.649, and that each group significantly differ from the other at $p<0.01$. The pairwise ANOSIM tests for the three intervals showed that the taxonomic composition of the assemblage significantly differs as follows: recovery and CIE R= 0.317, $p<0.02$; recovery and pre CIE R= 1, $p< 0.02$; CIE and pre CIE R= 0.683; $p<0.1$. During the CIE there was a wider separation between samples (SIMPER, 53% similarity) compared with the pre CIE (SIMPER, 74% similarity) or the recovery (SIMPER, 76% similarity). This may be due to the high level of ecological stress recorded during the PETM warming

The nmMDS plot also showed six subgroupings: one each for the pre-CIE and the recovery, and four subgroups for the CIE. These subgroupings of samples during the CIE could imply that there may have been a number of distinct environmental changes during the PETM. Overall ordination shows a horseshoe (Figure 3.8) structure proceeding from the pre-CIE, through several substages of the CIE, and then the recovery. The recovery samples showed a clear separation from the pre-CIE and CIE groups.

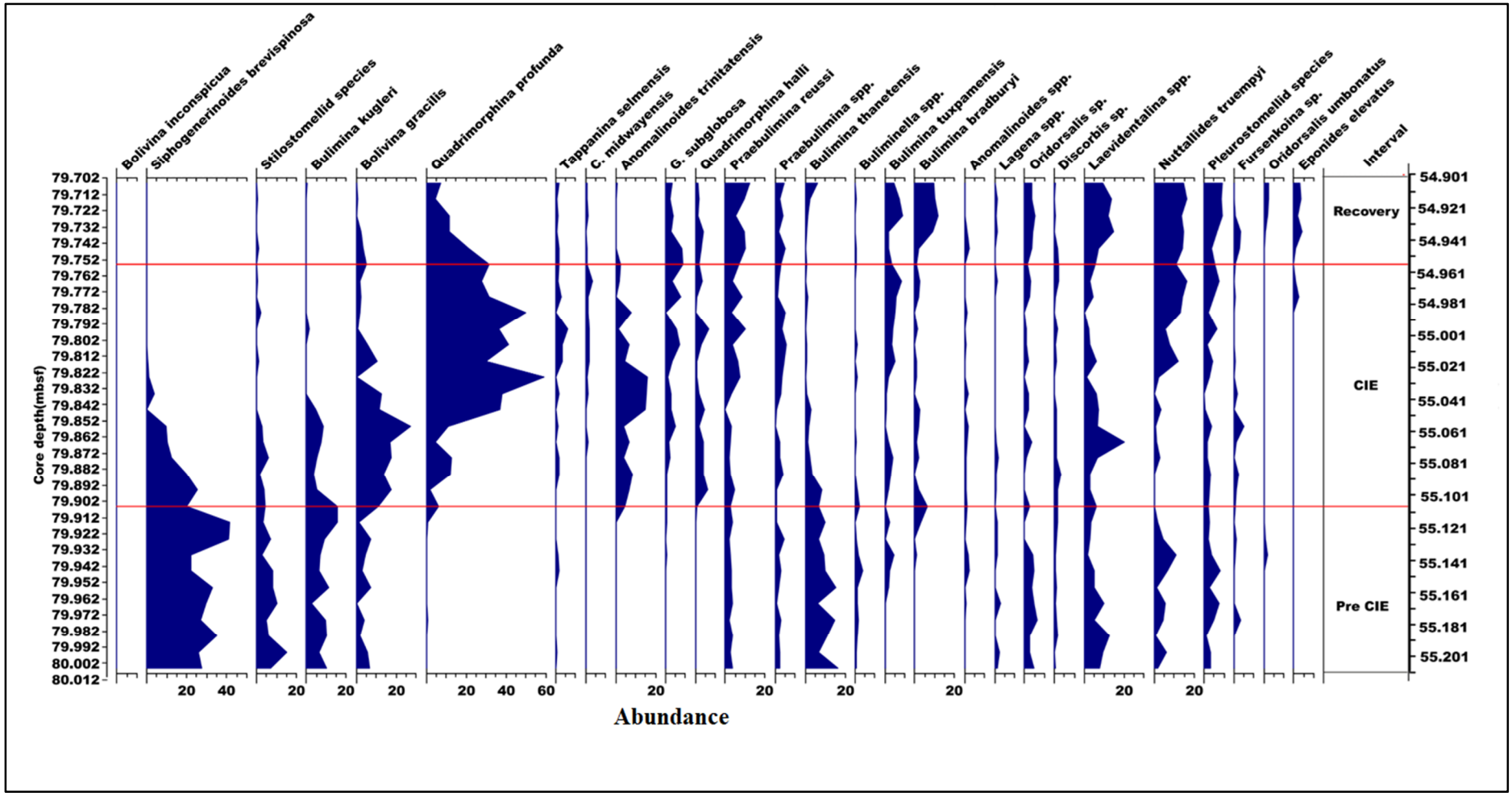

Figure 3.7: Benthic foraminiferal distribution across the PETM at ODP Site 1212B. Sample depth in mbsf is plotted on the left-hand side while the age is plotted in the right-hand side.

Depth 79.745 mbsf which was classified within the recovery interval (using the carbon isotope curve) but ordinated with one of the CIE groups, meaning that it was similar in composition to this subgroup of the CIE than the recovery. The transitional nature of the sample from 79.745 mbsf suggests that even although $\delta^{13}C$ may have started to recover to the background levels, the benthic communities were yet to recover from the ecological stress caused by the hyperthermal.

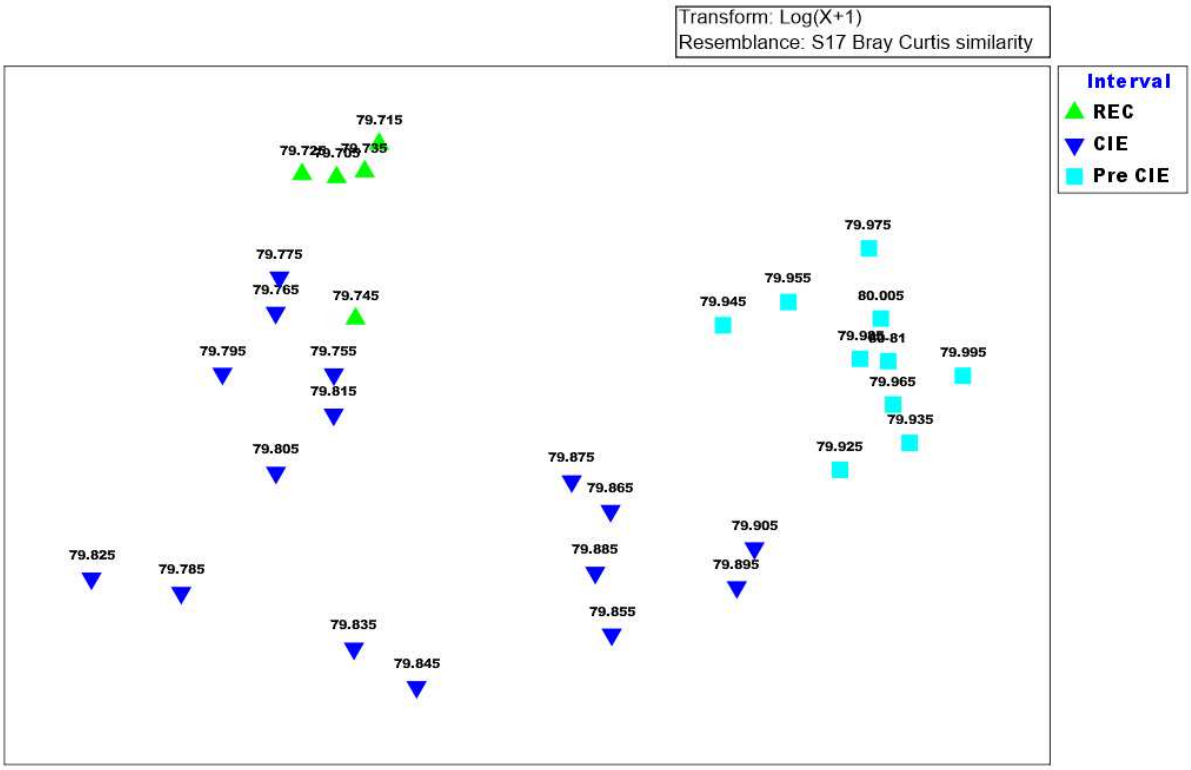

Figure 3.8: Non-Metric Multidimensional Scaling ordination of foraminiferal taxonomic composition (transformed with log x+1) of Bray-Curtis similarity from Site 1212B on the Shatsky Rise, Pacific Ocean. The sample groupings indicate taxonomic relationship across the CIE events. The dispersal in the CIE interval could indicate biotic disturbance.

Results of the SIMPER showed that only five taxa accounted for 56% of the dissimilarity between the CIE and recovery interval (Table 3.4). During the CIE there were relatively higher abundances of *Q. profunda* and *Bolivina gracilis*, whereas, during the recovery Buliminids, Pleurostomellids and *N. truempyi* were two-four times more abundant (Table 3.4).

The four taxa that accounted for 50% of the dissimilarity between the pre-CIE and the CIE were *Bulimina thanetensis*, *Siphogenerinoides brevispinosa, Quadrimorpha profunda* and *Bolivinia gracilis. Bulimina thanetensis* and *Siphogenerinoides brevispinosa* were more

abundant during the pre CIE while *Quadrimorpha profunda* and *Bolivinia gracilis* were more abundant during the CIE (Tables 3.5; 3.6). The differences in abundance of *Siphogenerinoides brevispinosa* and *Quadrimorpha profunda* together accounted for about 40% of the dissimilarity between the two intervals.

The taxonomic composition of the recovery interval differed from the pre-CIE by containing more Buliminids, Pleurostomellids, *Q. profunda* and *N. truempyii*. In contrast, pre-CIE had higher abundances of *B. kugleri* and *B. inconspicua* (Table 3.6) than the recovery.

Table 3.4: Mean abundance of taxa contributing to the most dissimilarity between the recovery and the CIE intervals (56% cut off) at Site 1212B

Species	**Mean abundance**		**Contribution to dissimilarity (%)**
	Recovery	**CIE**	
Quadrimorphina profunda	11.39	**26.89**	18.29
Nuttallides truempyi	**14.61**	5.68	8.81
Bolivina gracilis	1.32	**9.76**	8.50
Laevidentalina spp.	**11.40**	5.18	7.09
Bulimina bradburyi	**8.33**	1.50	6.73
Siphogenerinoides brevispinosa	0.00	**6.39**	6.20

Table 3.5: Mean abundance of species contributing to the most dissimilarity between the recovery and the pre-CIE intervals at Site 1212B (54% cut off)

Species	**Mean abundance**		**Contribution to dissimilarity (%)**
	Recovery	**Pre-CIE**	
Siphogenerinoides brevispinosa	0.00	**30.44**	23.85
Quadrimorphina profunda	**11.39**	0.32	8.68
Nuttallides truempyi	**14.61**	4.34	8.03
Bulimina kugleri	0.07	**8.67**	6.72
Bulimina thanetensis	2.23	**10.75**	6.66

Table 3.6: Mean abundance of species contributing to the most dissimilarity between the CIE and the pre-CIE intervals at Site 1212B (55% cut off).

Species	Mean abundance		Contribution to dissimilarity (%)
	CIE	Pre-CIE	
Quadrimorphina profunda	**26.89**	0.32	21.81
Siphogenerinoides brevispinosa	6.39	**30.44**	19.79
Bulimina thanetensis	2.02	**10.75**	7.20
Bolivina gracilis	**9.76**	4.20	6.21

3.2.5. Changes in foraminiferal trait composition at ODP Site 1212B

The nmMDS ordination of trait composition showed that the pre-CIE, CIE and recovery intervals were clearly separate from each other (Figure 3.9) and ANOSIM showed that they significantly differed at global R = 0.542 and $p<0.01$. The section analysed during the recovery was short and did not show a significant change in the areal diagram (Figure 3.11)

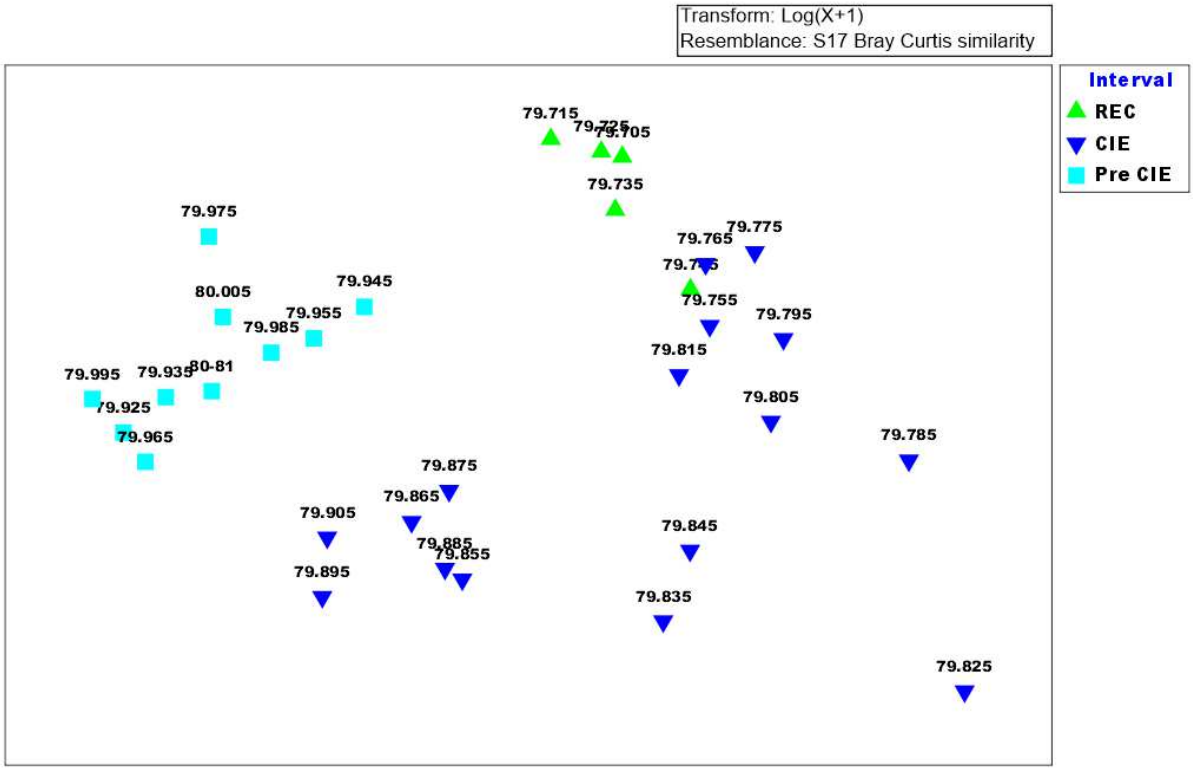

Figure 3.9: Non-metric Multidimensional Scaling ordination of foraminiferal traits composition (transformed with log x+1) of Bray-Curtis similarity from Site 1212B on the Shatsky Rise, Pacific Ocean. The widespread of the CIE trait composition was a reflection of the faunal turnover during the PETM. The outlier 79.825mbsf indicates the position of BEE.

Pairwise ANOSIM showed that the trait composition of the assemblage present during the pre-CIE and the CIE differed significantly at $p<0.01$. The recovery and CIE also differed but at lower significance ($p<0.04$). During the CIE, samples were highly variable as shown by the lowest percentage (79%) in SIMPER group similarity, the pre CIE samples were 88% similar, and the recovery sample similarity was 91%.

The nmMDS for trait composition was very similar to that of the taxonomic composition. The main CIE ordinates in three subgroups (Figure 3.9) with samples from depth 79.865 – 79.895 mbsf ordinating within one subgroup, samples from depth 79.755 – 79.815mbsf clustered fairly together, and depth 79.835mbsf -79.845 mbsf formed the third subgroup between the other two CIE subgroups. Samples from depth 79.785mbsf and 79.825mbsf lay separately from the rest (Figure 3.9). The clustering of the CIE samples into three groups could be an evidence of environmental perturbation during the hyperthermal, and the outlier (sample 79.825mbsf) marks the BEE interval.

Trait distribution deduced from raw data before statistical analysis (Figure 3.11) indicated that species with spiral test shape, hyaline aragonite, and planispirally test blossomed during the main period of the CIE when global temperature was highest. A coeval increase in species with tubular shape, arcuate apertures, fine perforations, shallow infaunal life habits as well as sessile lifestyle was also recorded at the CIE interval. While species with elongate tests, agglutinated forms, uniserial chamber arrangement, terminal apertures, and macro-perforation increased in relative abundance at the pre-CIE but their abundance plummeted drastically with further warming close to the CIE section.

The similarity percentage analysis (SIMPER) showed that 24 trait modalities accounted for 50% of the dissimilarity between the three PETM subdivisions (Figure 3.10). Six traits predominated at the pre-CIE, these include elongate tests, uniserial chamber arrangements, terminal apertures with neck, agglutinated tests, micro perforation and semi-circular chamber shape. Taxa with spiral tests, hyaline aragonite, fine perforation, planispiral coiling, umbilical apertures, no ornament, arcuate shaped apertures and grazers that live in the shallow infauna niche were more abundant during the CIE (Figure 3.10). The recovery interval recorded the highest abundance of the porcellanous test, trochospiral test shape, triangular/trapezoid chambers, slit-like apertures, and basal interiomarginal apertural position, non-perforated test and deposit feeders. During the period of recovery, almost all the species with macro-

perforations in their test and semi-circular chambers that was present during the pre-CIE had disappeared from the trait composition (Figure 3.10).

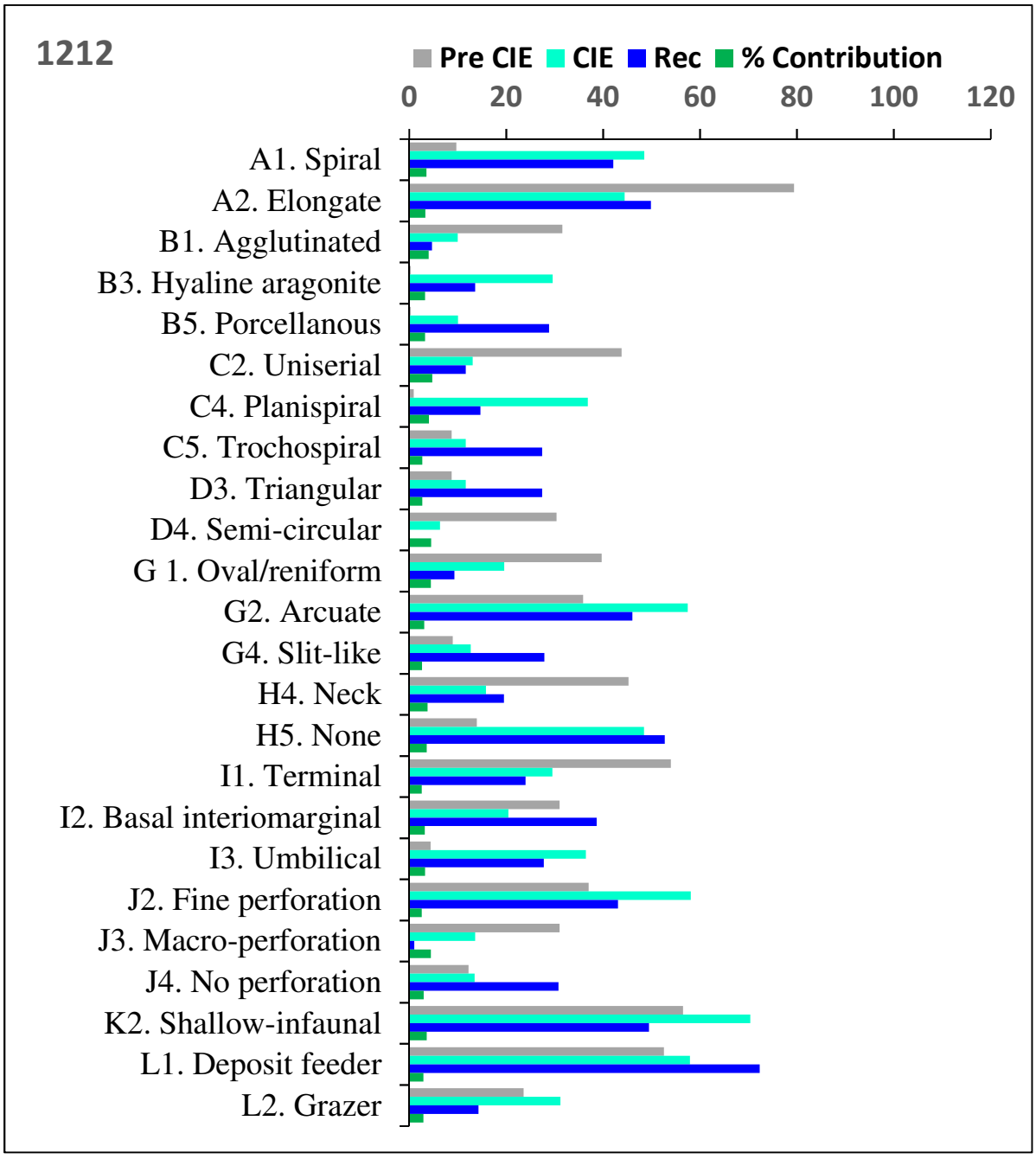

Figure 3.10: SIMPER result of the most significant trait (at 50% cut off) that contributed to the differences in benthic foraminiferal trait composition across the CIE events at Site 1212B. Grey bars = pre-CIE; sky blue bars = CIE core; deep blue bars= Recovery; green bars = % contribution of each trait.

Other trait modalities that were predominant at the pre-CIE but decreased in abundance during the recovery include elongate shape, uniserial test arrangement, terminal apertures, and

agglutinated tests (Figure 3.10). Nevertheless, there was an increase in taxa with deposit feeding habit, umbilical apertures and spiral test during the recovery.

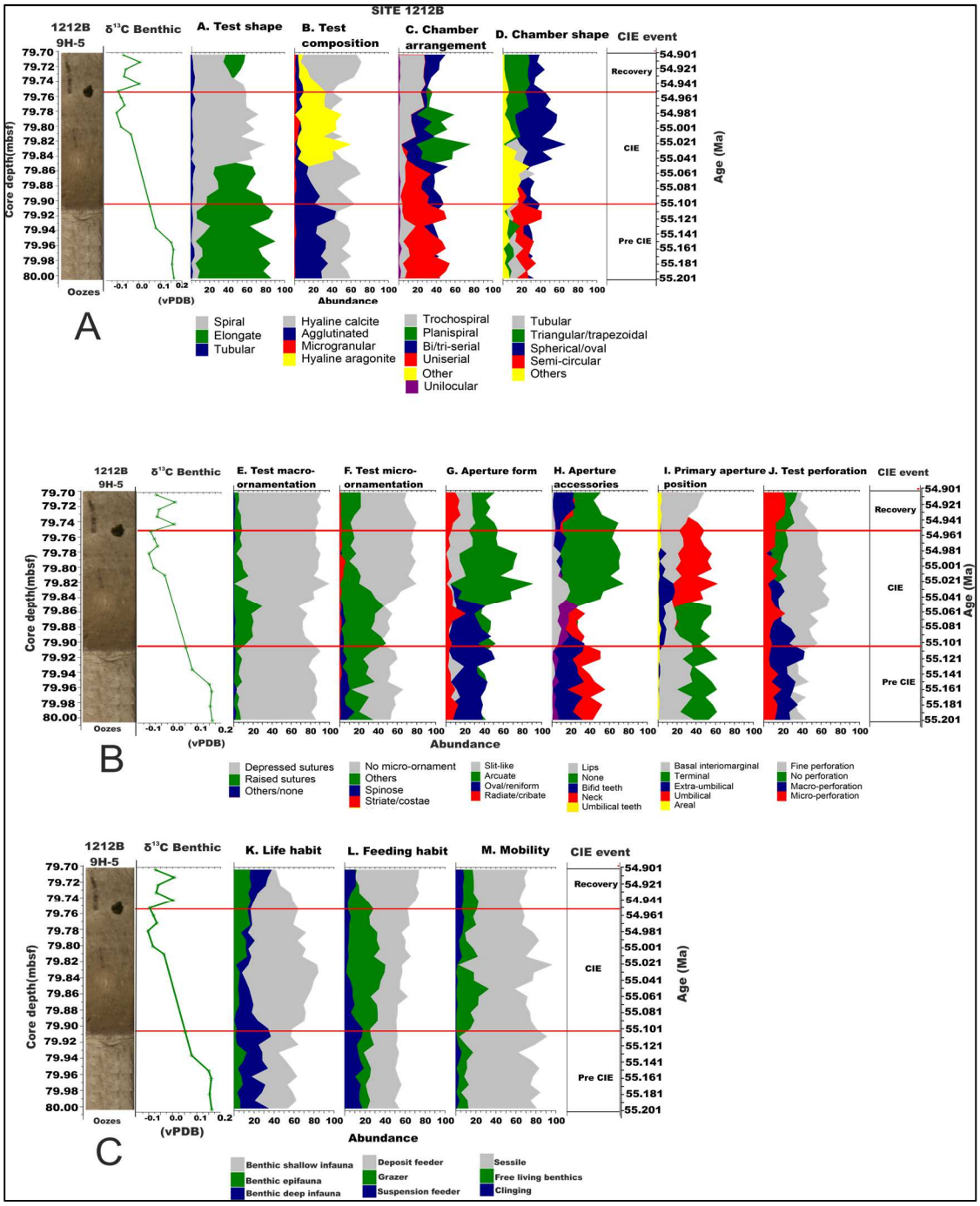

Figure 3.11: Benthic foraminiferal trait composition and distribution of the CIE events at Site 1212B. On the left: Core depths, lithology and carbon isotope record (derived from benthic foraminifera) used in association with other data to determine the CIE event. The numerical age is plotted on the right-hand side of the figure. A. shows the test composition and morphologically related traits. B. Contains ornamentations and aperture related traits C. Traits associated with the life habit. The lithostratigraphy s not to scale but was used to indicate the changes in the calcareous oozes coeval to the PETM.

The most affected traits at Site 1212B during the peak of the CIE were trochospirally coiled, semi-circular chamber shape, benthic epifauna and suspension feeding taxa as shown in the raw data (Figure 3.11). However, species with sessile lifestyle, deposit-feeding habit and depressed sutures did not show any significant changes across the studied interval and these could be the traits that sustained ecological functioning during the hyperthermal (Figure 3.10)

3.2.6 Alamedilla age model

The age model for the Alamedilla section was derived from a combination of planktic foraminiferal and calcareous nannofossil zones identified by Arenillas and Molina (1996), Molina *et al*. (1999) and Monechi *et al.* (2000). The timing of the CIE was inferred by comparing the shape of δ^{13} C bulk carbonate isotope from Alamedilla sediment to similar isotope record from ODP Site 690, where Rohl *et al.* (2007) developed a high-resolution age model using cyclostratigraphy.

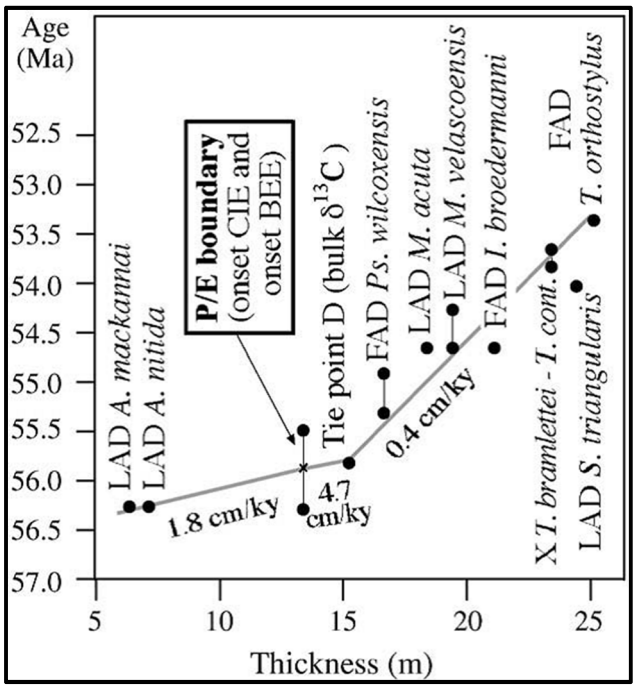

Figure 3.12: Age model for Alamedilla outcrop based on the integration of biostratigraphy, isotope stratigraphy derived from ODP Site 690 and Leg 208 (Alegret et al., 2009). A = Acarinina; I = Igorina; M = Morozovella; Ps = Pseudohastigerina; S= Subbotina; T=Tribrachiatus; T. cont=T. contortus. Numerical ages and sedimentation were inferred from ODP Leg 208. LAD = Last appearance datum, FAD = First appearance datum

Six inflecting points were chosen from the $\delta^{13}C$ record on the assumption that the kicks reflect inputs and sinks of light carbon during the PETM (Algret *et al.,* 2009). The P/E boundary was designated as 0 ky to mark the datum for this age calibration. Point A-F in figures 2.4 and 3.12 reflects the age estimation base on the correlation with Site 690. The isotope stratigraphy correlation of Alamedilla section and Site 690 is not very robust due to differences in sample resolution. The absolutes age and sedimentation rates for Alamedilla section was extrapolated from the timescales applied to ODP Leg 208 (Zachos *et al.*, 2005; Algret *et al.,* 2009). The absolute is shown in figure 2.4.

3.2.7 Changes in taxonomic composition at Alamedilla section

The fauna composition in Alamedilla indicated highly diverse and rich assemblages especially in the section before the CIE. About 117 species and over 6000 specimens of foraminifera were counted from this location (Alegret *et al*., 2009). The foraminiferal assemblage was dominated by calcareous taxa accounting for about 85% while the agglutinated taxa were about 15% of the overall count. The details of foraminifera composition at Alamedilla is contained in appendix 3 as the volume could not allow it to be displayed here. The most common morphogroup was the infauna comprising mostly of taxa from the superfamily Buliminacea (*Aragonina Bolivina, Brizalina, Bulimina, Buliminella, Coryphostoma, Dorothia, Fursenkoina, Marsonella, Praebulimina, Quadratobuliminella, Siphogenerinoides, and Tappanina)* and the *Abyssamminids.* The epifauna taxa consisted of *Cibidoides, Globocassidulina, Gyroidinoides, Nonion, Nuttallides, Oridorsalis, Pullenia* and *Stensioena* (a.k.a. *Gavellinella*). The pre-CIE interval has the highest species richness and abundance, but more than 26 species that existed within this interval went into extinction during the CIE.

Some of the taxa that disappeared during the CIE include; *Angulogavelinella avnimelechi, Anomalinoides rubiginosus, Arenobulimina truncata, Bolivinoides delicatulus, Cibicidoides species, Coryphostoma midwayensis, Dorothia pupa, Gyroidinoides subangulatus, Marssonella oxycona, Neoflabellina jarvisi, Nuttallinella florealis, Osangularia velascoensis, Pullenia coryelli, Siphogenerinoides brevispinosa* and *S. beccarriformis (*Alegret *et al.,* 2009*).* The species richness decreased upward from the pre-CIE to the recovery. The CIE interval was characterised by the prevalence of *Anomalinoides spp., Globocassidulina subglobosa, N. truempyi, O. umbonatus, Osagulina spp., Q. profunda, T. selmensis* and *Trochamminids*. Only three samples were analysed during the recovery interval and this must have been responsible

for the fewer species recorded within the section. Species of Abyssaminid*s*, Bolivinoides, *Cibicidoides pseuodoperlucidus, Lenticulina* spp., *Nonion* spp., and *Quadrimorphina profunda* exhibited "resurrection attribute" at the CIE interval. They appeared before the CIE, disappeared during the peak of the CIE and reappeared after the warming. This means that the reproduction of these species may have dropped significantly during the PETM but were not totally wiped out. Nevertheless, the acme of *Anomalinoides spp, Aragonia aragonensis,* Buliminids, *Globocassidulina subglobosa, Laevidentalina spp., N. truempyi, O. umbonatus, Osangularia spp., Paralabamina hillbrandti, Q. profunda Repmanina charoides, T. selmensis* and *Trochaminids* occurred at the CIE interval (Alegret *et al*., 2009 and appendix 3).

The nmMDS plot of foraminiferal taxa abundance in Alamedilla showed that only the pre-CIE samples were clearly separated from the rest of the intervals (Figure 3.13). The depths (13.5, 13.6 and 13.7 mbsf) representing the early stage of the CIE coeval to the BEE distantly ordinate away from the rest of the group while sample 15.40 mbsf designated as the recovery based on the carbon isotope clustered with the CIE group. This left only two out of the three recovery sample ordinated together. The sample ordination could mean that foraminifera from sample 15.40mbsf designated as a recovery interval was still having the impact of the hyperthermal. The CIE outliers indicate the depth with very few agglutinated taxa and absence of calcareous foraminifera. The absence of calcitic taxa at this depth was due to the massive carbonate dissolution associated with the PETM.

The ANOSIM value (global r=0.624; $p<0.01$) showed that the pre-CIE, CIE and recovery intervals significantly differed in taxonomic composition, while the pairwise ANOSIM showed that all three groups significantly differed except when the CIE and the recovery interval was compared. However, the number of samples from the period of recovery was smaller than those from the other two intervals.

The SIMPER result for foraminiferal abundance data from Alamedilla indicated the dissimilarity across the studied section as 71%. The comparison between the taxa that contributed to the dissimilarities between the CIE and recovery as well as the CIE and the pre-CIE (Tables 3.7 and 3.9) showed that all the taxa were higher in abundance during the CIE than any of the two intervals during the PETM. *Nuttalides truempyi* and *Oridosalis umbonatus* were more cosmopolitan whereas *Globbocassidulina subglobosa, Repmanina charoides, Anomalinoides* Spp. and *Osangularia* spp. tend to be the CIE markers for this section.

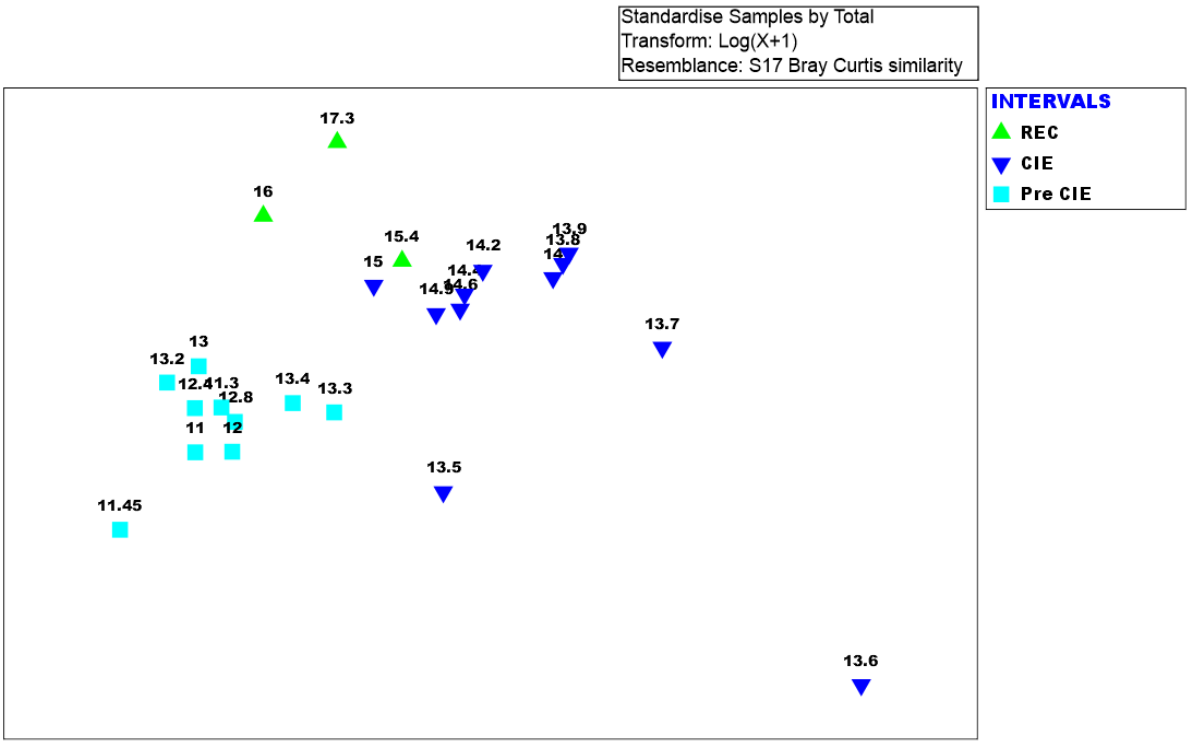

Figure 3.13: Non-metric Multi-dimensional Scaling of foraminiferal traits composition of Bray-Curtis similarity from the Alamedilla outcrop, Spain. Taxonomic abundance was standardised by total resemblance. The outlier 13.6 mbsf indicates the position of BEE.

Table 3.7: Mean abundance of species making a cumulative contribution to the dissimilarity between the CIE and the recovery intervals at Alamedilla section (Data cut off 52.98%)

Species	**Mean abundance**		**Contribution to dissimilarity (%)**
	Recovery	**CIE**	
Globocassidulina subglobosa	2.00	**61.64**	13.67
Repmanina charoides	1.30	**18.55**	5.16
Nuttallides truempyi	17.10	**25.18**	4.29
Oridorsalis umbonatus	8.60	**24.45**	4.29
Anomalinoides spp.	10.90	**19.73**	3.61
Osangularia spp.	10.90	**19.27**	3.43
Tappanina selmensis	2.90	**15.55**	3.25
Stilostomella spp.	**13.70**	2.18	3.23
Abyssamina quadrata	**11.70**	5.91	2.97
Anomalinoides cf. zitteli	**13.20**	3.18	2.86
Quadrimorphina profunda	5.70	**11.73**	2.86
Anomalinoides ammonoides	**9.70**	1.18	2.45

Table 3.8: Mean abundance of species making a cumulative contribution of ~50% to the dissimilarity between the pre-CIE and recovery intervals at Alamedilla section

Species	Mean abundance		Contribution to dissimilarity (%)
	Recovery	Pre-CIE	
Stilostomella spp.	**13.70**	4.33	4.19
Anomalinoides cf. zitteli	**13.20**	3.67	4.05
Abyssamina quadrata	**11.70**	4.00	3.88
Anomalinoides spp.	**10.90**	4.33	3.44
Nonion havanense	3.90	**9.33**	3.26
Stensioeina beccariiformis	**8.10**	0.00	3.17
Osangularia spp.	**10.90**	10.67	2.91
Nuttallides truempyi	17.10	**21.67**	2.91
Nonionella sp.	**7.70**	0.67	2.89
Laevidentalina spp.	7**.80**	1.00	2.78
Anomalinoides ammonoides	**9.70**	5.33	2.64
Bulimina kugleri	**9.20**	3.67	2.43
Pleurostomella sp.	4.70	**8.33**	2.16
Paralabamina hillebrandti	**6.20**	1.33	1.98
Oridorsalis umbonatus	**8.60**	3.67	1.98
Quadrimorphina profunda	5.70	**6.33**	1.94
Trochamminids	**6.10**	2.33	1.91
Coryphostoma midwayensis	**4.30**	0.00	1.69

Table 3.9: Mean abundance of species making a cumulative contribution of ~50% to the dissimilarity between the CIE and pre-CIE PETM intervals at Alamedilla.

Species	Mean abundance		Contribution to dissimilarity (%)
	CIE	Pre-CIE	
Globocassidulina subglobosa	**61.64**	4.33	18.66
Repmanina charoides	**18.55**	0.33	8.97
Oridorsalis umbonatus	**24.45**	3.67	6.92
Nuttallides truempyi	**25.18**	21.67	6.80
Anomalinoides spp.	**19.73**	4.33	5.99
Osangularia spp.	**19.27**	10.67	5.65

18 taxa accounted for 50% of the dissimilarity between the pre-CIE and recovery intervals (Table 3.8). SIMPER analysis clearly revealed that *Stensioeina beccariiformis* and *Coryphostoma midwayensis* disappeared before the recovery (Table 3.8) All the species showed higher abundance during the recovery interval except for the opportunists; *Nonion havanense, Nuttallides truempyi, Quadrimorphina profunda* and *Pleurostomella* sp.

3.2.8. Changes in foraminiferal trait composition at Alamedilla section

The nmMDS of trait composition at Alamedilla showed that most of the CIE samples clustered with part of the pre-CIE group but the recovery samples grouped in more or less longitudinal axis with notable separations (Figure 3.14). The ordination of trait composition was more dispersed than that of faunal composition, signalling that foraminiferal trait and by extension, it's functioning in the ecosystem was stretched during the CIE. The ANOSIM indicated that the trait composition of foraminifera across the three intervals significantly differed at global R= 0.496 and p <0.01. Also, the pairwise test also revealed that the pre-CIE and the recovery were the most dissimilar interval with p<0.02 while the recovery and the CIE were the most similar at p<0.01 and there was a significant dissimilarity (p>0.5) between the pre-CIE and the CIE.

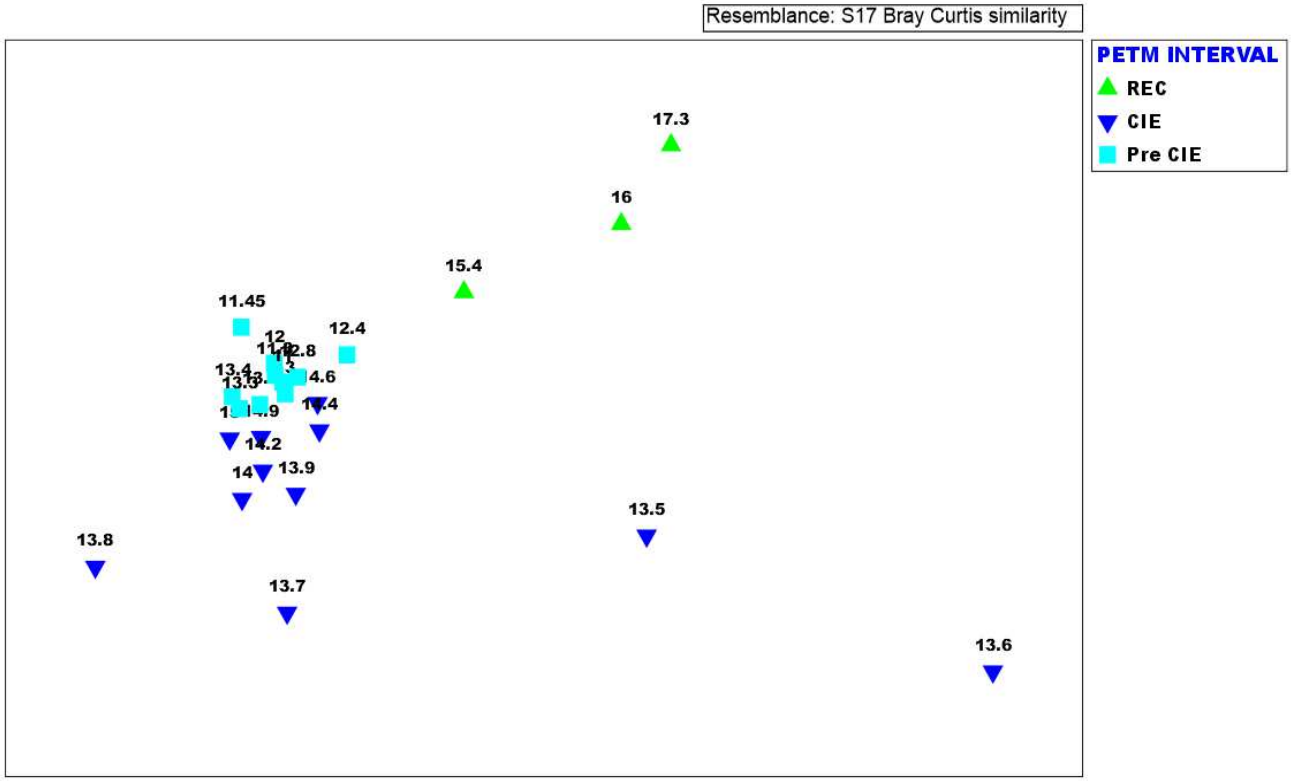

Figure 3.14: Non-metric Multidimensional Scaling ordination of foraminiferal traits composition from Alamedilla (transformed with total resemblance) of Bray-Curtis similarity indicating the grouping of samples across the CIE events.

The SIMPER result showed that the pre-CIE interval recorded the lowest abundance of all the traits identified from Alamedilla section (Figure 3.15). There were more spiral, hyaline

aragonite, porcellanous, uniserial, and trochospiral test, triangular/trapezoid, semi-circular chamber shape and arcuate apertures during the CIE than at the recovery. While elongate test shape, agglutinated test, planispiral coiling, oval/reniform- slit-like apertures and apertural neck were more during the recovery than at the CIE (Figure 3.15).

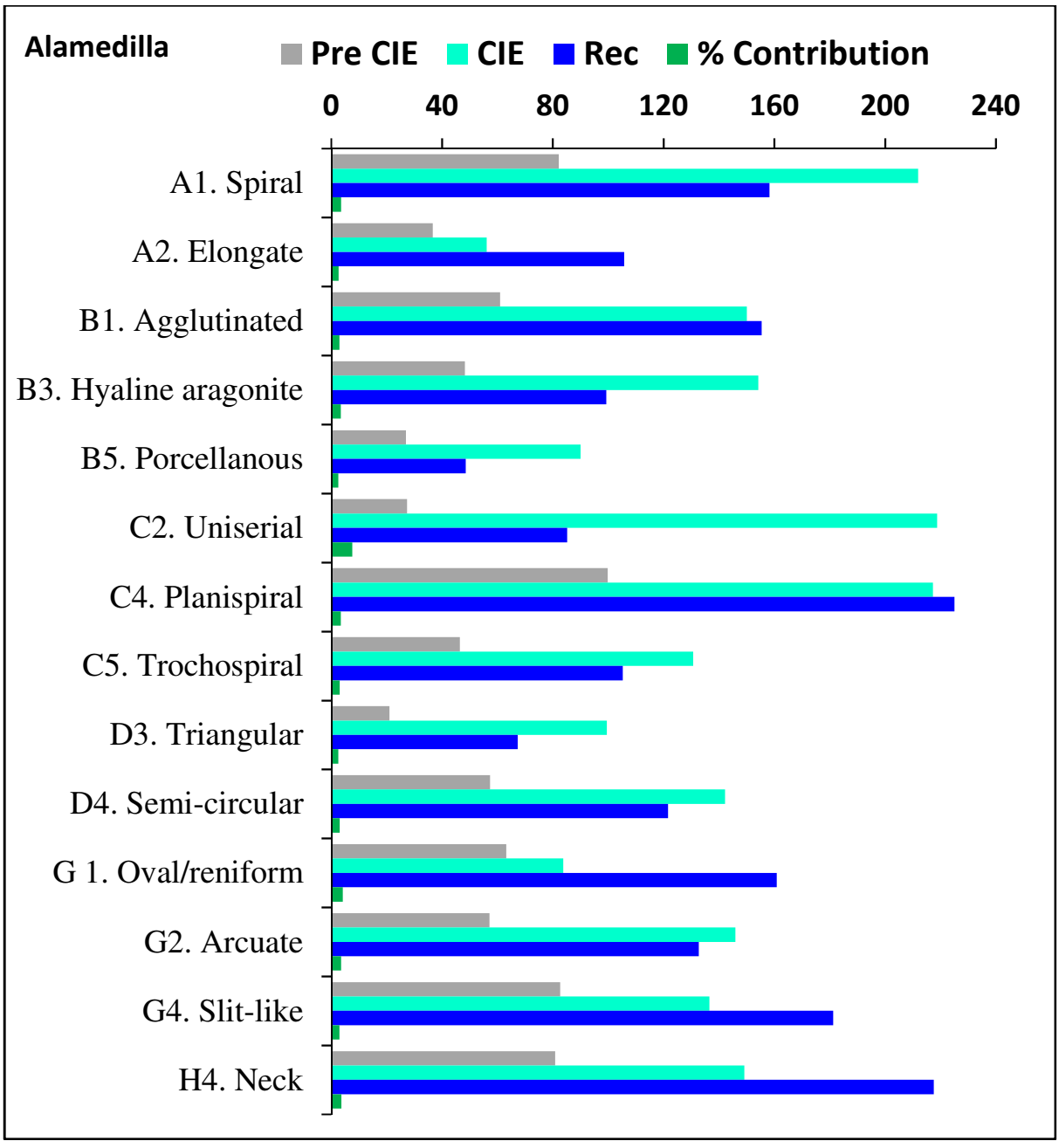

Figure 3.15: Similarity percentage (SIMPER) showing traits that cumulatively contributed ~50% to the differences in benthic foraminiferal trait composition across the CIE events at Alamedilla section, Spain

The overview of the trait distribution from the raw data at Alamedilla revealed spiral, elongate, tubular, and globose as the major test shapes of foraminifera identified from Alamedilla. The spiral shape was the most abundant with ~50% in total abundance (Figure 3.16A). The highest abundance of this shape occurred above the BEE at the CIE interval and significantly decreased during the recovery. Elongate test constituted about 40% of the four shapes that existed in foraminifera from Alamedilla. This trait recorded the highest abundance at the pre-CIE but dropped to near zero at the depth 13.50 mbsf, afterwards it resurrected and remained relatively uniform up to the top of the section.

Nevertheless, the abundance at the CIE interval was slightly higher than at the recovery. The tubular test was the second to the least in the abundance of test identified at Alamedilla, it indicated continuous occurrence at the pre-CIE section only, after which the abundance of the trait during the CIE and the recovery was more or less patchy. Globose test existed at the pre-CIE interval only and went into extinction at the BEE. It was the lowest in the abundance of foraminiferal trait in the test shape category from Alamedilla, constituting only ~3% of the four test shape identified.

The test composition of benthic foraminifera identified from the raw data (Figure 3.16) at Alamedilla comprises of hyaline calcite, porcelaneous, agglutinated, micro-granular and hyaline aragonite. Foraminifera with calcitic tests were the most abundant amounting to approx. 40% of the total test composition. The highest abundance of hyaline calcite test was after the BEE in the CIE interval but decreased remarkably during the recovery period (Figure 3.16B).

Porcelaneous test composition was relatively moderate and uniform across the study section except for some spikes at 13.20, 14.5 and 15.5 mbsf, it constituted about 25% of the total test composition. The agglutinated test was most abundant at the pre-CIE, it conspicuously increased in abundance at the BEE where most of the other traits decreased and dropped afterwards during the recovery. The micro-granular test was only recorded shortly after the BEE and no other evidence of its occurrence was found in the section (Figure 3.16B). The highest abundance of hyaline aragonite was at the CIE interval, followed by the pre-CIE, while the recovery interval recorded the rarest abundance of foraminifera with aragonite test.

Trochospiral coiled test was the most abundant among the foraminifera identified from Alamedilla. Its highest abundance was recorded at the CIE immediately after the BEE. Bi/triserial test, on the other hand, was the second most abundant trait with its highest occurrence at the pre-CIE interval and lowest at the recovery. Planispiral coiled taxa nearly mirrored the trend of the bi/triserial occurrence.

The uniserial test also recorded relative high abundance at the pre-CIE, but decreased significantly at the CIE interval and picked up again during the recovery. The unilocular test was sparingly present at the pre-CIE and went into extinction at the CIE interval while other miscellaneous test arrangement occurred in random with relatively high abundance at the BEE before going extinct at the CIE interval. Foraminiferal taxa with tubular chamber were the most abundant across the study section, and it exceptionally increased at the BEE and recorded the highest abundance at the CIE. Triangular/trapezoid was the second most abundant chamber shape; its highest occurrence was recorded at the pre-CIE while the recovery recorded the lowest occurrence.

The macro-ornamentation in foraminifera found in Alamedilla was predominantly depressed sutures representing about 70%. It increased in abundance from the pre-CIE to the CIE and remarkably dropped during the recovery. Another significant macro ornamentation identified from the studied section was raised sutures, the highest occurrence of this trait was at the pre-CIE while the recovery interval recorded the lowest abundance of the trait. Other miscellaneous macro ornamentation mimicked the raised sutures trend while keeled and cancellate sutures occurred only at the pre-CIE and CIE interval respectively. Foraminifera taxa without any recognisable micro-ornamentation on their test were the most abundant in the studied section with highest relative abundance at the CIE and lowest at the recovery (Figure 3.16F). This trait was closely followed by miscellaneous micro-ornamentation with the highest occurrence at the pre-CIE. Spinose and striate/costae test indicated significantly high abundance at CIE and low abundance at both pre-CIE and recovery intervals. While hispid ornamentation occasionally appeared from the pre-CIE and went extinct at the CIE interval.

Arcuate aperture recorded the highest abundance at Alamedilla and was closely followed by slit-like apertures. Both apertural forms indicated a similar trend, showing high abundance at the pre-CIE, relative increase during the CIE and lowest abundance at the recovery. Oval/reniform apertures indicated moderate abundance at the pre-CIE and CIE intervals but

slightly increased during the BEE. Radiate/cribate apertures also showed moderate abundance at the pre-CIE but went into extinction within the CIE interval.

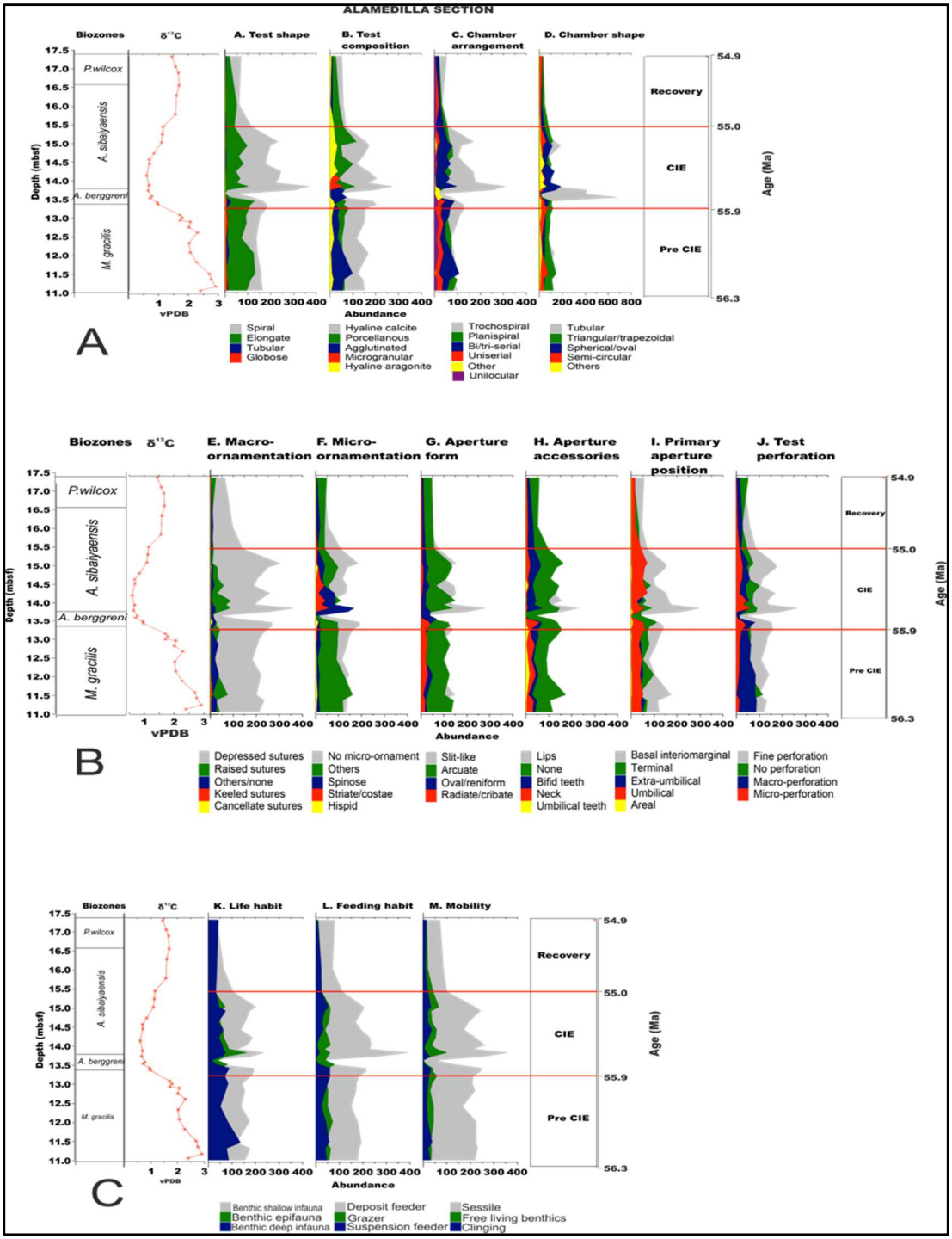

Figure 3.16: Benthic foraminiferal trait composition and distribution across the CIE events at Alamedilla section. The numerical age is plotted on the right-hand side of the figure. A. Shows traits for test composition and morphology. B. Test ornamentation and aperture traits. C. Traits associated with life habit.

Taxa with no apertural accessories were the most abundant in the studied section, followed by those with lips, bifid teeth, neck, and umbilical teeth in that order. They were abundant at the pre-CIE, relatively increased during the CIE and decreased in abundance at the recovery (Figure 3.16G).

The majority of foraminifera taxa in Alamedilla had their apertural position at the basal interiomarginal (~45%), the relative occurrence of others are terminal (~25%), extra-umbilical (~20%), umbilical (~18) and areal (~2%). They were all moderately abundant at the pre-CIE, relatively increased during the CIE and decreased in abundance at the recovery interval except for the areal apertures which occurred sparingly at the CIE interval. Perforations in foraminifera identified from Alamedilla showed a decreasing abundance from fine perforation, non-perforated, macro and micro perforations. They display a similar trend of high abundance at the pre-CIE, relatively increase during the CIE and decrease at the recovery (Figure 3.16J).

The life habit of benthic foraminifera at Alamedilla was dominated by shallow infauna (~50%), deep infauna (~30%) and epifauna (~20%), whereas the feeding mode was predominantly deposit feeding (65%), grazers (20%) and 15% for suspension feeders (Figure 3.16). Over 80% of the identified foraminifera taxa were stationary (sessile), free-living benthic constituted only 12% while clinging trait accounted for ~8%.

The most significant event in the trait composition at Alamedilla from areal plot (Figure 3.16) was the total collapse of all the trait at depth 13.50 mbsf. This depth was interpreted to be coeval to the benthic extinction event (BEE). Traits that showed relative increase at this point were agglutinated test and tubular chamber arrangement. Nevertheless, most of the traits recovered after the BEE except those with globose shape, apertural neck, radiate shaped apertures and uniserial chamber arrangement. The species with suspension feeding strategy and elongate test shape were found to be most susceptible traits during the CIE at Alamedilla.

3.3 Discussion

Biological trait analysis of the benthic foraminiferal taxa and trait composition in the tropical Pacific Ocean and Alamedilla (Tethys Sea) have enabled us to understand faunal turn over and trait reorganization during the period of extreme climate conditions associated with the PETM. The changes in trait composition are consistent with foraminiferal turnover during the PETM in all the studied sections. However, our result showed that the disappearance of some taxa did

not immediately affect the change in trait composition and hence the ecological functioning performed by them as seen in Site 1209B. Foraminifera reacted by either increase in the abundance of the taxa that shared similar traits or taxa with cosmopolitan behaviour that can tolerate a wide range of ecological changes, this continued until ecological function was stretched to the tipping point (example during the BEE at Alamedilla). In addition, the extinction of some trochospiral and macro perforated taxa did not lead to the immediate disappearance of those traits (Figure 3.17) as other taxa reacted by increase in abundance (Figure 3.2) and thereby sustaining the ecological functioning. The changes in foraminiferal traits were found in most case to lag behind the taxonomic turnover.

3.3.1 Similarities in trait compositions across the tropical Pacific Ocean and Tethys Sea.

The near coincidence of changes in foraminiferal traits with changes in environmental conditions as shown in Figure 3.17 may have been as a biological adjustment to the physio-chemical changes such as carbon fluxes, nutrient supply and oxygen concentration in the ocean during the PETM. These changes as inculcated into the fabric of foraminifera may be used to identify some vital climate events. A high occurrence of traits like elongate and spiral foraminiferal test shape were common in all the studied sites. Foraminifera with elongate tests were most abundant across the Pacific Ocean sites but significantly decreased during the CIE interval during which time spiral tests became more abundant (Figure 3.17). In the Tethys Sea (Alamedilla section), spiral tests were highly abundant and showed a relative increase during the CIE while elongate tests showed a concomitant decrease in abundance. Considering the differential thickness of the sections studied at the three sites (2 m in Alamedilla, compared with ~15 cm at the Pacific sites) we believe there is still a positive correlation between test shapes in both oceans (Figure 3.17). Taxa with spiral test shapes were more opportunistic and may have tolerated a wide range of environmental perturbation during the PETM. This was reflected in the high abundance of spirally coiled taxa such as *Nutallides,* Abyssaminids *and Oridosalis* taxa (Tables 3.1; 3.6; 3.7) during the CIE intervals. Increased abundance of opportunistic taxa during environmental upheavals have been reported for many PETM sections and other ocean anoxic events (OAE) in the geologic record (Thomas 2007; Giusberti *et al.,* 2009; D'haenens *et al*., 2012). In addition, high abundances of forms with elongate tests have been associated with periods of ecological disturbance in benthic communities by Ortiz and Kaminski (2012). The dominance of elongate tests in the Pacific sites is consistent with

this pattern. Despite the differences in the geological/palaeoenvironmental setting and faunal composition between Alamedilla and Shatsky Rise, there remains a relative decrease in the abundance of the elongate taxa during the CIE in both locations. This decrease may be an indication of a change in palaeoproductivity or preferential dissolution of the elongate test during the hyperthermal.

The typically common hyaline calcite tests predominated at all the studied sites. At Alamedilla, hyaline test composition relatively increased during the CIE just above the benthic foraminiferal extinction event (BEE), but at Shatsky rise (Figure 3.17) it slightly decreased during the CIE. The second most abundant test composition in Alamedilla was porcellanous and aragonite at the Pacific sites. There was also a significant amount of agglutinated test at Alamedilla and Site 1212B, but very little was recorded at Site 1209B. At Alamedilla, the agglutinated test relatively increased coeval to the BEE where there was a total absence of other test composition, also hyaline aragonite tends to increase both at Alamedilla and Shatsky Rise. The possible explanation for the increase in agglutinated test at the same time with the BEE could be as a result of calcite dissolution or because agglutinated taxa are more tolerant to higher organic flux and decrease in oxygen content under low sedimentation of fine-grained materials or that the sediment may have originated from the continental margin where higher abundance and diversity of agglutinated forms exist, (Kamiski and Gradstein, 2005). The decrease in agglutinated test at Shatsky Rise could be related to the prevailing foraminifera ooze in the area.

There was a decrease in the abundance of taxa with uniserial and bi/triserial chamber arrangement during the CIE at all sites except Alamedilla. Uni/bi/triserial chamber arrangements are usually traits exhibited by infauna taxa (Corliss and Emerson, 1990), it could mean that some epifauna and shallow infauna took refuge deeper in the sediment to reduce the impact of the hyperthermal and competed with the 'true' infaunal taxa in the utilization of nutrient and available oxygen leading to decrease in the abundance of uni/bi/triserial trait. Another explanation to this could be as a result of preferential dissolution as un/bi/triserial taxa are more susceptible to dissolution than other hyaline calcite taxa (Nguyen *et al.,* 2009; Mancini *et al.,* 2013). Nevertheless, trochospiral test increased significantly at Alamedilla during the CIE and shortly in the beginning of the CIE at the Pacific sites (Figure 3.17).

A near perfect similarity of chamber shapes occurred across the two oceans in the trait distribution chart (4.15). There was a decrease in the spherical/oval chambers in both sites at the beginning of the CIE but increase towards the later part of the hyperthermal. Triangular/trapezoids and semi-circular chamber decreased in abundance during CIE across all sites. Nevertheless, tubular chambers increased remarkably during CIE at Alamedilla and 1212B. Tubular chambers seem to be the most tolerant trait because they stick their head above the sediment surface Ortiz and Kaminski (2012) and may have been adapted to high organic carbon and low oxygen concentration.

In terms of macro ornamentation, most of the foraminiferal taxa identified had either depressed or raised sutures. At Alamedilla, the highest abundance of depressed sutures was recorded at the CIE interval, but at Shatsky rise, the CIE only marked the beginning of the increase in abundance. Raised sutures also relatively increased at the CIE in both sites. Most of the foraminifera have some sort of depressed sutures on them, and macro ornamentation does not seem to be a very critical trait in foraminifera in case of these sites. Decrease in micro ornamentation was observed across all the studied sites as shown by the dominance of taxa without recognisable ornaments. This decrease is believed to be responsible for the decrease in abundance of foraminifera, especially at the CIE interval. Micro ornamentation is crucial of the survival of foraminifera in the environment (Dubicka *et al.,* 2015), and the absence of ornamentation in foraminifera recovered across sites during the PETM could be responsible for their inability to cope with the extreme environmental changes. Dubicka *et al.* (2015) demonstrated that foraminifera utilise body ornament to sort food particles into different shapes and sizes, removing harmful substances and disaggregating larger particles prior to ingestion. They also use body ornamentation as protection from predators. The absence of ornamentation in foraminifera may have increased their vulnerability during the hyperthermal leading to the decrease in abundance and ecological function as well as the coeval extinction of some benthic foraminifera during the PETM.

There was no recognisable trend in aperture form in all the study sites. In Alamedilla section, slit-like increased during the CIE but remained relatively uniform at Site 1209B while decreasing in abundance at site 1212B. Arcuate apertures were moderately abundant and relatively increased during the CIE in all the three sites. Oval/reniform apertures composition was relatively uniform throughout the PETM sections, though it decreased during the BEE at

Alamedilla and Site 1209B. At Site 1212B it was relatively abundant before the CIE but decreased significantly after BEE. Radiate apertures were present on taxa from Alamedilla and Site 1212B, but no significant pattern could be observed at Site 1209B.

The abundance of aperture accessories varies across the sites. Lip, for instance, was the most abundant accessory at Alamedilla but the least in the Pacific sites. However, the common trend in this trait was its relative increase during the CIE in all the sites studied. Taxa without any recognisable apertures also indicated a relative rise in abundance during the CIE. Bifid teeth decreased during the CIE at the Pacific sites but increased at Alamedilla. While taxa with neck decreased in all the sites and those with umbilical teeth decreased at the beginning of the CIE at two sites but increased at the same time in Site 1209B. We cannot provide a convincing explanation for the decrease in aperture accessories during the PETM, but a similar scenario has been recorded by Dubicka *et al.* (2015) which observed a decrease in the apertural accessory of *Haynesina germanica* during the extreme rise in CO_2 and *p*H in the Barents seas. Because accessories like teeth are used in breaking down larger food particles, the majority of the foraminifera may have adopted assimilation of dissolved particles rather than feeding on solid food to reduce the energy spend on metabolism.

In terms of aperture position, there was a big increase in basal interiomarginal (BIM) aperture during the CIE at Alamedilla, but the trait relatively decreased at the Pacific sites. The increase in BIM aperture at Alamedilla may be linked to the continued existence of trochospiral taxa whose aperture mostly occur at the BIM, some of these taxa, however, went into extinction at the Pacific site at the beginning of the CIE. Terminal apertures decreased across the three sites at the CIE interval while umbilical/extra-umbilical apertures increased across all the sites. The decrease in terminal apertures can also be linked to the decrease in the abundance of uni/bi/triserial trait reported above. This needs more investigation because one should expect an increase in terminal apertures which are predominantly infauna morphotypes during the hyperthermal.

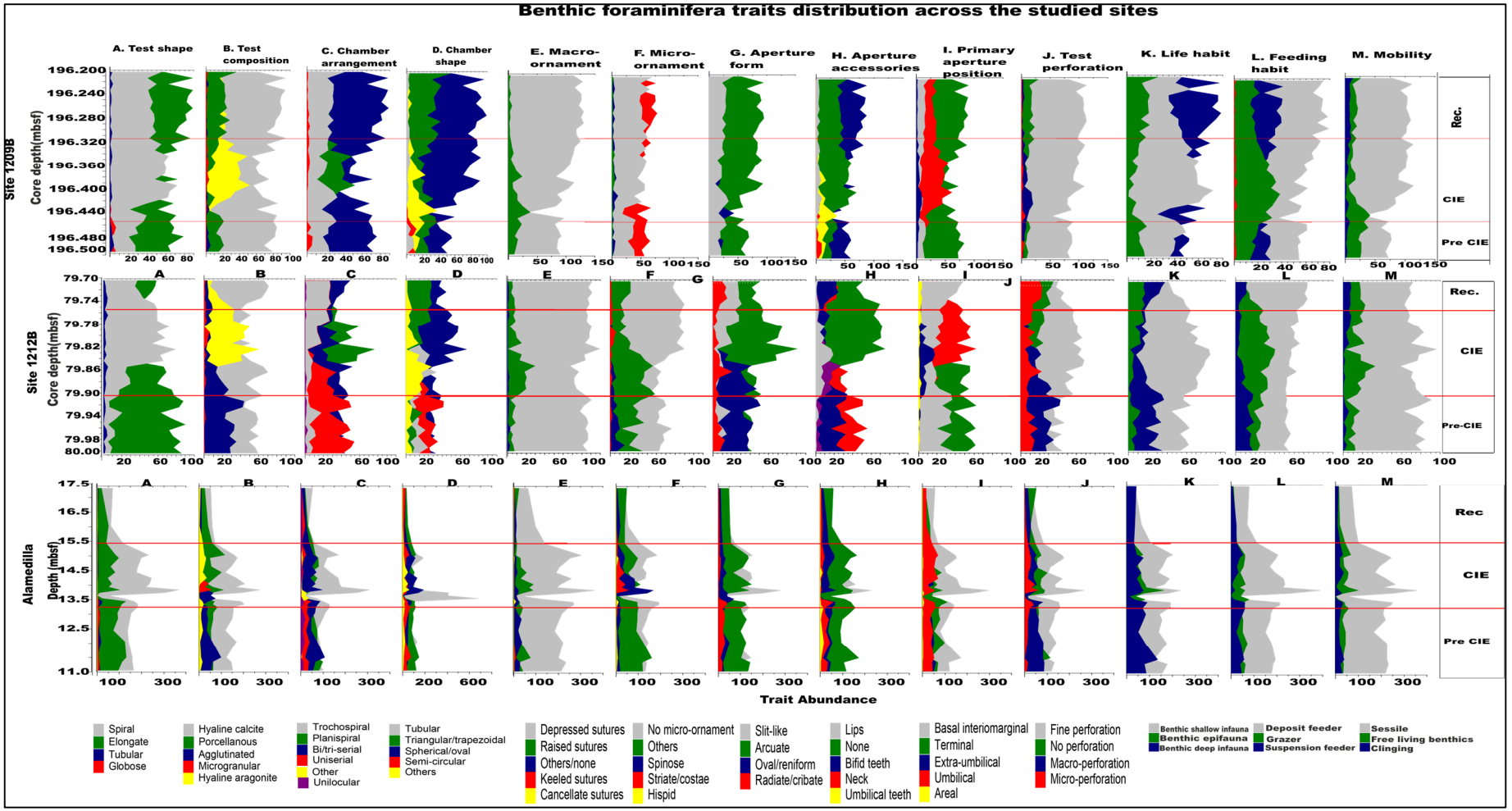

Figure 3.17: Composite trait composition from the Tethys Sea and the tropical Pacific Ocean to show some trait similarities across the studied sites. The colour used in a particular modality is uniform across all the sites. The trait abundance below each plot represents the absolute count of traits after standardisation. Site location and core depths are plotted at the left-hand corner of the figure and the PETM events at the right.

Test perforation in the studied sites indicates that fine perforation relatively increased during the CIE, both at Alamedilla and Pacific sites. Decrease in macro-perforation occurred at Site 1212B and Alamedilla but relatively increase at Site 1209B which had a sparse occurrence of this trait. Smooth tests (no perforation) showed a decrease in abundance at the Pacific sites but a relative increase occurred at Alamedilla. Micro perforation increased in abundance in all the three sites. Test perforation is a very important functional trait in foraminifera. The size, pattern and density of pores found in benthic foraminifera reflect the amount of oxygen available in the ecosystem they lived (Kuhnt *et al.,* 2013). Perforations in foraminifera have been linked to their ability to live in very low oxygen concentration as it is believed to play a role in the nitrate respiration and in the material exchange between the foraminifera and its symbionts. The increase in fine perforation and decrease in macro perforation could imply that hyperthermal favoured the taxa with smaller pores whose oxygen requirement was less than macro pores. The extinction of Gavellinids during the PETM (Thomas, 2007; Giusberti *et al.,* 2016) was attributed in part to the large perforations found in the taxa which required elevated oxygen concentration to survive but the species could not survive with a decrease in oxygen concentration during the hyperthermal. In other words, large pores are possessed by species (*G.becarriformis*) in a well-oxygenated environment while species found in the low oxygen environment have smaller pores (Jorissen, 2007). It is worthy to state that there are exceptions to this case depending on the prevailing environmental conditions and fauna assemblages. Taxa with large pores could also be more vulnerable to dissolution because the pores can create access for fluid to invade the test and disintegrate them.

Shallow infauna and grazers were the traits that correlated positively across the study sites during the CIE by a concurrent increase in abundance. There was a decrease in epifauna at Pacific sites during the hyperthermal but an increase was recorded at Alamedilla. Deep benthic infauna and deposit feeders indicated a similar trend with an increase in abundance at Alamedilla and a decrease in the Pacific sites. Suspension feeders indicated a relative decrease in abundance at the CIE in all the sites. Our results also demonstrate that shallow infauna was the most favourable habitat during the hyperthermal, with the trait been the most abundant as well as showing a relative increase during the CIE in all the sites (Figure 3.17). There is a possibility that shallow benthic infauna lived a dual life style migrating to the surface to feed when the environment is favourable and back into the sediment when the condition becomes unfavourable. The increase in epifauna at Alamedilla could be traced to the survival of some Gavelinidae and other epifauna taxa in the section during the hyperthermal. Deep infauna are

the next to shallow infauna in terms of success during the CIE. The habitat is mostly likely to be protected from the water column corrosiveness by the sediment. Their decrease in the Pacific sites could be attributed to the absence of agglutinated forms.

The classification of foraminiferal mobility was a tricky one as the Paleobiology Database and other literatures used in this study classified most of them as stationary. We hope that this is correct as our data showed sessile trait to be most dominant. Sessile trait relatively increased at the PETM and free-living trait, which was much less, slightly increased as well at Alamedilla and Site 1212B but decreased after the BEE at Site1209B during the same period. There is a general decrease in the abundance of clinging taxa in all the three sites. The increase in the sessile trait could be that most shallow and deep infauna live sessile lifestyle conserve energy and hide from predators. Nevertheless, despite the predominance of sessile trait, we cannot say that we have enough evidence to show that sessile was more favourably disposed towards foraminifera survival during the extreme warmth.

3.3.2 Interpreting ecological function base on changes in foraminifera fauna and traits

3.3.2.1 Nutrient supply in the Pacific Ocean during the PETM

Nutrient supply to the benthic zone was inferred from the faunal composition, infaunal/epifaunal ratio, species and trait turnover from the statistical analyses. The faunal assemblages in the Pacific Ocean (Sites 1209B and 1212B) are dominated by calcareous infauna taxa primarily by *Buliminids, Stilostomellids/Pleurostomellids* and *Bolivinids.* These taxa in the modern and ancient oceans thrive in the area of high and sustained food supply and low oxygen (Alegret and Thomas, 2004; 2009; Jorissen *et al.,* 2007; Mancini *et al.*, 2013; Arreguin-Rodriguez *et al.,* 2016). The relative dominance of infauna morpho-groups with a coeval high abundance of *Buliminids* at the Pacific sites (Tables 3.1- 3.6; Figure 3.7; Takeda and Kaiho, 2007) suggest a significant supply of nutrient to the seafloor during the PETM. The result from our SIMPER analyses between the pre-CIE and other intervals showed an increase in high nutrient flux indicators such as *Bulimina kugleri* and *Bolivina inconspicua* (Table 3.1). The nutrient supply started to decrease within the CIE interval as shown by a decrease in the *Bulimina* taxa (Figure 3.18; 3.19). The lowering in the number of *Buliminids* and *Stilostomellids* in the samples across this interval (Figure 3.16) was a good indicator of oligotrophy. The abundance of these taxa may not have been extremely affected by carbonate dissolution since they live inside the sediment and also very low carbonate dissolution was recorded in the Pacific Ocean during the PETM (Takeda *et al.,* 2006).

There was an initial increase in the *Buliminid* abundance at the beginning of the CIE (Figure 3.18) which could be as a result of preliminary increase in the surface productivity encouraging more phytodetrital rain to the sea floor but when the further rise in temperature resulted to enhanced metabolic efficiency of pelagic phyto and zooplankton (Thomas, 2003), they consumed more refractory organic particle in the upper water column and reduced the quantity and quality of food material reaching the bottom water. Food availability was made worse for the bottom-dwelling taxa as the rise in temperature resulted to increase in the opportunistic taxa (e.g. *Quadrimorphina profunda* and *Nuttalides truempyi*) that out-competed the epifauna and shallow infauna by consuming the limited food supply (Algret and Thomas, 2009; Table 3.4).

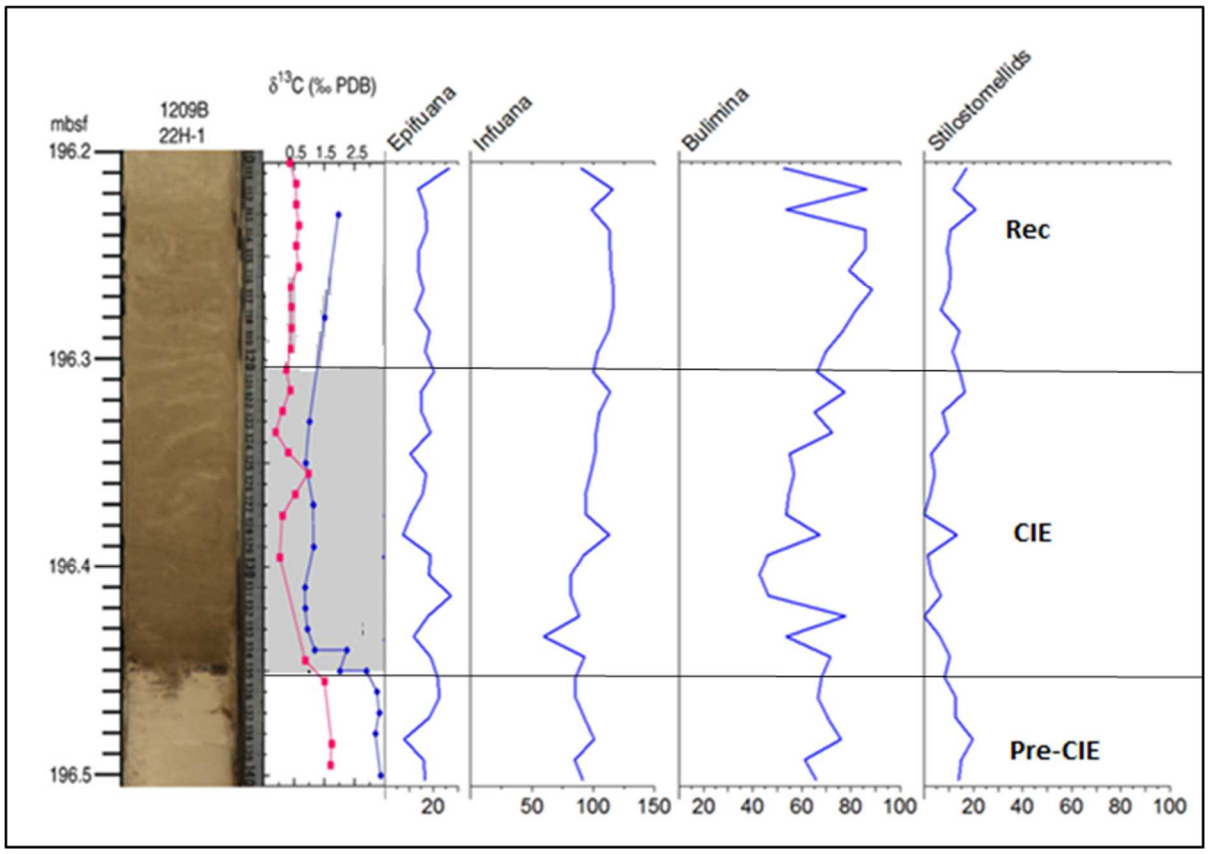

Figure 3.18: Litho, bio and geochemical stratigraphy of PETM section in core 1209B-22H-1. The lithostratigraphy and $\delta^{13}C$ record are those of Takeda and Kaiho (2007) while the morph groups and taxa curves plotted with absolute abundance were created in this study.

The faunal composition from the raw data at the recovery interval demonstrated a period of highest and most stable supply of quality nutrients to the sea floor. The highest abundance of the deep infauna morphogroup, as well as other high organic carbon influx indicators across this interval (Figure 3.18), strongly supports this observation. The high nutrient supply during

the recovery may be attributed to the enhanced continental weathering (Winguth, 2011) supplying nutrients to the ocean and less number of species competing for available resources after the PETM.

The results of trait evaluation indicate that the prevailing conditions at the sea floor before the CIE favoured species with elongate and uniserial test; neck and bifid teeth as well as bi/triserial forms (Corliss and Chen, 1988). These species are well adapted to infauna lifestyle and are predominantly *Stilostomellids, Pleurostomellids and Buliminids*. In general, the trait composition that constituted 50% similarities across the three PETM interval show that fine perforation, deep infauna, sessile, deposit feeder, terminal aperture, hyaline calcite test, bifid teeth, elongate, uniserial and shallow infauna and spherical aperture (Figure 3.11) were the most significant traits during the CIE across the studied section. These traits demonstrate high tolerance to high organic carbon influx to the bottom ocean and extreme environmental conditions (Corliss and Chen, 1988).

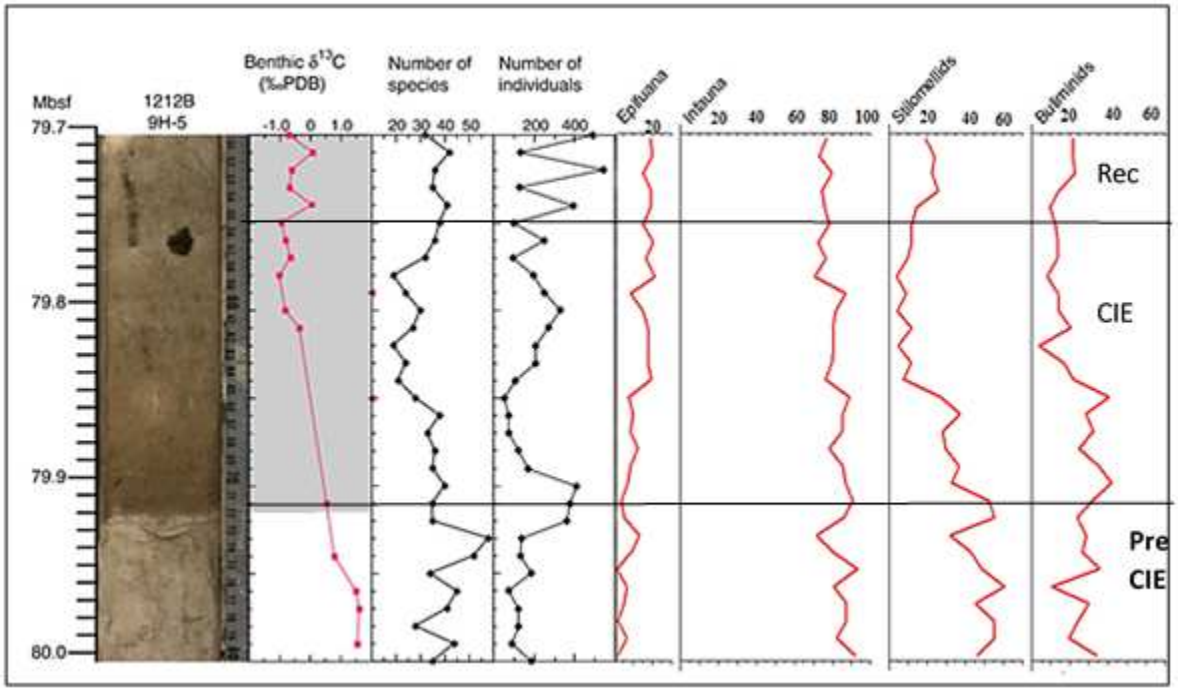

Figure 3.19: Litho, bio and geochemical stratigraphy of PETM section in core 1212B-9H-5. The lithostratigraphy, $\delta^{13}C$ record, number of species and number of individual are those of Takeda and Kaiho (2007) while epifauna, infauna, Stilostomellids and Buliminids percentage curves were created in this study.

Taxa with coarse perforations, trochospiral coiling and epifaunal habit (e.g. *G. beccariiformis*) was extirpated during the PETM perhaps because they required high dissolved oxygen and lowered organic matter to thrive, but high organic matter influx that resulted in bottom water

anoxia and acidification making the bottom water uninhabitable for them. Foraminifera with traits such as elongate cylindrical, flabelliform or biserial architecture were reported to have high surface to volume ratio that enables them to successfully adapt in the infaunal habitat with high organic matter inundation and anoxia (Mancin *et al.,* 2016). Additionally, this form of chamber arrangement provide communication/exchange link at each end and this can reduce the rate of protoplasm mixing between the inside and outside of the test leading to decreased metabolic activity within the foraminiferal cell. This anatomy could reduce oxygen and nutrient requirement of the organism. Excessive organic carbon rain from the upper water column may have contributed to the decrease in some less competent epifaunal taxa because high abundance of organic matter in the sea floor hinders pseudopodia function as they are usually overwhelmed by algal growth (Boltovkoy *et al*., 1991; Arreguin-Rodriguez *et al.,* 2016).

3.3.2.2 Nutrient supply to the Tethys Sea during the PETM as interpreted from Alamedilla section

Nutrient supply to the benthic zone in the Tethys Sea during the PETM was similar to that of the Pacific, with overall high organic matter influx from the pre-CIE till the recovery. The high organic content in the seafloor sediment at the Tethys Sea was indicated by the high abundance of *Buliminids* and other infauna morphotypes (Figure 3.20). However, enigmatic scenario occurred at the interval (13.4m) where BEE was recorded (Figure 3.20) with a total collapse in the food supply as indicated by a significant reduction in the abundance of *Buliminids,* infauna and epifaunal taxa (Figure 3.20). The only foraminifera that survived within this interval were the agglutinated taxa of *Rapmanina* and Trochaminids and it appears to be the most severe benthic foraminiferal extinction recorded in any PETM section across the globe (Alegret *et al.,* 2009).

The period of highest organic flux to the sea floor occurred just before the onset of the CIE (Figure 3.20). This suggests optimal primary and export production at the beginning the PETM warming but when the ecological threshold of the benthos was exceeded, the whole system collapsed due to a combination of other extreme climatic factors including insufficient food supply. The food supply to the benthic environment, however, returned and increased again after the BEE, 21ky years before the PETM recovery (see Figures 3.18; 3.20; Alegret *et al*., 2009). In general, there was more supply of quality food product to the Tethys sea floor because epifaunal richness indicated sustained the supply of nutrient suitable for both epifauna and infauna to flourish.

It seems there was a sufficient supply of quality food material before and after the CIE from the dominant taxa (*Buliminids*) that constituted 50% similarities in SIMPER analysis (Figure 3.15), However, nutrient supply at the main CIE interval was more or less episodic with the supply of low degraded organic matter at one point and fresh phytodetritus at another (Arreguin-Rodriguez *et al*., 2016) as suggested by high abundance of *G. subglobosa* and *O. umbonatus* (Tables 3.7 – 3.9).

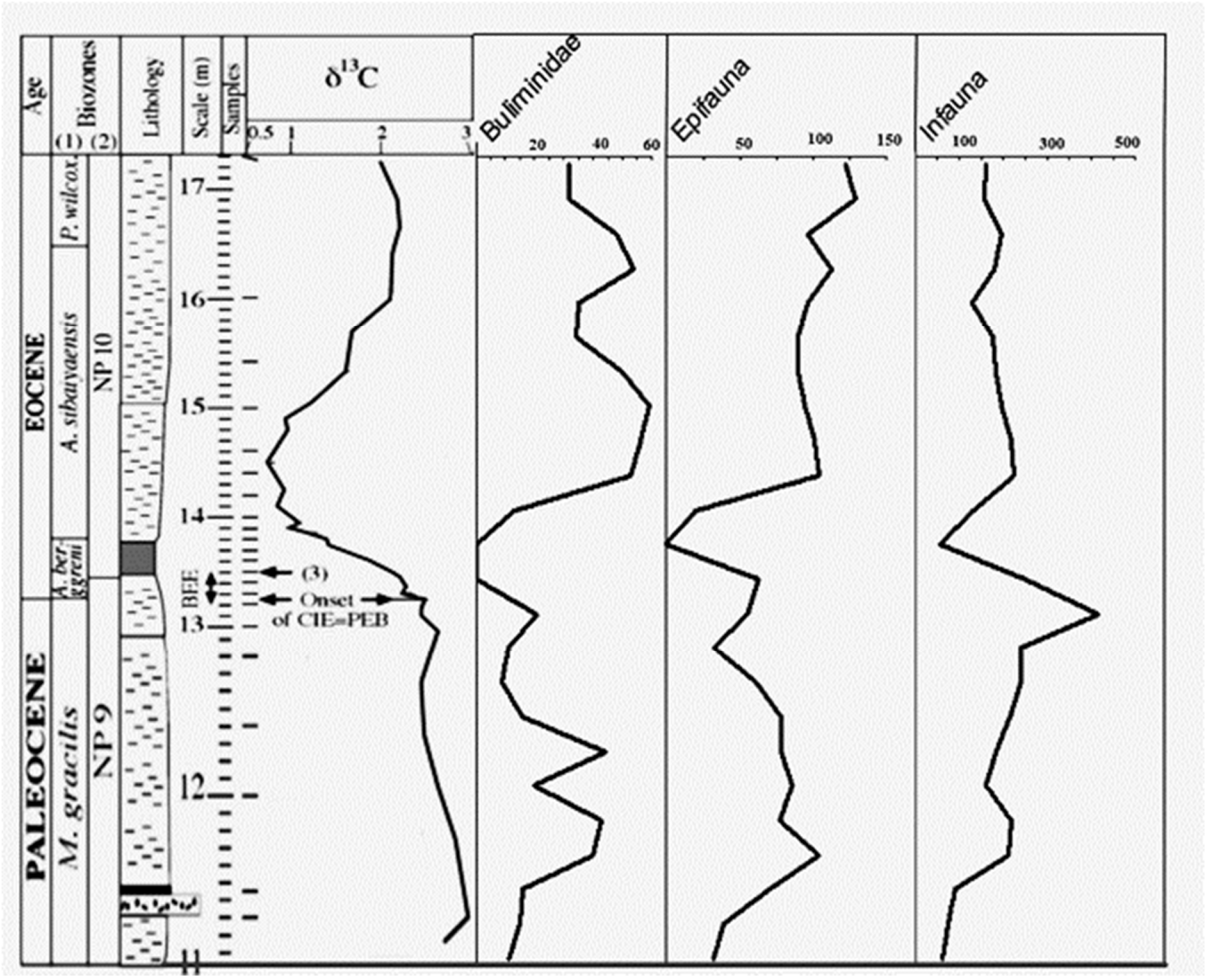

Figure 3.20: Stratigraphic profile of Alamedilla section. The arrow labelled 3 marks the top of BEE. The chronostratigraphy, lithostratigraphy and $\delta^{13}C$ record were modified from Alegret et al. (2009) while the biostratigraphy (Buliminidae, Epifauna and Infauna) curves were made with faunal data from Alegret et al. (2009).

The traits identified as the drivers of ecological function at Alamedilla includes; tubular, spiral and trochospiral test, hyaline calcite test composition, depressed sutures, fine perforation, slit-like and basal interiomarginal apertures, oval/spherical apertural shapes, apertures with lips, deposit feeder, sessile and shallow infauna. The complex test composition and apertural

framework composed in these traits provide some hints on the ability of the benthic foraminifera to utilise available food material in their environment. Mancin *et al.* (2013) hypothesised that complex apertures and test wall could provide suitable structures to develop numerous pseudopodia for capturing more food particles and break them down for easier digestion.

3.3.3 Productivity/global carbon cycle

3.3.3.1 Palaeoproductivity/global carbon cycle in the Pacific Ocean

Palaeoproductivity in the Pacific Ocean interpreted from fauna and trait results from sites 1209B and 1212B varied across the PETM intervals. The diversity and abundance of both the benthic and planktonic foraminifera [PF data in Petrizzo, (2007)] as well as the $\delta^{13}C$ signature of the biogenic carbonates (Figure 3.21) supports this assertion. The carbon isotope record of the surface-dwelling planktonic foraminifera and bottom-dwelling taxa strongly suggests high primary productivity in the surface ocean and significant export production to the seafloor denoting efficient benthopelagic coupling. The evidence of high export production in the Pacific Ocean was further supported by a notable abundance of taxa regarded as a good indicator of high export production such *Siphogenerinoides brevispinosa, Stilostomellids* and *Buliminids* (Arreguin-Rodriguez *et al*., 2016; Tables 3.1-3.6) at Sites 1209B and 1212B.

The productivity at the main CIE section was not very clear perhaps as a result of massive carbonate dissolution that led to shoaling of CCD globally during the PETM. All the proxies indicate a collapse in both pelagic (surface) and benthic productivity. The rise in temperature that resulted from the PETM must have increased the metabolic rate of the pelagic primary producers (Thomas, 2007). The high temperature recorded during the peak of the CIE must have caused encystment of many phytoplankton and reduced primary production (with episodic productivity when the environment is conducive to reproduce) while the zooplankton may have moved deeper into the water column and thoroughly foraged all the available organic matter and diminished the quality and quantity of organic carbon reaching the seafloor.

Enhanced foraging of the upper water column would mean that less phytodetritus will be reaching the ocean floor resulting in food scarcity and increased competition. In addition, increase in the solubility of calcium carbonate resulting from higher CO_2 concentration and lowered pH in the ocean will stimulate foraminifera to reduce calcification by building smaller and thinner test walls which are less likely to be preserved in the sediment record.

Palaeoproductivity picked up again after the BBE as indicated by the increase in the relative abundance of both planktonic and benthic foraminifera at Site 1209B (Takeda and Kaiho, 2007; Petrizzo, 2007), though this was not reflected on the $\delta^{13}C$ record as it remained relatively low throughout the rest of the studied interval in the Pacific. The lowering of $\delta^{13}C$ record in benthic foraminifera even when the abundance of biomass increased could be attributed to vital effect[5].

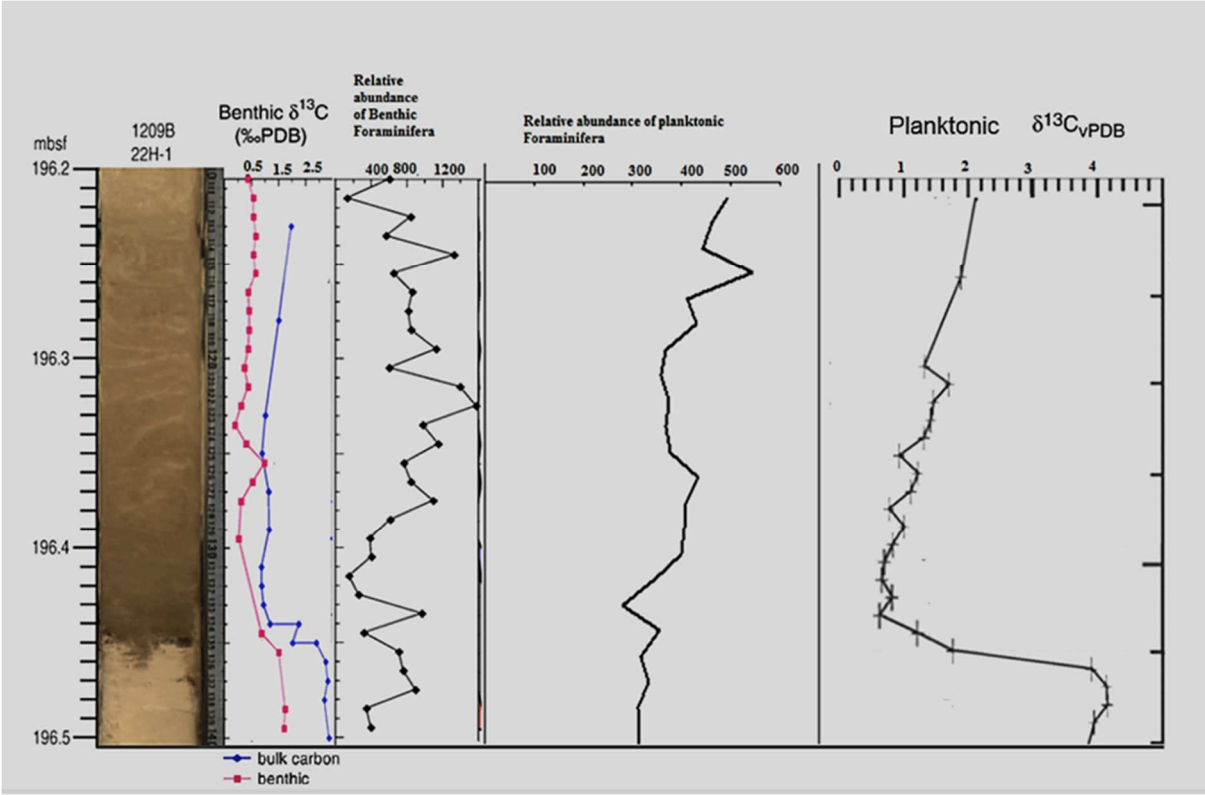

Figure 3.21: Records of benthic and planktonic foraminiferal abundance and $\delta^{13}C$ record from Site 1209B indicating changes in litho, bio and isotope stratigraphy during the PETM. Benthic foraminifera abundance and benthic isotope record was plotted from Takeda and Kaiho (2007) while the planktonic foraminifera abundance and isotope record was plotted from Petrizzo, (2007)

The connection between trait composition and productivity has not been well publicised in foraminiferal research. Jorissen *et al*. (2007) believed that cylindrical spherical and planispiral morphogroups usually with infaunal habit are common in the area of high productivity. In the PETM section at the Pacific Ocean, trait composition was dominated by the terminal apertures, fine perforation, grazers, infauna, planispiral, elongate test, sessile, biserial-triserial and

[5] Vital effect is the impact of ecological and environmental variability on the geochemical signatures of biominerals. For instance planktonic foraminifera may change their depth of habitat during ontogeny for specific nutrient or ecological requirement and return to their normal habitat adult stage. This affects the isotopic composition of their test (See Schiebel *et al.,* 2017 for more details).

complex apertures (Figures 3.5, 3.6; 3.10 and 3.11). These trait assemblages strongly support the Jorissen *et al.* (2007)'s hypothesis. Another possible explanation for the increase in cylindrical and bi-triserial traits may be related to their response function towards environmental perturbation and not really to productivity increase. Increase in the abundance of oligotrophic taxa such *N. trumpyi, Q. profunda and G. subglobosa* may suggest lowered productivity or well-functioning bentho – pelagic coupling[6]. This is also in line with the deduction on the food supply that suggested sustained mesotrophy during the PETM in the Pacific Ocean. In addition, the topography of elevated platform like the Shatsky Rise (Figure 2.3; Altenbach *et al.,* 1999), trophic focusing has been identified as the cause of disparity between food supply and productivity. Trophic focusing involves winnowing of the fine organic particle by current and concentrating them on a particular part of the ridge. (Arreguin-Rodriguez *et al*., 2016; Heinz *et al*., 2004). Kelly *et al*. (2006) also reported a decrease in calcareous nannoplankton abundance during the PETM in the Pacific Ocean. This decrease could also be a result of carbonate dissolution associated with the event.

In summary, i believe that the initial increase in the ocean-atmospheric CO_2 and the coeval rise in temperature before the CIE resulted in an increase in productivity with enhanced organic matter rain to the seafloor but with a further rise in temperature, phytoplankton productivity optimum was exceeded in the surface ocean leading to lowered export production. More so, the increased ocean acidification resulted in reduced calcification in the form of smaller and thinner test walls in benthic foraminifera and increase in bacterial activity in the sea floor. Increase in the opportunistic and resilient taxa utilised more bicarbonate in the upper water column and acted as a sink to the CO_2. The increase in silicate weathering from the continents enhanced this process and triggered the recovery of PETM. However, export production to the benthic realm never returned to the pre-CIE scenario as suggested by bulk carbonate and foraminiferal $\delta^{13}C$ records in figures 3.19 and 3.21.

[6] Benthic – Pelagic coupling refers to the exchange of mass, nutrients/organic materials or energy between benthic and pelagic habitats of the ocean (Griffiths *et al.,* 2017)

3.3.3.2 Palaeoproductivity/global carbon cycle in the Tethys Ocean as interpreted from fauna and trait composition from Alamedilla section

The high abundance and diversity of foraminifera, as well as high bulk carbon values (Alegret et al., 2009) at Alamedilla section, was interpreted as the high flux of organic matter resulting from strengthening primary (surface ocean) and export productivity. Before the initiation of the CIE, $\delta^{13}C$ record of bulk $CaCO_3$ was as high as 3‰ with a remarkable increase in the epifauna and infauna (Figure 3.20). The co-occurrence of epifauna and infauna indicates optimum productivity condition and deep water ventilation as well as efficient solubility and biological pump that could allow highly heterogeneous fauna to thrive in the sedimentary record (Guisberti *et al.,* 2016). Increase in both primary and export productivity has also been reported in the western Tethys at Forada section (Italy, Guisberti *et al*., 2016). The climax of benthic productivity was attained after the BEE with the deposition of clay horizon rich in organic matter and iron oxide free from calcium carbonate. This layer marks the peak of the PETM warming at Alamedilla. Similar organic carbon-rich layers have been reported in other PETM sections in deep water and continental deposits such as Contessa and Forada (Italy) as well as Zumaia (Spain) in the western Tethys. $\delta^{13}C$ record of bulk carbonate suggests a significant decrease in the carbonate content after the BEE and a coeval increase in silicate mineral in the sediments (Alegret *et al*., 2009), but there was also an increase in the abundance of *Buliminids* (indicator of high productivity) as well as higher abundance of epifauna morphotypes. This suggests oligotrophic bottom water conditions. The decrease in the $\delta^{13}C$ content in the bulk sediment could be attributed to the global dissolution of $CaCO_3$ during the PETM and does not necessarily imply a decrease in palaeoproductivity. Also, the increase in abundance of epifauna during this period of rising in temperature could tilt the foraminiferal assemblage towards oligotrophy (Alegret *et al.,* 2009) because the rise in temperature increases the metabolic efficiency of foraminifera (Thomas, 2007) and encourages thorough pasturage of available food material. Infauna morpho-groups remained relatively low in abundance after BEE because more epifauna consumed most of the organic matter at the sediment-water interface reducing the food reaching the deeper infaunal niche. The $\delta^{13}C$ content increased in this section indicating deepening of the CCD and PETM recovery but the carbonate concentration did not return to the pre-extinction value suggesting that the benthic ecology never recovered from the PETM perturbation.

The trait composition across the studied section showed strong similarity with those of the Pacific Ocean. The traits were dominated by tubular, elongate and spiral, and hyaline calcite test, sessile, shallow infauna and deposit feeding habit and a combination of simple and complex apertures with fine perforation (Figures 3.5; 3.10; 3.15). This trait assemblage suggests high organic carbon influx to the seafloor but not so high as to destroy the epifaunal niche as observed in the open ocean of the Pacific. Nevertheless, there was a notable high abundance of trochospirally coiled and agglutinated taxa such as *Glomospira spp*., *Repmanina charoides* and *Trochamina* spp. that bloated the frequency of spiral, trochospiral and basal interiomarginal traits.

Tubular, hyaline calcite, shallow infauna, sessile, deposit feeding, fine perforation and complex apertures are noted for the traits that sustained carbon cycling in the benthic ecosystem during the PETM extreme condition because of their increase in abundance during the PETM.

3.3.4 Oxygen concentration in the seafloor

Estimating the amount of dissolved oxygen in the sea floor using faunal association is complicated but has been successfully demonstrated by Kaiho (1994). This is because oxygen concentration in the bottom water also depends on the interaction between the quantity of organic matter reaching the seafloor, deep water circulation pattern, temperature and faunal composition. Another difficulty lies in the fact that some taxa (especially epifauna) considered to be abundant at a particular amount of oxygen concentration does not spend their whole lifetime in a single niche but migrate within a wide range of variable oxygen concentration environment during their life (Jorissen *et al.,* 2007). Nevertheless, the study by Kaiho (1994) identified critical dissolved oxygen concentration markers for estimating the amount of oxygen available in the benthic ecosystem.

3.3.4.1 Pacific Ocean

Foraminiferal composition in the Pacific Ocean (Sites 1209B and 1212B) indicates low oxygen concentrations throughout the PETM. Prior to the initiation of the CIE, the faunal assemblage was composed of dysoxic (moderate oxygen concentration) indicators characterised by a mixture of low oxygen taxa such as *Bolivina inconspicua, Buliminids* and *stilostomellids* (Table 3.1) and oxic fauna like *Gavelinella spp., Anomalinoides* and *Gyroidinoides* species occurring together in the sediment.

The high abundance of deep infauna, (Figure 3.5) in association with a few number of epifauna taxa reveals that oxygen level was already low in the benthic environment, but just slightly enough to keep the species that needed higher oxygen concentration on life support. The threshold of taxa that require high oxygen concentration was probably reached at the onset of the CIE that resulted in the benthic foraminiferal extinction (BEE). The BEE may largely have been caused by low oxygen concentration because high porosity epifauna taxa like *Gavelinella beccariiformis* needed high dissolved oxygen for their metabolic requirements but could not get enough. Low amount of dissolved oxygen accompanied by high organic carbon influx to the sea floor plus water column stratification combined to exterminate the susceptible (highly perforated) epifaunal species. Other epifaunal species that survived this hypoxia are well adapted to low oxygen concentration and had the ability to tolerate high organic carbon influx or are able to move up and down the sediment column.

The acme of *Bolivina gracilis* as well as a significant increase in the abundance of opportunistic taxa (*Q. profunda)* have been interpreted as a marker for low oxygen concentration at the peak of the CIE (Takeda and Kaiho, 2007). The amount of dissolved oxygen slightly increased after the peak of the CIE and at the beginning of the PETM recovery as suggested by high abundance of infaunal taxa (*Buliminids*) and the reduction in the opportunistic taxa (Takeda and Kaiho, 2007; Table 3.3) because more oxygen was available in the sediment and the infauna could favourably compete with the opportunistic taxa for the accessible nutrients.

The trait composition from SIMPER results revealed that the dominant traits driving ecological changes in Sites 1209B and 1212B during the PETM are deep infauna, sessile, elongate, no ornamentation, fine perforation, terminal apertures, planispiral and bi/trispiral test shape (Figures 3.5; 3.6). These trait assemblages strongly suggest adaptation to low oxygen condition, Kaiho (1994) describes the morphological characteristics of low oxygen taxa as thin wall, elongate, spiral and multi-serial. These attributes help them to maximise available oxygen to continue their metabolic activities in the face of hypoxia. Elongate and biserial taxa such as *Bolivina* have been reported to respiring nitrate in the absence of oxygen (Keating-Bixonti *et al.,* 2017). Some species of foraminifera found in the oxygen minimum zone have also been reported to lack ornamentation (Boltovskoy *et al.,* 1991) and no ornamentation trait was relatively high in the SIMPER result as shown in Figures 3.5 and 3.10. There was a mixture of traits like basal interiomarginal, trochospiral, and species with umbilical apertures. Such traits are indicating an increase in the abundance of opportunistic taxa across PETM events and

suggest environmental disturbance or periods of episodic bloom as a result of a seasonal increase in oxygen concentration.

3.3.4.2 Tethys Ocean

The oxygen concentration in the Tethys Sea was not as low as in the Pacific. The high taxa abundance, diversity and heterogeneity in the Alamedilla section are a positive indicator of the well-oxygenated environment (Jorissen *et al*., 2007) in the latest Palaeocene. The epifauna and infauna morphotypes are relatively high in abundance, an indication that the bottom water, sediment surface and down to few centimetres had enough oxygen to sustain both morphotypes successfully. The main body of the CIE interval at Alamedilla did not seem to experience extreme anoxia as reported in other open ocean (Walvis Ridge, Wendell and Southern Ocean (Thomas, 2003; 2007; Zachos *et al*., 2008; Dunkley-Jones *et al*., 2013) during the PETM. Iron enrichment and bioturbation (Alegret *et al.,* 2009), as well as the highest abundance of oxic environment indicators (*G. subglobosa* and *O. umbonatus*), occurred at the main CIE interval (see Arreguin-Rodriduez *et al*., 2016; Tables 3.7 and 3.9). There was no significant increase in the infaunal morphotypes as shown in Figure 3.20 because the increase in oxygen concentration meant that the epifauna thrived and competed favourably with the deeper dwelling taxa. Increase in the heavily calcified taxa like *Anomalinoides* species and *Osangularia spp*. further supports the oxic nature of the CIE interval at Alamedilla. The cause of BEE at the Tethys may have been extreme temperature and other ecological perturbation but not necessarily low oxygen concentration (Alegret *et al.,* 2009).

The trait composition in Alamedilla was similar to those that occurred in the Pacific Ocean (Figure 3.17). However, the magnitude of interiomarginal, trochospiral and spiral are relatively the same as the hypoxic indicators (Figure 3.16). This strongly correlates with the faunal distribution that showed co-habitation of epifauna and infauna in a suboxic environment.

3.4 Conclusions

This study is a novel one and it pioneered the utilization of trait changes in fossil foraminifera as indices for paleoecological changes in the benthic system. We have shown that trait composition in conjunction with faunal assemblages can be used as indices for palaeoecological changes and to detect ecological disturbance in the marine ecosystem. Detail examination of foraminiferal traits across the PETM sections at Northeastern Pacific and Tethys seas indicated that mostly heavily calcified and perforated benthic foraminifera taxa

went into extinction during the PETM but a significant number survived. This suggests that foraminifera could tolerate a wide range of ecological changes and withstand extreme ecological conditions through various trait manoeuvring such as increasing the abundance of taxa with resilient traits during environmental perturbation.

The results from this study also showed that changes in foraminiferal traits does not occur at the same time as the faunal turn-over in foraminiferal taxa, implying that traits of foraminifera are conserved. Careful examination of foraminifera census data from Takeda and Kaiho (2007) and Alegret *et al* (2009) revealed a very dynamic changes in foraminiferal events across the studied sites, however, the foraminiferal trait diagrams in Figures 3.6; 3.11; 3.16 showed a more uniform and predictable bioevents. The similarities in trait events in Figure 3.17 and Table 3.10 indicate that some foraminiferal trait are redundant meaning that different species share similar traits and when one goes into extinction similar species sharing the same trait can still maintain ecological functioning in the ecosystem.

Our results also have shown strong evidence that the trait composition of foraminifera can be used to characterised climatic events and sedimentary facies across basins as exemplified by trait similarities during the hyperthermal in both basins (Table 3.10). Nevertheless, some trait modalities such as hyaline calcite tests have been affected by the intensity of carbonate dissolution in both basins because of the ocean acidification. The decrease in the hyaline calcite in the Shatsky Rise indicates that carbonate dissolution in the Pacific Ocean may have been more severe during the PETM than at Alamedilla contrary to claim by Algret *et al.* (2009).

Table 3.10: Summary of trait occurrence patterns across the PETM events in the tropical Pacific and Tethys Oceans

Traits	Traits that showed the same pattern in all sites	Traits that increased in abundance at the same interval	Traits that decreased in abundance at the same interval	Traits with no pattern between sites
Test shape	Elongate, spiral test	Spiral test	Elongate	Tubular test , globose
Test Composition	Hyaline aragonite, porcelaneous	Hyaline aragonite	Porcelaneous,	Hyaline calcite, agglutinated
Chamber arrangement	Uniserial, trochospiral	Trochospiral test	Uniserial	Bi/triserial
Chamber Shape	Spherical/oval, tubular, triangular/trapezoids and semi-circular	Tubular chamber	Spherical/oval, triangular/trapezoids and semi-circular	
Test macro-ornamentation	Raised sutures, depressed sutures	Raised sutures, depressed sutures		
Micro ornamentation	No ornament, Spinose	Spinose,	No ornament	Striate
Aperture form	Arcuate, oval/reniform	Arcuate	Oval/reniform	Slit like, Radiate
Apertural accessories	Lip	Lip	Neck	Bifid teeth
Primary aperture position	Terminal apertures, umbilical/extra-umbilical	Umbilical/extra-umbilical	Terminal apertures	Basal interiomarginal
Test perforation	Fine perforation, macro perforation, micro perforation	Fine perforation, macro perforation		No perforation
Living habit	Shallow infauna and grazers, deep infauna and deposit feeders	Shallow infauna and grazers, deep benthic infauna and deposit feeders		epifauna
Mobility	Sessile, free-living	Sessile, free-living		

The trait distribution partly conforms to the taxonomic composition of foraminifera from which they were derived, however, the biological trait analysis demonstrated how foraminifera maintained benthic functioning in the face of an extreme climate event that led to the extinction of numerous benthic foraminifera. For instance, the extinction of taxa with highly calcified and mega perforated taxa like Gavellinidae at the Shatsky Rise was followed by an increase in smaller-sized opportunistic taxa such as *Q. profunda*; (Table 3.2) with micro-perforated tests that require less dissolved oxygen and well adapted to high organic rain.

The biological traits analysis of foraminiferal turnover from the Shatsky Rise (Pacific Ocean) and Alamedilla section (Tethys Sea) across the PETM has revealed the ecophenotypic responses of the benthic foraminiferal community to the environmental perturbations. The increase in temperatures and dissolved inorganic carbon associated with the event resulted in

enhanced food supply, decreased the amount of dissolved oxygen and palaeoproductivity in the Pacific Ocean. The excessive supply of organic material to the seafloor and lowered oxygen concentration resulted in the extirpation of the highly porous trochospirally coiled epifaunal taxa. However, in the Tethys, high productivity, moderate supply of oxygen and nutrient to the sea floor as indicated by high abundance of both the infauna and epifauna suggest effective bentho – pelagic coupling. The cause of extinction in the Tethys Sea is probably high temperature and ocean acidification as revealed by organic-rich clays found across the central and western Tethys (Giusberti *et al*., 2016; Arreguín-Rodríguez *et al*., 2018).

In both oceans, the statistical result showed that infaunal, sessile life habits, cylindrical elongate and bi-triserial test forms, complex terminal apertures and omnivorous feeding modes were the most resilient traits during the hyperthermal (Figures 3.5; 3.10; 3.15). Along with other opportunistic taxa the *Buliminids, Bolivinids, Pleurostomellids* and *Stilostomellids* may have utilised their facultative anaerobic metabolism enhanced by cytoplasmic streaming to sustain calcification and drew down the excess dissolved inorganic carbon in the water column. Increase in populations of foraminifera during the recovery intervals in all the studied sites together with high temperature feedbacks such as increase in precipitation and silicate weathering would have eventually returned the ocean to its normal state.

CHAPTER FOUR

The impact of high palaeoproductivity on the test and ecological function of foraminifera in the equatorial Pacific Ocean during the PETM

4.1 Introduction

Productivity in the modern equatorial Pacific is reportedly the highest compared to any other pelagic biomes in the world (Moore *et al*., 2004). Equatorial Pacific is estimated to have the largest primary production of 20%–60% in the modern oceans most of which is exported to the benthic zone (Lyle and Wilson, 2006). It hosts the largest reservoir of carbon and nutrients, and so it makes a major contribution to the global carbon budget through its regulation of global organic/inorganic carbon and atmospheric CO_2 partial pressure (pCO_2). Although the physical and chemical properties of the Pacific Ocean may have differed somewhat from what they are now during the Palaeogene, high palaeoproductivity has also been reported in the North equatorial tongue during the Eocene (Moore, 2005) and the PETM (Faul and Paytan, 2005; Ma *et al.,* 2014) at which time the equatorial Pacific also accounted for significant volume (60%) of the global ocean (Lyle and Wilson, 2006).

Ocean productivity is the main driver of foraminifera composition/changes in the benthos ecology as its a major food source, but also controls the amount of oxygen available for faunal utilisation (Altenbach *et al*., 1999; Jorissen *et al.,* 2007). Benthic foraminifera are a very useful tool for the reconstruction of the palaeoflux of organic matter on the sea floor because they constitute a major proportion of the benthic biomass in the open ocean (Altenbach and Sarnthein, 1989; Licari *et al*., 2003; Cavan *et al.,* 2017). The main source of food to the benthic organism is the detrital rain from the particulate organic matter produced by the plankton in the surface ocean except where hydrocarbon seeps and hydrothermal vents are present (Cavan *et al*., 2017).

The response of foraminifera to the organic carbon flux in the ocean floor is controlled by the quantity and quality of the organic material reaching the ocean floor. Hence adequate knowledge of the past changes in primary production and export production as it relates to foraminifera is crucial to the understanding the biological carbon pump which is a major driver of ocean productivity and in extension climate change (Chisholm 2000, Birch *et al.,* 2016).

Barite accumulation rate (BAR) during the PETM indicated that high pCO_2 had a fertilising effect on the primary producers which led to increase in reproduction and coeval increase in export production during the event (Ma *et al.* 2014). Although the evaluation of palaeoproductivity is difficult, biogenic barium is a good indicator of biological productivity because it is well preserved in pelagic settings (Paytan *et al*., 1996; Bains *et al.,* 2000). The high rate of BARs correlates well with the increase in export production, i.e. carbon flux from the surface water to the intermediate and deep waters (Dymond *et al.,* 1992) which is also a function of primary production. Increases in the temperature of the ocean can also lead to increased in bacterial activity and organic matter regeneration and nitrogen fixation (Ma *et al.,* 2014) thereby increasing the efficiency of the biological carbon pump and higher export production. More so, increase in nutrients in the ocean, either by continental runoff or upwelling from the deep sea, causes blooms of phytoplankton and increased export production to the ocean beds.

The PETM section of equatorial Pacific Ocean is reported to have the highest export production when compared to any site at a rate of 112g C m^{-2} yr^{-1} compared to 28 – 48g C m^{-2} yr^{-1} in the Atlantic and Southern Oceans (Ma *et al.,* 2014). The evidence of high organic matter content in the Central Pacific is present in the cores recovered from Site 1215A (Figure 4.1). And as stated in previous chapters, the understanding of the impact of the enhance palaeoproductivity during the PETM in the benthic ecosystem will give an insight on how current global warming will affect the deep sea benthic

The focus of this chapter is to examine the foraminiferal abundance and trait composition across the PETM section at Site 1215A, analysed them using the BTA and scanning electron microscopy (SEM).

See chapter two for details on the location, materials and methodology.

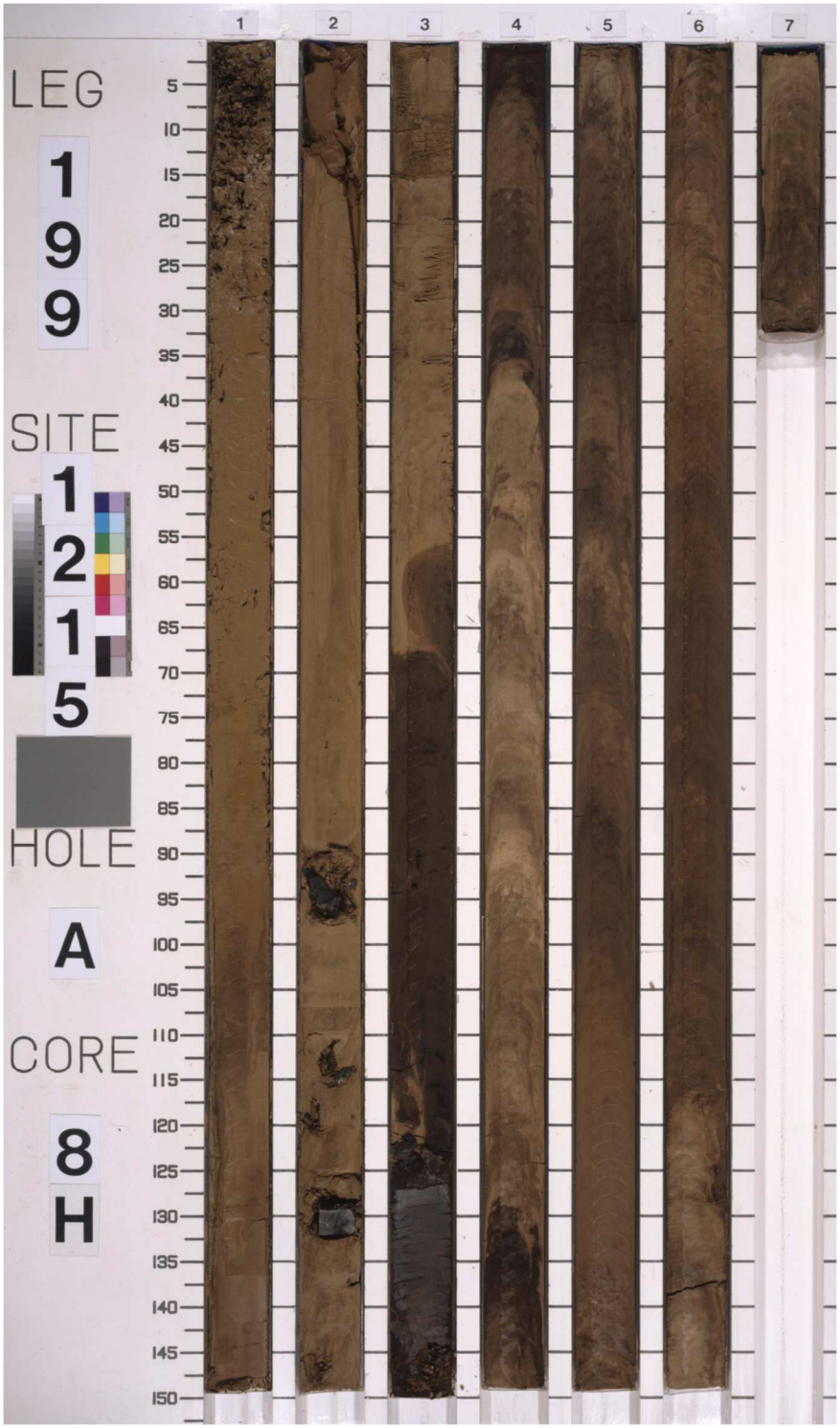

*Figure 4. 1: Digital core photograph of Core H8, ODP Site 1215A. The brown colouration is an indication of high organic matter content in the central tropical North Pacific Ocean. The PETM occurred in the darkest part of section 3 (*http://web.iodp.tamu.edu/OVERVIEW)

4. 2 Results

4.2.1 Core description

The detailed lithologic description of core 1215A 6H and 8H sampled for this work is outlined below from bottom to the top.

Core 8H-07 was the base of section sampled for this analysis; it was a short core of 32cm in total length that grades from light brown calcareous oozes at the top to dark brown nannofossil at the bottom.

Core 8H-06 composed of an intercalation of dark brown – very dark brown oozes. It is made of dark brown oozes from the core top to the 44cm interval, very dark brown at 45 – 116cm while the section from 117 -150TD was composed of light brown oozes.

Core 8H-04 composed of black nannofossil oozes from the core top to about 6cm interval. There was a diapiric intrusion of the lighter coloured ooze from 7-11cm and alternation of dark to very dark layers from the 12-38cm interval. However, a lighter brown interval underlain the intercalation from 38 – 98cm interval. Below this was another 18cm thick of very dark brown ooze. The onset of the CIE is situated in the upper part of this core.

Figure 4.2: A section of core 8H-03 showing sediment diapir and soft sediment deformation

The lithologic composition of core 8H -03 is the same nannofossil oozes, but it contains some small chert at the 8cm interval as well as 123 cm interval. There is evidence of a break in sedimentation and a sort of sediment deformation on this core (Figure 4.2). Two bigger lumps of chert also occurred at the 123cm interval with a little mixing of lighter coloured sediment. The black nannofossil oozes continued to the 144cm interval where another sediment

disintegration occurred around some chert fragments. 128-148 cm interval is interpreted as the P/E boundary and the core of the PETM.

Core 8H-02: The prevailing colour of the sediment on this section of the core was dark brown oozes, but there was a spectacular feature which I interpreted as a micro fault that runs from 11cm interval and sidetracks through 55cm of the core (Figure 4.3). This is not unusual considering the location of the site near the Molokai fracture zone. A dark coloured chert occurred at 90 – 98 cm, 111-116cm 119 – 120cm and 128 – 133 cm intervals. Carbon Isotopic Excursion (CIE) started at this section of the core.

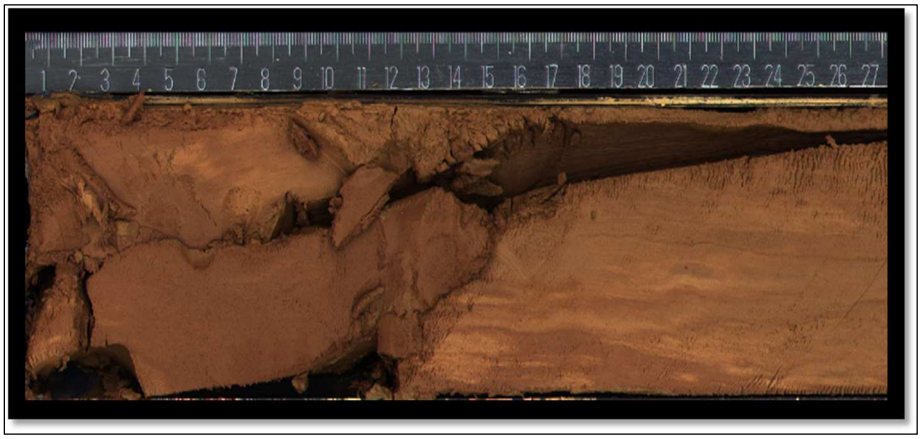

Figure 4.3: A section of core 8H-02 showing a fracture across the core

Core 8H- 01 was composed of predominantly dark brown nannofossil ooze. Some sort of soupy sediment occurred from the core top to the 31cm interval (Lyle *et al.,* 2002), and a mixture of stable/flowing sediments was recognised from 32cm – 91cm interval. The rest of the core from 91cm to the TD- 150cm was made of more stable and very dark brown ooze.

N/B Core section 7H of Site 1215A recovered only a black chert and was not analysed for this study (Figure 4.5, Leon – Rodriguez and Dickens, 2010).

Core 6H- 06 was mainly a dark brown ooze, the intervals from 9-13cm, 30 -33cm, 39 -42cm and 45 – 49cm were very dark, while the rest were dark brown. The total depth of this core was 78cm.

Core 6H -05: The core top up to 6cm interval was composed of dark brown nannofossil ooze, while 7-28 cm interval was light brown, 28-39 dark brown, 40-80cm light brown, 81-89 dark brown and 90 -100TD light brown.

Core 6H-04 also consisted of predominantly dark brown nannofossil ooze, apart from the intervals from 30-37, 52-68, 77-88, 114 -124 and 138-149TD which were light brown in colour. A black chert occurred between 89-113cm interval.

The top of core 6H-03 was a light brown nannofossil ooze, except at 5cm interval where a dark brown clay lens pierced in between the nannofossil sediment (Figure 4.4) reflecting a mixture of sediment of different ages. Also, there was a lump of chert and dark mineral fragments suspected to be igneous materials at 46 – 55cm interval.

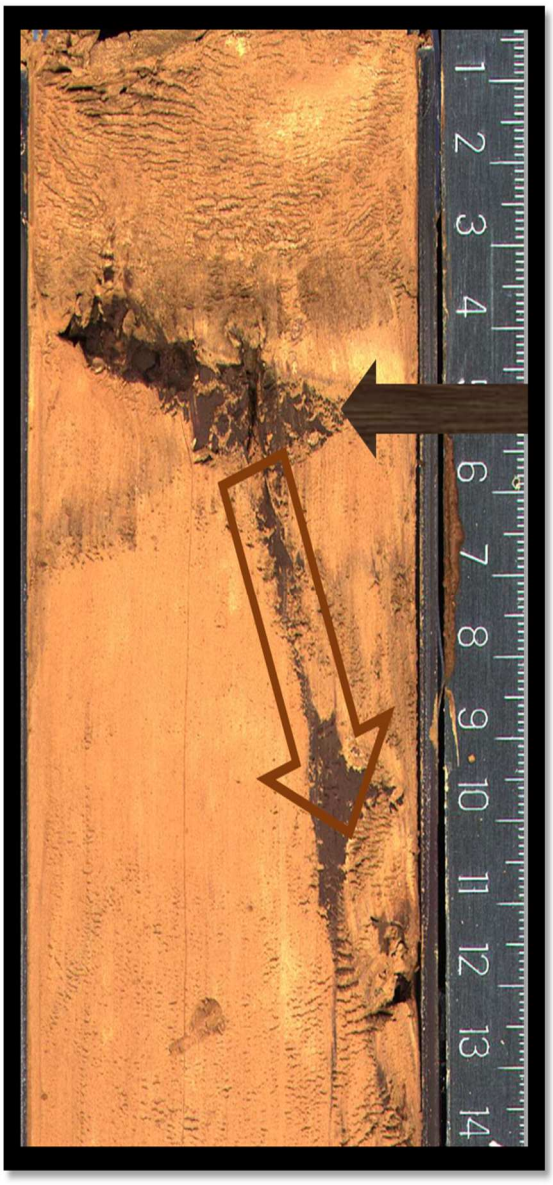

Figure 4.4: A section on core 6H-03 showing sediment mixing within the core. Arrows show directions of sediment deformation in this core. The flow in structure could affect the quality of biostratigraphic data collected from this section of the core.

The lower section of the core was interbedded with darker coloured oozes. The interval between 69 -73cm was dark brown, 91-96cm (dark brown), 118- 122cm (very dark brown), 135 – 138 (very dark brown) while other intervals composed of lighter brown sediment. The total depth (TD) of the core is 150cm.

Core 6H-02 comprised of inter-bedded dark and light brown nannofossil ooze and clay. Dark brown ooze occurred from the 1-7cm interval, underlain by light brown sediment from 7-26cm, and another dark brown interval occurred from 26-37cm. The inter-bedding continued from 38 -54 (light brown), 55 – 67cm (dark brown), 68 – 85 (light brown), 87-89 (dark brown), 99 – 113(light brown). There was evidence of flow-in and sediment mixture on this core section.

4.2.2 Chronology

The age model for the studied section of Site 1215A was based on the paleomagnetic information and magnetic susceptibility data from Shipboard Scientific Party Leg 199 and biostratigraphic events from Leon-Rodriguez and Dickens, 2010.

Unit II of Site 1215A was assigned Chron C24r from the identified palaeomagnetic reversal and anomalies (Agnini *et al*., 2007; Figure 4.5). Calcareous nannofossil was the best tool for the high-resolution age model for this section. The occurrence of *Fasciculithus richardii*, and *F. shaubii* at 55.38 mbsf mark the top of calcareous nannofossil zone NP9 (Raffi *et al.,* 2005) and the last downhole occurrence (LDO) of *Tribrachiatus bramlettei* found at 54.32 mbsf correspond to the base of NP 10. The absolute ages of the studied section (Figure 4.5) were derived by correlating shifts in the bulk carbonate isotope data from Leon-Rodriguez and Dickens (2010) work with the trends in the $\delta^{13}C$ records from ODP Site 690 for which a high resolution and orbitally tuned age model have been established by Rohl *et al*., 2007. The average sedimentation rate for Unit II was approx. 8.5m/m.y.

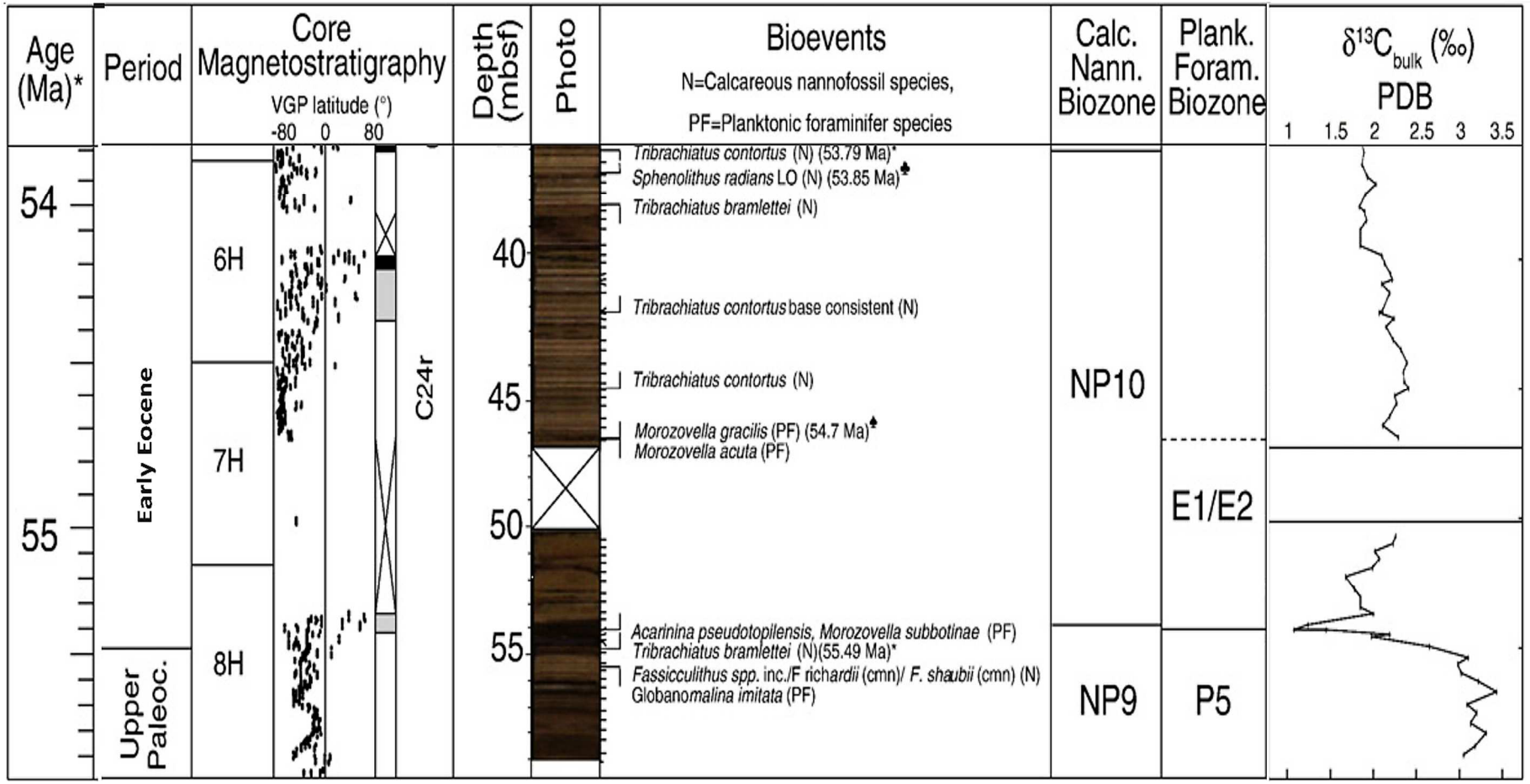

Figure 4.5: Chronology and stratigraphy of the studied section of ODP Site 1215A, cores 6H -8H (Adapted from Leon-Rodriguez & Dickens, 2010)

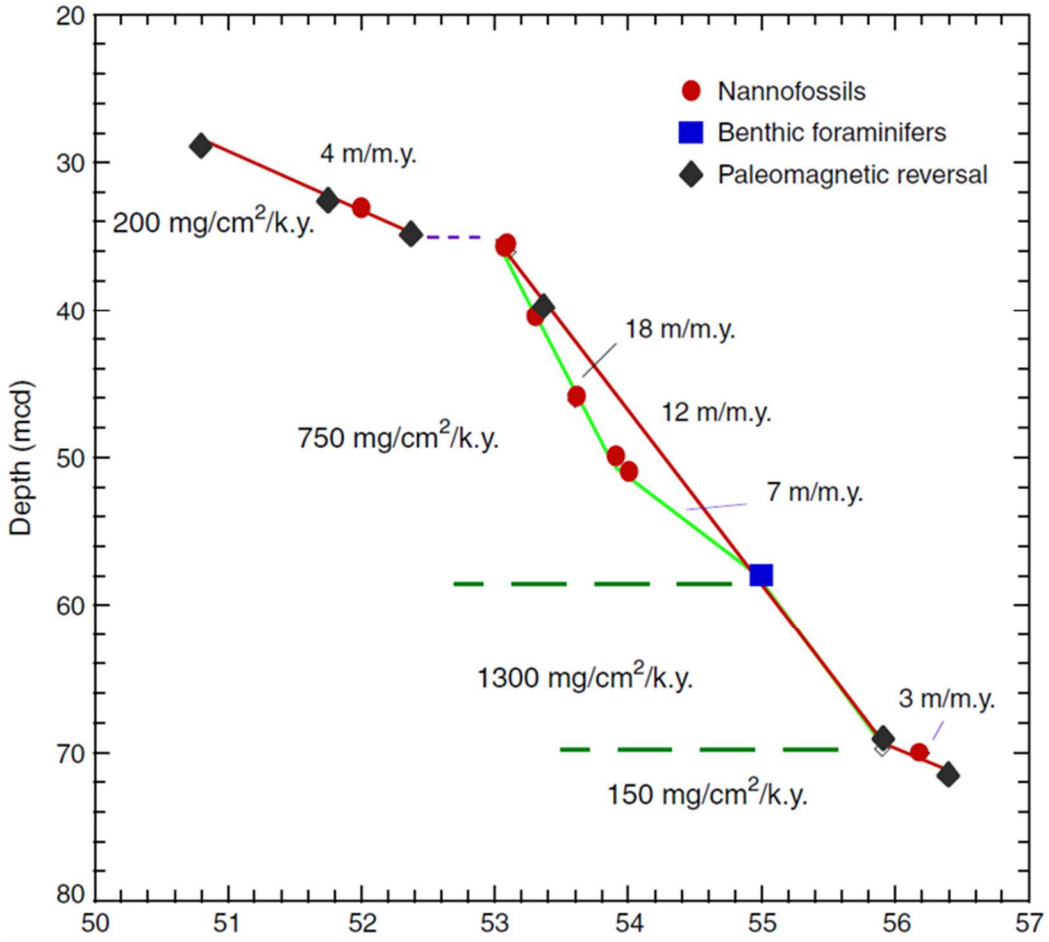

Figure 4.6 Age – depth model and sedimentation rate for Site 1215A (Taken from Lyle et al., 2002)

To calculate the sedimentation rate, the age-depth model was first derived using age dating techniques, and the sedimentation rate was derived from age-depth formula (See Lyle *et al.,* 2002). The line of best fit was drawn through all the bioevents and palaeomag data over a successive depth interval (Figure 4.6; Lyle *et al.,* 2002).

4.2.3 Benthic foraminiferal taxa composition and changes through time in Site 1215A

The benthic foraminiferal composition and assemblage in Site 1215A were dominated by calcareous hyaline taxa, with agglutinated forms constituting less than 10% of all the identified fauna. The strong dominance of benthic foraminifera with the calcareous hyaline test in the recovered taxa indicates that the studied section was deposited above the lysocline, and carbon compensation depth (CCD). However, poor preservation of planktonic and benthic foraminifera tests suggest that the lysocline may have been really close to the depositional depth especially during the PETM when the preservation was worst affected. 117 species constituting 4065 specimens of benthic foraminifera were identified and counted. The faunal

assemblage was predominantly infaunal morphotypes (~60% relative abundance), including *Bulimina, Abyssamina*, and cylindrical taxa like *Pleurostomella, Nodosaria,* and *Stilostomella*. The epifauna was relatively less (approx. 40%) with mainly cosmopolitan deep water Velasco-type taxa such as *Nuttalides*, *Anomalinoides, Cibicidoides, Gyrodinoides and Valvalabamina* (Figure 4.8; Table 4.1).

The nmMDS of taxa composition (Figure 4.7) showed a direct opposite of what we observed in other sites with the CIE samples clustering more tightly together than the other intervals. Most of the pre-CIE samples spaciously clustered at the base of the plot except for a sample from 56.5 mbsf. The CIE samples clustered more tightly at the upper part while the recovery samples clustered in between the pre-CIE and the CIE. The samples from the recovery interval were the most dispersed when compared to the other intervals. The ordination also showed that the recovery fauna were more closely related to their CIE counterpart than to the pre-CIE. The three samples from the CIE that clustered closer to the pre-CIE were those from the onset of the excursion, suggesting that they are more related. The clustering together of the CIE samples is interpreted as evidence of similarity in taxonomic composition and may also reflect a higher sampling resolution of that interval as the pre-CIE and the recovery were sampled at a lower resolution (Table 2.2). The recovery samples with wider dispersal were those at the transition from the CIE to the recovery; this suggests that fauna at the interval just before the recovery were still experiencing some perturbation. In general, the samples that did not ordinate with the respective group were those related to either the beginning or termination of the negative carbon isotopic excursion. Sample 41.01mbsf was an exception but it was the first sample analysed for this study and was basically a training sample.

The ANOSIM test indicated that the foraminifera communities from three intervals differed significantly from each other with the global R= 0.20 and $p<0.05$.

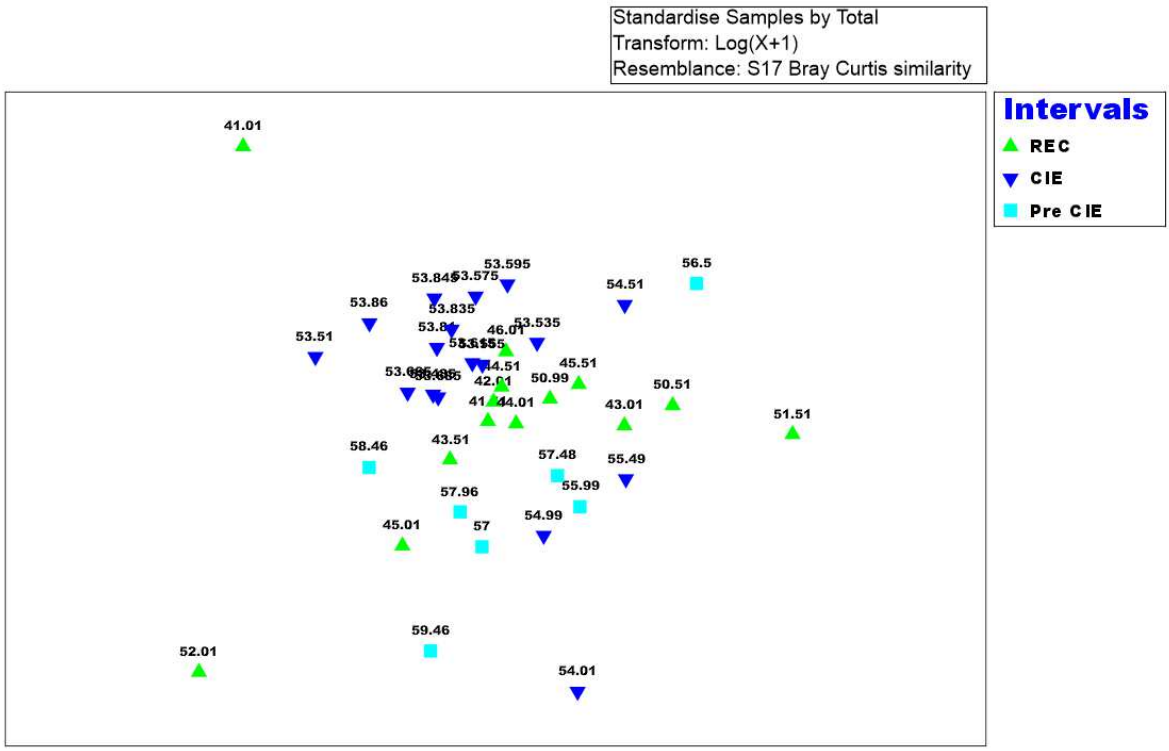

Figure 4.7: Non-metric Multidimensional Scaling ordination of benthic foraminifera taxa composition (transformed with total resemblance) of Bray-Curtis similarity from Site 1215A ODP Leg 199, Central equatorial Pacific Ocean.

The SIMPER result indicated that 24 taxa were the major contributor to the differences/ similarities observed in the faunal composition of the PETM intervals studied at Site 1215A. The highlighted species were predominantly cosmopolitan and composed of both infauna and epifauna morphotypes (Table 4.1). The pre-CIE was characterised by increase in the abundance of both robust/heavily calcified taxa as well as small disaster taxa. The CIE was characterised by increase in the small disaster taxa only and the recovery interval was characterised by mostly heavily calcified taxa (Table 4.1).

The mean abundance of the taxa present in the similarity percentage result showed that *Paralabamina elevata, Valvalabamina praeacuta, Buliminella beaumonti, Globorotalites micheliniana, Paralabamina lunata, Aragonia aragonensis, Oridorsalis umbonatus, Valvalabamina sp.2, Gyroidinoides subangulatus, Neoeponides hillebrandti,* and *Pullenia subcarinata* were relatively higher during the pre-CIE than in other intervals. The foraminifera assemblage above were dominated by epifauna taxa with few *Buliminid*s (Table 4.1). Despite the high number of species in this interval, their % contribution to the total dissimilarity was very low.

Table 4.1: Mean abundance of taxa that contributed the most dissimilarities observed in faunal distribution across the CIE intervals at ODP Site 1215A. Data is limited to 50% cumulative contribution.

Species	**Mean Abundance**			**Contribution to dissimilarity (%)**
	REC	**CIE**	**Pre CIE**	
Abyssamina quadrata	1.85	**2.36**	1.28	5.3
Nuttallides truempyi	2.08	**2.77**	1.38	5.12
Tappanina selmensis	1.78	**1.81**	0.41	4.08
Paralabamina elevata	0.13	0.24	**1.59**	2.99
Valvalabamina praeacuta	0.6	1.04	**1.57**	2.87
Anomalinoides praeacutus	**1.56**	0.63	1.04	3.35
Buliminella beaumonti	0.53	0.12	**1.32**	2.62
Quadrimorphina profunda	**1.26**	1.15	0.58	3.4
Nonion havanese	**0.91**	0.29	1.2	2.07
Globorotalites micheliniana	0.7	0.7	**1.04**	2.49
Paralabamina lunata	0.67	0.04	**0.85**	1.94
Aragonia aragonensis	0.19	0.48	**0.66**	1.92
Bulimina midwayensis	**0.47**	0.27	0.9	1.9
Oridorsalis umbonatus	0.64	0.57	**0.87**	1.89
Valvalabamina sp.2	0.1	0.24	**1.21**	1.89
Paleopleurostomella pleurostomelloides	0.51	**1.59**	0.77	3.1
Cibicidoides eoceanus	**0.57**	0.04	0.41	1.66
Cibicidoides subcarinatus	0.48	0.24	**0.49**	1.58
Gyroidinoides subangulatus	**0.54**	0.28	0.35	1.56
Neoeponides hillebrandti	0.05	0.13	**0.51**	1.54
Coryphostoma crenulata	0.23	**0.71**	0.55	2.16
Bulimina tuxpamensis	0.79	0.15	**0.84**	1.71
Pullenia subcarinata	0.61	0.27	**1.28**	1.67

The CIE interval recorded the highest mean abundance of *Abyssamina quadrata, Nuttallides truempyi, Tappanina selmensis, Paleopleurostomella pleurostomelloides* and *Coryphostoma crenulata* and these taxa made the greatest contribution to the dissimilarity (50% cut off) between the pre-CIE and the recovery (Table 4.1).

Quadrimorphina profunda, Bulimina midwayensis, Nonion havanese, Anomalinoides praeacutus, Cibicidoides eoceanus, Gyroidinoides subangulatus and *Bulimina tuxpamensis* were the most abundant species during the recovery interval. These species are associated with moderate oxygen level and seasonality in productivity from upwelling and surface water mixing (D'haenens *et al*., 2012; Arreguin-Rodriguez *et al*., 2016)

In the raw taxa composition, the late Palaeocene (Pre-CIE, 59.5 – 54.6 mbsf) section was characterised by the restricted occurrence of *Valvalabamina depressa, Ribdamina Sp, G. beccarriformis, Spiroluculina Spp., Neoflabellina rugosa, Stilostomellia plumerae, Coryphostoma midwayensis, Falsoguttulina wolburgi, Orthokarstonia clarki, Hemorobulina arcuta, Dorothia retusa, Brotzonella monterelensis, Marsonella trochoides, Oolina globosa, Ellipsoglandullina chilostoma* and *Ellipsoidella cuneiformis* (Figure 4.8).

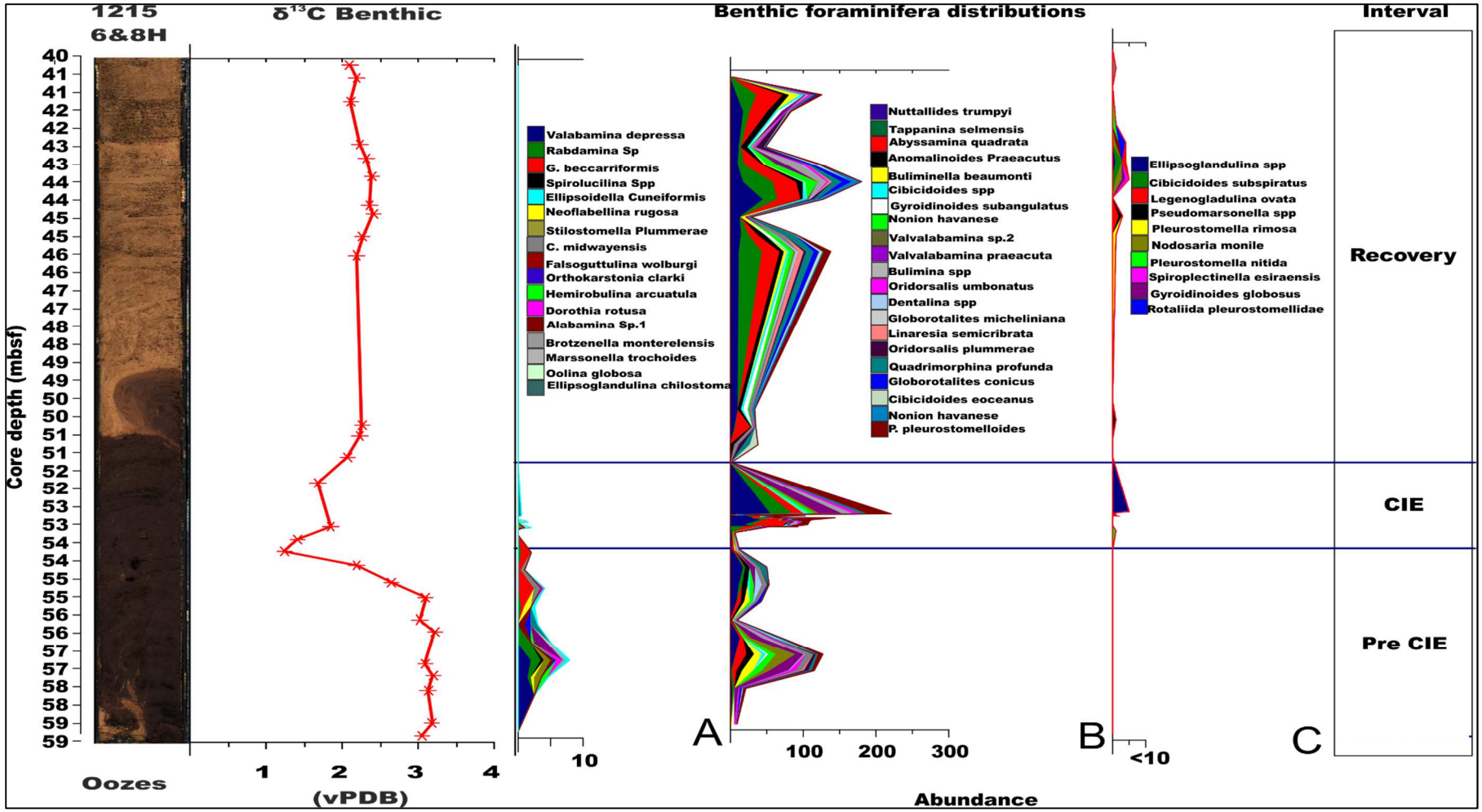

Figure 4.8: Benthic foraminiferal events in ODP Site 1215A. A- The distribution of some important opportunistic taxa. B- Extinction taxa; C- Taxa that originated during or after the CIE. N/B: There is colour overlap across three events due to limited colour range in Tilia.

Most of the listed taxa went into extinction before or during the PETM. Other cosmopolitan fauna that showed high relative abundance in this interval were *Nuttallides truempyi, Nonion havanese, valvalbamina praeacuta, Buliminella beaumonti* and *Bulimina spp, Cibicidoides Sp.3 Neoeponides hillebrandti and Paralabamina elevata* (Figure 4.8)

The main CIE (54.6 – 51.5 mbsf) interval was characterised by blooms of opportunistic taxa such as *Abyssamina quadrata, N. truempyi, Paleopleurostomella pleurostomelloides, Oridosalis umbonatus, Bulimina Spp., and Cibicidoides Spp*., (Figure 4.8) indicating an ecological disturbance in the benthic ecosystem. Other taxa which occurrences were restricted to the PETM include *Ellipsoglandulina Spp., Cibicidoides subspiratus, Leganogladulina ovata, Pseudomarsonella Spp., Pleurostomella nitida, Gyrodinoides subglobosa, Spiroplectinella esiraensis* and *Rotaliida pleurostomellidae*. These benthic foraminiferal species also went into extinction after the PETM. Agglutinated taxa were the most affected group of foraminifera (Figure 4.8) during the CIE in the equatorial Pacific, probably because they build their test with rock fragments and the majority of the fragment in the open ocean are a biogenic carbonate. The taxa that survived or increased in abundance during the PETM were mainly opportunistic epifauna and triserial infaunal morphotypes (Figure 4.8) and are predominantly of the small test sizes. Foraminifera have been reported to produce smaller test during the period of low oxygen concentration and decreased carbonate concentration due to early reproduction as a preadaptation measures to extreme ecological condition (Winguth *et al.,* 2012; Foster *et al.,* 2013).

Recovery section (51.5 – 41.0 mbsf) was characterised by the significant increase in diversity and abundance of taxa that survived the CIE including: *N. truempyi, Tappanina selmensis, A. quadrata, N. havanense, Bulimina Spp., Orisadolis plumerae, Anomalinoides praeacuta, Q. profunda Bulimina trinitatensis, B. tuxpamensis, Aragonina valescoensis Pullenia subcarinata* and *Cibicidoides Spp*. The ratio of epifauna to infauna also increased, the majority of the infauna were *Buliminids* and *Abyssaminids* while the *Pleurostillomellids* decreased in abundance during this period. The increase in both the surface-dwelling epibenthic and the deep sediment dwelling infauna at the recovery interval suggest improved ecological condition after the CIE.

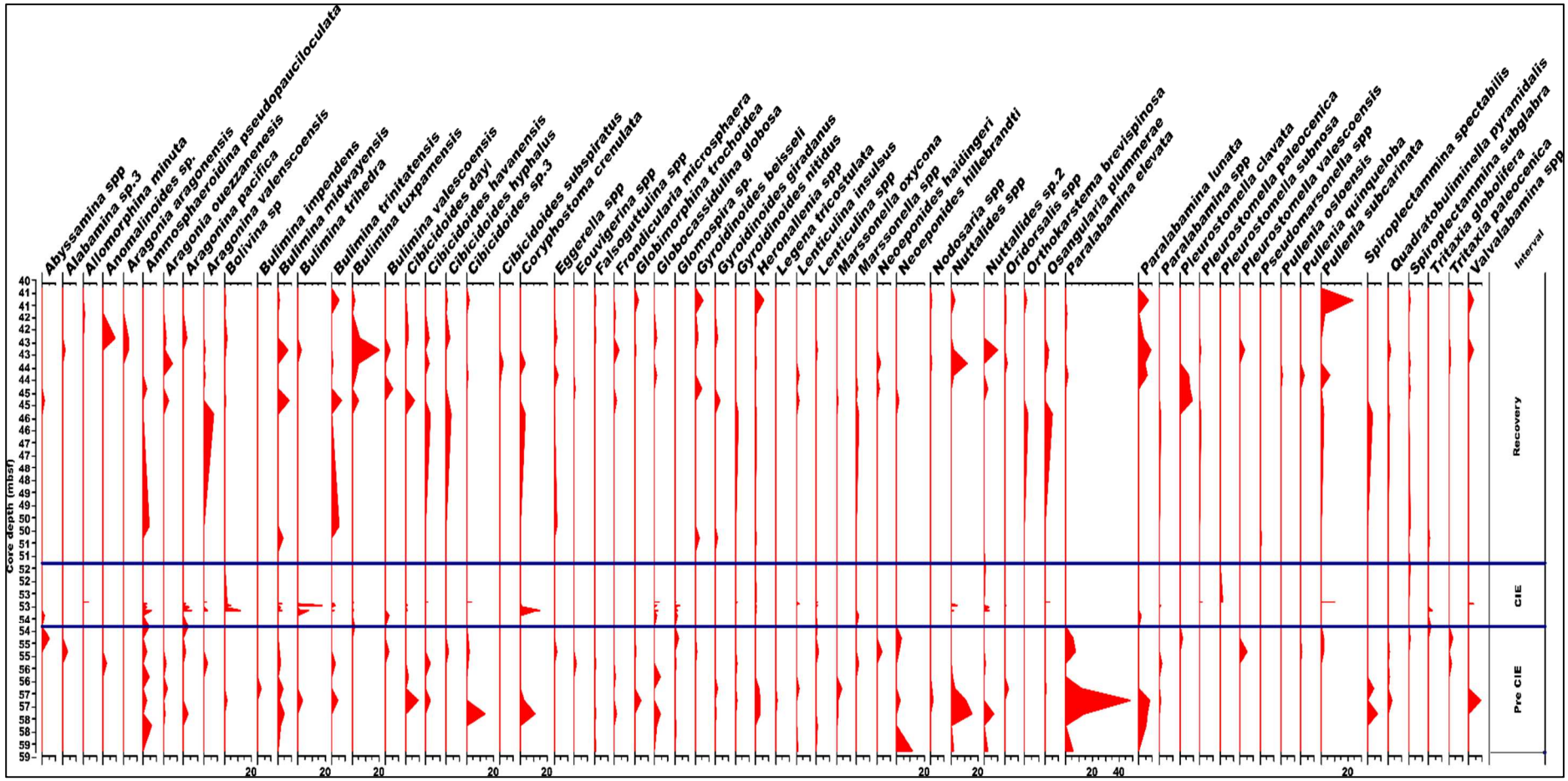

Figure 4.9: Distribution of cosmopolitan benthic foraminifera in ODP Site 1215A

4.2.4 Benthic foraminiferal traits composition in the equatorial Pacific Ocean

There were two separations in the nmMDS of traits composition at Site 1215A but unlike the previous sites where the ordinations were linked to the ecological stability of different intervals of the PETM, the trait nmMDS at Site 1215A depicted a different scenario. All the intervals clustered together in two groups (Figure 4.10). Samples at group A represent the core of the three intervals of PETM while samples at group B represent the boundaries between each interval. The ANOSIM value of global R= 0.08; p >0.05 indicated that intervals differed but at a low level. The ordination suggests that most of the benthic foraminifera that lived in the Central equatorial Pacific shared similar traits, possibly because the area was very eutrophic even before the PETM and all the taxa adapted similar traits to enable them to survive. Samples 41.01mbsf and 52.01mbsf were outliers and we could not explain the cause.

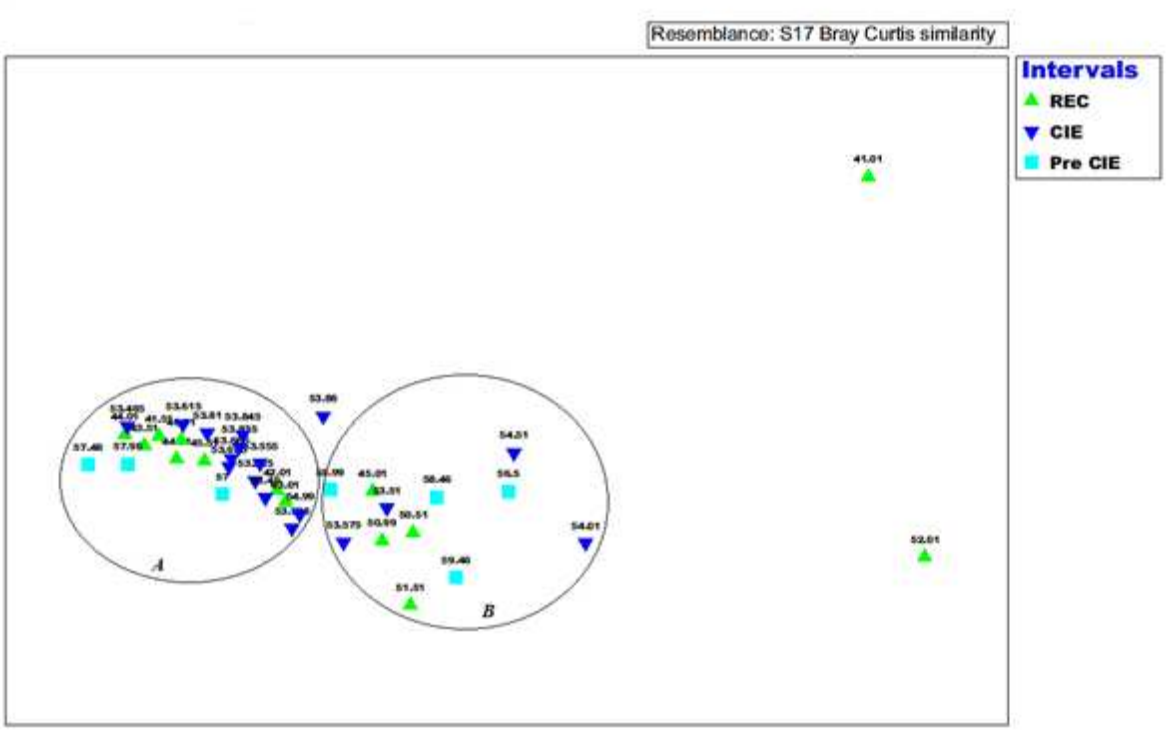

Figure 4.10: Non-metric Multidimensional Scaling ordination of foraminiferal traits composition (transformed with total resemblance) of Bray-Curtis similarity from Site 1215A ODP Leg 199, Central equatorial Pacific Ocean.

The result from the analysis of trait modalities with SIMPER indicated 22 trait modalities contributed to the similarities present in Site 1215A (Figure 4.11). Spiral test, planispiral chamber arrangement, triangular/trapezoid chamber shape, depressed sutures, and fine test

perforation increased in relative proportion during the pre-CIE. However, at the CIE interval, hyaline calcite test, trochospiral test, bi/triserial chamber arrangement, spherical/oval chamber shape, no ornament, slit-like apertures, terminal apertures, micro perforation and deposit feeding mode increased in abundance. The recovery interval was characterised by increase in elongate test, raised sutures, arcuate apertures, apertures with lips, shallow infauna and deposit feeding.

Another trait modality that showed significant variation in abundance across the three intervals were spherical/oval and triangular/trapezoid chamber shapes. Spherical/oval increased during the CIE but decreased afterwards but not as low as it was at the pre-CIE while triangular/trapezoid trait decreased significantly at the CIE and increased during the recovery but not as much as the pre-CIE values. The increase in the proportion of spherical/oval still points to the high abundance of some taxa *like Q. profunda and A. quadrata* during the CIE. The triangular/trapezoid trait is difficult to pin point to any taxa because it could be found in both elongate and spiral forms.

The mean values of depressed sutures retrogressively decreased from the pre-CIE to the recovery, while raised sutures progressively increased from the pre-CIE to the recovery. There were a general decrease in ornamentation and apertural accessories with the increase in carbon concentration in the ocean; this may have probably as a result of a decrease in the survival rate of the organism as ornamentation is associated with feeding and defence mechanism of foraminifera (Mancin *et al.,* 2013). Perforation also decreased during the CIE while the mode of life shifted toward a shallow infauna habit (Figure 4.11).

In the raw trait composition, five functional traits events (two during the pre-CIE, one at the CIE and two during the recovery) were recognized. (Figure 4.12). The trait composition (Figure 4.12) showed a more harmonised system of biotic event when compared to the taxonomic composition indicating that functional redundancy (i.e. multiple taxa performing similar ecological role) existed in the foraminifera communities from Site 1215A.

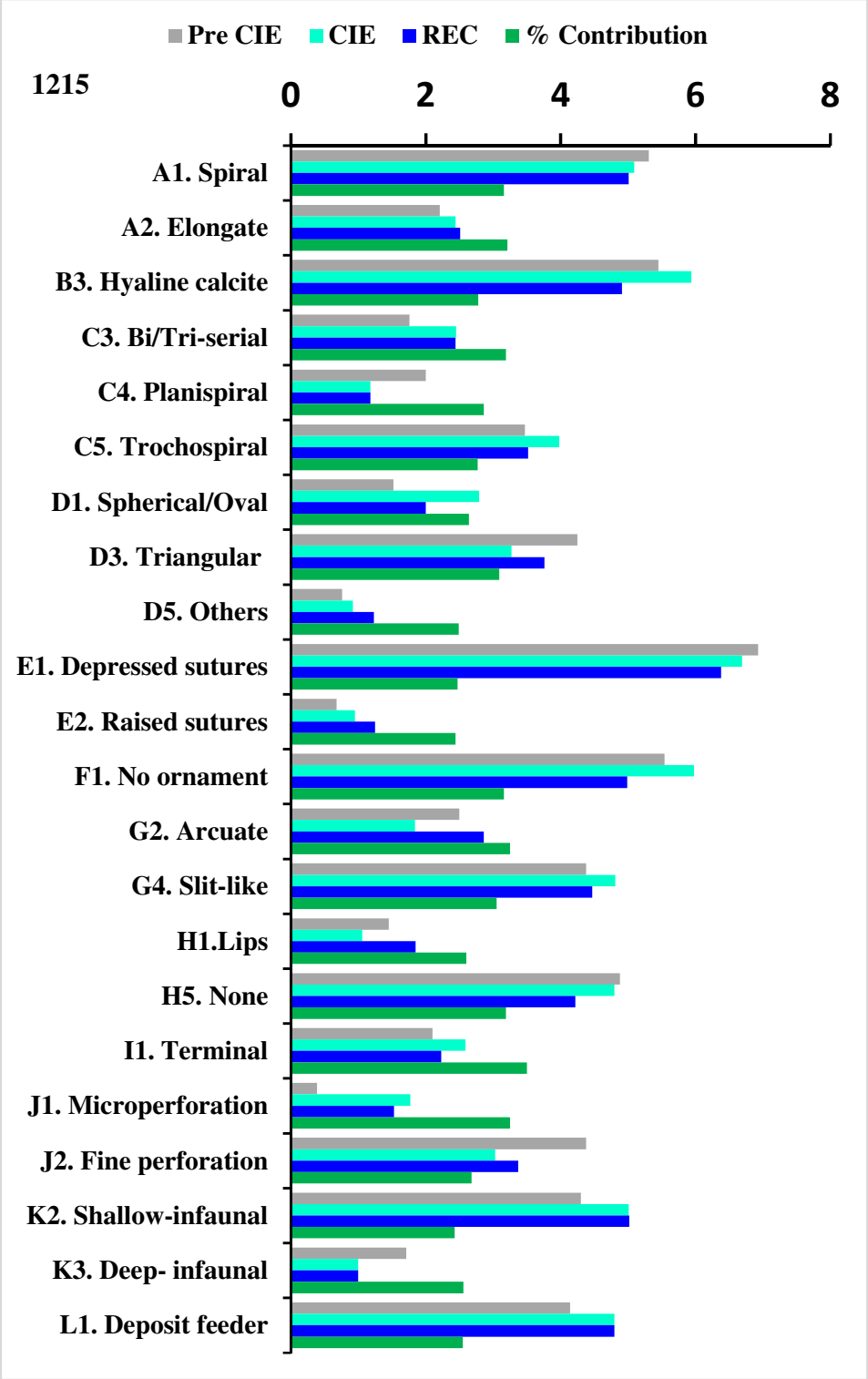

Figure 4.11: SIMPER result of the most significant trait (at 50% cut off) that contributed to the differences in benthic foraminiferal trait composition across the CIE events at ODP Site 1215A. Grey bars = pre-CIE; sky blue bars = CIE core; deep blue bars= Recovery; green bars = % contribution of each trait.

The spiral test was the most abundant category in the test shape modality with ~55%, accompanied by elongate ~40% (Figure 4.12A), while tubular and globose shape occurred in a very small proportion during the pre-CIE and recovery. Because spirally coiled foraminifera comprise of a wide range of taxa including epifauna and infauna, and elongate are dominantly infauna, the test shape can be said to reflect the higher abundance of infauna taxa. The overall test composition was predominantly hyaline calcite, however, hyaline aragonite moderately occurred at the pre-CIE and the CIE intervals but decreased significantly during the recovery (Figure 4.12B). Micro-granular tests originated during the CIE and slightly increased during the recovery. Agglutinated and porcelaneous tests frugally occurred across the studied section with the lowest abundance occurring during the CIE (Figure 4.12B).

The chamber arrangement modality indicated that trochospiral abundance was slightly higher than bi/triserial and planispiral which also occurred in significant quantity across the studied interval. The three chamber arrangements correlated with the events in the trait composition, however, bi/triserial chambers recorded the lowest occurrence before the CIE. Uniserial, unilocular and other chamber arrangements occurred in very small abundance at few depths across the analysed section.

Triangular/trapezoid was the most abundant in the chamber shape category, followed by spherical/oval. There was a relatively low abundance of tubular chamber across the studied section, but they significantly increased during the CIE, the semi-circular chamber also occurred sparingly before and after the CIE but none was recorded at the CIE interval. Other chamber shapes that did not fall under the above categories but was grouped as others occurred in low abundance at the pre-CIE but increased from the CIE to the recovery. Depressed and raised sutures were the two major macro ornamentations found in the identified foraminifera, the depressed sutures constituted about 80% and mirrored the general trend in trait composition. Raised sutures were very low in abundance at the pre-CIE interval but increased at the main CIE, it later dropped to zero and increased again during the recovery. In micro ornamentation category, no ornamentation trait was the most abundant, striate/costae structures were also significantly abundant during the CIE and recovery but low at the pre-CIE interval. Other micro ornamentations only occurred in a very small proportion across the studied interval.

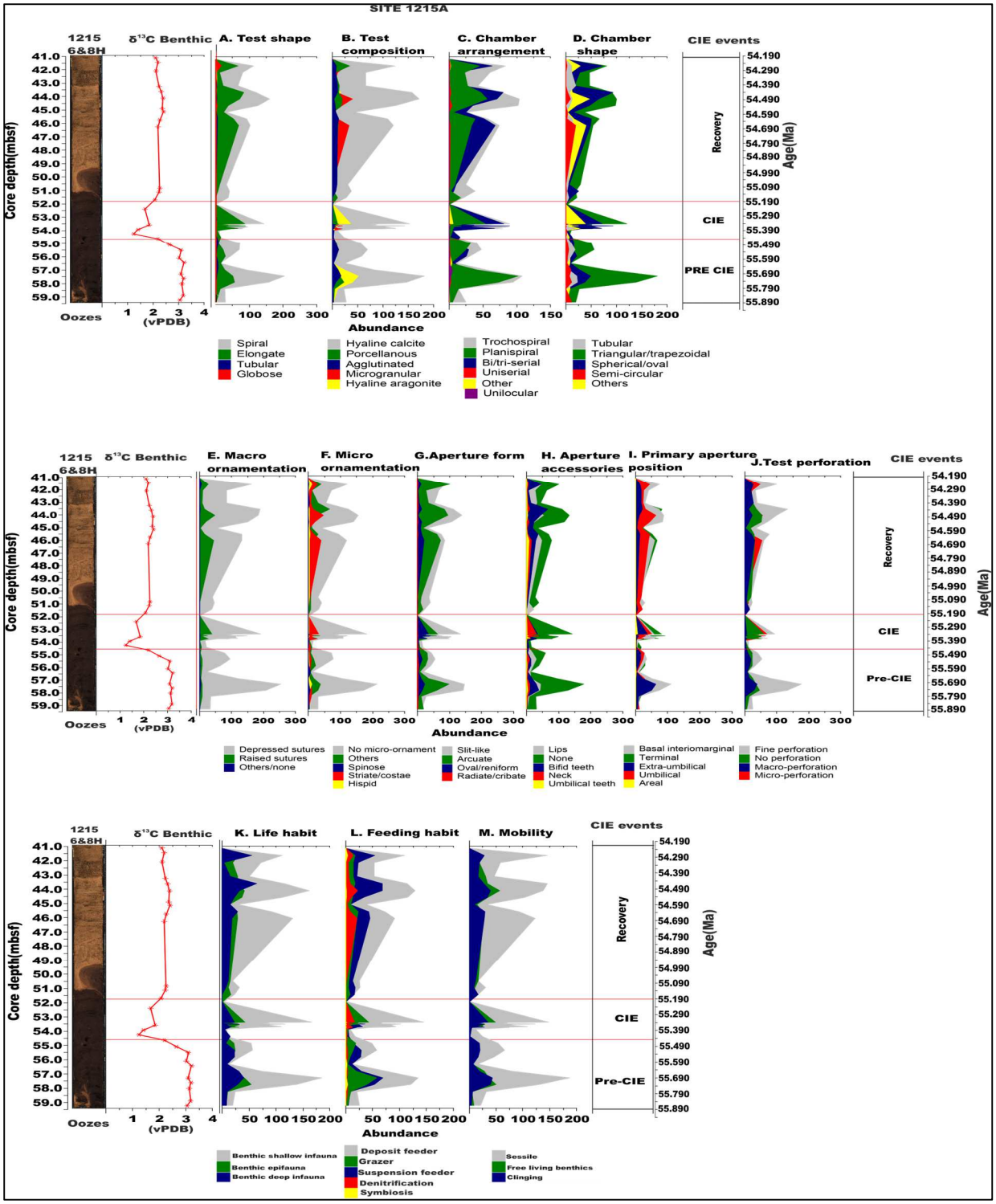

Figure 4.12: Benthic foraminiferal traits distribution in ODP Site 1215A. The core depth (left) in mbsf is followed by composite core photo of hole 6 &8; the $\delta^{13}C$ benthic record was plotted from Leon-Rodriguez & Dickens (2010); trait distribution with legends directly below them and the age (Ma) of the analysed section at the extreme right.

Slit-like aperture recorded the highest abundance ~45% in the apertural form category, followed by arcuate aperture ~ 35%; oval/reniform 18%; while other apertural forms constitute less than 2%. Foraminifera with no apertural accessories predominate the identified assemblages, those with lips constitute about 22%, teeth ~20% and neck ~10%. Foraminifera with neck show low abundance in pre-CIE and after the CIE but significantly increased during the main CIE interval. Primary aperture position category showed high trait richness and diversity; basal interiomarginal (BIM) was the most abundant in the primary aperture modality (Figure 4.12I), followed by a terminal aperture which was almost of the same abundance with the BIM aperture. The relative abundance of the terminal aperture was the lowest during the pre-CIE, and BIM aperture was the lowest during the CIE. Apertures in the umbilical positions were equally abundant but recorded the lowest occurrence at the pre-CIE, Invariably, extra-umbilical aperture recorded the highest occurrence at the pre-CIE section. Areal aperture constituted less than 1% of the total trait richness in this category and only occurred during the CIE.

Perforations in the identified foraminifera were dominated by finely perforated taxa ~30%, followed by micro perforation ~25%, and macro perforation ~20%. Other perforations followed the general trend of trait composition in this site, however, macro perforation significantly decreased in main CIE interval, this could be related to the disappearance of coarsely perforated taxa such *G. beccarriformis* during the CIE. There were a significant amount of none perforated taxa ~22 % across the studied section, indicating that the taxa shifted towards less perforation during the CIE.

The shallow benthic infauna was the most abundant trait in the living mode of foraminifera, constituting over 60%, the benthic epifauna and benthic infauna constitute ~20% each, suggesting that the shallow infauna was the most conducive habitat during the CIE. Deposit feeding mode was also the predominant feeding habit in the identified foraminifera with ~48%, suspension feeding ~25%, grazing 15%, and significantly high denitrifying taxa of about 10%. Our data also showed that half of the taxa analysed were sedentary with over 60% sessile trait and the rests were swimmers as well as those attached to the hard substrate.

4.3 Discussion

4.3.1 Interpreting the ecological functioning of the seafloor from the fauna and trait composition of benthic foraminifera

The faunal composition of the studied section indicates an assemblage associated with severe ecological disturbance due to the dominance of opportunistic taxa such as *Abyssamina quadrata, Nuttallides truempyi, Tappanina selmensis, P.pleurostomelloides, Quadrimorphina profunda, Bulimina midwayensis* and *Bulimina tuxpamensis.* The prevalence of opportunistic taxa in an ecosystem is evidence of ecological stress (Oschmann, 1998; Caswell and Frid, 2013). Similar foraminifera assemblages have been reported in many extreme climatic events such as Cretaceous/Palaeogene boundary event (Alegret and Thomas, 2009), Middle Eocene Climatic Optimum (MECO; Boscolo Galazzo *et al*., 2015) as well as the PETM (Thomas 2003, 2007; Takeda and Kaiho, 2007; Alegret *et al.,* 2009; D'haenens *et al*., 2012; Stassen *et al*., 2015 and Arreguin-Rodriguez *et al*., 2016). The extinction of *G. beccarriformis, Neoflabellina, Dorothia retusa and Marsonella trochoides* that occurred in this location have been reported in other PETM sections confirming the existence of the biotic changes that occurred during the hyperthermal at the equatorial Pacific (Alegret *et al.,* 2009; Takeda and Kaiho 2007; Speijer *et al.,* 2000, Aref and Youssuf 2004). The disappearance of other taxa recorded in Site 1215A may be as a result of local extinctions.

The pre-CIE interval was strongly dominated by epifauna and agglutinated taxa as well as few hyaline calcareous infauna (Figure 4.8). The extinct taxa were known to have wide distribution during the late Palaeocene in deep and epicontinental seas before their extinction in the early Eocene. The high abundance of infauna taxa is an indication of moderate and sustained food supply and/or reduced oxygen concentration to the seafloor (Jorissen, 2007). Also, the faunal composition in this interval indicated a mesotrophic condition, with seasonally fluctuating oxygen and transient high food environment (Sen Gupta and Machain-Castillo, 1993; Thomas, 2003; Kuhnt *et al*., 2007; Alegret and Thomas 2009; Arreguin-Rodriguez *et al*., 2016)

The composition of taxa at the CIE interval (Table 4.1; Figure 4.8) are dominated by opportunists, characteristic of low-productivity and possibly thriving in continuously stressed dysoxic sea-bottom conditions (Giusberti *et al.,* 2014). These species are reported to be common in the deep sea especially around the BEE (Alegret *et al.*, 2009a; Stassen *et al.,* 2012, Frenzel 2000; D'haenens *et al*., 2012; Giusberti *et al.,* 2009; Arreguin-Rodriguez *et al.,* 2016).

The relatively low abundance of low oxygen indicators may be due to preservation as bi/triserial taxa go into solution before other taxa during carbonate dissolution (Nguyen *et al.,* 2009). And the high level of dissolution in foraminiferal assemblage from this site may have affected the taxonomic composition by skewing the preserved specimens toward more resistant taxa.

Overall, there was a reduction in the abundance of taxa with a spiral test from the pre-CIE to the recovery interval and taxa with elongate test indicated an inverse trend as they rather increased from the pre-CIE through to the recovery interval. This result suggests that elongate bi/triserial tests were more resilient to the increase in the acidification of the ocean as most taxa that increased in abundance at the CIE interval have elongate bi/triserial tests.

Elongate test shape is associated with taxa like *Bulimina; Bolivina; Pleurostomelloides, Stilostomella,* and *Coryphostoma* and these taxa are well known as disaster taxa (Alegret *et al.,* 2009). These taxa have been reported to be tolerant to increased phytodetritus rain to the sea floor, reduced oxygen content and unstable ecological condition (Giusberti *et al.,* 2009; Arreguin-Rodriguez *et al.,* 2016). Spiral tests are found in a large number of heavily calcified epifauna that are susceptible to changes in the benthic ecosystem. The increase of bi/triserial chamber (Figures 4.11 and 4.12) also supports the increase of elongate test during the CIE as a proxy for stress in the seafloor ecology. Elongate traits have also been identified as the most dominant during the CIE in the Atlantic and Tethys seas (see Chapter 3 and 5). Trochospiral test showed a relative increase in abundance during the CIE and returned to the pre-CIE values at the recovery interval (Figure 4.11). The increase in this trait modalities during the CIE could be linked to the increase in the opportunistic taxa like *A. quadrata; N. truempyi; O. umbonatus and Q. profunda* which have trochospiral chamber arrangement.

The high abundance of near-surface dwelling spiral taxa and the deep living elongate form in trait composition could mean that most of the preserved benthic foraminifera lived in a dual habitat, staying on the sediment surface when it is conducive and diving deeper inside when the sediment surface becomes harsh. Jorissen *et al.* (2007) pointed out that species classified as epifauna in the modern ecosystem may have lived a similar dual lifestyle as they co-occur with deep infauna taxa, though this hypothesis still needs more investigation.

The ecological functioning of the benthic foraminifera will, therefore, be complicated to interpret due to the loss of some taxa that contributed to functioning that may have been lost to dissolution. Nevertheless, our BTA analysis shows that ocean acidification caused by high

export productivity had a significant impact on the traits and by extension functioning of benthic foraminifera as shown in the alternation of trait composition (Figure 4.12).

The high abundance of highly calcified taxa indicated by the predominance of hyaline calcite, spiral, trochospiral, elongate, bi/triserial (Figures 4.8; 4.11; 4.12) suggests a continual sequestration of carbon by foraminifera and that ocean acidification may not have reduced the ability of this organism to calcify, instead it destroyed the test of the organism after burial. This is contrary to the current observation in the modern ocean where ocean acidification is said to reduce the calcification of calcifying organism (Heinze *et al.,* 2015; Riebesell *et al.* 2017). This is because, despite the high degree of dissolution observed in the foraminiferal assemblage, taxa with calcareous test still dominate. Foraminifera during this period may have utilised more inorganic carbon (DIC) than the organic carbon (OC) for their nutritional needs as the DIC is more labile than the OC. The residual organic matter may have contributed to a large amount of organic material and other detrital rain from the surface ocean to the sea floor, and the bacterial oxidation of this organic matter may have sustained the acidification for a long period in the equatorial Pacific.

The ocean acidification leads to the loss of ornamentation in the identified foraminifera. The result from this study indicated a prevalence of the no ornament trait (Figure 4.11 and 4.12). Loss of ornamentation in benthic foraminifera is linked to extreme ecological conditions and has been previously reported by Dubicka *et al.* (2015) in the modern ecosystem. Ornamentation in foraminifera is important in feeding, protection, movement, and prey -predation relationship (Dubicka *et al*. 2015; Georgescu *et al.,* 2011). They are used for sorting food particles into different shape and sizes, disaggregating larger particles into smaller pieces before ingestion, removing of harmful stuff as well as an adaption for escaping from predators (Dubicka *et al*. 2015). The outer ornamentation of foraminifera would likely be the first point of attack by the corrosive bottom water. More so, organisms could reduce structural/anatomical complexity to conserve energy in the period of ecological stress and thereby enriching taxa with no ornamentation in the foraminiferal assemblage. The relatively high abundance of striate/costate structures may have been to enhance absorption of dissolved nutrients since the ornamentation is negative (depressed into the test).

The apertural modality of the foraminifera assemblage was dominated by simple slit-like and arcuate form. Because the majority of the foraminifera are shallow infauna and deposit feeders, these forms of apertures are suitable for absorbing dissolved nutrient rather than ingesting food

particles. Our result also shows a significant decrease in apertural complexity across the studied section with no aperture accessory being the most abundant trait in the aperture accessories category. The decrease in apertural complexity has also been reported in some species of foraminifera (*Haynesina germanica)* during the period of carbon dioxide increase in the Barent Sea (Dubicka *et al*., 2015). Nevertheless, there was a significant number of taxa with teeth and neck which are linked to suspension feeding habit. In general, there was a shift towards nutrient assimilation over foraging behaviour among foraminifera during the PETM in the equatorial Pacific Ocean. Perforation also decreased with the increase in acidification as indicated by the lowest occurrence of macro perforation at the CIE section and the dominance of finely perforated taxa. Perforations are known to enhance dissolution of foraminiferal tests because pores are points of reaction in the test (Figure 4.12), hence the decrease in size of perforation during the CIE may be an artefact of carbonate dissolution as well as the result of the extinction of some coarsely perforated epifauna taxa. It is difficult to relate perforation to the ecological function due to high dissolution and unstable ecological conditions observed in the study area but the BTA has shown that prevailing traits in the recovered foraminifera encourage accumulation of large quantity of organic material because most taxa derive nutrients from the dissolved organic carbon and only a few preys on the smaller plankton that contributed to the organic carbon. This could be the reason for the high organic matter deposition and prolonged acidification in the equatorial Pacific during the late Palaeocene – early Eocene period.

4.3.2 Preservation of foraminiferal test in the equatorial Pacific during the PETM

The scanning electron microscope (SEM) images of some recovered foraminifera have revealed evidence of dissolution/etching, extreme recrystallisation/neomorphism and secondary calcite cementation on the test of both planktic and benthic foraminifera. The SEM imaging focused on the quality of preservation in selected foraminifera, and we have documented different stages of foraminifera test alteration during the PETM at Site 1215A.

The SEM imaging revealed that some of the foraminiferal specimens that showed glassy appearance in the light microscope have evidence of dissolution under the SEM and the frosty specimens showed a high level of dissolution and recrystallisation (plates 4.1 – 3). For example specimens 4.1 A - D would appear to be well preserved under the light microscope, but under the SEM, A is showing an early stage of alteration. The initial protruding part of the test has been dissolved indicating that foraminifera test dissolution usually starts from the last chamber of a spiral test and progresses to different parts of the test.

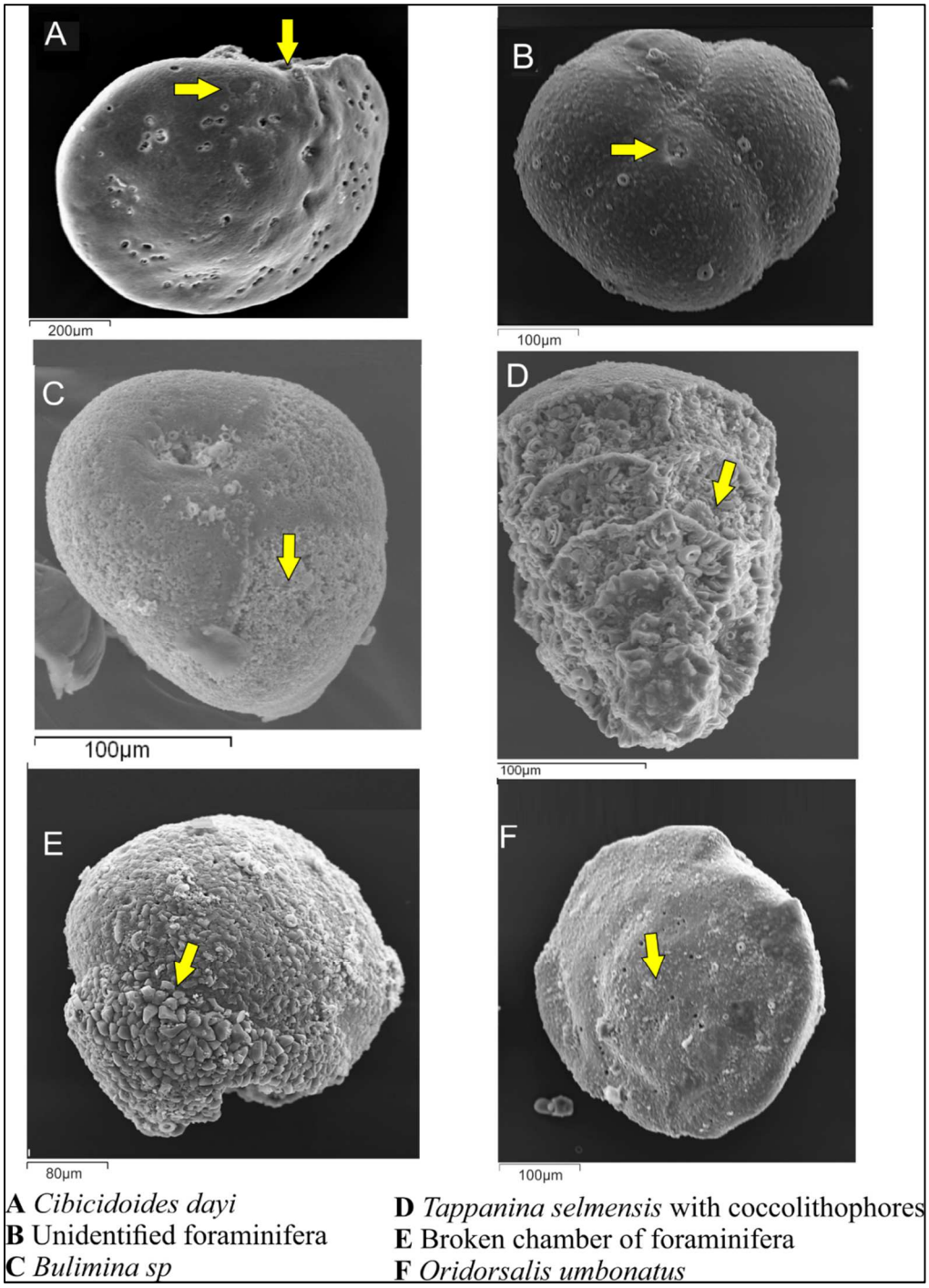

Plate 4.1: Foraminifera test from sample 1215A_8H-03_60-62 showing evidence of early stage of diagenesis. A) shows a test of Cibicidoides dayi with the arrows pointing at the broken edge and peeling on the surface of the test. Under the light microscope, this test will appear glassy indicating good preservation. B) is a test of unidentified planktonic foraminifera with the outer layer of the test completely removed. It is difficult to identify this species because all the outer features have been completely dissolved. C) is showing a partially dissolved outer layer of B. tuxpamensis? It could still be identified based on shape and aperture position. D) is showing coccolith plates exposed by partial dissolution in T. selmensis test. Note (yellow arrow) how the nannofossil are arranged in different parts of the test with some sort of order. E) a piece of the foraminifera chamber is showing the peeling of the second layer of the test. The dissolution of this test has reached an advanced stage. F) is a test of O. umbonatus with the outer layer completely removed.

The specimens also show that the test architecture plays a role in the susceptibility or resistance of a test to abrasion or dissolution. The surfaces around the broken part were beginning to roughen and exfoliate as shown by the arrow in specimen A. Specimen B shows a completely exfoliated specimen, all the diagnostic features and ornamentation have been removed, and the size of previously small pores are beginning to increase as a result of dissolution. This specimen appears frosty under the light microscope and could be identified based on the shape to the family level, but in SEM where all the surface features have been completely removed, it is identified as unknown foraminifera. Specimen C and F showed the test that was undergoing dissolution and still retained their original shape and ornamentation which was used in their identification, more so, the evidence of widening of pores in specimen F is conspicuous. The surface of specimen D (*T. selmensis)* is partially removed by dissolution and coccolith plates embedded in the test have been exposed.

The last chamber at the bottom of the specimen still retained the secreted crystals; we think that this species may have a dual method of calcification; secreting hyaline calcite to build its test and incorporating coccolith plates during the later period of calcification. Specimen E shows a test that has undergone many layers of exfoliation, the size of existing crystals in the original test has been enlarged by recrystallization, and the chamber has been detached from the parent test. This specimen is hyaline calcite and at an advanced stage of dissolution.

The process of foraminifera test alterations starts with the roughening/etching of the initially smooth surface (Plate 4.1, A and C), as the dissolution continues there may be partial peeling of the test or breaching of the last chamber depending on the morphology of the foraminifera test (Plate 4.1A and 4.2A) at this point the last chamber may be broken and more or less missing with total removal of the surface ornamentation or suture and widening of surface pores.

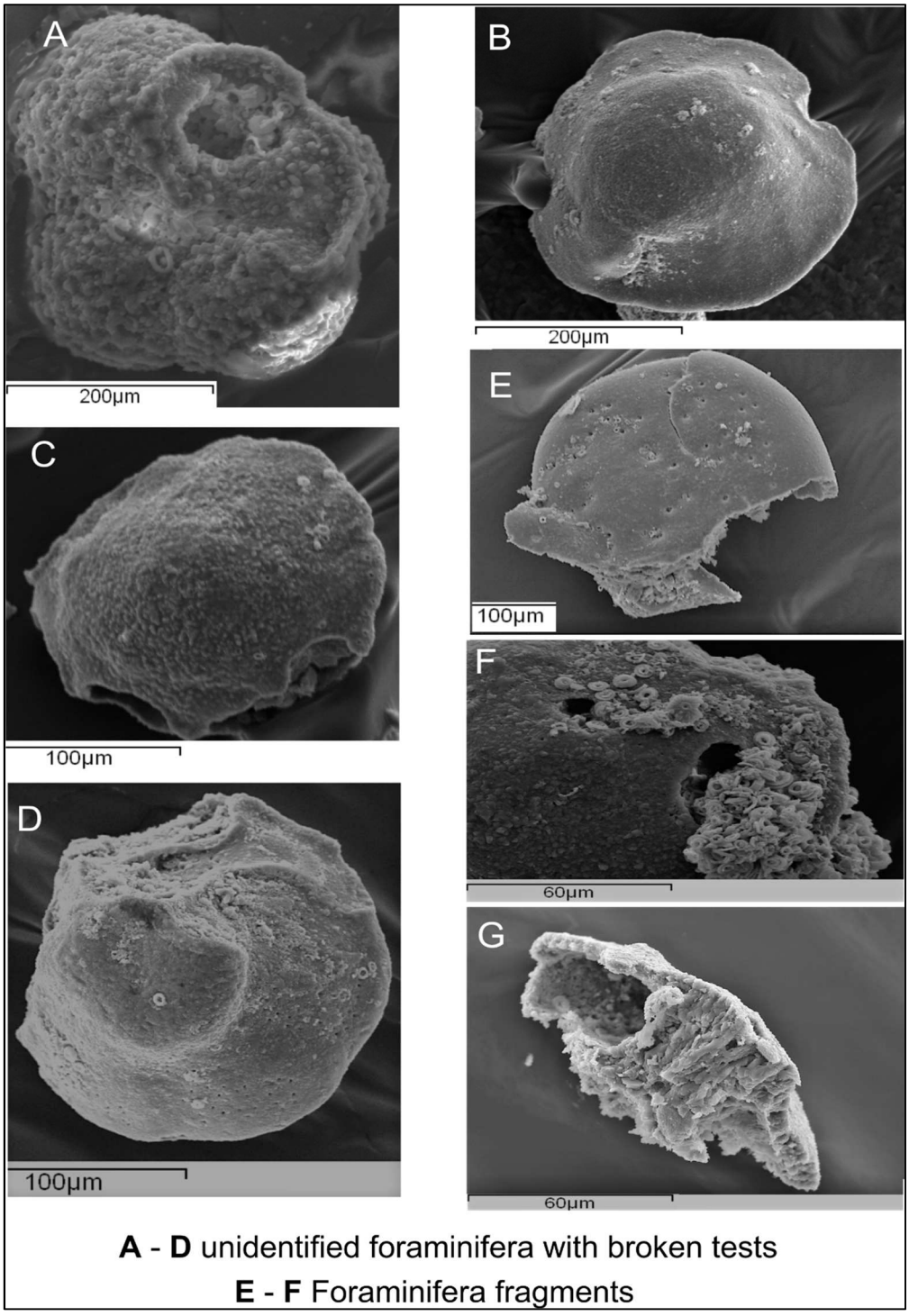

Plate 4.2: Foraminiferal test at an advanced stage of dissolution. All the specimens were picked across the PETM interval. A shows extreme dissolution, calcite overgrowth and neomorphism of planktonic foraminifera. Dissolution has destroyed all the ornamentation, enlarged the pores spaces and removed some chambers. B – D shows advanced stages dissolution and thinning of the test walls with fragmentation setting in. E – G are fragments of foraminifera test at the final stage of dissolution. Note the coccolithophores on specimen F; it is a post-depositional attachment unlike the previously described test with nannofossil incorporated in the test fabric.

Advanced stages of dissolution are characterised by significant thinning of the test, missing chambers/disappearance of some part of the test and scattered holes (Plate 4.1 E and Plate 4.2 A – D), and most of the last whorl may be totally exfoliated. The last stage shows less than 50% of the test preserved, and the test becomes so thin that it could crumble on the touch of a picking brush, (Plate 4. 2, E- G, Plate 4.3 A- E). Also, the original calcite crystal may have been replaced by neomorphism and overgrowth (Plate 4. 2 A – G). At this point, the test may be destroyed beyond possible taxonomical identification.

Many specimens of foraminiferal test recovered from this study showed evidence of coccolith incorporation in foraminiferal test (Plate 4. 3). The amount of coccolith incorporated in the test of some foraminifera in this study has generated some curiosity as to which method(s) does foraminifera calcify in the open ocean. Plate 4.3A, C & E are foraminiferal fragments composed entirely of calcareous nannofossil. One may argue if these fragments are sediments recovered with the foraminifera, but specimens 4.3B, 3D, 3G, and 3F showed part of foraminiferal test composed of coccolith plates. Nannofossil incorporation in foraminifera has been reported as part of the post-depositional diagenetic process of foraminifera (Bearman, 1989; Hecht *et al*., 1975. Some agglutinating taxa have also been reported to use coccolith plates as part of their test (Henrikson et al., 1998) but the nature of coccoliths plate association (Plates 4.1 and 4. 3) with foraminifera test in this study makes us argue that some foraminifera species may have dual calcification method of building their test with secreted hyaline as well as incorporating coccolith plates by agglutinating method as they develop.

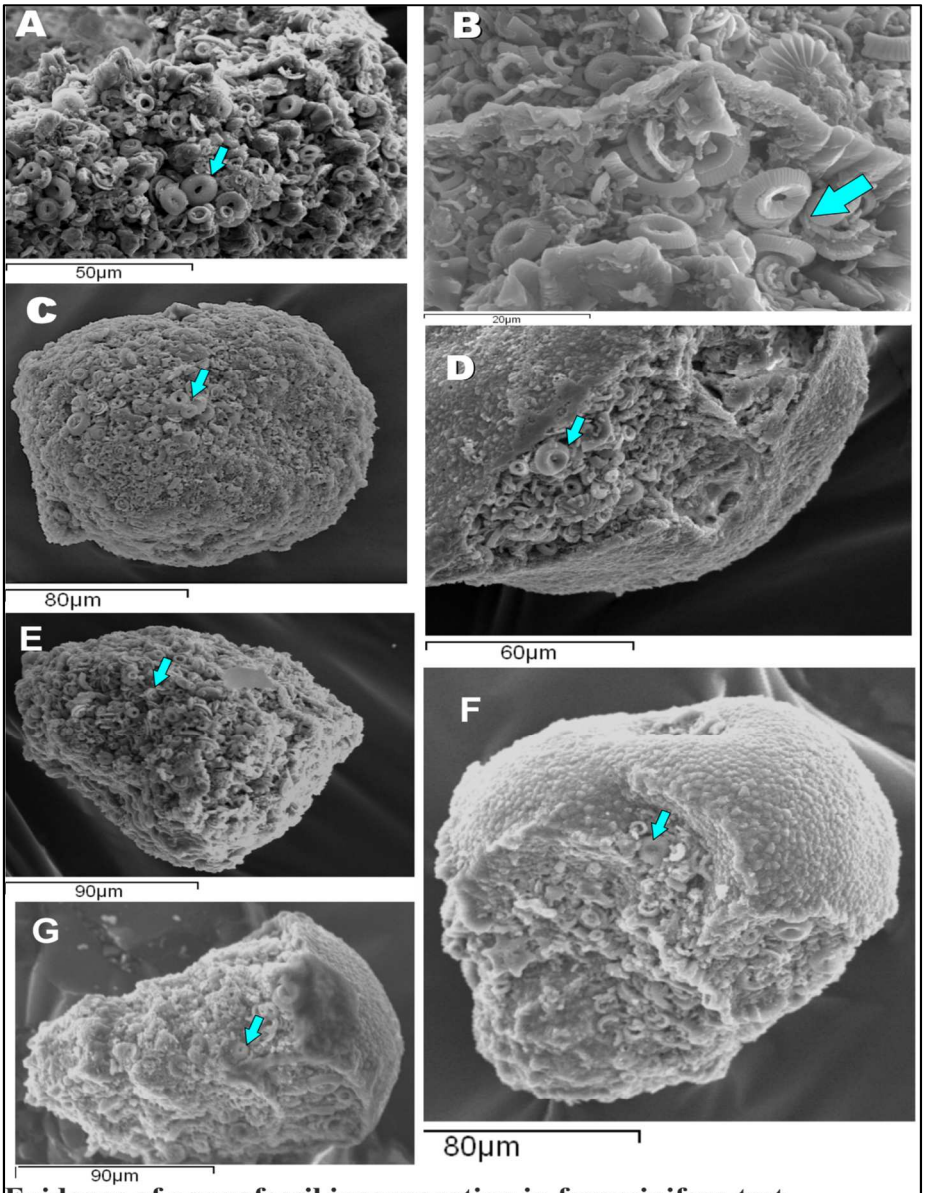

Evidence of nannofossil incorporation in foraminifera test.
A. Foram fragment with coccolithophores
B. Magnified part of *T. selmensis* test with many *Toweius sp and Discoaster* sp
C. Foram fragment with coccolithophores
D. Unidentified foraminifera with coccolithophores inside the test
E. Foraminfera fragment with coccolithophores
F. *T. selmensis* coccolithophores
G. *T. selmens*is coccolithophores

Plate 4. 3: Evidence of nannofossil incorporation in foraminifera test from sample 1215A_8H-03_130-132. A, C &E are broken pieces of foraminifera test resulting from extreme dissolution. Note in the arrows showing nannofossil incorporation in foraminifera test. B) is the enlarged part of T. selmensis showing a combination of secreted hyaline test and embedded coccolith plates. This test composition suggests that foraminifera could calcify in dual processes (agglutinating and secreted hyaline). D) shows advanced stages dissolution and thinning of O. umbonatus? test wall with fragmentation setting in. G & F are further evidence of incorporation of nannofossil in foraminifera.

In general, foraminiferal test is known to undergo different types of diagenetic processes after the death of the organism from the water column to period of deposition and burial. Dissolution of foraminifera tests usually starts as the test sinks in the water column to the seafloor (Edgar *et al*., 2015) and it results to altering the appearance of the test morphology and removal of delicate ornamentation such as the spine, roughening of the previously smooth surface, etching (i.e. stripping of upper layers of the test surface) and enlargement of pores and perforations (Nguyen *et al*., 2009). Recrystallization (neomorphism) is caused by modification of the crystal structure of the calcite test or growth of small crystals on the existing test walls (Bearman, 1989). These crystals eventually increase in size and deform pre-existing ornamentation, sometimes changing the morphology of the test entirely. The existence of secondary calcite cementation on the test of foraminifer is also common (Bearman, 1989), the cementation could be in the form of the calcite layer over the test or encrustation with coccolith plates. In the deep sea, fine-grained carbonate detritus often accumulate in the open part of foraminifera and fuses with it (Nguyen *et al.,* 2009). These could obscure the original ornamentation and/or alter the chemical composition of the test.

There are many factors that could cause changes to the preservation of foraminifera test after deposition. The composition, internal wall structure and microfabrics of the test are major factors; the high Mg/Ca porcellaneous taxa dissolve faster than the low Mg/Ca of hyaline making the aragonitic test more susceptible to dissolution than the calcitic test. The lithologic composition and post-burial sedimentation rate also play a crucial role in the preservation and alteration of foraminifera (Nguyen *et al*., 2009). Tests deposited in the very fine-grained (clay) sediment are better preserved than those buried in very coarse sediment (Bearman, 1989). Very fine clays have low porosity and do not easily allow fluid and oxygen penetration for bacterial activity to degrade the test. High porosity and permeability, on the other hand, are critical to the processes of foraminifera test alteration as they provide fluid pathways and greater surface area for reaction to proceed (Sexton *et al*., 2006). The pH of the surrounding interstitial pore in which the test is submerged also controls the alteration and preservation of the test (Nguyen *et al*., 2009).

Dissolution and etching set in when the pH of the pore fluid is less than 7.0. $CaCO_3$ saturation of the surrounding seawater and burial rate after deposition also control the nature of foraminifera test preservation (Edgar *et al.,* 2015). The paleobathymetry of the depositional environment is another factor in the preservation potential of foraminifera; test deposited in the

continental shelf are better preserved than those deposited in the abyssal depth of the open ocean (Sexton *et al*., 2006). The increase in dissolution with depth is related to the undersaturation of carbonate [CO_3^-] below the lysocline.

The combined effect of an increase in atmospheric pressure, decreasing hydrothermal gradient and fluctuating pCO_2 is the cause of $CaCO_3$ underestimation in deeper waters. The poor preservation noticed on the foraminifera test identified from this study could ascribe to the core depth, ocean acidification and high organic flux to the bottom water during the PETM.

The incorporation of some nannofossils in their test of foraminifera may be a result of post-depositional diagenetic processes, however, some species of foraminifera may have constructed their hard parts by dual processes, i.e. by crystallising the inner part of their test during the early stage of test formation from the chemical composition of the surrounding seawater as well as incorporating some coccolith plate into their test later in life by agglutinating process. Some agglutinating foraminifera has been reported to use coccolithophores for feeding and plastering their test with coccolith plates (Noel, 1958). A close look at the SEM image of some of our elongate infauna taxa (Plates 1 and 3) showed the nannofossil incorporated on the test of some *Buliminids* are in fact part of the test and not a diagenetic artefact. Most of the nannoliths are of *Toweius and Discoaster* taxa indicating that the coccolith plates were preferentially selected. If it were to be diagenetic in origin, the composition of the coccolithophores might have varied, and nannofossils usually dissolve before foraminifera (Kelly *et al.,* 2006). A similar scenario was reported by Henrikson *et al.* (1998) where *Gaudryina cribrosphaerellifera* constructed their test entirely with *Cribrosphaerella ehrenbergii. T. selmensis* (Plate 4.3) for instance was described as being entirely composed of hyaline calcite only, but our result has shown that the species and other deep infauna *Buliminids* may have been hyaline and agglutinated (Plate 4.3).

4.4 Conclusions

This study has further improved the knowledge of benthic foraminiferal composition and palaeoecology from Site 1215A. New benthic foraminiferal dataset has been generated and analysed for faunal and trait composition with biological trait analysis which has not been previously applied to foraminifera data from this site. The results from this study has revealed the ecological disturbance associated with high organic matter flux to the seafloor as a result of increased surface productivity and upwelling. Our interpretation supports the idea that the paleoredox changes from enhanced organic carbon influx during the period of increased

temperature and carbon dioxide concentration created highly acidified oceanic conditions that resulted to poor preservation of the recovered foraminifera and ecological disturbance in the sea floor. Evidence of benthic ecological perturbation was indicated by the turn over in taxa and trait composition of the recovered foraminifera as well as the dominance of opportunistic taxa in assemblages.

Post-depositional dissolution is believed to be a significant factor that influenced the faunal composition and invariably the associated traits and ecological functions. Dissolution is suspected to have selectively removed more susceptible taxa, smaller specimen and taxa with rough ornamentation as well as coarsely perforated taxa. However, results from the biological trait analysis suggest that functional redundancy (i.e. some species performing the same function) existed in the foraminiferal assemblage studied. The technique highlighted some crucial foraminiferal traits responsible for running the benthic ecosystem in the studied section and how they were affected.

In terms of faunal composition, the BTA identified *Paralabamina elevata, Valvalabamina praeacuta, Buliminella beaumonti, Globorotalites micheliniana, Paralabamina lunata, Aragonia aragonensis, Oridorsalis umbonatus, Valvalabamina sp.2, Cibicidoides subcarinatus* and *Pullenia subcarinata* (Table 4.1) as drivers of ecological functioning before the onset of the CIE. This assemblage is characterised by heavily calcified epifaunal species and a few deep infaunal taxa, and it correlates with a relatively low perturbed and less acidified seafloor with a moderate and sustained supply of food materials. *Abyssamina quadrata, Nuttallides truempyi, Tappanina selmensis, Paleopleurostomella pleurostomelloides* and *Coryphostoma crenulata* were the taxa with highest relative abundance during the CIE interval; these are small, deep infauna taxa known to bloom during ecological disasters (see Tekeda and Kaiho, 2007; Algret *et al.,* 2009; Arreguin-Rodriguez *et al.,* 2016). The increase in the abundance of these opportunistic taxa during the PETM may be as a result of biotic turnover resulting from extinction and/or stifling of reproduction in the bigger taxa that require more energy to flourish. This assemblage suggests a stressed ecosystem caused by additional pressure from the carbon isotopic excursion on the already perturbed benthic habitat.

The foraminifera assemblage associated with the recovery in this study (Table 4.1) included: *Anomalinoides praeacutus, Quadrimorphina profunda, Nonion havanese, Bulimina midwayensis, Cibicidoides eoceanus, Gyroidinoides subangulatus* and *Bulimina tuxpamensis*. The faunal composition indicates a return of heavily calcified taxa and a combination of

epifaunal and infaunal morphotypes. There is still a number of cosmopolitan taxa suggesting the benthic ecosystem have not fully recovered from the effect of PETM even when the carbon isotope signal had fallen back to the pre CIE values.

Based on trait composition, this study suggested that taxa with spiral and elongate test shape, secreted hyaline calcite test composition as crucial traits for the regulation of carbon content in the ecosystem. Bi/tri-serial, planispiral and trochospiral chamber arrangement, as well as spherical/oval, triangular/trapezoid shape chambers, depressed or raised sutures and taxa with no ornament, are indicated as resilient traits during the period of ecological disturbance because their proportion increased or remained constant during the CIE. These traits are found on a wide range of taxa with opportunistic lifestyle (Figure 4.11). Aperture forms such as arcuate or slit-like apertures with lips or no apertural accessories and terminal aperture position are indicators of successful feeding strategies critical to the survival of the benthic foraminifera. Also, the existence of micro and fine perforation in the SIMPER result (Figure 4.11) suggested a reduction in the size of perforation. Finer perforation reduces oxygen requirement of foraminifera as well as the impact of dissolution by creating smaller reaction surface. More so, the absence of coarse perforation suggests that taxa with such traits require higher oxygen concentration and less corrosive bottom water to survive.

Benthic fauna shift their habitat towards shallow-infaunal and deep- infaunal with deposit feeding mode during the period of ecological disturbance (Figure 4.11), and only those taxa that were suited to such lifestyle were able to survive. There are possibilities that some taxa currently classified as epifauna may have lived infaunally and migrated to the sediment surface to feed or acquire oxygen and move back later into the sediment to take refuge.

This study also suggests that some deep infaunal taxa like *T. selmensis* might have constructed their test in a dual process of secreted hyaline calcite and incorporation of coccolith plate by agglutinated processes. Further sample cleaning procedures, high-resolution SEM imaging and tomography are therefore recommended to understand the calcification in this taxa better.

The application of BTA in understanding the ecological functioning of microfossils is still at its pioneering state, and we hope that with increasing interest among palaeoecologists on the application of the tools, more discoveries of its value would be appreciated. In this study, it has been very useful in combining faunal assemblages and trait composition and mapping them to the related ecological functioning. Also, it synthesises large data sets across the lateral and temporal scale in a well-structured and understandable manner.

CHAPTER FIVE

Biological trait composition and ecological functioning of foraminifera in the SE Atlantic Ocean during the PETM (to be submitted as a paper)

5.1 Introduction

Foraminifera contribute to some important ecological functions in the oceans such as nutrient cycling, carbon sequestration and source of food for organisms at the higher trophic levels. Because the shells of most foraminifera are composed of calcium carbonate, they are the largest contributor to biogenic inorganic carbon sequestration globally (Petrizzo *et al*., 2008). Foraminifera are very sensitive to ocean chemistry and tend to incorporate the chemical composition of sea water within their calcified shells and thereby record the prevailing local conditions. Thus foraminiferal test composition (hereafter referred to as test) can be used as proxy for interpreting palaeoenvironmental conditions such as temperature, carbon saturation, salinity, palaeocirculation, oxygen concentration and hydrodynamics during their lifetime (e.g. Thomas, 2007; Aze *et al.,* 2014b; Boscolo Galazzo *et al*., 2014; Littler *et al.,* 2014; Nwojiji *et al.,* 2014; Palike *et al.,* 2014; Schiebel and Hemleben 2017).

The physiological makeup of foraminifera plays a huge role in the surviving strategies they adopt while alive and has been demonstrated in the fossil and modern species records to have a close relationship with environmental parameters (Keating-Bitonti and Payne, 2017). Several palaeoecological studies have linked vertical separations (stratification) in the ocean to the morphological stratification of foraminiferal ecosystem both at the pelagic and benthic zones (Luciani *et al.,* 2007; Arreguin-Rodriguez *et al*., 2016; Schiebel and Hemleben, 2017). In the modern ocean, the planktonic foraminifera found in the mixed layer of the surface water is dominated by rounded globular test, such Globigerinids with an algal symbionts. Moreover, the species found deeper below the thermocline are predominantly flattened discoidal, or conical forms representing Globorotalids morphologies with herbivorous feeding habit (Hemleben *et al.,* 1989). In the benthic zone, the epifauna species are composed of smooth trochospirally coiled and coarsely perforated forms while the infauna species are significantly rough, bi-triserially chambered and elongate forms (Corliss and Chen, 1998; Jorrisen *et al*., 2007).

Due to the rapid changing of global marine ecosystem as a result of anthropogenic (e.g. climate change, habitat loss, and environmental pollution) and natural (e.g. orbital forcing, volcanism)

pressures, extreme climatic changes are forecasted for the next few millennia (Zebee and Zachos, 2013). The climatic extreme could lead to mass extinction and permanently alter the current climate system (Barnosky *et al.,* 2011). The present study considers the Palaeocene – Eocene Thermal Maximum (PETM) hyperthermal event 55 – 56 million years ago that had similar magnitude and rate of greenhouse emission as present value (Zebee and Zachos, 2013). The PETM is characterised by 2 - 3‰ carbon isotopic excursion (CIE) due to a massive injection of isotopically light carbon into the Earth system that coincided with eccentricity maxima (McInerney and Wing, 2011). Extensive ocean anoxia and the acidification in the deep-sea led to the burndown of existing calcite deposit in the ocean and a significant rise in the lysocline and carbon compensation depth (CCD) during the PETM (Babila *et al.,* 2018). These changes in ocean chemistry have significant effects on marine ecosystems including faunal turnover such as the extinction of benthic foraminifera, subsequent diversification and migration of planktonic foraminifera (Williams *et al.,* 2007; more details in Chapter one).

Because of the significant role that foraminifera play in the global carbon sequestration and food supply, it is important to understand how their turnover during the PETM as well as the impact of the climatic extremes on the essential services provided by foraminifera. The result from this study will help us to speculate the impact of the current climate change on foraminifera and their ecological functions. To achieve this aim, we have selected ODP core samples from the southeastern Atlantic Ocean (Leg 208 Site 1265). ODP Site 1265 is located at bathyal water depths (Zachos *et al*., 2004; Figure 5.1) in a broad channel at the base of the westward trending slope of the Walvis Ridge. ODP Leg 208 was the first to recover an intact and undisturbed continuous sequence of Palaeocene – Eocene (P/E) boundary because of the drilling strategy that adopted advanced piston corer (APC) techniques. The recovered cores were used to constrain the nature of both long and short-term changes in the vertical dimension of PETM (Zachos *et al.,* 2004).

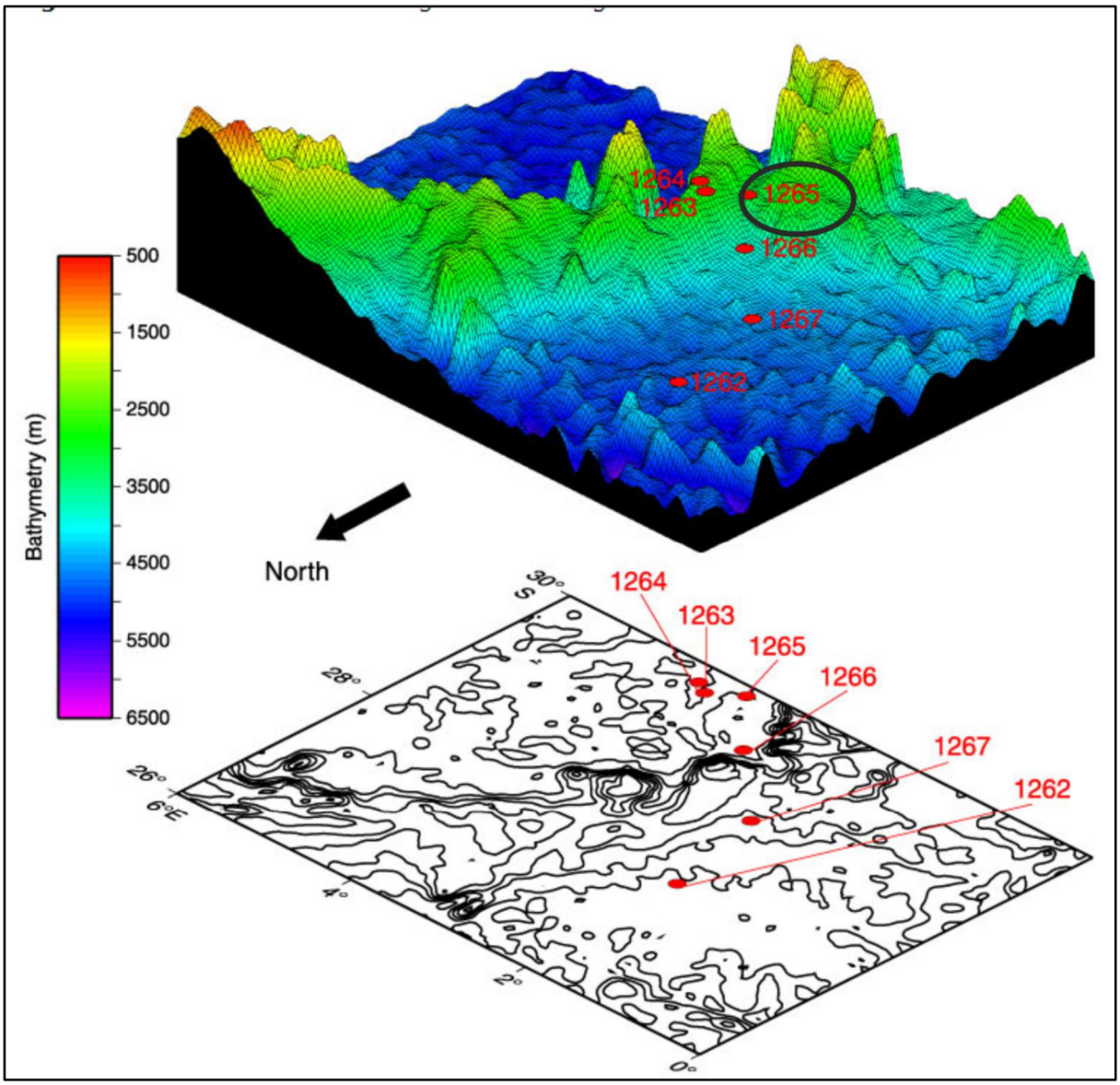

Figure 5.1: Three-dimensional diagram of the Leg 208 drill sites showing the location of Site 1265A and its associates with corresponding bathymetry (adapted from Zachos et al., 2004).

In this chapter, we present the foraminiferal abundance and distribution from thirty-five sediment samples (core depths 266.31 mbsf – 276.66 mbsf) across the PETM section in ODP Site 1265A. Biological traits analysis (BTA; Bremner *et al.* 2006) was used to quantify changes in the trait, and by inference of functional composition. The recovered foraminiferal assemblage in conjunction with the trait composition helped to understand how the ecological functioning of foraminiferal assemblage changed during the hyperthermal. Furthermore, determining which characteristics the benthic foraminifera that became extinct or survived during the PETM had, can provide a clue to the response of foraminifera during an extreme climatic event in the future.

5.2 Results

5.2.1 Core description

The detailed description of individual core section (Table 3.3) analysed for this study showed that Core 29H-01 compose of brown ooze from the core top to 10cm interval while the rest part of the core was a grey foraminifera ooze. This description is based mainly on the change in colour across the core sections. Changes in colour is known to reflect climate variability in deep-sea sediment across the time slice they were deposited with lighter colour indicating cooler climate and dark brown for a warmer climate (core 29H-07 in Figure 2.2). Core 29H-02 was predominantly chalky ooze with light brown intervals at 55-65cm and 97-112cm. There is only a 5cm interval of light brown ooze at 29H-03 while the rest of the section was grey in colour. The interval from 88 – 134 cm composed a mixture of soupy and semi-solid sediment. Core 29H-04 consisted of light grey calcareous oozes with brown intervals at the core top to 30cm and at 56-63cm sections. The whole section of cores 29H-05 and 06 were made of light grey foraminifer-bearing nannofossil ooze.

Core 29H-07 is the core of major interest. The reddish-brown section of this represents the CIE interval at Site 1265A. The 50cm (22-72cm) interval of this core composed of nannofossil-bearing clay. The clay enrichment in this section is evidence of carbonate dissolution widely associated with the PETM across the globe. The clay was evident during the foraminifera processing with the sediments forming pellets and sticking to the mesh. Less than 5% of the foraminiferal residue was recovered from this section compared to 30-40% (estimated) recovered from the section below and above this section. The contact between the PETM (CIE) onset and late Palaeocene sediment was not sharp as expected, and this has been interpreted as evidence of sediment reworking resulting from bioturbation during the hyperthermal. Lightening of the core towards the top was a sign of carbonate enrichment associated with PETM recovery.

5.2.2. Chronology

The age model for Site 1265A was derived from a combination of cyclostratigraphy, XRF (Fe and Ca) curves, carbon isotope stratigraphy and biochronology. The PETM section is located within the magnetic polarity zone of Chron C24r (Aubry *et al.,* 1996). The chronology of ODP Leg 208 cruise of which Site 1265A was one of the holes developed by Zachos *et al*., (2005). The age model was based on high resolution astronomically turned time frame correlated with $\delta^{13}C$ isotope records from ODP Site 690 (the Weddell Sea, Rohl *et al*., 2000). As mentioned in Chapter 1, the PETM interval coincided with eccentricity maxima, and Rohl *et al.* (2000) used spectral analysis to ordinate orbital cyclicity and high-resolution geochemical records and developed absolute age for each major shift in carbon isotope $\delta^{13}C$ record across the PETM. The datum for the time scale was placed at the first negative shift of $\delta^{13}C$, and this point was regarded as 0ky ±P/E boundary relative to the strata above (Figure 5.2; Zachos *et al.,* 2005; Littler *et al.,* 2014). In the original age model from Site 690 (Rohl *et al.,* 2000) the duration of PETM was categorised from A – H (0 ky, A=0.75 ky, B=21.90 ky, C=42.38 ky, D=71.25 ky, E=81.17 ky, F=94.23 ky , G=200 ky, H=240 ky; Figure 2.4; Alegret *et al.,* 2009) corresponding to key inflection points in the carbon isotope record. Based on these estimation, it took 50 ky from the base of the clay enrichment (reference datum) to the point of minimum carbon isotope excursion (CIE) value and another 50 ky from the lowest value of $\delta^{13}C$ to the 'ankle' of the curve where the isotope record levelled off and showed initial sign of recovery. The details of the chronology are shown in figure 5.2. Cautiously, we have to state that the chronology is only relative and has been linearly extrapolated to the rest of the core bearing in mind the uncertainties that may be associated with this method. Age estimate across the PETM is highly complicated because the boundary is based on the basal part of the clay layer which has been affected by the extreme dissolution of previously deposited $CaCO_3$ and a period of non-deposition due to the shoaling of the CCD. It is more problematic for Site 1265A where the lowermost section of the clay layer was not recovered (Zachos *et al.,* 2004; 2005). The age estimate for the upper section of the core was more robust due to the uniform carbonate deposition and clearer signal in the $\delta^{13}C$ record.

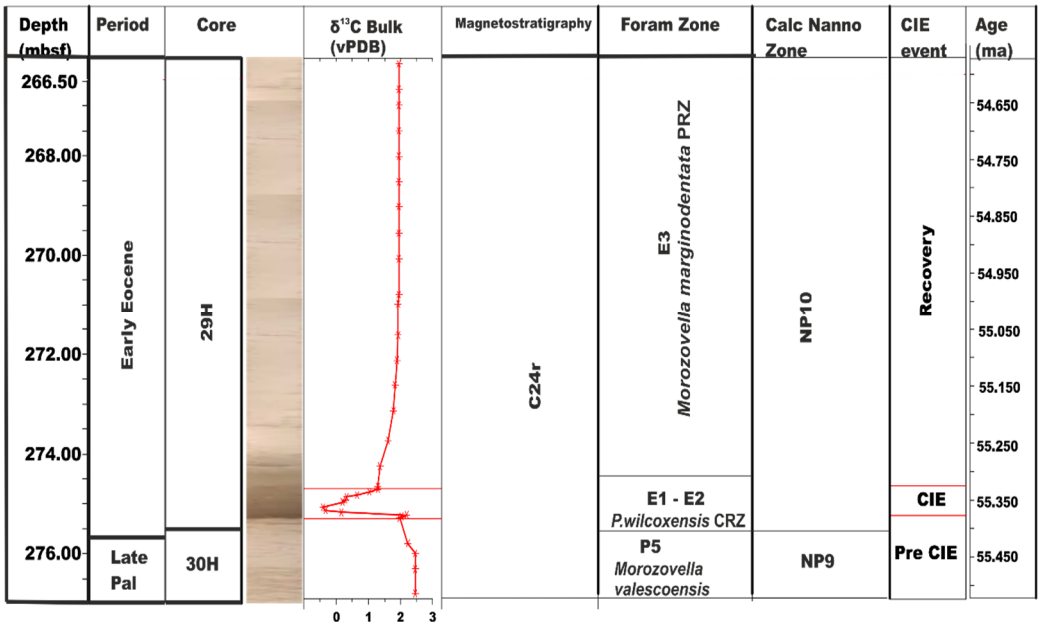

Figure 5.2: Chronostratigraphy of the studied section of Site 1265A. Carbon isotope, paleomag, and Calcareous nannofossil zones were modified from (Zachos et al., 2004; 2005) while foraminifera zonation is from this study.

Sedimentation rates in subunit IIC was moderate, and carbonate content of the sediment was high in accordance with the equatorial location of the site and its relatively shallow depth. The average linear sedimentation rate is approx. 18 m/m.y (Figure 5.3) and the mass accumulation rate ranges from 0.55 – 3.1 g/cm^2/k.y (Zachos *et al.*, 2004)

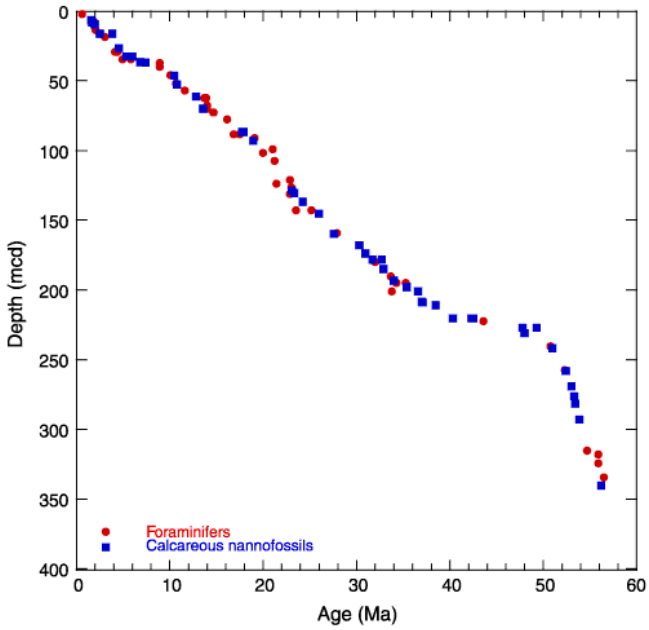

Figure 5.3. Linear sedimentation rate and Age – depth curve of Site 1265A (taken from Zachos et al., 2004)

5.2.3 Planktonic foraminiferal distribution

5.2.3.1 Taxa composition and changes through time

From the 35 core samples analysed for planktonic foraminifera across the PETM section in Site 1265A, a total of 79,706 foraminiferal specimens were counted. These represented 59 species with *Acarininidae, Morozovellidae, Subbotinidae, Chiloguembellinidae* and *Globanomalinidae* being the dominant taxa. Base on ANOSIM result, planktonic foraminiferal composition at Site 1265A significantly differed between the pre-CIE, CIE and recovery (global R = 0.673, $p<0.01$), and pairwise tests showed that all three intervals significantly differed from each other ($p<0.01$). The result also show that each interval insignificantly differed from each other as follows; recovery and CIE, R= 0.632 ($p< 0.01$); recovery and pre-CIE, R= 0.918, ($p< 0.02$); CIE and pre-CIE (R= 0.335) ($p< 0.01$). The sample ordination during the pre-CIE was distinct and the recovery samples were tightly grouped. However, the CIE was clearly different because the grouping was more or less longitudinal, forming a transect between the pre-CIE and the recovery groups (Figure 5.4). The high dissimilarity (R= 0.335; $p< 0.01$) of planktonic foraminifera composition during the CIE suggests evidence of environmental disturbance (Figure 5.4). While the greater similarity (R= 0.918, ($p< 0.01$) pre-CIE and during the recovery imply a more stable ecosystem (Figure 5.4).

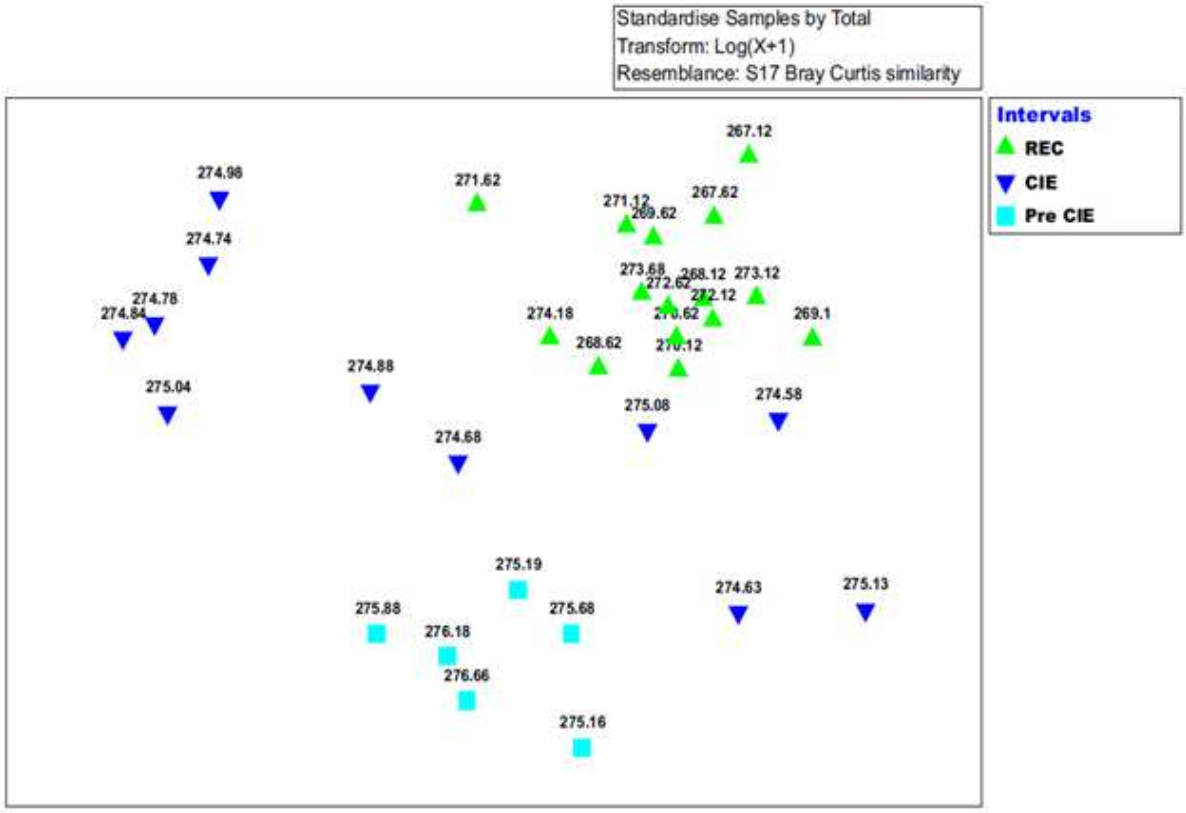

Figure 5.4: Non-Metric Multidimensional Scaling ordination of planktonic foraminiferal taxonomic composition (transformed with log x+1) of Bray-Curtis similarity from Site 1265A.

Similarity percentage routine (SIMPER) results showed that six taxa contributed to 50% of the dissimilarity between the CIE and the recovery intervals, and notably *Morozovella* spp contributed 17.78% of the dissimilarity being 5 fold more abundant during the CIE. The high abundance of this taxa during the CIE was attributed to their increase during the PETM (Petrizzo, 2007; Aze *et al*. 2014b). Nevertheless, *Chiloguembelina trinitatensis*, *Subbotina patagonica, Morozovella subbotinae* and *Globoturborotalia brassriverensis* were more (Table 5.1) during the recovery than in the CIE interval.

Subbotina spp., *Acarinina* spp., *Morozovella* spp were more in abundance at the CIE than during the recovery. The high abundance of *Subbotina* spp and *Acarinina* spp during the CIE period (Tables 5.1 and 5.3) was due to the high level of dissolution witnessed within the interval that made the identification to species level difficult. *Chiloguembelina trinitatensis, C. crinita S. patagonica, M. subbotinae, G. brassriverensis* and *A. interposita* maintained higher abundance during the recovery compared with during the CIE. *G. brassriverensis* originated during the CIE and the absence of *M. aqua* at the same interval showed that the species went extinct before the recovery period.

Table 5.1: Mean abundance of species contributing to the most dissimilarity between the recovery and the CIE intervals at site 1265A (data cut off 50%)

Species	**Mean abundance**		**Contribution to dissimilarity (%)**
	REC	**CIE**	
Morozovella spp.	5.15	**26.02**	17.78
Acarinina spp.	1.28	**12.27**	8.5
Chiloguembelina trinitatensis	**11.98**	2.78	7.48
Subbotina patagonica	**10.95**	3.89	6.17
Morozovella subbotinae	**10.58**	5.09	6.1
Globoturborotalia brassriverensis	**9.75**	2.14	6.03

Table 5.2: Mean abundance of species contributing to the most dissimilarity between the recovery and the pre-CIE intervals at Site 1265A. Data cut off at 50% cumulative similarity.

Species	**Mean abundance**		**Contribution to dissimilarity (%)**
	REC	**Pre CIE**	
Chiloguembelina trinitatensis	**11.98**	2.93	7.72
Globoturborotalia brassriverensis	**9.75**	0.00	7.36
Morozovella subbotinae	**10.58**	2.78	6.18
Subbotina spp	1.70	**8.51**	5.76
Subbotina patagonica	10.95	6.11	5.38
Acarinina spp	1.28	**7.71**	5.13
Acarinina interposita	7.33	3.37	5.02
Morozovella aequa	0.00	**6.25**	4.72
Chiloguembelina crinita	**6.10**	3.73	3.97

The dissimilarity between the CIE and pre-CIE indicated that *Morozovella* spp*., Acarinina* spp., *Acarinina Soldadoensis, Acarinina nitida* were higher in abundances during the CIE than during the pre-CIE. However, *Subbotina* spp*., Subbotina patagonica, Acarinina coalingensis* abundance were more before the CIE than in the main CIE. The abundance of *Subbotina* spp at the pre-CIE interval indicated that the taxa test dissolution started before the CIE making the identification of the specimen to species level very difficult.

Table 5.3: Mean abundance of species contributing to the most dissimilarity between the CIE and pre-CIE intervals at Site 1265A. Data cut off at 50% cumulative similarity.

Species	**Mean abundance**		**Contribution to dissimilarity (%)**
	CIE	**Pre-CIE**	
Morozovella spp.	**26.02**	5.76	17.79
Acarinina spp	**12.27**	7.71	7.27
Acarinina Soldadoensis	**14.58**	6.71	6.46
Subbotina spp	1.50	**8.51**	5.48
Subbotina patagonica	3.89	**6.11**	4.61
Acarinina coalingensis	2.86	**6.84**	4.34
Acarinina nitida	**5.25**	5.03	4.30

In general, the preservation of the recovered foraminiferal specimen range from moderate to very poor. In most cases, it was difficult to see distinguishing features like muricae, spines, or perforations under the light microscope, and in such cases identification was made based on the shape, number of chambers and other visible ornamentation (see Chapter 4 for more discussion on test preservation)

The result from raw faunal composition showed that the pre-CIE interval (276.66 - 275.19 mbsf; latest Palaeocene) was marked by the restricted occurrences of *Acarinina nitida, Acarinina strabocella, Chiloguembellina morsi, C. wilcoxensis, Globanomalia australiformis, G. compressa, G. pseudomenardi, G. planoceanica, Morozovella pasionensis, M. valescoensis, M. angulata, Parasubbotina pseudobulloides, Parasubbotina variata, Subbotina cancellata, Subbotina triagularis, S. triloculinoides,* and *S. trivalis* (Figure 5.5A). The pre-CIE interval was characterised by high abundances of all the major taxa with relatively good preservation, however, fragmentation and dissolution significantly increased just prior to the benthic foraminiferal extinction event at 275.68 mbsf. *Acarinina* was the most abundant taxa in this interval; it was followed by *Subbotina* and *Globanomalia* while *Morozovella* was least abundant (Figure 5.5). *Globanomalia* were abundant only in the fine fraction.

The CIE interval was marked by a significant reduction in the abundance and preservational quality of all the species present. The Subbotinidae family (which included taxa like *Parasubbotina and Globoturborotalia*) decreased from 500,000 at the pre-CIE to >100 at the main CIE interval (Appendix 5.2 for census data). Nineteen (19) planktonic foraminifera species including: *A. nitida, M. aquea, S. trivalis, G. chapmani, G. pseudomenardi, S.*

triagularis, S. cancellata, P. pseudobulloides, G. planoceanica, M. occulosa, C. morsi, W. claytonensis, S. valescoensis, M. passionensis, S. triloculinoides, M. acuta, M. acutispira and A. strobocella became locally extinct at Site 1265A (Figure 5.5A) and the first appearance of eight taxa (Figure 5.5B) was recorded within the CIE interval. The interval was characterised by high abundances of *Morozovella acutispira, Morozovella aqua, Morozovella gracilis, Morozovella spp., Acarinina spp., and Subbotina spp.* No excursion taxa were recorded in the interval of main carbon isotopic excursion as reported in the Pacific, Tethys and continental seas (Petrizzo 2006; Giusberti *et al*., 2007; Aze *et al.,* 2014b). However, *Globoturborotalia brassriverensis* which has been reported as an excursion taxa in the PETM section of Bass River (Pearson *et al.*, 2006) made its first appearance at 275.19 mbsf coinciding with the BEE. *Acarinina sibaiyaensis* widely reported as excursion taxon was found in the later part of the recovery interval (Figure 5.5B)

The recovery interval occurred between 274.5–266.6 mbsf and was characterised by a remarkable increase in abundance of most species that survived the local extinction such as *Acarinina soldadoensis, A. coalingensis, A. interposita, Chiloguembelina crinta, Chiloguembelina trinitatensis, Subbotina patagonica, Subbotina hornibrooki*, *Globoturborotalia brassriverensis and Zeauvigerina* spp (Figure 5.5C). There was a significant increase in the abundance of *Morozovella* during the recovery, making it the most abundant taxa. The abundance of *Subbotina* and *Acarinina* species were relatively similar, while the genus *Chiloguembelina* replaced the *Globanomalia* as the fourth most abundant taxa.

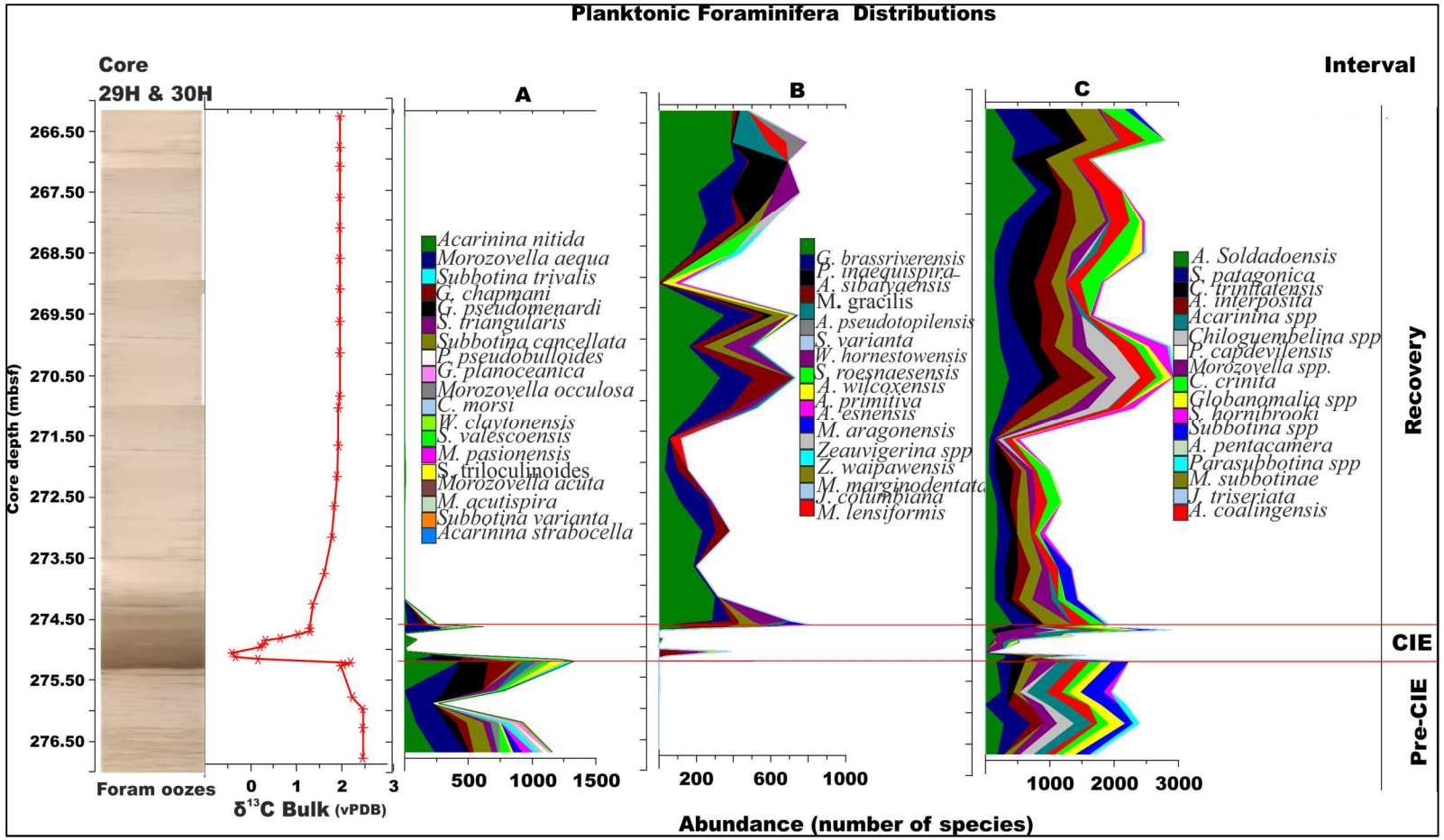

Figure 5.5: The distribution of planktonic foraminiferal species from the PETM section of Site 1265A. A -species that went extinct during or shortly after the CIE. B Species that originated during or after the CIE. C-Cosmopolitan species. The abundance and diversity of all the species were significantly affected by carbonate dissolution with the CIE interval. The bulk carbon isotope record and lithology were plotted with supplementary data from Zachos et al. (2005).

5.2.3.2 Trait composition and changes through time

The result from our statistical analysis indicated that only taxa with smooth, trochospiral test and semi-circular chamber shape were more at the pre-CIE interval than at the main CIE and recovery intervals (Figure 5.7). Taxa with muricae structures, triangular/ trapezoidal chambers, micro and macro perforations, extra-umbilical apertures, surface dwelling and grazing habits were more during the CIE than at the pre-CIE and recovery. While taxa with fine perforation, depressed sutures, elongate test, bi/triserial chambers, terminal aperture, no apertural accessories, deep dwelling and suspension feeding habit were more during the recovery than at the CIE and pre-CIE intervals (Figure 5.7). The high abundance of the trochospiral chamber arrangement during the pre-CIE indicate that taxa such as *Acarinina, Morozovella, Subbotina* and *Globanomalia* which are trochospiral in shape were more during this period. The high proportion of traits such as muricae, surface dwellers and triangular/trapezoid chamber and macro-perforation at the CIE interval is linked to the increase in the abundance of *Acarinina* and *Morozovella* taxa during the hyperthermal. While the high values of elongate, bi/triserial, terminal apertures, deep dwellers and suspension feeding traits during the recovery indicate the preponderance of *Chiloguembelina* species after the CIE.

The similarity analysis (ANOSIM) of trait composition indicated that all the three intervals slightly differ in terms of their trait composition at R=0.45 and $p<0.01$. The comparison of each interval with the other indicated that the recovery interval significantly differs from the CIE at R=0.564; $p<0.01$; also the recovery interval significantly differs from the pre-CIE at global R=04; $p<0.02$ signifying that the PETM significantly impacted on the traits composition of planktonic foraminifera across the studied intervals. However, there was a slight difference between the trait composition at the CIE and pre-CIE with the R-value =0.206 and $p>0.05$ (Figure 5.7).

The nmMDS ordination of planktonic foraminiferal traits composition is entirely different from that of the taxonomic composition. Three groupings A, B and C could be identified from the trait ordination (Figure 5.6). Group A contain samples from the core of the CIE, though not all the the samples at the core of the CIE is contained in group A, the ordination of other samples (274.63mbsf, 274.68 mbsf and 274.88 mbsf) from the CIE section towards the pre-CIE samples (Figure 5.6) could represent a period after the initial perturbation when the traits tried to readjust to buffer the effect of the extreme condition. Hence statistics think they are different and more similar to the pre-CIE.

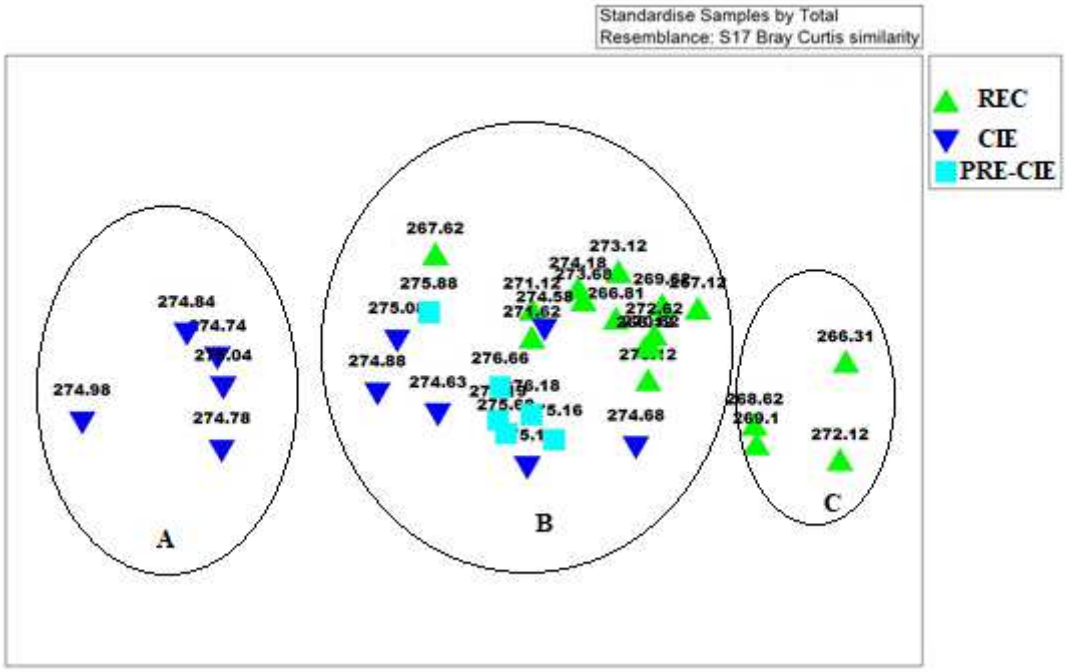

Figure 5.6: Non-metric Multidimensional Scaling ordination of planktonic foraminiferal traits composition from Site 1265A (transformed with total resemblance) of Bray-Curtis similarity indicating sample ordination across the CIE events.

Sample 274.58 classified as CIE based on the carbon ($\delta^{13}C$) isotope ordinated close to the recovery and this suggests that at this point the trait has not been affected by the change in the chemical condition of the sea water. Or because the $\delta^{13}C$ was measured on the bulk carbonate, the record may have been affected by reworking or diagenesis. The same applies to sample 275.13 mbsf. Group B represents the samples that are relatively less perturbed. Even though the samples came from different sections, statistics found them to be more similar than groups A and C. In general, the mixture of samples from different intervals is believed to be a reflection of ecological perturbation that occurred during the PETM. This suggests that the extreme climate condition during the CIE has a significant impact on the trait composition of planktonic foraminifera. Group C contains the samples from the upper part of the recovery interval. The grouping of these samples may suggest the onset of other warming event in the early Eocene such as ETM 2 (Zachos *et al.,* 2008), nevertheless, we do not have sufficient evidence to verify this assertion.

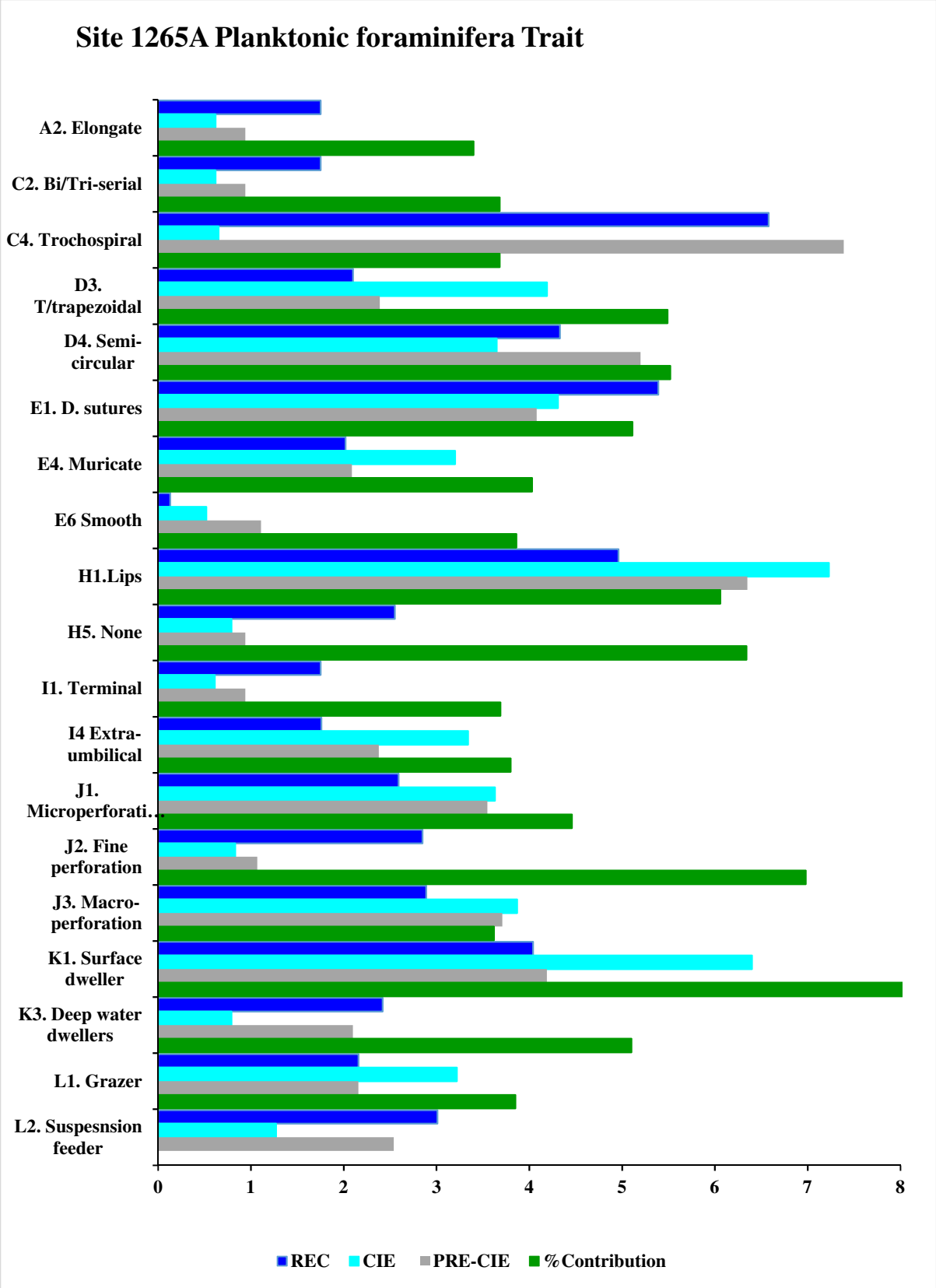

Figure 5.7: Mean abundance of planktonic foraminiferal traits driving the main differences in distribution across the PETM interval at Site 1265A (Data cut off 50%)

Qualitatively, 38 trait modalities were identified in planktonic foraminifera from Site 1265A. The trait composition as shown in figure 5.8 indicated high variability from the pre-CIE to the recovery. The trait distributions can be described as serrated (Figure 5.8) signifying the changes in palaeoecological parameters across the studied interval. The intermittent nature of the trait distribution indicated alternation in the period of rich supply of the needed ecological resources and conducive environment for the foraminifera to thrive as well as a period of ecological stress and resource scarcity. The overview of the trait composition showed the trait richness at the pre-CIE as relatively high in diversity and stable for except spinose wall structure and circular/reniform apertures (Figure 5.8). The trait richness began to decrease in the later part of the pre-CIE and early part of the CIE. The fewest traits were represented during the CIE, while the highest trait diversity was recorded during the recovery. Most of the planktonic foraminifera (Figure 5.8) dropped to the minimum at the base of the CIE but later increase within the same interval. This suggests that planktonic foraminifera traits started to recover before the carbonate composition of the sea water.

In terms of individual traits, the most abundant modality in test shape was spiral, probably because all the three major planktonic taxa identified in Site 1265A were spirally coiled in the penultimate shells. Subquadrate and globose test shape were equally high in abundance, while elongate test shape was relatively low from the pre-CIE till 271.0 mbsf after which it increased remarkably.

All the identified planktic foraminifera from the study site were composed of entirely hyaline calcite base on the classification adopted for trait coding in this study. The collapse in trait richness in the planktonic at the beginning of the CIE was due to the carbonate dissolution that significantly reduced the faunal richness of the planktonics during the period.

Chamber arrangement in planktonic traits recorded only two modalities with trochospiral constituting ~70% and bi/triserial (30%). The chamber shapes were predominantly semi-circular, triangular/trapezoid, spherical/oval and few tubular in the order of decreasing abundance (Figure 5.8).

Wall texture in planktonic foraminifera was highly diverse. Depressed sutures were the most abundant, closely followed by muricate and much fewer cancellate structures. Taxa with smooth wall texture were common during the pre-CIE interval but disappeared after the CIE and occurred later at few depths within the recovery intervals. Only infinitesimal number of taxa with spinose wall texture was recorded across the studied section.

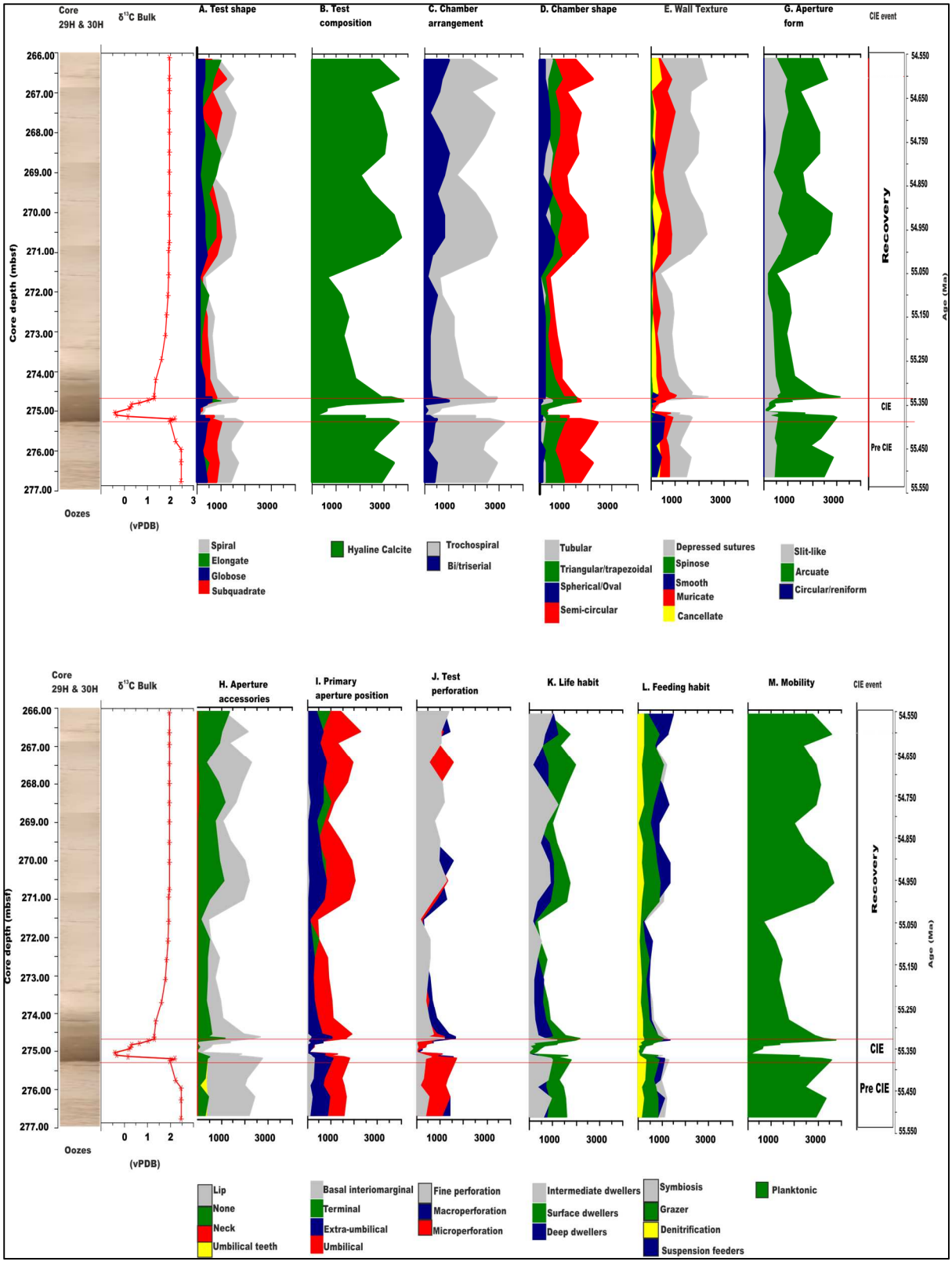

Figure 5.8: Planktonic foraminiferal traits distribution across the three intervals of PETM at ODP Site 1265A-South Atlantic Ocean shown with core depths (mbsf) on the left, bulk $\delta^{13}C$ record (extracted from Zachos et al., 2005) and age (Ma) on the far right.

Aperture form in the planktonic trait recorded approx. 70% arcuate and 28% slit-like apertures, while circular/reniform apertures occurred in a very insignificant number. The most abundant aperture accessories recorded in planktonic foraminifera was lip, umbilical teeth occurred sparingly across the studied section while the rest of the taxa lacked apertural accessories.

Umbilical – extra umbilical apertures recorded the highest abundance in terms of primary aperture position in planktonic foraminifera from this site. The abundance of terminal apertures was relatively moderate while basal interiomarginal aperture was the rarest and it only occurred consistently before the CIE.

All the planktonic foraminifera identified in Site 1265A were perforated. Macro and micro perforation showed a similar trend across the studied section and fine perforation indicated low abundance from pre-CIE through the CIE interval but increased during the recovery.

Surface dwellers were the most abundant life habit in planktonic foraminifera recovered from this study area. This was followed by deep and intermediate water dwellers in decreasing order of abundance. The highest abundance of surface dwellers reflected the preponderance of *Acarinina* and *Morozovella* across the studied sections, deep dwellers represent the Subottinid*s* while the population of Chiloguembelinids was reflected by the intermediate dwellers abundance. Traits indicated in the planktonic foraminiferal mode of feeding were grazing, suspension feeding, symbiosis and denitrification.

5.2.4 Benthic Foraminifera

5.2.4.1 Taxa composition and changes through time

A total of 6128 specimens of benthic foraminifera were counted in 33 samples analysed from Site 1265A. The assemblage was composed of one hundred and thirty-four (134) species comprising of 38 epifauna and 96 infauna morphological groups. The fauna were dominated by cosmopolitan/ opportunistic taxa and other late Palaeocene – early Eocene foraminifera assemblage. Faunal abundance and diversity were fairly high before the CIE and during the recovery period but slightly decreased at the CIE interval.

The ANOSIM test on the benthic foraminifera taxa composition indicated that the three groups: pre-CIE, CIE and recovery differed significantly at R= 0.659 and $p<0.01$. The pairwise test for the three groups also showed that the recovery and the CIE significantly differed by R=0.585, recovery and pre-CIE at 0.896 while the CIE and pre-CIE at 0.516 and $p>0.05$.

The nmMDS ordination of benthic foraminifera composition showed tight grouping during the recovery while those of the CIE and pre-CIE were more spread (Figure 5.9). The compact grouping of the recovery samples could be interpreted as environmental stability after the extremely warm conditions and ocean acidification. The CIE samples loosely grouped in the NW axis of the plot but samples from 275.08 mbsf and 275.13 mbsf classified as CIE lay far from the rest of the axis. More so, samples from 274.98 mbsf and 275.04 mbsf also classified as CIE grouped together with the recovery. We may not have an elucidating explanation for the scattered nature of the CIE interval, but it may not unrelated to the benthic ecological disorganisation associated with the CIE. The first two samples (274.98 mbsf and 275.04mbsf) outcropping as outliers may indicate the initial fauna turnover at the beginning when the methane oxidation reached the seafloor and after that period the microbenthos tried to readjust by enhancing their reproduction and that created the two samples (274.98 mbsf and 275.04mbsf) with high abundance similar to the recovery.

In addition, the nmMDS also showed that all the samples during the pre-CIE including the first four samples from the CIE interval were scattered across the whole NE – SE axis of the plot. The scattered nature of these pre-CIE samples could be related to the inception of the release of exogenous greenhouse gases that caused the hyperthermal during the CIE.

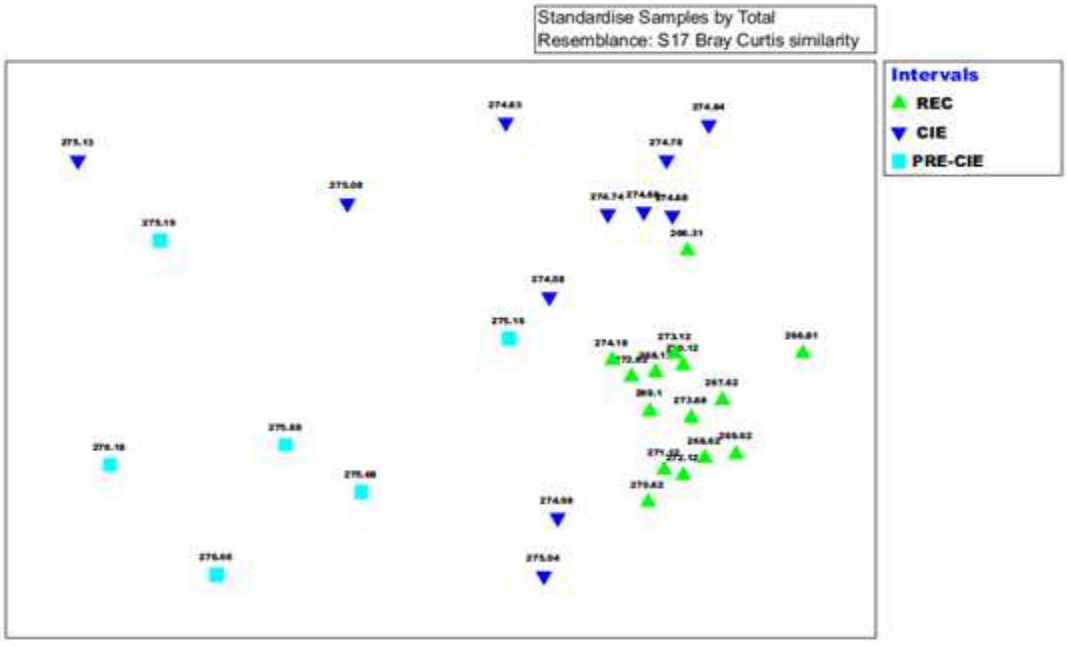

Figure 5.9: nmMDS ordination of Benthic foraminifera abundance in Site 1265A. Pre-CIE samples were clustered around the eastern axis, CIE at the NE and recovery on the SW axis of the plot.

The result from SIMPER analysis for pre-CIE and recovery indicated that the two intervals were 71.55% dissimilar. The result also highlighted taxa that existed at the pre-CIE but went into extinction during the recovery. The extinct taxa include *Gavelinella beccarriformis, Aragonina valescoensis, Praebulimina sp., Coryphostoma midwayensis, Osangularia sp.* (Table 5.4). The result also showed that taxa like *Cibicidoides* spp., *Nonion havanense, Marsonella oxycona*, and *Bolivina* Spp. were more than five times higher at the pre-CIE than during the CIE. The reduction in the mean abundance of *Gavelinella beccarriformis, Osangularia* spp*., Cibicidoides* spp*., Nonion havanense* and *Lenticulina* spp. could be related to the susceptibility of heavily calcified taxa like them to the ocean acidification during the PETM (Kennett and Stott, 1991; Pak and Miller, 1992; Luciani *et al.,* 2007; Thomas 2007). Other taxa that decreased in abundance during the CIE include; *Marsonella oxycona*, *Aragonina valescoensis Coryphostoma midwayensis* and *Bolivina* spp.

SIMPER also indicated a significant increase in the mean abundance of all the Buliminaceae and opportunistic taxa such as *Abyssammina quadrata, Quadrimorphina profunda, Nuttallides truempyi, Oridorsalis Paleopleurostomella pleurostomelloides umbonatus, Stillostomella plumaerae* and *Anomalinoides praeacuta* during the recovery, rather than in the CIE (Table 5.4). This supported the hypothesis that opportunistic (aka disaster) taxa began to increase during the CIE to take over the niche vacated by dissolution susceptible taxa during the PETM (Takeda and Kaiho, 2007; Alegret *et al*., 2009; D'haenens *et al.,* 2012 and this study). These disaster taxa were believed to have supported and sustained the ecological functioning in the benthic zone during the PETM.

Table 5.4: Site 1265A SIMPER results of the average abundance of benthic foraminiferal taxa and their respective percentage contribution within the recovery and pre-CIE intervals. (Data cut off 50%)

Species	**Mean abundance**		**Contribution to dissimilarity (%)**
	REC	**pre-CIE**	
Stillostomella plumaerae	**2.70**	0.34	3.44
Gavelinella beccarriformis	0.00	**2.41**	3.40
Aragonina aragonensis	**2.35**	0.30	3.02
Cibicidoides spp.	0.51	**2.49**	2.67
P.pleurostomelloides	**2.50**	0.85	2.65
Bulimina sp	**1.92**	0.68	2.14
Anomalinoides praeacuta	**2.09**	0.90	2.11
Nuttallides sp.1	**1.81**	0.73	2.05
Tappanina selmensis	**2.46**	1.26	1.97
Bulimina tuxpamensis	**2.58**	1.66	1.97
Q.pyramidalis	**1.43**	0.10	1.86
Nonion havenense	0.43	**1.62**	1.86
Abyssammina quadrata	**1.72**	1.53	1.79

Bulimina trihedra	**1.21**	1.02	1.78
Bulimina midwayensis	**1.77**	0.73	1.76
Praebulimina sp.	0.00	**1.36**	1.74
Aragonina valescoensis	0.00	**1.28**	1.72
Marsonella oxycona	0.24	**1.37**	1.71
Quadrimorphina profunda	**1.64**	0.63	1.71
Bolivina sp.	0.11	**1.44**	1.70
Coryphostoma midwayensis	0.00	**1.13**	1.53
Lenticulina sp	1.06	**1.38**	1.52
Oridorsalis umbonatus	**1.45**	0.81	1.49
Nuttallides truempyi	**3.07**	2.03	1.44
Osangularia sp	0.00	**1.02**	1.40

Table 5.5: Site 1265A SIMPER results of the average abundance of benthic foraminiferal taxa and their respective percentage contribution within the CIE and pre CIE intervals. (Data cut off 50%)

Species	**Mean abundance**		**Contribution to dissimilarity (%)**
	CIE	**pre-CIE**	
Gavelinella beccarriformis	0.45	**2.41**	3.22
Cibicidoides spp.	0.73	**2.49**	2.69
Nonion havenense	0.23	**1.62**	2.10
Aragonina aragonensis	**1.28**	0.30	2.03
Tappanina selmensis	**1.69**	1.26	1.93
Marsonella oxycona	0.27	**1.37**	1.90
Bulimina tuxpamensis	**2.23**	1.66	1.90
Nuttallides truempyi	**2.87**	2.03	1.89
Aragonina valescoensis	0.00	**1.28**	1.89
Bolivina sp.	0.50	**1.44**	1.85
Quadrimorphina profunda	**1.36**	0.63	1.83
Praebulimina sp.	0.19	**1.36**	1.81
Lenticulina sp	0.23	**1.38**	1.78
P. pleurostomelloides	**1.02**	0.85	1.77
Praebulimina reuss	**0.95**	0.71	1.71
Abyssammina quadrata	**1.85**	1.53	1.69
Oridorsalis umbonatus	**1.27**	0.81	1.63
Coryphostoma midwayensis	0.55	**1.13**	1.63
Bulimina trihedra	**1.19**	1.02	1.62
Bulimina midwayensis	**1.30**	0.73	1.57
Osangularia sp	0.35	**1.02**	1.54
Pleurostomella paleoceanica	**1.08**	0.20	1.51
Gyroidinoides globosa	0.00	**1.03**	1.49
Oridorsalis plummerae	0.16	**1.06**	1.49
Spiroplectammina spp	0.00	**1.06**	1.47
Anomalinoides praeacuta	0.33	**0.90**	1.46
Gavelinella sp	0.20	**1.06**	1.44
Gyroidinoides subangulatus	**0.64**	0.45	1.33

The average dissimilarity between the CIE and the pre-CIE was 71.46%, and the results indicated that *Gyroidinoides subglobosa, Spiroplectammina* spp. and *Aragonina aragonensis*

disappeared after the pre-CIE and did not record any occurrence during the CIE (Table 5.5). There were also more *Tappanina selmensis*, *Bulimina tuxpamensis, Praebulimina reuss, Oridorsalis umbonatus, Bulimina midwayensis, Bulimina trihedral, Paleopleurostomella pleurostomelloides, Abyssammina quadrata* and *Gyroidinoides subangulatus* during the CIE than the pre CIE. In the same vein, *Abyssammina quadrata, Quadrimorphina profunda* and *Pleurostomella paleoceanica* increased more than 5 fold during the CIE than the pre-CIE (Table 5.5). The pre-CIE was characterised by an increase in the mean abundance of heavily calcified taxa such as *Gavelinella beccarriformis, Cibicidoides* spp, *Nonion havanense, Osangularia* sp., *Gyroidinoides globose, Gavelinella* spp., *Anomalinoides praeacuta, Oridorsalis plumaerae* and *Lenticulina* spp. The mean abundance of most of these taxa dropped drastically during the CIE or became extinct (Figure 5.10) due to the effect of dissolution resulting from the ocean acidification and probably decrease in oxygen concentration.

Table 5.6: Site 1265A SIMPER results of the average abundance of benthic foraminiferal taxa and their respective percentage contribution within the recovery and CIE intervals. (Data cut off 50%)

Species	**Mean abundance**		**Contribution to dissimilarity (%)**
	REC	**CIE**	
Stillostomella plumaerae	**2.70**	0.00	5.38
Paleopleurostomella pleurostomelloides	**2.50**	1.02	4.11
Bulimina sp	**1.92**	0.16	3.59
Nuttallides sp.1	**1.81**	0.00	3.59
Anomalinoides praeacuta	**2.09**	0.33	3.58
Aragonina aragonensis	**2.35**	1.28	3.32
Abyssammina quadrata	1.72	**1.85**	2.81
Quadratobuliminella pyramidalis	**1.43**	0.00	2.69
Bulimina trihedra	**1.21**	1.19	2.62
Tappanina selmensis	**2.46**	1.69	2.49
Bulimina tuxpamensis	**2.58**	2.23	2.27
Nodosaria spp.	**1.10**	0.43	2.09
Quadrimorphina profunda	**1.64**	1.36	2.06
Lenticulina sp	**1.06**	0.23	2.01
Pleurostomella paleoceanica	0.05	**1.08**	1.92
Nuttallides truempyi	**3.07**	2.87	1.87
Praebulimina reuss	0.00	**0.95**	1.86
Oridorsalis umbonatus	**1.45**	1.27	1.85

The SIMPER result comparing the CIE and recovery indicated that the two intervals were 63.35% different. It highlighted the origination of *Stillostomella plumaerae, Nuttallides* sp.1, *Quadratobuliminella pyramidalis* after the CIE as well the extinction of *Praebulimina reuss* before the recovery (Figure 5.11; Table 5.6). The most remarkable event highlighted by SIMPER result for CIE and recovery was the replacement of the heavily calcified taxa that

dominated the pre-CIE by the more opportunistic ones during the recovery (Figures 5.10 and 5.11). The heavily calcified taxa were hugely affected by carbonate dissolution during the ocean acidification, and the niche they vacated was recolonised by the opportunistic taxa. In addition, *P. pleurostomelloides, Bulimina sp., A. praeacuta, A. aragonensis, B. trihedral, T. selmensis, B. tuxpamensis, Nodosaria spp., Q. profunda, Lenticulina sp., N. truempyi, O.umbonatus* were more during recovery than the CIE (Table 5.6). Nevertheless, *A. quadrata, P. paleoceanica, P.reuss* maintained a high relative abundance during the CIE.

In the raw data, the foraminiferal assemblage during the pre-CIE at Walvis Ridge was characterised by high abundance and diversity, with a combination of calcareous and agglutinated taxa. The pre-CIE foraminifera assemblage was dominated by late Palaeocene taxa comprising of 38 infauna and 10 epifauna taxa *(*Figure 5.10). The exact depth of BEE was difficult to pin point due to the incomplete recovery of the PETM section in the site and low sampling resolution, however, *G. beccariiformis, C. midwayensis, A. valescoensis, Praebulimina sp., Globorotalites mecheliniani, Gavellinella sp., G. conicus, Osangulina sp., Anomalinoides sp., Ellisoidella attenuate, Glandulina sp., Gyroidinoides globosa, Nodosaria limbeta and Gauddryina pyramidata* (Figure 5.10) went extinct at the beginning of CIE.

The CIE (274.5-275.19 mbsf) was characterised by the extinction of many foraminiferal taxa that existed at the latest Palaeocene. Over 30 species (Figure 5.10) became locally extinct within the CIE interval. The occurrence of *Arenobulimina sp.*, *Lenticulina howelli, Osangulina mexicana, Polymorphina cylindrical, Spiroplectinella dentata, Gaudryina nitida* and *Siphogerinoides sp.* (Figure 5.11) that were mainly infauna morphogroups locally originated and went into extinction within the CIE interval. Some taxa like *Cibicidoides dayi*, *Lenticulina* sp., *Fursekoina* sp., *Gyroidinoides beisseli, Laevidentallina gracilis, Linaresia semicrbrata, Marsonella oxycona, Nonion havenense* and *Pullenia coryelli* disappeared within the CIE interval and reappeared again during the recovery (Figure 5.12).

The recovery interval recorded the highest abundance and diversity of benthic foraminifera. It was characterised by increased abundance of *Anomalinoides praeacuta, A. quadrata, B. midwayensis, A. aragonensis, Bulimina* sp*., B. triletra, B tuxpamensis, Lenticulina* sp*., Nodosaria* sp*., P. pleurostomelloides, Quadratobuliminella pyramidalis, T. selmensis, S. plumerae* and *C. subcarinatus (*Figure 5.11). Most of the taxa were elongate – cylindrical infauna of Buliminidae and Stilostomellidae. There are couple of epifauna taxa but their abundance was not as rich as the infauna taxa. *Nonion spp., Bulimina elaganstissima,*

Spiroplectammina subglabra and *Valvalabamina depressa* only occurred within the recovery section. The increase in the abundance of the Buliminacae actually started at the CIE interval but attained their highest abundance during the recovery.

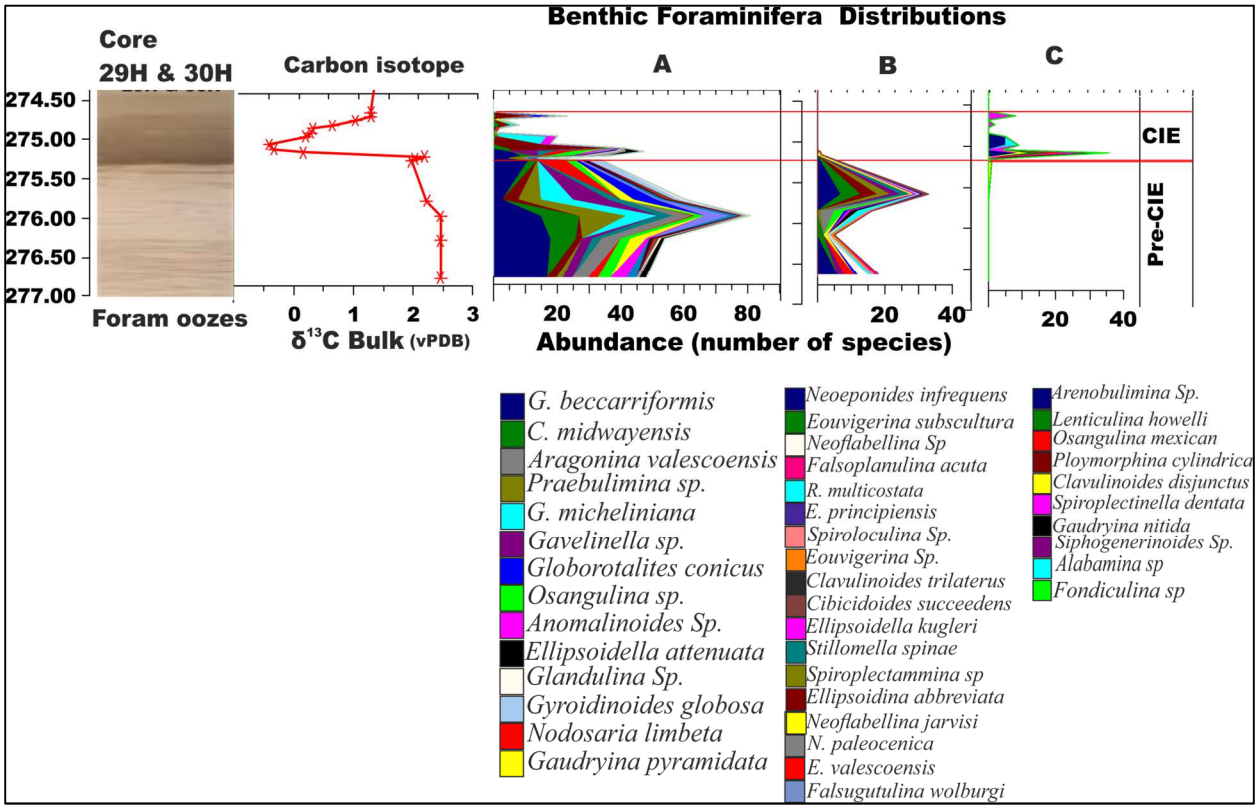

Figure 5.10: Benthic foraminiferal taxa present before and during the CIE at ODP Site 1265A. A - species that disappeared within the CIE interval. B – species whose occurrence were restricted to the Pre-CIE. C- species restricted to the main CIE interval. The bulk carbon isotope record and lithology were plotted with supplementary data from Zachos et al. (2005). The revenant nature of these species suggest that their reproduction during the PETM was extremely affected and only a few survived to continue their existence after the event. The benthic foraminiferal extinction (BEE) event in this study was placed at 275.08 mbsf with the last occurrence Gavellinella becarriformis.

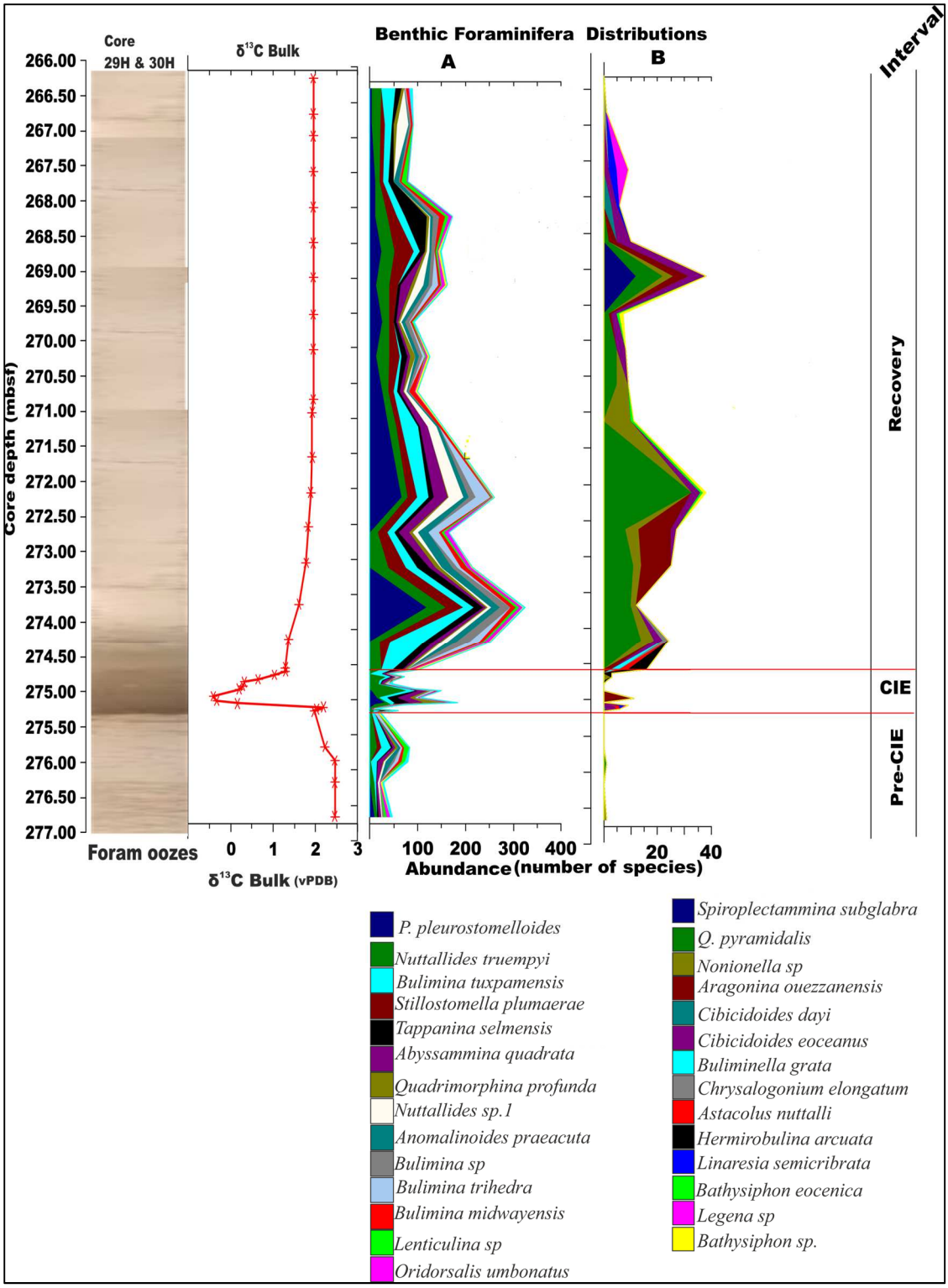

Figure 5.11: Faunal distribution of benthic foraminifera taxa that remarkably increased and/ or originated after the PETM at ODP Site 1265A. A - species that existed throughout the studied section but significantly increased after the CIE. B - species that originated after the CIE and increased in abundance during the recovery. The bulk carbon isotope record and lithology were plotted with supplementary data from Zachos et al. (2005).

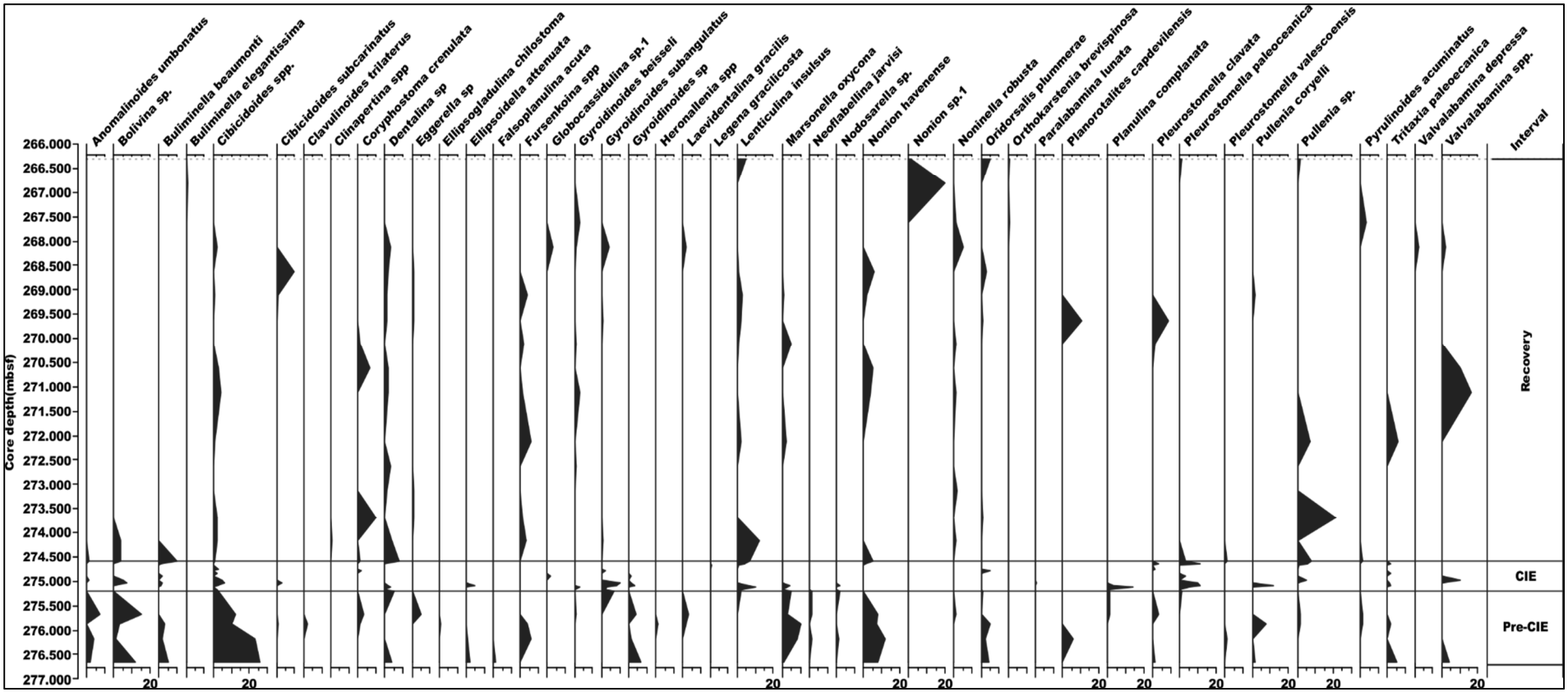

Figure 5.12: Other cosmopolitan benthic foraminifera recovered from ODP Site 1265A, most of which were present before the CIE but disappeared during the CIE and reappeared at the recovery interval

5.2.4.2 Trait composition and changes through time

More than 57 trait modalities were recorded in benthic foraminiferal trait composition from Site 1265A (Figure 5.14). The changes in trait composition across the PETM intervals as determined by ANOSIM test showed that the three intervals were different at global R = 0.117 but at a low level of $p>0.05$.

The similarities between the CIE and pre-CIE the showed that there were more porcellanous tests, arcuate and spherical/oval apertures, apertures with teeth, taxa with no apertural accessories as well as taxa without any recognisable apertures, elongate, tubular, spiral, trochospiral and bi/triserial test, deposit feeders and deep benthic infauna, basal interiomarginal and no ornamentation during the CIE than at the pre-CIE (Figure 5.13). However, more hyaline calcite tests, macro perforation, slit-like apertures, apertures with lips, triangular/trapezoidal chambers, fine test perforation, shallow benthic infauna and sessile habit occurred during the pre-CIE than during the CIE. From this result, we can see that porcellanous test composition, elongate test, deposit feeders, deep benthic infauna, an aperture with teeth, terminal apertures and bi/triserial began to increase in abundance from the CIE and continued through the recovery (Figures 5.13 and 5.14). Basal interiomarginal aperture, non-perforated test, unornamented, no apertural accessories were highest in abundance during the CIE while slit-like aperture, sessile lifestyle and apertures with lip decreased from the pre-CIE to the recovery. This shows that perforation, apertural complexity, ornamentation on the test decreased but sessile lifestyle increased. The mean abundance of hyaline calcite was highest during the pre-CIE and lowest during the CIE.

The average dissimilarities between the CIE and recovery interval indicated that basal interior marginal apertures, slit-like apertures, taxa with no apertural accessories, trochospiral, spiral and bi/triserial tests, triangular/trapezoidal chambers, non-perforated tests, taxa without any ornamentation, deposit feeders and deep benthic infauna traits were more during the CIE than the recovery. This result shows that apertural complexities and perforation, as well as ornamentation became reduced during the CIE similar to what was observed in the planktonic trait and taxa composition, living mode also shifted to deeper habitat and deposit feeding mode of life (Figure 5.13). Basal interiomarginal apertures must have been boasted by the opportunistic taxa that increased in abundance during the warming (Figure 5.13). However, porcellanous and elongate test, terminal, arcuate and spherical/oval apertures, hyaline calcite and micro perforation, as well as sessile traits, were more abundant during the recovery than

the CIE. The increase in hyaline test indicated improved carbonate deposition during the recovery, nevertheless, elongate taxa such as Buliminacae also increased and this could be linked to increase in the food supply to the benthic zone.

The dissimilarity between the recovery and the pre-CIE also showed that all the traits listed to have increased during the recovery interval (Figure 5.13) as well as bifid teeth and shallow benthic infauna were also more when compared with the pre-CIE interval but triangular/trapezoidal chambers, slit-like apertures, aperture with lips, macro perforation, no ornamentation and no apertural accessory traits were more at the pre-CIE than during the recovery. This shows that test perforation decreased from the pre-CIE towards the recovery and could be linked to the disappearance of macro perforated taxa such as Gavelinellids (Figure 5.10). There was also a shift from epifaunal lifestyle to infaunal from pre-CIE to recovery as well as from spiral to bi/triserial chamber arrangement which are related to taxa with terminal apertures.

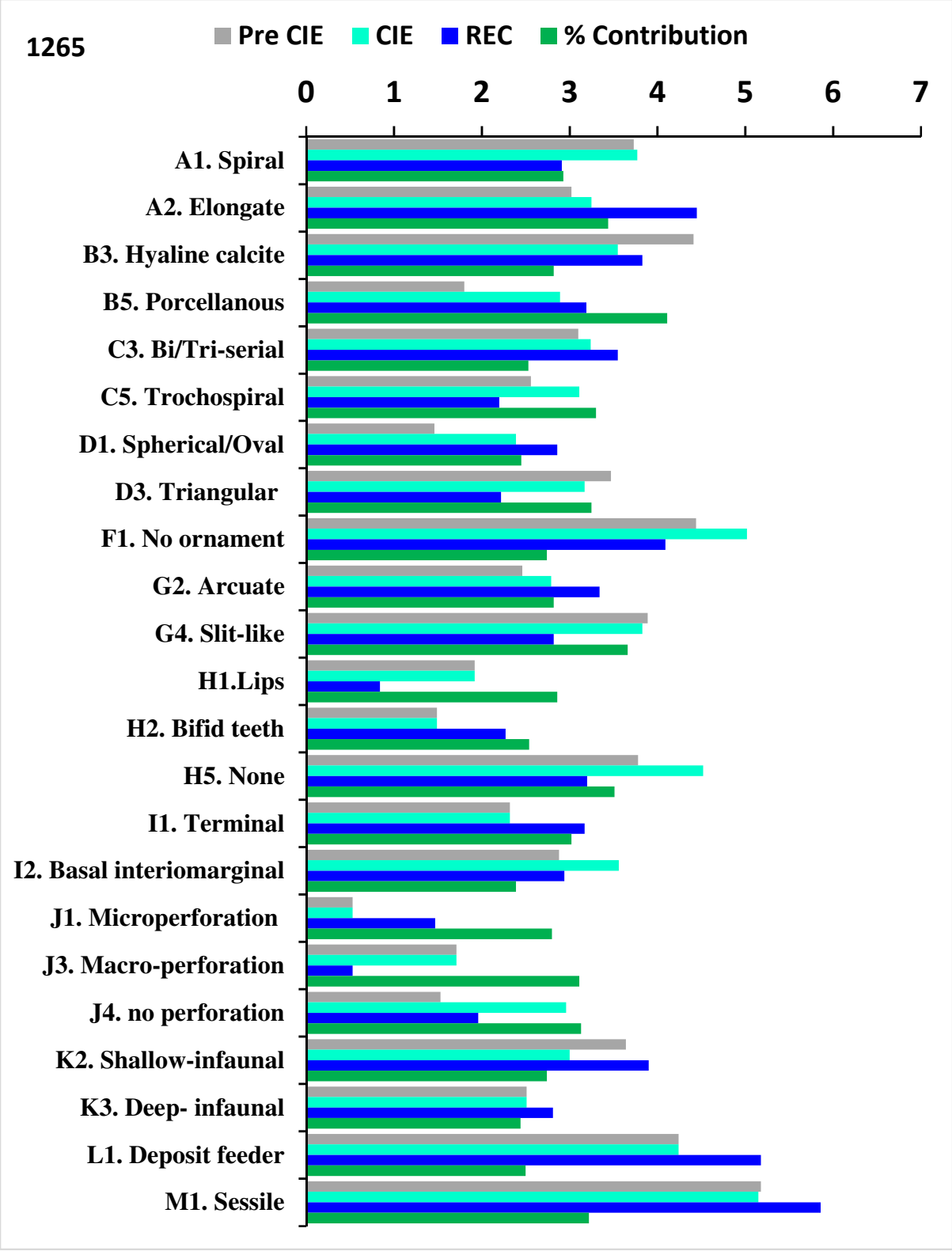

Figure 5.13: SIMPER result of the most significant trait (at 50% cut off) that contributed to the differences in benthic foraminiferal trait composition across the CIE events at Site 1265A. Grey bars = pre-CIE; sky blue bars = CIE core; deep blue bars= Recovery; green bars = % contribution of each trait.

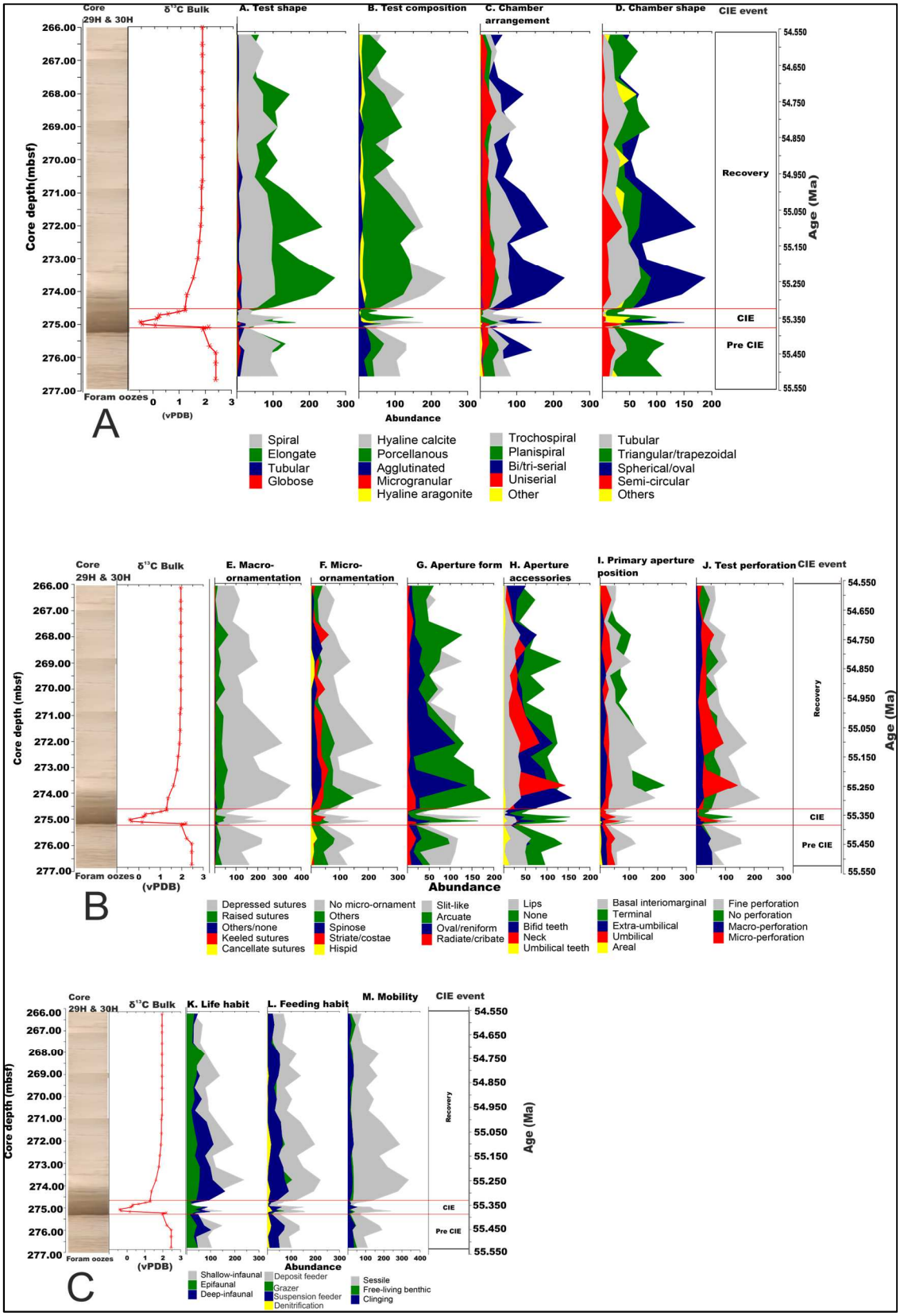

Figure 5.14: Changes in the traits of benthic foraminifera across the PETM at ODP Site 1265A shown with core depths (mbsf) on the left, $\delta^{13}C$ record (extracted from Zachos et al., 2005) and age (Ma) on the far right. A. Shows traits for test composition and morphology. B. Test ornamentation and aperture traits. C. Traits associated with life habit.

The nmMDS for trait composition was similar to the fauna ordination. Most of the samples from the recovery interval ordinated together, however with four other samples from the CIE and one sample from the pre-CIE (Figure 5.15). Only five samples at the core of the CIE with one sample from (266.81 mbsf) the lower most interval of the pre-CIE ordinated together. Two samples (275.08mbsf & 275.13mbsf) clustered closer to the pre-CIE while the other four samples (275.04mbsf, 274.98mbsf, 274.63mbsf & 274.58mbsf) from the earliest part of the CIE samples grouped with the recovery. From the whole ordination, we could observe that the trait re-organisation started at the pre-CIE and continued throughout the CIE. The spread in the ordination of the pre-CIE and the CIE samples suggested ecological disturbance with the input of the excessive greenhouse prior and coeval to the PETM.

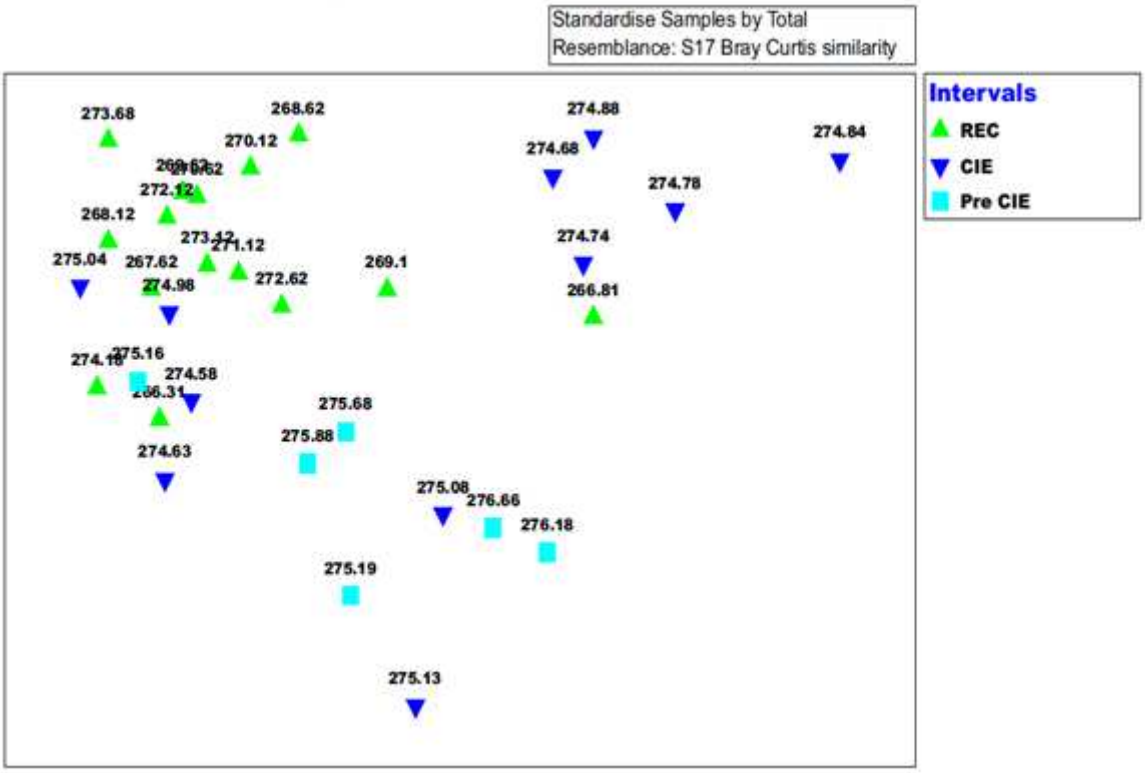

Figure 5.15: nmMDS ordination of benthic foraminiferal traits composition (transformed with log x+1) of Bray-Curtis similarity from ODP Site 1265A. CIE samples clustered at the SE axis, recovery around the SW axis while the pre-CIE samples clustered mostly on the top most part of the plot.

5. 3 Discussion

5.3.1 Changes in pelagic ecology as indicated by planktonic foraminifera

The benthic and planktonic foraminiferal assemblage at ODP Site 1265A at Walvis Ridge was characterised by the typical late Palaeocene to early Eocene fauna (Pearson *et al.,* 2006). The planktonic assemblage represented taxa from the full range of pelagic depth zones and life strategies according to Luciani *et al*. (2007; 2009) (Figure 5.16), e.g. the dominant taxa across the studied interval were *Morozovella* and *Acarinina* taxa (Figure 5.5; Tables 5.1-5.3) which are symbiont-bearing taxa that inhabit the upper water column and are warm water / oligotrophic indicators (Luciani *et al.,* 2007); *Chiloguembelina, Zeauvigerina* and *Pseudohastigerina* that dwell at intermediate depths and are tolerant of reduced oxygen (Berggren and Norris, 1997; Quillévéré and Norris, 2003; Zachos *et al.,* 2003; Dutton *et al*., 2005; Wade *et al*. 2006; Petrizzo, 2007; Luciani *et al*., 2010) as well as deep-water dwellers and colder-water indicators such as *Subbotina, Parasubbotina, Globanomalina* and *Planorotalites*.

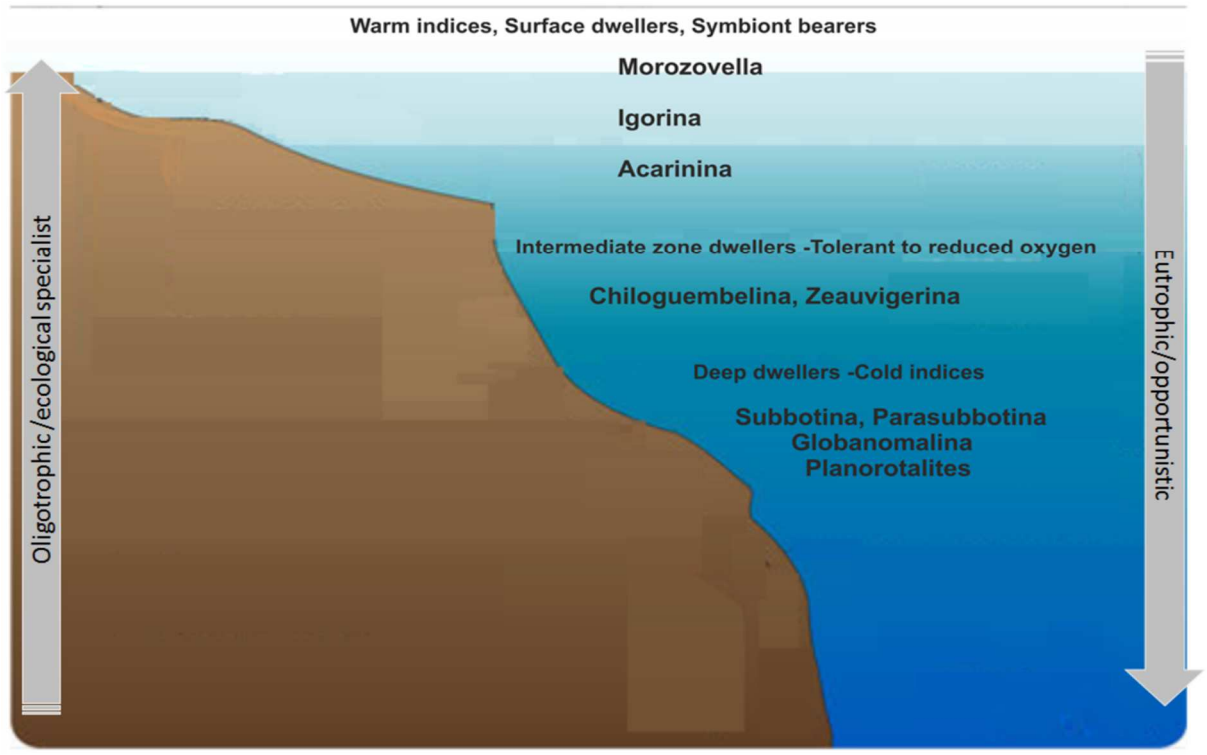

Figure 5.16: Summarised depth profile and life strategies of major Palaeocene – Eocene planktonic foraminifera (modified from Luciani et al. 2007; 2009). Oligotrophy and ecological specialisation increases from bottom to the top while eutrophy and opportunism increases with decrease in depth

Prior to the CIE interval, the planktonic assemblage contained high abundances of *Subbotina*, a moderate abundance of *Acarinina* and, relatively lower abundances of *Morozovella* and *Globanomalia* (Figure 5.5). This assemblage was indicative of eutrophic condition and relatively mild temperatures (Luciani *et al.* 2010). Similar increases in *Subbotina* were found before the CIE at the PETM section in Forada, Italy. In another study, Petrizzo (2007) reported a decrease in the abundance of the *Subbotina* at the Shatsky Rise during the PETM, however, the core analysed was relatively thin compared to this study and Forada section, and also closer to the onset of CIE. Also, low abundances of biserial forms were indicative of a weakly developed oxygen minimum zone (Luciani *et al.,* 2010).The co-occurrence of warm and cold water planktonic taxa was an indication that the ocean was beginning to warm in the late Palaeocene.

Increasing global temperatures during the CIE coincided with decreases in the abundance of the cold water indicators (*Subbotina and Globanomalina*), and corresponding increases in the warm water and nutrient depleted indicators (*Acarinina* and *Morozovella;* Table 5.3). A similar scenario was reported at the Forada section in Tethys Sea (Luciani *et al.* 2010), and in the equatorial Pacific Ocean and Weddell Sea (Kelly *et al.,* 1998; Petrizzo, 2007). The main excursion (CIE) interval was also marked by considerable dissolution of the tests of all three dominant taxa. *Subbotina* seemed to be most affected as shown by its low abundance and diversity among the major taxa. As also recorded in this study, the high abundance of *Acarinina* during the CIE has been widely reported for the equatorial Pacific, Southern Ocean and the Tethys Sea and could be related to the temperature increases and nutrient-depletion (Figure 5.16).

The high relative abundance of photosymbiotic taxa (*Acarinina and Morozovella*) at Site 1265A during the CIE and the decrease in *Subbotina* could be linked to the laters' susceptibility to carbonate dissolution as *Acarinina* and *Morozovella* are more heavily calcified. The depressed cancellate nature of *Subbotina* ornamentation makes them more susceptible to dissolution. Many studies (Pearson *et al*., 1993; Berggren and Norris, 1997; Olsson *et al*., 1999) of modern low – latitude tropical planktonic foraminifera showed that the spinose *Globigerina* a descendant of *Subbotina* are more susceptible to dissolution than the non-spinose taxa. Also, the size of the test also determines the sinking speed (Schiebel and Hemleben, 2017) with larger tests sinking faster. *Subbotina* being relatively smaller than the other taxa spends longer travel time in the water column and so are more likely to be destroyed by predation and dissolution.

High proportions of unidentified Subbotina species in the samples during the CIE interval corresponded with high levels of dissolution among the specimens.

During the recovery high abundance and diversity of *Acarinina, Morozovella, Subbotina* and *Chiloguembelina* occurred. When all the *Globigerinidae* (*Subbotina, Parasubbotina and Globoturborotalia*) were combined, they constituted the greatest proportion of the samples from this section. The pelagic environment must have cooled and been less stratified in order for the cold-water indicator *Subbotina* to proliferate. The abundance of smaller taxa such as *Globoturborotalia and Parasubbotina* were boosted by counting > 63-micron fraction. In previous studies, this fraction has been neglected; however in this study all fractions were included so as not to miss important taxa like *Globoturborotalia brassriverensis*. The high abundance of all major taxa (*Acarinina, Morozovella, and Subbotina*, Figure 5.5; Tables 5.1 – 5.3) during the recovery indicates that the pelagic zone experienced high seasonal variation, well stratified and highly productive surface water.

5.3.2 Benthic foraminiferal markers indicating ecological changes in the seafloor during the PETM at Walvis Ridge.

The benthic foraminiferal composition at Walvis Ridge had high heterogeneity in species richness, abundance and morphotypes. Calcareous taxa dominated the overall foraminiferal assemblage. The predominance of calcareous taxa in the identified fauna suggest that Site 1265A was deposited above the CCD but close to the lysocline during the PETM (Zachos *et al.,* 2005). The preservation of foraminifera was moderately good for the larger tests, however, there was also evidence of frosty calcite overgrowth, etching of test walls, thinning of test walls for some large specimens and many foraminifera from the fine (>63µm) fraction. SEM imaging further showed that even the specimens that appeared to be well preserved have been affected by dissolution and encrustation with secondary calcite and calcareous nannofossil (Plates 4.1-4.3). Dissolution seems to have occurred from highly corrosive carbonate under-saturated sea water rather than non-deposition within or below the CCD because dissolution was incomplete and some smooth, thin-walled *Praebulimina* spp and *Nonion* spp with glassy tests occurred.

The faunal assemblage was composed of 67% infauna and 33% epifauna, the dominance of infaunal *Buliminids* and uniserial taxa are associated with high organic flux and decrease in oxygen concentration (Guisberti *et al*., 2016). Similar benthic foraminifera have been used as an index for trophic conditions at the seafloor (Jorissen *et al.* 2007) and in this model infaunal *Buliminids* and other biserial/cylindrical taxa such as *Pleurostomella, Stillostomella* and

Siphonodosaria occurred in high abundance in eutrophic regions with sustained or highly seasonal phytoplankton productivity. These taxa are believed to have tolerated warm, locally oxygen-depleted and carbonate-corrosive bottom waters. Similarly, high abundances of these taxa have been reported from other PETM section as well as the black shale facies of Cretaceous ocean anoxic event II (Alegret and Thomas, 2009) and the middle Eocene climatic optimum (MECO; Boscolo Galazzo *et al*., 2015). They are reported to be adapted to low-oxygen conditions or can rapidly recolonise the seafloor during brief intervals of reoxygenation. In this study, the *Buliminids* had the most consistent species richness and abundance across the PETM. During the CIE all the species of Buliminidacea were abundant except for *Bulimina bradburyi* and high abundance of this species was recorded throughout the recovery. The statistical results from SIMPER also confirm higher abundance of *Bulimina* species at the CIE and recovery intervals than at the pre-CIE section (Table 5.3 – 5.6). *Bulimina* taxa are tolerant to low oxygen and high organic flux meaning they may occupy niches vacated by vulnerable taxa, and may dominate the foraminiferal assemblage. The prevalent occurrence of *Bulimina* in this study suggests that the taxa occurrence is more closely linked with nutrient and organic matter influx rather than oxygen depletion (Murray 1991; Gooday 1994; Schmiedl *et al*., 2000).

Nevertheless, interpreting palaeo-oxygen concentrations based on foraminiferal composition should be done with caution, because foraminifera can utilise alternative metabolic pathways during low oxygen conditions. For example species of *Globubulimina* and *Bolivina* store intracellular nitrate which they use in denitrification in the absence of oxygen (Keating-Bontonti and Payne, 2017). Oxygen minimum zones have been reported to be dominated by small thin-walled specimen of *Bulimina* (Boltovskoy *et al*., 1991; Kaiho 1994). The faunal assemblage from Site 1265A indicated high diversity of Bulimininidacea that were well-preserved as well as the co-occurrence of taxa that usually inhabit oxygenated environments. Irrespective of the high abundances of *Bulimina,* oxygen concentration is interpreted to be moderate. There was also a moderate abundance of oxic indicators such as *Oridorsalis umbonatus. O. umbonatus* was described as cosmopolitan and an indicator of well-oxygenated pore water but the sustained low flux of highly degraded organic matter (D'haenens *et al.*, 2012) and persistent strong bottom water current. The relatively moderate occurrence of this species across the studied interval suggests the oxygen concentration was moderate during the PETM.

The significant increase of the opportunistic taxa (*Nuttallides truempyi)* at the main CIE interval in this study has been previously associated with sluggish water circulation (Boscolo Galazzo *et al*., 2015). *N. truempyi* was consistently high in abundance during the CIE and throughout the recovery interval. This suggests that the thermohaline circulation may have slowed down during the PETM. In the present day ocean, the abundance of the extant analogue *N. umbonifera* usually coincides with blooms of phytoplankton linked with the formation of deep water mixing and upwelling that redistribute nutrients (Boscolo Galazzo *et al*., 2015). Therefore, the high abundance of *N. truempyi* at the CIE interval may be related to a relative increase in productivity during the PETM.

The high abundances of epifaunal foraminifera such as *Osangularia mexicana* during the CIE indicate that there was a period of seasonal increase in oxygen during the PETM. *Osangularia spp.* typically live opportunistically and repopulated the seafloor during short-term re-oxygenation phases of Cretaceous OAEs (Alegret and Thomas, 2009). They also have a high tolerance for organic enrichment and intermittent deoxygenation. Increase in the abundance of *Osangularia spp.* are reported across the PETM section in Alamedilla (Alegret *et al*. 2009; Friedrich, 2005;2009) and have made the species a PETM benthic foraminifera marker.

Tappanina selmensis, Siphogenerinoides Spp., Aragonina spp. are opportunistic species and indicators of high-productivity, continually stressed and dysoxic sea bottom conditions. (Thomas 2003, 2007; Giusberti *et al.,* 2009; Alegret *et al.,* 2009; D'haenens *et al.,* 2012). They are characteristic of hyperthermal sections in the open ocean sites and are capable of colonizing the sediment when productivity increases during environmental instability. In this study, these species relatively increased at the main CIE section and also showed rich abundance during the recovery.

The parameters used in the above interpretation must be applied with caution as many taxa described are already extinct and the relation between the morphology and the microhabitat is still under investigation. Buzas *et al*. (1993) estimated the current interpretation to be 75% correct and this work has also shown that there is no straightforward interpretation based on faunal assemblages with the mixture of divergent ecological conditions markers. According to Jorissen *et al.* (2007), paleoceanographic reconstructions in geologic records are not always uniform but time averaged. Fauna accumulation in sediment will contain a mixture of all different fauna that lived in the location over several decennia assuming there was no addition or loss of test due to basinal processes and lateral transport when these sediments are sampled

sediment cores may contain fauna from the period of seasonal blooms and period of severe ecological stress. A similar scenario occurs in terms of oxygen concentration, if ecological conditions were stable during the period under consideration, the composition of the fauna might accurately record the concentration of oxygen in the bottom water. Nevertheless, bottom water oxygen concentration (and oxygen penetration depth into the sediment) may in real situation experience significant seasonal variability, for instance when strong water column stratification, or pulsed phytodetritus deposits, cause seasonal hypoxia/anoxia (Jorissen *et al*., 2007). Such events may be annual, but can also be highly episodic, occurring once every 10 years, or even less often. In such cases, it will be extremely difficult (if not impossible) to extract the precise oxygenation history from the time-averaged faunas. More so, in cases when anoxic conditions persisted with low fauna occurrence if this was to be interrupted by short periods with oxic bottom waters characterised by rich and high oxygen content faunas.

Using benthic foraminifera as oxygen index may mix up the average long-term oxygen concentration in the environment. In other settings the duration and severity of the periodical hypoxia/anoxia may easily be overestimated, for instance during oligotrophic, well-oxygenated ecosystems are affected by short-term anoxia leading to the explosive development of a few low-oxygen tolerant taxa. The minor events recorded in our fauna distribution could be linked to the seasonal variation in phytodetrital input and oxygen concentration.

5.3.3 Trait indices in ecological function and community interaction in the Surface Ocean and Seafloor

Functional diversity (i.e. a representation of a range of biological traits and so functions) is a crucial attribute of a community as it measures the role that each organism contributes to ecosystem functioning. For both planktonic and benthic foraminifera identified from Site 1265A, the biological trait composition significantly differed between all three CIE (pre-CIE, CIE and Recovery) intervals. The benthic foraminifera was richer in trait composition compared with the planktonic assemblage and this reflects the differences in taxonomic richness of both.

The highest abundance of hyaline calcite tests in benthic foraminiferal trait during the pre-CIE when compared to the CIE and recovery (Figure 5.13) suggest that the carbonate ion concentration in seawater and carbonate deposition in ocean floor did not recover after the PETM at the Walvis Ridge. A similar circumstance has been documented in other PETM section such as the Shatsky Rise, Alamedilla and Bass River (Alegret *et al.,* 2009; Petrizzo,

2007; Aze *et al.,* 2014b; Takeda and Kaiho, 2007; Stassen *et al*., 2015). The increase in a porcelaneous trait in the benthic ecosystem during the CIE and the recovery raises the question of the solubility high magnesium calcite tests during ocean acidification. Previous studies argued that it goes into solution before the low Mg-Ca hyaline calcite but the increase in *Lenticulina* spp and *Praebuilima* spp (presumed to be porcelaneous) during the CIE suggest that foraminifera calcification during ocean acidification may be different from what is currently known.

Also, in benthic foraminiferal traits, there were increase in spiral and trochospiral test during the CIE. These traits are linked to cosmopolitan taxa such *A. quadrata, N. trumpyi*, and *Q. profunda, O. umbonatus* and *Cibicidoides spp.* They occur in wide range of environments and may be floaters, epifaunal to deep infaunal. The relative increases in these traits during the CIE could be interpreted as the increase in opportunist taxa during the PETM (Figures 5.10; 5.13). In the modern ocean, there have been wide reports of an increase in opportunistic taxa during environmental disturbances (Culver and Lipps, 2003; Bremner, 2006; Caswell and Frid, 2016). Trochospiral coiling is also argued to be advantageous for floating and attachment at the sediment-water interface during the times of disturbance in the bottom water (Boltovskoy *et al*., 1991; D'haenens *et al.*, 2012).

Significant reduction in the benthic foraminiferal wall structure was noticed during the CIE with increase in taxa with no ornament, no perforation and no apertural accessory. Reduction in ornamentation in foraminifera have been reported previously in modern ocean experiencing extreme ecological condition (Dubicka *et al*., 2015) and we believe that either it is the adaptive strategy adopted by benthic foraminifera or that taxa with complex wall structure are more vulnerable during extreme environmental events than those with no ornamentation in the test. No perforation recorded the highest occurrence during the CIE suggesting that ocean acidification and ecological disturbance may lead to loss of perforation in foraminifera. More so, benthic foraminifera tends to reduce perforation during the period of decrease oxygen concentration to conserve gas exchange during metabolism and reduce the amount of oxygen required by the cells.

Our data also show that the infauna habitat, sessile and omnivorous feeding were the preferred way of living among the benthic foraminifera during the PETM (Figure 5.13). Shallow epifauna recorded the lowest occurrence during the CIE while the abundance of deep infauna increased after the warming. The decrease in the occurrence of the shallow infauna trait could

be linked to the ecological stress created by the corrosive water in the upper sediment layer. While the increase in the abundance of the deep infauna during the recovery could be interpreted as a reflection of more oxygen reaching the deeper layer of the bottom sediment.

The trait composition of planktonic foraminifera in Site 1265A indicate that the pre-CIE section was relatively cooler than the CIE and the recovery as taxa with smooth, trochospiral and semi-circular chamber arrangement were higher in abundance before the CIE (Figure 5.7). Only *Globanomalia* have a combination of these traits and the species is regarded as cool water indicator (Luciani *et al.,* 2009). The traits that increased during the CIE are common in warm water indicators such as *Acarinina* and *Morozovella.* This supports that theory that temperature increased during the period. Taxa with perforations also increased during the CIE (Figure 5.7), the function of perforation in planktonic foraminifera tend to contrast that of the benthics. Because planktonic foraminifera were used to well-oxygenated surface water, the increase in perforation during the CIE may be an adaptation to enhance gaseous exchange during the hyperthermal when the oxygen concentration in the seawater was believed to be low. Increase in traits such as lips and umbilical-extra umbilical apertures (Figure 5.7) is a good adaption for the feeding mode (grazing) that thrived during the CIE in planktonic foraminifera community. Since foraminifera are passive predators (Grigoratou *et al.,* 2018), with wide aperture such as umbilical-extra umbilical planktonic foraminifera would be able to capture food while drifting on the surface of water and protect the food with their lips.

The planktonic foraminiferal traits that increased in relative abundance during the recovery suggest that the ocean have relatively cooled with increase in traits such as elongate tests, bi/triserial chamber arrangement, terminal apertures and deep dwellers that are associated with intermediate and cold waters taxa like *Subbotina, Chiloguembelina, Zeauvigerina, Jenkinsina* and *Woodringina.* These traits composition during the recovery also suggest that oxygen concentration was still low at the Walvis Ridge after the CIE (Figures 5.7; 5.8). In general, surface water dwellers and grazing taxa showed more resilience to extreme climate (by increasing significantly during CIE) than the deep water dwellers and suspension feeders whose abundance dropped during the CIE and increase during the recovery.

Despite the difference in the composition of planktonic and benthic foraminifera taxa with terminal apertures, SIMPER results showed some similarities in the trait of the two communities. In the planktonic community, taxa with terminal trait recorded the lowest average abundance at the CIE interval, because only *Chiloguembelina, Zeauvigerina, Jenkinsina* and

Woodringina have terminal apertures. The relatively low abundance of taxa with terminal aperture is interpreted as evidence of nutrient scarcity in the mesopelagic zone during the PETM. The increased temperature during the period must have encouraged thorough consumption of all the nutrients in the upper water column allowing very poor nutrient supply to the intermediate zone where most taxa with terminal apertures reside. As the temperature dropped and surface productivity increased resulting in a more efficient biological pump and increase of nutrient supply to the mesopelagic zone. This lead to the climax of terminal trait abundance in planktonic foraminifera during the recovery period. The trait occurrence in the benthic assemblage also indicates relatively low abundance before and during the CIE but significant increase during the recovery. In the benthic community, the terminal trait is also an indication of productivity changes. The moderate abundance of the trait during the pre-CIE and CIE period suggest that not much change occurs in seafloor productivity during those periods. But the increase in the abundance of terminal apertures at the recovery suggests an increase in export production and remineralisation after the PETM. This is because benthic species such as *Bulimina, Stilostomellids* and *Siphonodosaria* are characterised by terminal apertures and the increase in their abundance reflect an increase in the rain of particulate organic matter to the ocean (Thomas *et al.,* 2018).

There is a noticeable similarity in the occurrence of umbilical – extra umbilical apertures in the planktonic traits and basal interiormarginal apertures in benthic trait composition. Both apertures increased in relative abundance during the CIE. Linking traits with ecological change is not a straightforward task and more work is recommended. Nevertheless, because extra umbilical aperture cut across both sides of the trochospiral test it may be a good adaptation for increased metabolism as a result enhanced food consumption and excretion. Taxa with these apertures are mostly opportunistic group such as *Acarinina, Abssamina*, *Oridosalis* and their abundance was reduced during the recovery (Figures 5.5; 5.10).

The results from our biological trait analysis have shown some evidence of ecological stability or turbulence through the way each sample ordinates within and across the CIE interval. The closeness or disparity between each sample in the nmMDS plot demonstrates how each trait could work together to provide ecological functioning. The tightly clustered samples indicate trait working in harmony to provide the need and stability required for the optimal function of the ecosystem while sparsely diverse sample point to the magnitude of perturbation and hostility experienced by the fauna. Planktonic trait ordination (Figure 5.6) demonstrated a high

level of disorderliness, especially during the CIE. The CIE ordination is interpreted to portray the efforts made by species to counteract the ecological crisis during the PETM by occasionally utilising episodic seasonal bloom of opportunistic taxa to make up for the disappeared taxa. The samples before the CIE were tightly clustered indicating ecological stability. Some part of the recovery interval clustered together while a couple of samples disperse around the group. The grouping still indicated some harmony however, and we interpret the dispersed samples as a trigger to smaller hyperthermal that occurred during the early Eocene climatic optimum (EECO). Benthic trait nmMDS showed that seafloor experienced ecological disturbance even before onset carbon isotopic excursion and that the ecological turbulence persisted till the early part of the $CaCO_3$ recovery. Only the uppermost part of the recovery interval showed some level of coherence. We think that the release of methane clathrate which triggered the PETM started in the late Palaeocene and initiated benthic ecological disturbance which did not recover till the mid-early Eocene. The release of methane hydrate was hypothesised to have originated from the Atlantic Ocean before spreading to the other regions (Zachos *et al.,* 2005) and the disorderliness in benthic trait composition seems to support the idea.

5.4 Conclusions

During the PETM at the Walvis Ridge, considerable faunal turnover of the foraminiferal assemblage occurred that resulted in the mortality and extinction of both planktonic and benthic forms. In general, cosmopolitan taxa dominated during the CIE indicating extreme ecological perturbation. The benthic assemblage was more perturbed than the planktonic assemblage. Multivariate analyses of the assemblage composition demonstrated that the planktonic community was relatively stable before and after PETM, but experienced considerable ecological perturbation during the CIE resulting from increased CO_2 concentration and temperature. However, the taxonomic composition of the benthic assemblage was highly perturbed prior to the start of the CIE suggesting that there were environmental changes that impacted the benthos before the PETM sensu stricto. The greater disturbance of assemblages inhabiting the bottom waters suggests that the source of the isotopically light carbon may have originated beneath sea floor causing benthic ecological disturbance and progressively reaching the surface of the ocean. Thus, supporting the methane hydrate dissociation and or subsea volcanism as the main cause of the PETM.

The planktonic trait distribution also indicated a relatively calm pre-CIE and recovery but sign of ecological disturbance during the CIE. The clustering of the two samples classified as the

upper part of the CIE with the recovery group suggests that traits started to recover earlier than the carbon isotope records in the surface ocean. Planktonic fauna may have adjusted in such a way to favour taxa with traits that could enhance the recovery of the ecosystem. Nevertheless, benthic traits indicated evidence of ecological instability throughout the studied sections and we think that the location of the study site around the active seamount as well as the emission of methane from the seafloor is reflected on the ecological distress in the benthic ecosystem throughout the studied interval.

The fauna present in the planktonic community before the CIE were mesotrophic temperate taxa including Subbotina *spp., Acarinina spp., Subbotina patagonica, Acarinina coalingensis* and *Morozovella aequa.* During the CIE, the faunal composition shifted towards more typically warm-water and oligotrophic taxa comprising *Morozovella spp., Acarinina spp., Acarinina soldadoensis* and *Acarinina nitida*. The recovery fauna was typically eutrophic and cold water indicators such as *Chiloguembelina trinitatensis, Subbotina patagonica, Morozovella subbotinae, Globoturborotalia brassriverensis* and *Chiloguembelina crinita* (Figure 5.16 and Luciani *et al*., 2010).

The high prevalence of heavily calcified benthic foraminifera during the late Palaeocene (e.g. *Gavelinella beccarriformis, Cibicidoides spp., Nonion havenense, Praebulimina Spp., Marsonella oxycona, Bolivina sp., Coryphostoma midwayensis, Lenticulina Spp, Pleurostomella paleoceanica, Gyroidinoides globosa, Oridorsalis plummerae* and *Anomalinoides praeacuta)* indicated conditions were eutrophic before the PETM. However, the presence of crisis taxa such as *Aragonina valescoensis, Osangularia spp.* and *Spiroplectammina spp.* indicates environmental instability at the seafloor even before the PETM. There was a proliferation of opportunistic and ecological stressed fauna during the main CIE; these include *Aragonina aragonensis, Tappanina selmensis, Bulimina tuxpamensis, Nuttallides truempyi, Quadrimorphina profunda, Praebulimina reuss, Abyssammina quadrata, Oridorsalis umbonatus, Bulimina trihedral, Bulimina midwayensis, Abyssammina quadrata,* and *Praebulimina reuss.*

During the recovery, the assemblage was comprised of high proportions of heavily calcified epifauna and infaunal taxa (Table 5.4 – 5.6). This suggests that near the seafloor conditions were oxic and relatively stable with sufficient nutrient supply for epifaunal taxa with high oxygen and food requirements to thrive. The critical foraminifera traits that controled the ecological function in this site include test composition, chamber arrangement/ shape

ornamentation, primary aperture position, perforations and living/feeding habit (Figures 5.7; 5.13).

The biotic and trait records from our study suggest massive carbonate dissolution and relatively moderate oceanic productivity at the Walvis Ridge during the PETM. However, it is hard to interpret the amount of oxygen concentration probably because of the ridge topography with enhanced current activities including eddies and circular currents that prevail around the seamount and transport nutrient and oxygen from the surface to the seafloor (Arreguín-Rodríguez *et al.,* 2016). This is also made more complicated by the behaviour of some foraminifera in the low oxygen environment as it believed that they have an alternative method of respiring nitrate in the absence of oxygen.

In general, the BTA produced a quantitative and integrated picture of palaeoecological change at the Walvis Ridge during the PETM when compared to the conventional foraminiferal assemblage analysis and have clearly detected environmental disturbance from sample ordinations.

CHAPTER SIX

General Discussion

This thesis has presented a detailed benthic and planktonic foraminiferal analyses of ODP Sites 1265A (Southern Atlantic) and 1215A (North-eastern Pacific). The foraminifera census data from these sites and previously published foraminifera census data from ODP Sites 1209B, 1212B (Central Pacific) and Alamedilla (Spain) were used to investigate changes in the ecological functioning of foraminifera using faunal assemblage and Biological Trait Analysis (BTA) techniques.

6.1 The similarities in foraminiferal composition across the PETM intervals in all the studied sites

The composition of benthic foraminiferal assemblages across all the studied sites shows a close resemblance to the Velasco-type fauna (Bolli *et al.* 1994) of the late Palaeocene – early Eocene biostratigraphy. The faunal assemblage is characterised by high abundance of cosmopolitan taxa and very few marker species. All the study sites share a huge similarity in the overall foraminiferal composition, but each site is unique in its own taxa abundance, species richness and stratigraphic ranges/event. Site 1265A recorded the highest taxa abundance and diversity in the species of benthic foraminifera with over hundred taxa identified to the species level. Planktonic foraminifera were also analysed for this site, and the abundance was higher than the benthic composition with more than 79706 planktonic specimen and 59 species of *Acarinina, Morozovella, Subbotina, Chiloguembellina and Globanomalia* counted. Site 1215A and Alamedilla also recorded high benthic foraminiferal population, while sites 1209B and 1212B have the lowest. The species richness and faunal abundance are partly related to the analysers' interest and priorities, for instance, Takeda and Kaiho (2007) merged all the agglutinated species into one group without identifying them to the taxa or species level; *Stilostomellids* with many species were only identified at the genus level. Nevertheless, the advantage noticed with this method of taxonomy is the reduction in the number of species counted especially those with very few abundances which makes the biostratigraphic event more coherent and clearer. However, the disadvantage is that it could lead to the loss of essential species necessary to characterise the biostratigraphic event.

The palaeoecological interpretation of the foraminiferal assemblage from all the sites has been discussed in chapters 3, 4 and 5. In this chapter, sites will be compared, and an explanation of

how the assemblages reflected the overall changes across the PETM will be presented. Palaeoecological interpretation in the open ocean during this period is subjective because: 1) the ocean habitat is enormous; 2) benthic foraminifera reproduce through the sexual and asexual method and can rapidly recolonise their habitat during extreme ecological conditions (*Foster et al.* 2013). Nevertheless, some of the important taxa recognised across all the sites have been used to characterise the paleoecology of the studied sections in terms of pre-CIE, CIE and post CIE (recovery) relating to the release of exogenous carbon that caused the PETM.

6.1.1 Pre-CIE fauna

In all the sites, the interval before the CIE was characterised by the late Palaeocene – earliest Eocene foraminiferal assemblage and a restricted occurrence of taxa listed in table 6.1. The composition of benthic foraminifera in this interval is made of highly diverse and heterogeneous taxa comprising of heavily calcified, agglutinated, infauna and epifauna taxa. There was a low abundance of opportunistic taxa associated with the disturbance in the ecosystem at this interval while the high abundance of taxa associated with increased productivity and food availability was recorded.

At the Central Pacific Sites (1209B &1212B), there was an increase in *Siphogenerinoides brevispinosa, Bulimina thanentensis, Bolivina kugleri* and *Cibicidoide*s species with a corresponding decrease in the abundance of *O. umbonatus, Praebulimina* sp., *Globocassidulina globosa* and *T. selemensis.* During the same period in Site 1215A, increase in the species of *Cibicidoides, Valvalabamina, Anomalinoides, Globorotalites, Paralabamina clavata, Gyrodinoides globosa, Coryphostoma crenulata, Nonion havanese, Gaudryina pyramidata* and *Neoeponides hillebrandti* and a concomitant decrease *in Bulimina tuxpamensis, Aragonina* spp*., Osangulina,* Pleurostomellids*, T. selmensis* and *Q. profunda* were recorded

At the South Atlantic (Site 1265A), the foraminiferal composition during the pre-CIE was highly diverse and rich in both calcareous and agglutinated taxa. The abundance of very robust calcareous taxa such as *Cibicidoides, Gavelinella, Nonion havanese, Anomalinoides, Gyrodinoides, Neoeponides, Paralabamina*, as well as deep infauna taxa like *Marsonella oxycona, Aragonina valescoensis, Bolivina* sp*., Clavulinoides trileter*a*, Coryphostoma midwayensis,* and *Praebulimina* sp. increased at the same time when there was a decrease abundance of opportunistic taxa like *A. qudrata, B. tuxpamensis, N. truempyi,*

Paleopleurostomella pleurostomelloides, Stillostomellids, Q. profunda, T. selmensis, O. umbonatus, and *Quadratobuliminella pyramidalis*.

In Alamedilla, there was an increase in the abundance of Anomalinoides species, *Bolivina delicatus, Coryphostoma midwayensis*, *Nonion sp*., and Stilostomellids and a decrease in the species of *Aragonina, Abyssamina*, *B. tuxpamensis, B. valescoensis, G. subglobosa, O. umbonatus, Q. profunda and T. selmensis.* From the fauna composition above and in table 6.1, there was a preponderance of heavily calcified epifauna and infauna as well as the co-occurrence of taxa indicating oxic condition and reduced carbon saturation during the pre-CIE. The composition demonstrates that the biological carbon pump was effective before the PETM in most sites and there was enough nutrient for both the epifauna and the infauna morphotypes. It also indicates mesotrophic condition in the benthic ecosystem and a healthy ocean.

Previous studies have shown that species heterogeneity and diversity are controlled by the stability of an ecosystem (Schmiedl *et al*., 2003). Stable ecosystems reportedly favour the development of complex and highly diverse fauna such as recorded in the pre –CIE section of all the studied sites. The stability in the ecosystem is reflected in the high abundance of *Anomalinoides, Valvabamina and Nonion* taxa which are very robust and have a coarsely perforated test that requires high oxygen concentration and nutrient supply to thrive. More so, the relatively less abundant opportunistic taxa that decreased in abundance during this period supported this hypothesis. A similar scenario has been reported by Schmiedl *et al*. (2003) where the repopulation of these taxa occurred during the period of increased oxygenation in the eastern Mediterranean Sea. This assemblage also suggests high productivity and relatively stable benthic ecology ecosystem.

The planktonic foraminiferal composition at Site 1265A during the pre-CIE as discussed in Chapter five is characterised by taxa indicating mild temperature and high surface productivity. This suggests effective benthopelagic coupling at Site 1265A before the PETM. The highest abundance of *Subbotina* occurred in this section while *Chiloguembellina* recorded the lowest abundance. This taxa assemblage signifies a relatively mild temperature and a weakly developed oxygen minimum zone (Luciani *et al*., 2007). There were also high abundances of *Acarinina* and *Morozovella,* but the number was relatively lower than that of the *Subbotina*.

The high surface ocean productivity interpreted for this section is based on the amount of planktonic fauna recovered.

Table 6.1: Benthic foraminiferal assemblage that dominated the pre-CIE interval but became extinct after the CIE.

Alamedilla, Spain	**Sites 1209/1212BB**	**Site 1215A**	**Site 1265A**
Allomorphina sp	*Agglutinated forms*	*Abyssamina spp*	*Anomalinoides spp.*
Anomalinoides affinis	*Anomalinoides sp*	*Alabamina sp.1*	*Anomalinoides umbonatus*
Arenobulimina truncata	*B.inconspicua*	*Allomorphina minuta*	*Aragonina sp.*
Bolivinoides delicatulus,	*Bulimina kugleri*	*Bolivina sp*	*Aragonina valescoensis*
Bulimina valescoensis	*Fursenkoina sp.*	*B. monterelensis*	*Brazilina sp*
Buliminella grata	*Gavelinella spp.*	*Bulimina impendens*	*Cibicidoides succeedens*
Cibicidoides dayi	*Gyroidinoides spp.*	*Bulimina trihedra*	*Clavuloides triletera*
Cibicidoides eaceanus	*Lenticulina spp.*	*C. midwayensis*	*Coryphostoma midwayensis*
Cibicidoides hyphalus	*Paralabamina spp.*	*Dorothia retusa*	*Ellipsoidella attenuata*
Clavulinoides amorpha	*S. brevispinosa*	*E. chilostoma*	*Ellipsoidella kugleri*
C. midwayensis	*Stilostomellids*	*Ellipsoglandulina spp*	*Ellipsopolymorphina valescoensis*
Dorothia pupa		*E.cuneformis*	*Eouvigerina subscultura*
Gaudryina pyramidata		*Falsugutulina wolburgi*	*Falsoplanulina acuta*
Gaudryina sp. Juvenile		*G.beccarriformis*	*Falsugutulina wolburgi*
Gaudryina spp., indet		*Gyroidinoides globosus*	*G. micheliniana*
Globorotalites sp		*Hemirobulina arcuatula*	*Gaudryina pyramidata*
Globulina spp.		*Hormosina ovulum*	*Gavelinella beccarriformis*
Gyroidinoides beiseeli		*Lenticulina insulsus*	*Gavelinella sp*
Gyroidinoides globosus		*Marsonella trochoides*	*Glandulina sp.*
Hemirobulina spp.		*Marssonella oxycona*	*Glorobotalites conicus*
Nuttallinella florealis		*Neoflabellina rugosa*	*Gyroidinoides globosa*
Osangulina valescoensis		*Oolina globosa*	*Gyroidinoides sp*
Praebulimina sp		*Orthokarstonia clarki*	*Hermirobulina arcuata*
Pullenia coryelli		*Paralabamina elevata*	*Heronallenia spp*
Pullenia cretacea		*Pleurostomella paleocenica*	*Laevidentalina gracilis*
Quadratobul. pyramidalis		*Pleurostomella subnosa*	*Neoeponides infrequens*
Recurvoides spp.		*Ribdammina spp*	*Neoflabellina paleoocenica*
Spiroplectammina spectabilis		*Stilostomella plummerae*	*Neoflabellina sp*
G. beccarriformis		*Oolina globosa*	*Nodosaria limbeta*
		Tritaxia paleocenica	*Osangulina spp*
		Valvalabamina sp.2	*P.hillbrandti*
			Praebulimina sp.
			Reussolina apiculata
			Siphonodosaria hispidula
			Spiroplectammina spectabilis
			Stillomella spinae

6.1.2 CIE fauna

Many of the benthic foraminiferal species present at the pre-CIE section became extinct during the PETM (Table 6.1). The extinction rate at sites 1209B and 1212B, 1215A and 1265A is

approximately 27% respectively and 24% at Alamedilla. Site 1209B and 1212B recorded the lowest number of (eleven) taxa that disappeared after the CIE, followed by Alamedilla (29 taxa), Site 1215A (30 taxa) while the highest number of benthic foraminiferal extinction in this study occurred at Site 1265A with the disappearance of thirty-six (36 taxa). There is no common extinction pattern among the taxa across the sites except that the majority of the extinct taxa are infauna morphotypes and a reasonable number of epifauna (see Table 6.1). The overall composition of extinct taxa indicated the infauna morphotype to be the most affected, e.g. 20 out of the 29 taxa that disappeared from Alamedilla are infauna, 6/11 at 1209B and 1212B; 23/30 at 1215A and 22/36 at 1265A. The proportion of extinctions from each site reflects the general composition of the entire faunal assemblage and the extinct taxa represented a change from the late Cretaceous fauna to a more "Eocene" fauna.

The extinction of both infauna and epifauna in all the studied sites is a substantial evidence of environmental disturbance in the Open Ocean and continental seas during the PETM. Nevertheless, among all the taxa listed in table 6.1, only *Gavelinella* spp. and *Gavelinella beccariiformis* are known to have disappeared across all the studied sites. *Coryphostoma midwayensis* disappeared at Alamedilla, Sites 1215 and 1265A but occurred from the pre-CIE to recovery in the Site 1209B and 1212B. The differences in the taxa that went extinct after the PETM highlight the difficulty in characterising the event with specific taxa assemblage. The number of taxa affected at each site depends on the size fraction counted and the picking techniques. In as much as there are differences in the taxa that disappeared after the PETM, it is difficult to agree that the agglutinated taxa entirely went into extinction as indicated by data from Takeda and Kaiho (2007), as they occurred at other open ocean sites and Alamedilla from pre-CIE to recovery.

Other taxa that recorded the highest occurrence during the CIE were dominated by mostly opportunistic calcareous and deep infaunal taxa. At most of the sites, *Tappanina selemensis, Abyssamina quadrata, Nuttallides truempyi, Q. profunda, Anomalinoides species* and *Laevidentalina sp.* significantly increased in abundance during the CIE. *Bulimina kugleri* and *Bolivina gracilis* high occurrence during the PETM was restricted to central Pacific Sites (1209B and 1212B), while *Globocassidulina subglobosa, Lenticulina sp., Orisodalis umbonatus, Osangulina sp., Repmanina charoides, Stillostomella species* and *Trochaminids* occurred only at the Alamedilla section. At the Walvis Ridge (Site 1265A) in the South

Atlantic, *Coryphostoma crenulata, Aragonina aragonensis, Praebulimina reuss* and *Gyrodinoides subangulatus* were restricted to the CIE interval.

The high occurrence of these species during the PETM has been previously reported in other locations (Speijer, 1994; D'haenens *et al.,* 2012; Giusberti *et al*., 2016) and the ecological implication of these taxa has been explained in the previous chapters. In general, *Buliminds* are the most abundant taxa in all the studied sites, their occurrence usually peaks after the PETM in the deep sea site, but at Alamedilla their highest proportion occurred at the pre-CIE and began to drop during the CIE. The high occurrence of *Bulimina* taxa is an indication of increase productivity and low oxygen concentration. Their increase in this study (at the open ocean sites) began at the CIE interval and peak at the recovery. This suggests that ocean productivity did collapse during the CIE in the studied sites, corroborating the finding of Thomas (1998). More so, the co-occurrence of taxa indicating ecological stress and some taxa like *Pleurostomellids, Stillostomellids* that indicate high productivity could be evidence of vigorous water mixing and upwelling caused by intense hurricane (Handley *et al.,* 2012) that accompanied the extreme water condition during the PETM (see also the changes in hydrology during the PETM in Chapter 1).

The co-occurrence of oxic and mesotrophic taxa like *Globocassidulina subglobosa, Lenticulina* sp*., Orisodalis umbonatus, Osangulina* sp. and *Gyrodinoides subangulatus* during the CIE is an indication that the benthic ecosystem was relatively ventilated and have not been totally devoid of oxygen (Schmiedl *et al*., 2003). A robust and heavily calcified taxa *Oridosalis umbonatus* started to increase at the CIE interval and reached maximum abundance during the recovery at Site 1209B, 1266A and Alamedilla. At Site 1215A, it showed high abundance in the early part of the CIE, significantly increased during the CIE and decreased afterwards till the end of the recovery. *O. umbonatus* has been reported to increase in calcification and abundance after the PETM in the nearby Site 1263 (Foster *et al.,* 2013). The species has an opportunistic lifestyle and was reported to thrive in both oligotrophic and eutrophic environments (Giusberti *et al*., 2016) as well as in high carbonate-corrosive pore water conditions. The increase in the abundance of *O. umbonatus* during the CIE could be attributed to their resistance to corrosive pore water and the ability to reproduce rapidly during environmental perturbation (Giusberti *et al*., 2016).

The planktonic foraminiferal composition at the CIE section from Site 1265A is characterised by the highest occurrence of *Acarinina*, moderate abundance of *Morozovella* and a significant

reduction in the abundance of *Subbotina*. The high abundance of *Acarinina* and *Morozovella* are interpreted as evidence of a rise in temperature and reduction in the available nutrient. However, the overall population of planktonic foraminifera in this interval after a massive dissolution effect indicates that nutrient availability in the surface water must have been high to produce the volume of the biomass recovered. The increase in temperature enhances the metabolic activities in foraminifera (Schiebel and Hemleben, 2017) and this may have increased reproduction in planktonic foraminifera that reflected in the high export production recorded in the benthic zone during the PETM in this study. The decrease in the abundance of *Subbotina* is partly related to increase in temperature, increased utilisation of nutrient in the upper water column by *Acarinina* and *Morozovella* when their abundance increased as well as due to their susceptibility to dissolution in the highly corrosive sea water.

Also significant during the CIE was the extinction of *Acarinina nitida, Acarinina strabocella, Chiloguembellina morsi, G. chapmani, G. pseudomenardi, G. planoceanica, Morozovella pasionensis, M. valescoensis, M. occulossa, M. acuta, Parasubbotina pseudobulloides, Parasubbotina variata, Subbotina cancellata, Subbotina triagularis, S. triloculinoides, S. varianata, S. valescoensis, S. trivalis* and *Woodringina claytonensis.* The extinction of these taxa may be a local event as none of them has been reported in other PETM sections. More so, *Globoturborotalia brassriverensis* made its first appearance during the PETM (CIE interval) at Site 1265A, this foraminifera species was recently described and has been reported in the PETM section of Bass River as an excursion taxa (Pearson *et al*., 2006). Other excursion taxa previously reported in other locations during the PETM were not identified at Site 1265A.

6.1.3 Post CIE (Recovery) fauna

The section after the CIE was characterised by the first appearance of the benthic foraminiferal taxa listed in table 6.2 and a significant increase in most of the species that survived the ocean anoxic event (see chapters 3, 4 and 5). The origination of these taxa may not be related to the hyperthermal event because some taxa that made their first appearance in one location were also recorded as extinct in another site. Examples are *Cibicidoides dayi* and *C. eoceanus* whose occurrences at Alamedilla ended before the CIE, but both species made their first appearance after the CIE at the South Atlantic Site 1265A. Nevertheless, the reverse was the case for *Abyssammina sp.* and *Fursenkoina spp*.

It is difficult to compare both the pre- and post-extinction taxa in all the sites because of the sampling differences and resolution. This difficulty was also noticed by Thomas (1998) when

comparing post-extinction fauna at different ODP drilling sites and outcrop locations. She cited factors like the rapidity of the extinction, unconformity straddling the PETM intervals (as recorded in Alamedilla), differences in taxonomic concepts used by different authors and differences in the size fraction studied as the major cause of the cause of this difficulty (Thomas, 1998).

These factors also play a huge role in all the sites we studied; there is no uniformity on the sampling resolution, the foraminiferal census was done by different authors with different taxonomic biases, there are cases of unconformity, drilling disturbance and incomplete recovery core sections across the PETM. This led to the cause of the differences and difficulty in comparing the faunal composition across all the sites.

Despite these differences and difficulties in comparing the PETM fauna at various sites in this study, there are significant similarities in the faunal composition, though each location is composed of unique assemblages of foraminifera. The dominance of opportunistic taxa and re-coloniser such as *T. selmensis, Aragonina* species*, Abyssamina quadrata, N. truempyi* and *Q. profunda* in all the studied sites indicate ecological disturbance.

Table 6.2: Benthic foraminiferal assemblages that originated after the CIE in all the studied sites

Alamedilla	**Sites 1209/1212BB**	**Site1215A**	**Site1265A**
A. aragonensis	*Eponides elevata*	*Cibicidoides subspiratus*	*Aragonina ouozzanensis*
A. praeacuta		*Coryphostoma incrassata*	*Astacolus nutalli*
Abyssammina Sp		*Ellipsoglandulina* Spp.	*Bathysiphon eoceanica*
Brizalina Spp.		*Gyroidinoides globosus*	*Bathysiphon* Sp.
Dorothia Sp.		*Legenoglandulina ovata*	*Buliminella grata*
Ellipsopolymorphina Sp.		*Nodosaria monile*	*C. eoceanus*
Eouvigerina Sp.		*Pleurostomella nita*	*Chrysalogonium elongata*
Fursenkoina Spp.		*Pleurostomella rimosa*	*Cibicidoides dayi*
G. subglobosa		*Pseudomarsonella* Spp.	*Hermirobulimina arcuta*
Glandulina Spp.		*Rotaliida pleurostomellidae*	*Legena* Sp.
Nuttallinella Sp.		*Spiroplectinulla esiraensis*	*Linaresia semicribrata*
Quadrimorphina allomorphinoides		*Cibicidoides subspiratus*	*Spiroplectammina subglabra*
Spiroplectammina Sp.			

The rate at which these taxa increased during the CIE in all the studied sites indicate that they have less competition for nutrient and space by the disappearance of some extinct taxa.

Just as with the benthic foraminiferal composition, the planktonic foraminifera recorded an increase in the abundance of all the species that survived the hyperthermal event. There was a proliferation of *Subbotina* which suggests less stratified surface water, an increase in nutrient availability and high surface ocean productivity.

6.2 Mapping foraminiferal traits to their ecological functioning

Previous studies have shown that a literal reading of faunal composition could lead to a significant error in the understanding of palaeoecological changes especially during biotic crisis (Twitchett, 2006). The BTA has enabled us to quantitatively analyse both the faunal and trait compositions to pick out major drivers of ecological changes across the studied sites. The first impression from the BTA results is its strength in making biotic event coherent and more explicit (Figures 3. 17; 4.12; 5.8 and 5.14). One of the key objectives of this study is to understand the trait changes in foraminifera in relation to the ecological functioning during extreme climatic events. Previous studies have shown that the survival of organisms and ecological functions are entirely based on their trait composition. Though few studies have been done on the relationship between foraminiferal traits and ecology, this study has identified some preferential selectivity of traits over another during extreme climate and linked some traits to the functional ecology of foraminifera. In this study, traits whose proportion was not affected or those that increased in abundance during the CIE are considered resilient while those that significantly decreased in abundance or disappeared during the PETM are regarded as susceptible. The BTA has identified chamber arrangement/ shape, test composition, ornamentation, primary aperture position, perforations and living/feeding habit as traits crucial to the ecosystem functioning and survival of foraminifera in the marine environment. The occurrence of these traits in all the studied sites has been discussed in chapters 3, 4 and 5 and the general overview is given below.

6.2.1 Test shape

The BTA identified traits such as spiral and elongate shape as very important in the foraminifera test shape modalities (Figures 3.5; 3.10; 3.15; 4.11; 5.7 and 5.13). They are the most prevalent test shape across the sections in all the studied sites. Even though there are few occurrences of the tubular, globose and other test, they did not seem to have any significant impact on the test shape modality. The shape of foraminifera test is important for their feeding mode, reproduction and movement. The elongate shape is well adapted to living inside the sediment (Nagy *et al*., 1995; Corliss and Chen, 1998) while the spiral is more cosmopolitan

and capable of living in both sediment surface and inside the sediments as well as attaching on the hard or soft substrate. The spiral test is usually perforated which enhances the utilisation of oxygen as well as secretion of adhesive substances for attaching on a hard substrate. This trait enables foraminifera to thrive in a high oxygen environment and to escape from the predators. The consistent occurrence of a spiral and elongate traits in all the SIMPER results indicates that they are resilient and crucial in ecological function while globose, tubular, subquadrate and others are of less value.

6.2.2 Test composition

Hyaline calcite, hyaline aragonite, porcelaneous and agglutinated tests are the major test composition identified by BTA as being crucial to the ecological functioning of foraminifera in all the studied sites. However, only hyaline calcite and the agglutinated test can be distinguished using a light microscope. Porcellaneous and aragonite tests were classified based on the test lustre or the description by previous authors. Hyaline calcite showed the highest occurrence among all the tests across the studied sites. The high abundance of calcareous taxa in all the studied interval indicates that they lived above the lysocline. Some calcareous taxa such as *Gyroidinoides, Oridosalis* and *Lenticulina* have been found to increase during the CIE despite the extreme dissolution. These taxa would have been expected to dissolve or reduce in population during the CIE, but their increase shows that we are yet to fully understand how ocean acidification affects the dissolution of foraminifera test. Also, some laboratory experiment by Nguyen *et al*. (2009) observed that bigger and smooth foraminifera specimens are more resistant to carbonate dissolution during the OAE than their smaller and rough counterparts. Even though our result may partly conform to this observation, this experiment was conducted in a controlled environment, and the concentration of corrosive pore water fluid varies between the sediment surface (epifauna environment) and deep sediment (infauna environment). In addition, there are other marine ecological parameters that cannot be simulated in the laboratory, hence the results from Nguyen *et al*. (2009) should be interpreted with caution.

6.2.3. Chamber arrangement

The chamber arrangement was highlighted to be crucial to the functioning of foraminifera in the benthic ecosystem. Both the raw data and the multivariate statistical analyses indicated uniserial, bi/triesrial, trochospiral and planispiral as the critical traits in the running of the ecosystem while bi/triesrial, trochospiral and planispiral were the most resilient during the

acidification of the ocean. Bi/triserial arrangement showed the highest proportion in sites 1209B 1212B and 1265A while trochospiral proportion was highest at 1215A and Alamedilla during the CIE. It is difficult to link the impact of the OAE to the foraminifera chamber arrangement, however, Boltovskoy *et al*., (1991) associated change in coiling direction and reduction of surface ornamentation in foraminifera with a change in temperature or pH in the environment. Planispiral and porcelaneous tests tend to increase in proportion during the CIE, and this may be related to the ability of foraminifera to secret $CaCO_3$ during ocean acidification.

No significant variation in chamber shape could be satisfactorily confirmed as it followed a similar trend in all the studied sites from the pre-CIE to the recovery and we believe that the trait is not sensitive to the ecological change.

6.2.4 Ornamentation

Ornamentation in the identified foraminifera is dominated by depressed sutures and no ornamentation. Raised sutures are fewer in proportion than the former but increased during the CIE in almost all the sites except at 1212B and 1215A. Depressed sutures are very common in most foraminifera, and we regard this trait as being redundant. However, the high proportion of taxa without ornamentation during the CIE may be a feedback from the ocean acidification. Previous studies (Boltovskoy *et al*., 1991; Dubicka *et al*., 2015) reported a reduction in the ornamentation and apertural complexity with an increase in acidification of the ocean. The increase in the number of taxa with no ornament is interpreted as a functional response to reduce the structural complexity of foraminifera and conserve energy during the period of ecological stress. The reduction in structural complexity will make taxa more efficient and increase survival rates in the face of the extreme ecological conditions. Taxa such as *Lenticulina* have smooth surfaces, and they recorded an increase in abundance during the PETM due to their high resistance to dissolution. The increase in raised sutures trait seems to counter the reduction in structural complexity during the CIE as taxa with raised sutures such as *T.selemensis* occurred together with other taxa. However, there are other traits which could be responsible for the increase.

6.2.5 Apertures

There was a consistent increase in oval/reniform and slit-like apertures during the CIE in all the studied sites. Oval/reniform apertures are common with elongate taxa such as *Buliminids, Nodosaria* and *Stilostomella.* The increase in the proportion of this trait during the CIE may be

linked to increase in taxa listed above, hence the trait is regarded as a crucial functional trait. The decrease in arcuate trait during the CIE indicates that it is susceptible to ocean acidification.

Environmental change does not seem to have any significant impact on the apertural accessories of foraminifera as no identifiable pattern could be recognised from the studied sites except for a decrease in the aperture with neck during the CIE. Nevertheless, the most resilient trait in primary aperture position is the umbilical positions. Umbilical apertures increased in proportion during the CIE in most of the studied sites. We cannot convincingly explain how this is related to environmental change, but it is likely related to the ease at which gaseous exchange and dissolved nutrients can be assimilated through this form of apertures. Terminal apertures appeared to be prone to dissolution during the OAE, as it recorded the lowest abundance in all the studied core sites during the CIE interval except for Site 1215A. This could be that most of the taxa with terminal apertures are small in size or have a thin test which could easily dissolve during the ocean acidification.

6.2.6 Perforation

There is a significant decrease in the abundance of macro- perforation trait during the CIE in all the sites, making it the most susceptible test perforation in foraminifera. As discussed in previous chapters, macro perforation enhances dissolution by creating pathways for fluid penetration and reaction with the test. As taxa with micro-perforation require higher oxygen concentration to survive in an ecosystem, the decrease in the proportion of this trait during the CIE may be linked to the decrease in the oxygen concentration in the benthic environment during the PETM and the highly corrosive water associated with the ocean acidification. This same reason has been cited as the major cause of benthic foraminiferal extinction recorded during the PETM (Tekeda and Kaiho, 2007). No perforation, micro and fine perforation relatively increased in proportion during the CIE in all the studied sites indicating that these traits are very resilient.

6.2.7 Life habit

In terms of life habit, epifauna taxa decrease during the CIE while shallow infauna significantly increased in all the studied sites. Our data show that epifauna taxa were most affected by dissolution and suggest that most foraminifera vacated the epifauna habitat which was high in the corrosive water for the shallow infauna environment which was diluted with sediment and organic matter but still contained some oxygen, potentially just enough to survive. Also,

epifaunal taxa are composed of traits that make them susceptible to the impact of ocean acidification. Our result also showed that some species of foraminifera may have lived a dual lifestyle (fuzzy coding data), spending part of their life on the sediment surface to acquire oxygen and feed but move back through the soft sediment to the spend the rest of their life in the deep infauna habitat. In the deep infauna, they may be inactive for a long period of time in order to save energy. Past studies of traits that enhance the survivability of benthic fossils during extreme ecological events indicated infauna life habit as a crucial survival trait (Twitchett, 2006). The feeding habit and mobility traits closely mirrored each other in all the sites, there were high proportion of deposit feeders indicating that most of the foraminifera may have lived infaunally. Suspension feeding and grazing traits are less in proportion, with grazing increasing slightly in abundance during the CIE. Most of the foraminifera are indicated to be sessile, only a few clinging and swimming species were recorded.

6.2.8 Foraminiferal trait sensitivity/selectivity during the PETM across the studied sites

In general, our analyses show that functioning in foraminifera is driven by traits such as spiral test shape, elongate test shape, agglutinated test, hyaline calcite test, hyaline aragonite test, porcellanous test, bi/tri-serial chamber arrangement, uniserial chamber arrangement, planispiral chamber arrangement, trochospiral chamber arrangement, spherical/oval chamber shape, triangular chamber shape, semi-circular chamber shape, depressed sutures, raised sutures, no ornament, costae ornament, muricae ornament, oval/reniform aperture shape, arcuate aperture shape, slit-like aperture shape, terminal aperture, basal interiomarginal aperture, umbilical aperture, aperture with lips, aperture with bifid teeth, aperture with neck; micro-perforation, fine perforation, macro-perforation, no perforation, deep- infaunal, shallow-infaunal, deposit feeding, and grazing. In a real sense, the composition of these traits varies from site to site, but the list represents the overall observation. There are some evidence of functional redundancy in foraminifera as indicated by trait and faunal distribution and this could be the reason for their continual provision of ecological functioning even in a period of extreme perturbation.

In the planktonic category, traits such as hyaline calcite, triangular/trapezoid, muriae, lips, umbilical – extra umbilical apertures, perforations surface dwelling and grazing (Figure 5.7) were highlighted as resilient and traits that sustained function during the hyperthermal. These traits are associated with taxa that are tolerant to warm temperatures. Traits such as elongate, bi/triserial, terminal, deep dwellers and suspension feeding that increased during the recovery

suggest that more and quality food material got to the deeper water after the CIE and that the ocean has relatively cooled down but not as much as in the pre-CIE which were dominated by traits such as trochospiral, semicircular and smooth which is linked to a more cooler environment. Hyaline calcite is the only modality in test composition (Figure 5.8). There is no doubt that trait played a significant role in the ocean carbon cycle during the PETM, hence should be regarded as a crucial functional trait of the organism.

This study has contributed to the understanding of the impact of extreme conditions on the ecological functioning of the foraminiferal community using the BTA. Initial research by Caswell and Frid (2013); Frid and Caswell (2015, 2016) has documented the impact of the ocean anoxia on the macrobenthos through the change in their biological attributes and reported that changes in the biodiversity of the fauna are closely related to the ecological function they perform. In this study, we demonstrated a direct relationship between the fauna assemblage as well as trait composition and the degree of ecological disturbance associated with the PETM by linking traits to taxa and how both changed across the PETM event. The results from this study show that the more stable the ecosystem is, the more similarity in the faunal and functional composition is observed, but if the ecosystem is unstable, the faunal assemblage and the function they provide will reflect the dynamics of the changes taking place in the ecosystem and become much disorganised.

The non-Metric Dimensional Scaling (nmMDS) ordination of faunal assemblages at Site 1209B (Figure 3.3) indicates a stable pre-CIE and recovery communities because the samples in both communities grouped tightly together, however, the faunal community within the CIE (PETM) interval are more widely separated. The disconnected nature of the CIE community (samples), especially at the earlier part of the PETM, is interpreted as an evidence of ecological disturbance during the hyperthermal. Stability returned to the benthic ecosystem in the later part of the event as the upper part of the CIE sample ordinated with the recovery community. The similarity of the upper part of the sequence recovery may be related to the resolution and length of the interval analysed. The provision of the ecological function was shown to be stable before and after the PETM based on the ordination of trait composition (Figure 3.3), the traits at pre-CIE and recovery grouped nicely together indicating harmony and collaboration in the provision of ecological function while the traits of the CIE section are widely distributed which is a sign of constant change in the trait and functioning of the ecosystem and an indication of instability (see Figures 3.3 and 3.4).

Site 1212B faunal and trait composition ordinations (Figures 3.8 and 3.9) are very similar to the Site 1209B records. The pre-CIE and recovery clustered together in their respective groups suggesting stability in seafloor as well as services provided by benthic foraminifera during these periods. However, the CIE samples are widely scattered and in a sub-group of three which is interpreted as a sign of ecological extremis coeval to the stages in the release of greenhouse gases during the PETM. It also suggests that the provision of ecological services by foraminifera was disorganised by the hyperthermal but not completely terminated.

The ecological disturbance in Site 1215A is more difficult to understand as no definite pattern could be recognised from the nmMDS ordination of both faunal assemblages and trait composition (Figures 4.7 and 4.10). This could be as a result of the core location and high export productivity associated with the Northeastern Pacific Ocean (Ma *et al.,* 2014). The evidence from sedimentological and geochemical analyses indicate that high productivity and ocean anoxia in the area around Site 1215A (Ma *et al.,* 2014) existed prior to the PETM and persisted even after the hyperthermal. The clustering together of CIE samples within the entire sample is an indication of a change in ecology during the PETM (Figure 4.7), but the pattern of ordination is not clear enough to estimate the degree of ecological disturbance during the period. The clustering of all the communities (pre-CIE, CIE and recovery) together suggest that only the foraminiferal specimens resistant to ocean acidification were preserved, and all the evidence of the ecological change in the faunal composition, as well as ecological functioning, may have been lost due to high rate of test dissolution recorded at Site 1215A (see Chapter 4).

The nmMDS ordination of the benthic foraminifera assemblage at Site 1265A recorded the impact of the ecological disturbance on the composition of foraminifera before, during and after the PETM. The pre-CIE community shows wide separation in figure 5.9 indicating that the earlier release of methane hydrate that caused the PETM started perturbation in the benthic foraminiferal community even before the (CIE) peak of the warming. The CIE community (Figure 5.9) was scattered around the entire plot indicating extreme benthic ecological perturbation. Only the recovery community was grouped together suggesting that the benthic ecology at that time was stable. The disorganisation of the pre-CIE community supports the hypothesis of Zachos *et al.* (2005) that the methane hydrate that caused the PETM may have originated from the Atlantic Ocean. This may be the reason for the benthic ecological disturbance before the CIE in the Atlantic Basin. The trait ordination separated the samples

into three groups, with the most disturbed samples in group A, less perturbed samples in group B and an event which we could not interpret in group C.

The faunal community in Alamedilla also showed some evidence of ecological disturbance during the CIE but the samples before the PETM (pre-CIE) tightly grouped together to indicate stability in the benthic ecosystem. The early part of the CIE was the most affected as the samples are separated apart, and we interpret this as evidence of severe benthic ecological perturbation. The foraminiferal analysis recorded the lowest abundance of species at this interval (Alegret *et al.,* 2009) and the benthic foraminiferal extinction was the severest at Alamedilla when compared to the other sites studied. The nmMDS ordination indicates benthic ecological stability in the later part of PETM with nicely clustered samples. There were only a few (three) samples analysed in the recovery interval and it is not enough to speculate on the stability of the ecosystem during the recovery phase based on the number of samples studied. Just as for the faunal assemblage ordination, the trait composition indicates ecological stability in the section before the PETM and instability during the early part of the CIE. The recovery sample ordinated differently from the rest of the group by aligning on a straight transect and we cannot speculate the stability of ecology based on the ordination.

6.3 The past as the key to the future.

If the law of uniformitarianism, which states that the present is the key to the past, is an established geologic principle, it can also be right to say that the past is the key to the future. A lot of effort is being invested in understanding how the current change in climate will affect the marine environment and biodiversity in the future because it has been forecasted that 2000 to 4000 Gt of carbon will be released into the Earth system in the next few centuries. The impact of this large volume of CO_2 in the ocean has been forecast to be more severe than any ecological crisis experienced on Earth in the past 65 million years. Some authors have suggested that the sixth mass extinction has already started (Barnosky *et al*., 2011). One of the objectives of this study is to understand the feedback of calcareous marine micro-zooplankton to extreme climate in the future. Forecasting what will happen in the future is a herculean task because not only that all the parameters controlling the Earth system are not fully understood but also the Earth history is not entirely documented in the stratigraphic records due to hiatuses and poor preservation resulting from continual earth processes. Despite the incompleteness of the sedimentary record, the fossil data still have the potential to show us how ecosystems change over a longer timeframe. Predicting how the marine environment will look in the future

is particularly difficult because it involves an infinite number of complex systems and highly interconnected variables comprising of physical, chemical and biological processes. Though the exact prediction of the outlook of the future ocean may not be attainable, a clue from the past and contemporary events could help in making educated guesses.

For the fact that the CO_2 emission is increasing at an exponential rate (IPCC,2013) since the industrial revolution and that the future ocean will be warmer than they now are, means that acidification of the ocean will increase. The increase in ocean acidification will result in a wider spread of oxygen minimum zones and hypoxia (Aze *et al.,* 2014a; Secretariat of the Convention on Biological Diversity) across the globe. The global anoxia that will result from the environmental change will be more severe and unprecedented because of the domestic and industrial wastes including the plastics already residing in the present day ocean (Frid and Caswell, 2017). In addition, a rise in temperature will lead to an increase in rainfall and land runoff, eroding and transporting minerals from the continents to the ocean as reported during the PETM.

Another impact of the future environmental change in the ocean that also occurred during the PETM (Nunes and Norris 2006) will be a change in deep water circulation. The thermohaline circulation will become sluggish leading to less oxygen and nutrients reaching the benthic realm in the abyssal zone and a significant reduction in upwelling. In the present day ocean, the temperature differences between the tropics and poles ensure that high oxygen, cold and nutrient-rich deep water sinks at high latitudes and upwells at the equator and promoting high surface productivity, but this may be slowed entirely or reversed due to increase in temperature hence, resulting to productivity collapse in the future ocean (Birch *et al.,* 2016).

The primary feedback of these changes in the ocean on the marine fauna will be migration; surface dwellers will move deeper into the water column and distorting the marine trophic arrangement. The result from this study showed a significant decrease in epifauna taxa and increase in infauna taxa during the CIE. Also, a recent study on the changes in $\delta^{13}C$ and $\delta^{18}O$ of planktonic foraminifera showed that some surface dwelling species of *Acarinina* descended to the thermocline at the onset of the CIE (Si and Aubry, 2018) thereby invading other species habitat and resulting to competition with their indigenous species. Migration of *Apectodiunium augustum* from the tropics to the poles has also been reported during the PETM (Sluijs *et al.,* 2007) and with an increase in current global temperature; migration of species in search of a more comfortable ecosystem is inevitable. Already marine zooplankton are migrating towards

the poles at 23 km y^{-1} (Frid and Caswell, 2017). Also predicted is the reduction in species abundance at the equator to the tune of 50% in half a century from now. Lower temperature taxa will have no place to move to and may eventually disappear due to extreme environmental conditions. Nevertheless, a harsh environmental condition will result to increase in opportunistic and disaster taxa as well as an evolution of new species with complex morphology just as the excursion taxa recorded during the PETM. Our observation from this study and other studies across the PETM show a significant increase of opportunistic taxa during the event.

The decrease in ocean pH due to acidification will result to a significant reduction in calcification of foraminifera, and other calcareous marine organisms, taxa with high perforation such as *Haynesina germanica* will drastically reduce in abundance or evolve to a less perforated species. In general, the impact of the current environmental change will result to habitat loss, ecological stress and eventual mass extinction of taxa that cannot adapt to the environmental changes.

CHAPTER 7

General Conclusions

Foraminiferal census data from four ODP sites in the Pacific Ocean (1209B, 1212B, and 1215A), South Atlantic (1265A) and an outcrop of pelagic sediment at Alamedilla (Spain) have been studied to understand the changes in foraminiferal ecology during the Palaeocene-Eocene Thermal Maximum. The foraminiferal census data from ODP Sites 1215A and 1265A were processed, counted and analysed during this study while data from ODP Sites 1209B, 1212B and Alamedilla has been previously published by Takeda and Kaiho (2007) and Alegret *et al.* (2009) respectively. All the foraminifera taxa identified from this site were subjected to qualitative and quantitative analyses and used to study the fauna and trait changes in foraminifera during the PETM.

The main aim of this thesis as stated in chapter one was to explore the usefulness of biological trait analyses (BTA) in investigating the impact of extreme climate on the ecology of fossil foraminifera in the marine environment. The results from this study have shown that ecological changes could be characterised with the trait composition of foraminifera (Chapters three, four and five). BTA technique produced a more quantitative and integrated picture of palaeoecological change in all the studied sites when compared to results from the conventional faunal assemblage analysis. The results from this study also showed that changes in foraminiferal traits did not occur at the same time as the faunal turn-over in foraminiferal taxa, implying that traits of foraminifera are conserved. Although the faunal assemblage differed in composition at each of the studied sites, their trait composition was relatively similar, suggesting that BTA reduces the effect of synonymy from the taxonomic assemblage. The approach has proved to be useful in understanding the ecological functioning of foraminifera during an extreme ecological disturbance in the marine ecosystem, however, for this tool to be effectively deployed in foraminiferal studies, there is a need to update the trait composition of described foraminiferal taxa in the existing palaeobiological database.

The primary ecological functions provided by foraminifera are carbon sequestration and food source for a higher trophic organism such as marine snail, jellyfish, sea anemones and coral. To quantify the exact link between the traits and functioning is not a straightforward task but the calcification of foraminifera from the seawater carbonates serves as a carbon sink, and when they are fed on by the larger organism, they contribute to the sustenance of the marine food chain and the health of the oceans. The high occurrence of hyaline calcite test in all the

trait compositions indicates that carbon sequestration during the PETM was only reduced but did not collapse entirely. However, the feedback mechanism from the increased temperature leads to increased faunal abundance as well as functional diversity immediately after the hyperthermal. The increase in the abundance of foraminifera will also lead to increase in the organism feeding on them, the calcareous predator such as snails and other non-calcifiers will increase the drawdown of both organic and inorganic carbon from the ocean. This may have contributed to the recovery of the marine ecosystem after the PETM.

This study also indicated that changes in the trait composition of foraminifera are related to ecological parameters such as carbon fluxes, productivity, ocean acidification, nutrient/food supply oxygen concentration, and competition. The link between each trait and the ecological parameter is summarised in table 7.1 below.

Table 7.1: Foraminiferal traits and related ecological parameter

Traits	**Related ecological parameters**
Test composition	Carbon sequestration, ocean acidification,
Test shape and chamber arrangement	Productivity, ecological disturbance, oxygen concentration
Ornamentation	Ecological disturbance, ocean acidification
Apertures	Ocean acidification, productivity, nutrient/food utilisation
Perforation	Oxygen concentration, ocean acidification
Life habit	Ocean acidification, productivity, oxygen concentration, competition, nutrient/food utilisation

In general, findings from this study has improved the overall knowledge of the wide range of investigations that BTA can be used for and the technique has proved to be very useful in grouping taxa that share similar traits to understand how they are impacted during extreme climatic events. In this study, the results from the biological trait analysis did better than the conventional faunal assemblage interpretations techniques in the understanding the impact of ocean acidification on the palaeoecology of foraminifera. Because, the trait analysis provided a quantifiable synthesis for a better understanding of biostratigraphic events in all the studied sites. This was due to the synonomy and differences in taxonomic composition recorded across the studied sites. The results from this study have also shown that information on the morphological and physical characteristics of foraminifera can be used to characterised climatic events and changes in sedimentary facies across different basins.

Another interesting result from this study is that instability in faunal composition leads to the instability of functional ecology (nmMDS results). When ecological conditions change, the ecological function was often maintained for a substantial period by trait manoeuvring. This was different from what was observed at Alamedilla where there was a sudden extinction of most of the taxa leading to a total collapse of functioning (Chapter three). We cannot say how possible this scenario could be because there was a bloom of fauna immediately after the extinction; hence we think that the section recorded as dead zone may have been an unconformity layer and most of the taxa that existed at that time coeval to the BEE must have been eroded. This highlights the challenge of reconstructing ecological function in deep time, as the reconstructions similar to this study may have been constrained by the degree of preservation of fauna that existed in the community (Chapter 3). Because most foraminifera are reported to be calcareous, an enormous number of taxa must have been lost to dissolution considering the location of the cores and period studied. The lost taxa may have hugely affected the faunal composition and the understanding of foraminiferal ecology. Nevertheless, results from the BTA indicated that redundancy in trait composition compensated for the lost taxa. In most cases, foraminifera communities respond by increasing the abundance of opportunistic or crisis taxa to make up for the lost species.

This study also investigated the tenacity of foraminiferal traits in the face of the extreme ecological condition. Our data show that traits such as spiral and elongate test, bi/triserial and trochospiral chamber arrangement, triangular/trapezoid and spherical/ oval chamber shape, umbilical aperture, slit-like aperture, terminal aperture, basal interiomarginal aperture position, no aperture accessory, no perforation, fine perforation, no ornament, shallow infauna, deposit feeding and sessile lifestyle increased during the CIE in most of our study sites hence are regarded as resilient. Spiral and elongate test, bi/triserial, deposit feeding, terminal apertures are believed to be resilient to high organic matter influx (Chapter three, this study), and taxa with fine/ no perforations are resilient to low oxygen concentration while shallow infauna, deposit feeding slit-like aperture, umbilical aperture, basal interiomarginal aperture position are resilient to most ecological stress. The traits described as resilient in this study are related to the crisis taxa that predominate during the CIE. For instance, if the prevailing crisis taxa in a location is *N. truempyi* and *Q. profunda*, traits such as spiral, trochospiral and umbilical apertures will be highlighted as the resilient traits (Figure 3.5) but if taxa such *Buliminids* dominate during the period of ecological stress, trait such as elongate, bi/triserial, deposit feeding, terminal apertures, triangular/trapezoid would be highlighted as the most resistant trait

(Figure 4.11). This means that foraminiferal traits should not be interpreted independently of the taxonomic composition.

The results from nmMDS ordination in this study have also shown that the degree of ecological disturbance in the ecosystem can be interpreted based on the similarity in the faunal and functional (trait) composition of foraminiferal communities. The results indicated a disturbance in the benthic and pelagic ecology in all the studied sites during the CIE. Only Site 1265A recorded the onset of instability in the benthic ecosystem at the pre-CIE interval, probably because of the site proximity to the source of the exogenous carbon pool that caused the PETM. Other evidence of ecological disturbance is the arrival of new (invasive) species or the disappearance of the pre-existing taxa during the CIE which was recorded in all the studied sites.

The results from the faunal composition showed that foraminiferal assemblages identified from all the studied sites were poorly preserved due to the ocean acidification associated with the PETM. Benthic foraminiferal extinction was recorded in all the studied sites, but the extinction pattern differed in all of them, only the extinction of *G. beccariiformis* was common in all the sections studied. The benthic foraminiferal extinction did not wipe out all the Valesco –type fauna from our studied sites and no established excursion taxa were present in the planktonic foraminiferal composition of Site 1265A. The primary cause of the biotic turnover and extinctions during the PETM is probably the increase in temperature resulting from climate change and natural cycles.

The bigger picture from this study suggests that the current environmental change will result in the migration of foraminiferal species from their original habitat and create an extreme ecological crisis and eventual mass extinction. The mass extinction that will result from this current climate change may be more severe than that of the PETM because of the rate of change as well as the domestic and industrial wastes including the plastics residing in the present-day ocean. The thermohaline circulation may be revised or become sluggish, and this will lead to less oxygen and nutrient reaching the benthic ecosystem, a significant reduction in upwelling and possible productivity collapse in the ocean.

Future work

This thesis has assisted in developing the application Biological Trait Analysis (BTA) to understand the ecological functioning of foraminifera in the marine environment and investigating the impact of extreme climate on the foraminiferal assemblages as well as its functions. The findings from the study are significant as they will enable us to understand the impact of current climate change on the functioning of these organisms in the future. However, the study has also raised some exciting avenues for consideration and for future research such as why there is still an abundance of foraminifera during the OAE with some low oxygen taxa co-occurring with oxic indicators and coccolith incorporation in foraminifera. There is a need to investigate this further and to track size changes in foraminiferal species across the PETM as well as harmonise the traits classification.

In the future, we hope to follow up this work by investigating the nitrate respiration in foraminifera to understand which foraminifera respire nitrate in the absence of oxygen as reported by Ren *et al.* (2015) and Keating-Bitonti and Payne (2017). Results from previous studies recognised that some species of foraminifera could denitrify and can incorporate ^{15}N in their test during calcification (Straub *et al.,* 2013; Ren *et al.,* 2012 and 2015). To understand how foraminifera survived during the period of extremely low oxygen concentration, there is a need to study in detail the composition of ^{15}N on the test of foraminifera before, during and after the CIE. Even though the ecology may have changed over the years, significant similarities still exist between the palaeorecords and the present. To constrain the variability of ^{15}N isotope during the PETM, the values from the foraminiferal isotopes will be compared to those of the bulk sediment, living foraminifera and water samples from the present oxygen minimum zone as a control for the palaeo-records.

Nitrogen isotopes incorporated in foraminifera test can be used as good proxy for changes in nutrient condition and cycling of fixed nitrogen in recent and deep time ocean sediment (Galbrait, *et al.,* 2008; Granger, *et al.,* 2008; Sigman *et al.,* 2009; Meckler, *et al.,* 2011). Studying the nitrogen isotope composition during the PETM will provide a better understanding of the nutrient conditions in the ocean at that time and provide some insight into nitrate respiration by foraminifera.

There are conflicting classifications of some foraminiferal traits especially living and feeding habits in the existing publications and future work should consider harmonising/updating the

traits classification existing in online databases and other publications to reduce the problem of synonymy in foraminifera taxonomy.

The data on the diagenesis of foraminifera in Chapter 4 has raised the need to investigate more on the coccolith incorporation in the foraminiferal test to understand if it is a diagenetic artefact or process of calcification by foraminifera. Even though some studies in the past (Henrikson et al., 1998) reported that some agglutinated foraminifera taxa use coccoliths to build their shells, some species previously described as entirely hyaline calcite (Holbourn *et al.,* 2013) are found in this study to be composed of huge amount of coccoliths in their test and this needs more investigation to ensure that foraminifera test composition is appropriately classified in future biological trait analysis.

References

Abbott, A.N., Haley, B.A., McManus, J. (2016). The impact of sedimentary coatings on the diagenetic Nd flux. Earth and Planetary Science Letters, 449: 217-227

Adl, S. M., Simpson, A. G. B., Farmer, M. A., Anderson, R. A., Anderson, O. R., Barta, J. A., Bowser, S. M., Brugerolle, G. Fensome, R. A., Fredericq, S., James, T. Y., Karpov, S., Kugrens, P., Krug, J., Lane, C. E., Lewis, L. A., Lodge, J., Lynn, D. H., Mann, D. G., McCourt, R. M., Mendoza, L., Moestrup, O., Mozley-Standridge, S. E., Nerad, T. A., Shearer, C. A., Smirnov, A. E., Speigel, F. W. and Taylor, M. F. J. R. (2005). The new higher level classification of Eukaryotes with emphasis on the taxonomy of Protists. Journal of Eukaryotic Microbiology 52(5): 399–451

Alegret, L. and Thomas, E. (2004). Benthic foraminifera and environmental turnover across the Cretaceous/Paleogene boundary at Blake Nose (ODP Hole 1049C, Northwestern Atlantic). *Palaeogeography, Palaeoclimatology, Palaeoecology*, 208(1-2), 59-83. https://doi.org/10.1016/j.palaeo.2004.02.028

Alegret, L. and Thomas, E. (2009). Food supply to the seafloor in the Pacific Ocean after the Cretaceous/Paleogene boundary event. Marine Micropaleontology, 73(1-2), 105-116

Alegret, L., Ortiz, S., Orue-Etxebarria, X., Bernaola, G., Baceta, J.I., *et al*. (2009a). The Paleocene-Eocene thermal maximum: new data on microfossil turnover at the Zumaia section, Spain. Palaios 25:318–28

Alegret. L., Ortiz, S and Molina, E. (2009b). Extinction and recovery of benthic foraminifera across the Paleocene- Eocene Thermal Maximum at the Alamedilla section (Southern Spain). Palaeogeogr. Palaeoclimatol. Palaeoecol. 279:186–200

Alegret, L., Ortiz, S., Arenillas, I., and Molina, E. (2010). What happens when the ocean is overheated? The foraminiferal response across the Paleocene-Eocene Thermal Maximum at the Alamedilla section (Spain), Geol. Soc. Am. Bull., 122, 1616–1624,

Alegret, L., Arreguin-Rodriguez, G and Ortiz, S. (2013). Glomospira Acme during the Paleocene-Eocene Thermal Maximum: Response to $CaCO_3$ Dissolution or to Ecological Forces? The Journal of Foraminiferal Research 43(1) 40-54

Altenbach, A. V and Sarnthein, M. (1989). Productivity record in benthic Foraminifera, in Berger, W. H., Smetacek, V. S., and Wefer, G. (eds.), Productivity of the Ocean: Present and Past, John Wiley and Sons Ltd., New York, 255–269.

Altenbach, A.V., Pflaumann, U. Schiebel, R., Thies, A., Svenn T. and Trauth M. (1999). Scaling percentages and distributional patterns of benthic foraminifera with flux rates of organic carbon. J. Foraminifera. Res., 29 (3), 173-185

Alve, E. and Goldstein, S. T. (2003). Propagule transport as a key method of dispersal in benthic foraminifera (Protists), Limnol. Oceanogr., 48, 2163–2170.

Anagnostou E., John E. H., Edgar K. M., Foster G. L., Ridgwell A., Inglis G. N., Pancost R. D., Lunt D. J., Pearson P. N. (2016). Changing atmospheric CO_2 concentration was the primary driver of early Cenozoic climate. Nature 533, 380–384

Aref, M. and Youssef, M. (2004). The benthic foraminifera perturbation across the Paleocene-Eocene Thermal Maximum event (PETM) from Southwestern Nile Valley, Egypt. N.Jb. Geol. Paleont. Abh 234(1-3): 261-269.

Armstrong, H. A., Brasier, M. D. (2005). Microfossils. Second Edition. Blackwell Publishing. 304p

Arreguín-Rodríguez, G. J., Alegret, L. and Thomas E. (2016). Late Paleocene-middle Eocene benthic foraminifera on a Pacific seamount (Allison Guyot, ODP Site 865): Greenhouse climate and superimposed hyperthermal events, Paleoceanography, 31, 346–364, doi:10.1002/2015PA002837.

Arreguín-Rodríguez, G.J., Thomas, E., D'haenens, S., Speijer, R.P., Alegret, L. (2018). Early Eocene deep-sea benthic foraminiferal faunas: Recovery from the Paleocene Eocene Thermal Maximum extinction in a greenhouse world. PLoS ONE 13(2) 1- 47

Aubry, M.P, Lucas, S. and Berggren, W.A., eds. (1998). Late Paleocene-Early Eocene Climatic and Biotic Events in the Marine and Terrestrial Records. New York: Columbia Univ. Press. 600p

Aubry, M.P., Berggren. W. A., Stott. L. and Sinha. A. (1996). The upper Paleocene-lower Eocene stratigraphic record and the Paleocene Eocene boundary carbon isotope excursion: lmplications for geochronolory. In Knox. R. W O'B., Corfield, R. M. and Dunay, R. E. (eds.).

Correlation of the early Paleogene in Northwest Europe, Geological Society Special Publication No 101. 153- 380.

Aze, T., Barry, J., Bellerby, R.G.J., Brander, L., Byrne, M., Dupont, S., Gattuso, J-P., Gibbs, S., Hansson, L., Hattam, C., Hauton, C., Havenhand, J., Fosså, J. H., Kavanagh, C., Kurihara, H., Matear, R.J., Mark, F. C., Melzner, F., Munday, P., Niehoff, B., Pearson, P., Rehdanz, K., Tambutte, S., Turley, C. M., Venn, A., Warnau, M., Young J. R. (2014a). An Updated Synthesis of the Impacts of Ocean Acidification on Marine Biodiversity Secretariat of the Convention on Biological Diversity. Montreal, Technical Series No. 75, 99.

Aze, T., Pearson, P. N., Dickson, A. J., Badger, M. P. S., Bown, P. R., Pancost, R. D., Gibbs S. J., Huber, B. T., Leng, M. J., Coe A. L., Cohen, A. S., Foster, G. L. (2014b). Extreme warming of tropical waters during the Paleocene–Eocene Thermal Maximum. Geology 42, 739–742

Aziz, A. H., Hilgen, F.J., Van Luijk, G.M., Sluijs, A., Kraus, M., Pares, J.M., Gingerich, P.D. (2008). Astronomical climate control on paleosol stacking patterns in the upper Palaeocene-lower Eocene, Willwood Formation, Bighorn Basin, Wyoming. Geology 36:531–34

Babila, T.L., Penman, D.E., Hönisch, B., Kelly, D.C., Bralower, T.J., Rosenthal, Y. and Zachos, J. C. (2018). Capturing the global signature of surface ocean acidification during the Palaeocene–Eocene Thermal Maximum. Phil. Trans. R. Soc. A 376: 20170072. 1- 19.

http://dx.doi.org/10.1098/rsta.2017.0072

Baczynski, A. A., McInerney, F. A. Wing, S. L., Kraus, M. J., Bloch, J. I. Ross S. (2017). Constraining paleohydrologic change during the Paleocene-Eocene Thermal Maximum in the continental interior of North America. Palaeogeography, Palaeoclimatology, Palaeoecology 465: 237–246

Bains, S., Corfield, R.M., Norris, R.D. (1999). Mechanisms of climate warming at the end of the Palaeocene. Science 285:724–27

Bains, S., Norris, R. D., Corfield, R. M. and Faul, K. L. (2000).Termination of global warmth at the Palaeocene/Eocene boundary through productivity feedback. Nature 407: 171-174

Barnosky, A. D., Matzke, N., Tomiya, S., Wogan, G. O., Swartz, B., Quental, T. B., Marshall, C., McGuire, J. L., Lindsey, E. L., Maguire, K. C., Mersey, B. Ferrer, E. A. (2011). Has the Earth's sixth mass extinction already arrived? Nature, 471: 51–57

Bé, A.W.H. and Anderson, O.R. (1976). Gametogenesis in planktonic foraminifera. Science, 192: 890-892.

Bearman, G. (1989). Waves, Tides, and Shallow-Water Processes. The Open University. Oxford (Pergamon Press). 187p

Beauchard, O., Veríssimo, H., Queirós, A.M., Herman, P.M.J. (2017). The use of multiple biological traits in marine community ecology and its potential in ecological indicator development. Ecol. Indic. 76:81-96. http://dx.doi.org/10.1016/j.ecolind.2017.01.011.

Beck, R.A., Sinha, A., Burbank, D.W., Sercombe, W.J., Khan, A.M. (1998). Climatic, oceanographic, and isotopic consequences of the Paleocene India–Asia collision, in: M.-P. Aubry, S. Lucas, W.A. Berggren (Eds.). Late Paleocene–Early Eocene Climatic and Biotic Events in the Marine and Terrestrial Records. Columbia University Press, New York, 103–117

Beerling, D. J. and Royer, D. L. (2011). Convergent Cenozoic CO2 history, Nat. Geosci., 4: 418–420, doi:10.1038/ngeo1186.

Bell, M.A., Travis, M.P., Blouw, D.M. (2006). Inferring natural selection in a fossil threespine stickleback. Paleobiology 32: 562–577.

Bellier, J.P., Mathieu, P., Granier, B. (2010). Short treatise on foraminiferology (Essential on modern and fossil Foraminifera). Carnets de Géologie - Notebooks on Geology, Brest, Book 2010/02 (CG2010_B02), 104p.

Berggren, W.A, Norris, R.D. (1997). Biostratigraphy, phylogeny and systematics of Palaeocene trochospiral planktic foraminifera. Micropaleontology. 43:1-116.

Berggren, W.A. and Ouda, K. 2003. Upper Paleocene-lower Eocene planktonic foraminiferal biostratigraphy of the Dababiya section, Upper Nile Valley (Egypt). Micropaleontology, 49: 61–92

Berggren, W.A., Kent, D.V. and Flynn, J.I. (1985). Paleogene planktonic foraminiferal biostratigraphy and magnetobiochronology. Micropaleontology, 34: 362-380

Berggren, W.A., Kent, D.V., Swisher III, C.C., Aubry, M.P. (1995). A revised Cenozoic geochronology and chronostratigraphy. In: Berggren, W.A., Kent, D.V., Aubry, M.P., Hardenbol, J. (Eds.), Geochronology, Time Scales and Global Stratigraphic Correlation: A Unified Temporal Framework for an Historical Geology: SEPM Spec. Publ., 54: 129–212.

Berggren, W.A., Pearson, P.N. (2005). A revised tropical and subtropical Paleogene planktonic foraminiferal zonation. J. Foramin. Res. 35: 279–298

Bice, K.L. and Marotzke, J. (2002). Could changing ocean circulation have destabilized methane hydrate at the Paleocene/Eocene boundary? Paleoceanography, 17 (2): 8.1-8.13 doi:10.1029/2001PA000678.

Bijl, P. K., Pross, J., Warnaar, J., Stickley, C. E., Huber, M., Guerstein, R., Houben, A. J. P., Sluijs, A., Visscher, H. and Brinkhuis H. (2011). Environmental forcings of Paleogene Southern Ocean dinoflagellate biogeography. Paleoceanography 26:PA1202.

Bijl, P.K., Bendle, J.A.P., Bohaty, S.M., Pross, J., Schouten, S., Tauxe, L., Stickley, C.E., McKay, R.M., Röhl, U., Olney, M., Sluijs, A., Escutia, C., Brinkhuis, H., Expedition 318 Scientists. (2013). Eocene cooling linked to early flow across the Tasmanian Gateway. Proceedings of the National Academy of Sciences 110, 9645–9650.

Birch, H. S., Coxall, H. K., Pearson, P. N., Kroon, D and Schmidt D. N. (2016). Partial collapse of the marine carbon pump after the Cretaceous- Paleogene boundary. Geology, 44 (4), 287–290

Bolle, M.P. and Adatte, T. (2001). Palaeocene–early Eocene climatic evolution in the Tethyan realm: Clay mineral evidence. Clay Minerals, 36: 249–261.

Bolli, H., Beckmann, J., and Saunders, J. (1994). Benthic foraminiferal biostratigraphy of the South Caribbean region. Cambridge University press 408p

Boltovskoy, E., Scott, D.B. and Medioli F.S. (1991). Morphological variations of benthic foraminiferal tests in response to changes in ecological parameters: A review J. Paleontol., 65: 175-185

Boscolo Galazzo, F., Giusberti, L., Luciani, V., and Thomas, E. (2013). Paleoenvironmental changes during the Middle Eocene Climatic Optimum (MECO) and its aftermath: the benthic foraminiferal record from the Alano section (NE Italy), Palaeogeogr. Palaeocl. 378: 22–35.

Boscolo Galazzo, F., Thomas, E., and Giusberti, L. (2015). Benthic foraminiferal response to the Middle Eocene Climatic Optimum (MECO) in the Southeastern Atlantic (ODP Site 1263). Palaeogeogr. Palaeocl. Palaeoecol. 417: 432–444.

Boscolo Galazzo, F., Thomas, E., Pagani, M., Warren, C., Luciani, V., and Giusberti, L. (2014). The middle Eocene climatic optimum (MECO): A multiproxy record of paleoceanographic changes in the southeast Atlantic (ODP Site 1263, Walvis Ridge), Paleoceanography, 29: 1143–1161.

Bowen GJ, Koch PL, Gingerich PD, Norris RD, Bains S, Corfield R. (2001). Refined isotope stratigraphy across the continental Paleocene-Eocene boundary on Polecat Bench in the northern Bighorn Basin. Univ. Mich. Pap. Paleontol. 33:73–88

Bowen, G. J. and Zachos, J.C. (2010). Rapid carbon sequestration at the termination of the Palaeocene-Eocene Thermal Maximum. Nat. Geosci. 3:866–69

Bowen, G. J., Beerling, D. J., Koch, P. L., Zachos, J. C. and Quattlebaum, T. (2004). A humid climate state during the Palaeocene/Eocene thermal maximum. Nature 432: 495–499. (doi:10.1038/ nature03115

Bowen, G.J and Bowen, B.B. (2008). Mechanisms of PETM global change constrained by a new record from central Utah. Geology 36:379–82

Bralower, T. J. (2002). Evidence of surface water oligotrophy during the Paleocene-Eocene thermal maximum: nannofossil assemblage data from Ocean Drilling Program Site 690, Maud Rise, Weddell Sea. Paleoceanography 17:1023

Bremner, J., Rogers, S.I., Frid, C.L.J. (2006). Methods for describing ecological functioning of marine benthic assemblages using biological traits analysis (BTA). Ecological Indicators 6(3): 609-622.

Bremner, J. (2008). Species' traits and ecological functioning in marine conservation and management. Journal of Experimental Marine Biology and Ecology 366(1-2): 37-47.

Bremner, J., Frid, C. L. J. and Rogers, S. I. (2005). Biological traits of the North Sea benthos: does fishing affect benthic ecosystem function? American Fisheries Society Symposium 41: 477–489.

Buzas, M. A., Culver, S. J., and Jorissen, F. J. (1993). A statistical evaluation of the microhabitats of living (stained) infaunal benthic foraminifera, Mar. Micropaleont., 29: 73–76

Caballero, R. and Huber, M. (2013). State-dependent climate sensitivity in past warm climates and its implications for future climate projections, Proc. Natl. Acad. Sci. U.S.A., 110(35): 14,162–14,167, doi:10.1073/pnas.1303365110.

Cardinale, B. J., Duffy, J. E., Gonzalez, A., Hooper, D. U., Perrings, C. Venail, P. Narwani, A., Mace, G. M., Tilman, D., Wardle, D. A., Kinzig, A. P., Daily, G. C., Loreau, M., Grace, J. B., Larigauderie, A., Srivastava D. S. and Naeem, S. (2012) Biodiversity loss and its impact on humanity. Nature, 486: 59-67, 10.1038/nature11148.

Castella, E. and Speight, M.C.D. (1996). Knowledge representation using fuzzy coded variables: an example based on the use of Syrphidae (Insecta, Diptera) in the assessment of riverine wetlands. In: *Ecological Modelling*, 85, 1: 13-25. https://archive-ouverte.unige.ch/unige:72896

Caswell, B. A. and Coe, A. L. (2014). The impact of anoxia on pelagic macrofauna during the Toarcian Oceanic Anoxic Event (Early Jurassic). Proceedings of the Geologists' Association 125(4): 383-391.

Caswell, B. A. and Frid, C. L. J. (2013). Learning from the past: functional ecology of marine benthos during eight million years of aperiodic hypoxia, lessons from the Late Jurassic. Oikos 122(12): 1687-1699.

Caswell, B.C. and Frid, C. L. J. (2017). Marine ecosystem resilience during extreme deoxygenation: the Early Jurassic oceanic anoxic event. Oecologia, 1–16.

Cavan, E. L., Henson, S. A., Belcher, A and Sanders, R. (2017). Role of zooplankton in determining the efficiency of the biological carbon pump. Biogeosciences, 14: 177–186. doi:10.5194/bg-14-177

Ceballos G. and Ehrlich P. R. (2018). The misunderstood sixth mass extinction. Science 360, 6393: 1080-1081

Charvet, S., Kosmala, A. and Statzner, B. (1998). Biomonitoring through biological traits of benthic macroinvertebrates: perspectives for a general tool in stream management. Arch. Hydrobiol. 142, 415–432.

Charvet, S., Statzner, B., Usseglio Polatera, P. and Dumont, B. (2000). Traits of benthic macroinvertebrates in semi-natural French streams: an initial application to biomonitoring in Europe. Freshwater Biology, 43: 277–296.

Chevenet, F, Dolédec, S. and Chessel, D. (1994). A fuzzy coding approach for the analysis of long-term ecological data. Freshwater Biology 31:295–309.

Chisholm, S W. (2000) Oceanography: Stirring times in the Southern Ocean. Nature, 407: 685-686

Clarke, K.R. (1993). Non-parametric multivariate analyses of changes in community structure. Aust. J. Ecol. 18:117-143

Clarke, K.R. and Gorley, R.N. (2006). Primer v6 Plymouth Marine Laboratory, Roborough, Plymouth, UK. 225-244 <www.primer-e.com>

Coadic, R., Bassinot, F., Dissard, D., Douville, E., Greaves, M. and Michel, E. (2013). A core-top study of dissolution effect on B/Ca in Globigerinoides sacculifer from the tropical Atlantic: Potential bias for paleo-reconstruction of seawater carbonate chemistry, Geochem. Geophys. Geosyst., 14: 1053–1068. doi:10.1029/2012GC004296.

Collinson, M., Hooker, J., Grocke, D. (2003). Cobham Lignite Bed and penecontemporaneous macrofloras of southern England: A record of vegetation and fire across the Paleocene–Eocene Thermal Maximum. Acta Palaeobotanica 47(1): 109–125

Corliss B.H. and Emerson, S. (1990). Distribution of Rose Bengal stained deep-sea benthic foraminifera from the Nova Scotian continental margin and Gulf of Maine. Deep-Sea Res., 37: 381-400

Corliss, B. H. (1985). Microhabitats of benthic foraminifera within deep-sea sediments. Nature, *314* (6010): 435–438.

Corliss, B.H. and Chen, C. (1988). Morphotype patterns of Norwegian Sea deep-sea benthic foraminifera and ecological implications: Geology, 16: 716–719.

Costello, M.J., Claus, S, Dekeyzer, S., Vandepitte, L., Tuama, É.Ó., Lear, D. and Tyler-Walters H. (2015) Biological and ecological traits of marine species. *PeerJ* 3:e1201: 1 -29. https://doi.org/10.7717/peerj.1201

Cramer, B. S. and Kent, D. V. (2005). Bolide summer: The Paleocene/Eocene thermal maximum as a response to an extraterrestrial trigger. Palaeogeography, Palaeoclimatology, Palaeoecology, 224: 144–166

Cramer, B. S., Toggweiler, J. R., Wright, J. D., Katz, M. E. and Miller, K. G. (2009). Ocean overturning since the Late Cretaceous: Inferences from a new benthic foraminiferal isotope compilation, Paleoceanography, 24, PA4216

Crouch, E. M., Raine, J. I., Kennedy, E. M., Handley L. and Pancost, R. D. (2009). New Zealand terrestrial and marginal marine records across the Paleocene-Eocene transition. In E. M. Crouch, C. P. Strong, and C. J. Hollis [eds.], extended abstracts from international conference Climatic and Biotic Events of the Paleogene (CBEP 2009), Wellington, New Zealand. GNS Science Miscellaneous Series 18: 40–43.

Cui, Y., Kump, L. R., Ridgwell, A. J., Charles, A. J., Junium, C. K., Diefendorf, A. F., Freeman, K. H., Urban, N. M., and Harding I. C. (2011). Slow release of fossil carbon during the Palaeocene-Eocene thermal maximum, Nat. Geosci., 4(7): 481–485, doi:10.1038/ngeo1179.

Culver, S.J. and Lipps, J.H. (2003). Predation on and by Foraminifera P. Kelley, M. Kowalewski, T. Hansen (Eds.), Predation in the Fossil Record, Kluwer Academic/Plenum Publishers, New York: 7-32

Cushman, J.A. (1951). Paleocene foraminifera of the Gulf Coastal region of the United States and adjacent areas. U.S. Geol. Surv. Prof. Pap., 232:1–75.

D'haenens, S., Bornemann, A., Stassen, P. and Speijer, R. (2012). Multiple early Eocene benthic foraminiferal assemblage and $\delta^{13}C$ fluctuations at DSDP Site 401 (Bay of Biscay - NE Atlantic): Marine Micropaleontology, 88–89: 15–35.

Daniel, S. M. and Hain, M. P. 2012. The Biological Productivity of the Ocean. Nature Education Knowledge 3(6):7

DeConto, R.M., Galeotti, S., Pagani, M., Tracy, D., Schaefer, K., Zhang, T., Pollard, D., Beerling, D.J. (2012). Past extreme warming events linked to massive carbon release from thawing permafrost. Nature 484 (7392): 87–91.

Dickens, G.R. (2000). Methane oxidation during the late Paleocene Thermal Maximum. Bulletin de la Société Géologique de France, 171: 37-49.

Dickens, G.R., Oneil, J.R., Rea, D.K., Owen, R.M. (1995). Dissociation of oceanic methane hydrate as a cause of the carbon-isotope excursion at the end of the Paleocene. Paleoceanography 10:965–71

Doledec, S. and Chessel, D. (1994). Co-inertia analysis: an alternative method for studying species–environment relationships. Freshwater Biology 31:277–294

Dubicka, Z., Złotnik, M. and Borszcz, T. (2015). Test morphology as a function of behavioral strategies — Inferences from benthic foraminifera. Marine Micropaleontology 116: 38–49

Dunkley Jones T., Lunt D. J., Schmidt D. N., Ridgwell, A., Sluijs, A. Valdes P. J. and Maslin, M. (2013). Climate model and proxy data constraints on ocean warming across the Paleocene–Eocene Thermal Maximum. Earth Sci. Rev. 125:123–145.

Dunkley Jones, T., Ridgwell, A., Lunt, D.J., Maslin, M.A., Schmidt, D.N. and Valdes, P.J. (2010). A Paleogene perspective on climate sensitivity and methane hydrate instability. Philosophical Transactions of the Royal Society A 368: 2395–2415.

Dutton, A., Lohmann, K. C. and Leckie, M. R. (2005). Insights from the Paleogene tropical Pacific: Foraminiferal stable isotope and elemental results from Site 1209, Shatsky Rise, Paleoceanography, 20, PA3004, doi:10.1029/2004PA001098.

Dymond, J., Suess, E. and Lyle M. (1992). Barium in Deep-Sea Sediment: A geochemical proxy for paleoproductivity. Paleoceanography 7: 163-181.

Edwards, R.J., Van de Plassche, O., Gehrels, W.R., Wright, A.J. 2004a. Assessing sea-level data from Connecticut, USA, using a foraminiferal transfer function for tide level. Marine Micropaleontology 51: 239–255.

Eldrett, J.S., Greenwood, D.R., Polling, M., Brinkhuis. H. and Sluijs, A. (2014). A seasonality trigger for carbon injection at the Paleocene-Eocene thermal maximum. Climate of the Past, 10: 759 – 769. doi:10.5194/cp-10-759-2014.

Elena, N. I., Alain, F. Z and Chris, S. E. (2010). A protocol for data exploration to avoid common statistical problems. Methods in Ecology and Evolution, 1: 3–14

Fairon-Demaret, M., Steurbaut, E., Damblon, F., Dupuis, C., Smith, T. and Gerrienne, P. 2003. The in situ Glyptostroboxylon forest of Hoegaarden (Belgium) at the Initial Eocene Thermal Maximum (55 Ma). Review of Palaeobotany and Palynology 126: 103 – 129.

Farrell, J.W., and Prell, W.L. (1989). Climatic change and $CaCO_3$ preservation: an 800,000 year bathymetric reconstruction from the central equatorial Pacific Ocean. Paleoceanography, 4(4):447–466.

Faul, K. L., and A. Paytan (2005), Phosphorus and barite concentrations and geochemistry in Site 1221 Paleocene/Eocene boundary sediments, in Proceedings of the Ocean Drilling Program, Sci. Results, edited by P. A. Wilson, M. Lyle, and J. V. Firth, Ocean Drilling Program, College Station, Tex. 1–23

Fensome, R. A., H. Gocht, and G. L. Williams (1996). The Eisenack Catalog of Fossil Dinoflagellates. E. Schweizerbart'sche Verl., Stuttgart, Germany 2: 632p

Fontanier, C., Jorissen, F.J., Chaillou, G., Anschutz, P., Grémare, A. and Griveaud, C. (2005). Live foraminiferal faunas from a 2800 m deep lower canyon station from the Bay of Biscay: faunal response to focusing of refractory organic matter. Deep Sea Res. 52: 1189–1227.

Foreman, B. Z., Heller P. L. and Clementz M. T. (2012). Fluvial response to abrupt global warming at the Palaeocene/Eocene boundary. Nature, 491(7422):92-5 doi: 10.1038/nature11513

Foster, G. L., Hull, P., Lunt, D.J., Zachos, J.C. (2018). Placing our current 'hyperthermal' in the context of rapid climate change in our geological past. *Phil. Trans. R. Soc. A* 376: 20170086. http://dx.doi.org/10.1098/rsta.2017.0086

Foster, L. C., Schmidt, D. N., Thomas, E., Arndt, S., and Ridgwell, A. (2013). Surviving rapid climate change in the deep-sea during the Paleogene hyperthermals. Proc. Nat. Acad. Sci., 110: 9273-9276; http://dx.doi.org/10.1073/pnas.1300579110

Frenzel, P. (2000). Die benthischen Foraminiferen der Rügener Schreibkreide (unter-Maastricht, NE Deutchland). Neue Paläontologische Abhandlungen, 3: 1–361.

Fricke HC, Wing SL. 2004. Oxygen isotope and paleobotanical estimates of temperature and δ^{18}O-latitude gradients over North America during the early Eocene. Am. J. Sci. 304:612–35

Frid, C.J.L., Paramor, O.A.L., Brockington, S. and Bremner, J. (2009). Incorporating ecological functioning into the designation and management of marine protected areas. Hydrobiologia, 606: 69-79

Frid, C. L. J and Caswell B. A. (2015). Is long-term ecological functioning stable: The case of the marine benthos? Journal of Sea Research 98: 15-23.

Frid, C. L. J and Caswell, B. A. (2016). Does ecological redundancy maintain functioning of marine benthos on centennial to millennial time scales? Marine Ecology, 37(2): 392–410.

Frid, C. L. J. and Caswell B. A. 2017. Marine Pollution. Oxford University Press. 268p

Frid, C. L. J., Harwood, K. G., Hall, S. J. and Hall, J. A. (2000). Long-term changes in the benthic communities on North Sea fishing grounds. ICES Journal of Marine Science 57: 1303-1309

Friedrich, O., Herrle, J. O. and Hemleben, C. (2005). Climatic changes in the Late Campanian through Early Maastrichtian: micropaleontological and stable isotopic evidence from an epicontinental sea. Journal of Foraminiferal Research, 35(3):228-247, https://doi.org/10.2113/35.3.228

Friedrich, O., Erbacher, J., Wilson, P. A., Moriya, K. and Mutterlose, J. (2009). Paleoenvironmental changes across the Mid Cenomanian Event in the tropical Atlantic Ocean (Demerara Rise, ODP Leg 207) inferred from benthic foraminiferal assemblages. *Marine* Micropaleontology, 71(1-2): 28-40

Frieling, J., Gebhardt, H., Huber, M., Adekeye, O. A., Akande, S. O., Reichart G. J., Middelburg, J. J., Schouten S. and Sluijs A. (2017). Extreme warmth and heat-stressed plankton in the tropics during the Paleocene-Eocene Thermal Maximum. Sci. Adv. 3(3) e1600891: 1 - 9

Frieling, J., Svensen, H. H., Planke, S., Cramwinckel, M. J., Selnes, H. and Sluijs, A. 2016 Thermogenic methane release as a cause for the long duration of the PETM. Proc. Natl. Acad. Sci. 113: 12059–64

Galbraith, E. D., Kienast, M., Jaccard, S. L., Pedersen, T. F., Brunelle, B. G., Sigman, D. M. and Kiefer, T. 2008 Consistent relationship between global climate and surface nitrate utilization in the western subarctic Pacific throughout the last 500 ka, Paleoceanography, 23: PA2212, doi:10.1029/2007PA001518.

Galbraith, E. D., Kienast, M., Jaccard, S. L., Pedersen, T., Brunelle, B. G., Sigman, D. M. and Kiefer, T. (2008). Consistent relationship between global climate and surface nitrate utilization in the western subarctic Pacific throughout the last 500 ka, Paleoceanography, 23(PA2212): doi:10.1029/2007PA001518.

Galeotti, S., Krishnan, S., Pagani M., Lanci L., Gaudio A., Zachos, J. C., Monechi, S., Morelli G., Lourens, L. (2010). Orbital chronology of Early Eocene hyperthermals from the Contessa Road section, central Italy. Earth and Planetary Science Letters, 290: 192–200

Gavrilov, Y.O., Shcherbinina, E.A. and Oberhansli, H. (2003). Palaeocene-Eocene boundary events in the northeastern Peri-Tethys. Geol. Soc. Am. Spec. Pap. 369:147–68

Gayraud, S., Statzner, B., Bady, P., Haybachp, A., Scholl, F., Usseglio-Polatera, P. and Bacchi, M. (2003). Invertebrate traits for the biomonitoring of large European rivers: an initial assessment of alternative metrics. Freshwater Biology, 48: 2045-2064.

Gehler A., Gingerich, P. D. and Pack, A. (2016).Temperature and atmospheric CO_2 concentration estimates through the PETM using triple oxygen isotope analysis of mammalian bioapatite. Proc. Natl. Acad. Sci. U.S.A. 113: 7739–7744

Georgescu, M.D., Arz, J.A., Macauley, R.V., Kukulski, R.B., Arenillas, I., Pérez-Rodríguez, I. (2011). Late Cretaceous (Santonian-Maastrichtian) serial foraminifera with pore mounds or pore mound-based ornamentation structures. Rev. Esp. Micropaleontol. 43: 109–139.

Gibbs, S. J., Sheward, R. M., Bown, P. R., Poulton, A.J., Alvarez, S. A. (2018). Warm plankton soup and red herrings: calcareous nannoplankton cellular communities and the Palaeocene–Eocene Thermal Maximum. Phil. Trans. R. Soc. A. 376: 20170075. http://dx.doi.org/10.1098/rsta.2017.0075

Gibbs, S. J., T. J. Bralower, P. R. Bown, J. C. Zachos, and L. M. Bybell (2006b). Shelf and open-ocean calcareous phytoplankton assemblages across the Paleocene-Eocene Thermal Maximum: Implications for global productivity gradients, Geology, 34: 233–236, doi:10.1130/G22381.1

Gibson, T. G., L. M. Bybell, and J. P. Owens (1993). Latest Paleocene lithologic and biotic events in neritic deposits of southwestern New Jersey, Paleoceanography, 8(4): 495–514, doi:10.1029/93PA01367.

Gibson, T.G., Bybell, L.M. and Mason, D.B. (2000) Stratigraphic and climatic implications of clay mineral changes around the Paleocene/Eocene boundary of the northeastern US margin. Sedimentary Geology, 134: 65–92

Gibson, T.G., Bybell, L.M., and Owens, J.P. (1993). Latest Paleocene lithologic and biotic events in neritic deposits of southwestern New Jersey. Paleoceanography, 8:495–514.

Giusberti, L., Rio, D., Agnini, C., Backman, J., Fornaciari, E., Tateo, F. and Oddone, M. (2007). Mode and tempo of the Paleocene–Eocene Thermal Maximum in an expanded section from the Venetian Pre-Alps Geological Society of America Bulletin, 119: 391-412;

Giusberti, L., Coccioni, R., Sprovieri, M. and Tateo, F. (2009). Perturbation at the sea floor during the Paleocene–Eocene Thermal Maximum: Evidence from benthic foraminifera at Contessa Road, Italy: Marine Micropaleontology, 70, 102–119.

Giusberti, L and. Luciani, V. (2014). Reassessment of the early–middle Eocene planktic foraminiferal biomagnetochronology: new evidence from the Tethyan Possagno section (NE Italy) and Western North Atlantic Ocean ODP Site 1051, J. Foramin. Res., 44, 187–201.

Giusberti, L., Boscolo Galazzo F. and Thomas E. (2016). Variability in climate and productivity during the Paleocene–Eocene Thermal Maximum in the western Tethys (Forada section). Clim. Past. 12, 213–240

Gleason, J. D., Thomas, D. J., Moore Jr., T. C., Blum, J. D., Owen, R. M. and Haley B. A. (2007). Water column structure of the Eocene Arctic Ocean recorded by Nd-Sr isotope proxies in fossil fish debris, Geochim. Cosmochim. Acta, 71, A239. 1- 18

Goldstein, S. T. (1999). Foraminifera: A biological overview. In B. K. Sen Gupta (Ed.), Modern foraminifera, Great Britain: Kluwer Academic Publishers. 37–56

Goldstein, S.T. and Alve E. (2002). Resting stage in benthic foraminiferal propagules: a key feature for dispersal? Evidence from two shallow-water species. Journal of Micropaleontology, 21, 95–96.

Gooday A.J. (1994). The biology of deep-sea foraminifera: A review of some advances and their applications in paleoceanography, Palaios, 9: 14-31

Gooday, A. J., Bernhard, J. M., Levin, L. A., and Suhr, S. B. (2000). Foraminifera in the Arabian Sea oxygen minimum zone and other oxygen-deficient settings: Taxonomic composition, diversity, and relation to metazoan faunas. Deep-Sea Research Part II-Topical Studies in Oceanography, 47(1–2): 25–54.

Gooday, A. J., Levin, L. A., da Silva, A. A., Bett, B. J., Cowie, G. L., Dissard, D., Woulds, C. (2009). Faunal responses to oxygen gradients on the Pakistan margin: A comparison of foraminiferans, macrofauna and megafauna. Deep-Sea Research Part II-Topical Studies in Oceanography, 56(6–7):488–502

Gooday, A.J. (1994). The biology of deep-sea foraminifera: a review of some advances and their applications in paleoceanography. Palaios 9: 14-31.

Gooday, A.J. and Jorissen, F.J. (2012). Benthic foraminiferal biogeography: controls on global distribution patterns in deep-water settings. Annual Review of Marine Sciences, 4: 237–262.

Gooday, A.J. and Levin, L.A. (1992). Possible roles for xenophyophores in deep-sea carbon cycling. G.T. Rowe, V. Pariente (Eds.), Deep-Sea Food Chains and the Global Carbon Cycle, Kluwer Academic Publishers, The Netherlands, 93-104

Gradstein, F. M., Kaminski, M. A., Berggren, W. A., Kristiansen, I. L. and D'ioro, M. A. (1994). Cenozoic biostratigraphy of the North Sea and Labrador Shelf. Micropaleontology, 40: 152.

Gradstein, F. M., Ogg, J. G. and Smith, A. G. (2004). A Geologic Time Scale 2004. Cambridge University Press, Cambridge

Granger, J., Sigman, D. M., Lehmann, M. F. and Tortell, P. D. (2008). Nitrogen and oxygen isotope fractionation during dissimilatory nitrate reduction by denitrifying bacteria, Limnol. Oceanogr., 53, 2533–2545, doi:10.4319/lo.2008.53.6.2533.

Griffith, J., Kadin M., Nascimnento F.J.A., Tamelander T., Törnroos A., Bonaglia S., Bonsdorff E., Büchert V., Gårdmanrk A., Järnström M., Kotta J., Lindegren M., Nordström M.C., Norkko A., Olsson J., Weigel B., Zydelis R., Blenckner T., Niiranen S., Winder, M. (2017). The importance of benthic–pelagic coupling for marine ecosystem functioning in a changing world. Global Change Biology. 23: 2179–2196, doi: 10.1111/gcb.13642

Grigoratou, M., Monteiro, F. M., Schmidt, D. N., Jamie, D. W., Ben, A. and Ridgwell, A. A trait-based modelling approach to planktonic foraminifera ecology. Biogeosciences Discuss., https://doi.org/10.5194/bg-2018-483

Groeneveld, J. and Filipsson, H. L. (2013). Mg- Ca and Mn/Ca ratios in benthic foraminifera: the potential to reconstruct past variations in temperature and hypoxia in shelf regions, Biogeosciences, 10: 5125–5138, https://doi.org/10.5194/bg-10-5125-2013.

Gutjahr, M., Ridgwell, A., Sexton, P. F., Anagnostou, E., Pearson, P. N., Pälike, H., et al. (2017). Very large release of mostly volcanic carbon during the Palaeocene-Eocene Thermal Maximum. Nature, 548: 573. https://doi.org/10.1038/nature23646

Handley, L., O'Halloran, A., Pearson, P.N., Hawkins, E., Nicholas, C.J., Schouten, S., McMillan, I.K., Pancost, R.D. (2012). Changes in the hydrological cycle in tropical East Africa

during the Paleocene-Eocene Thermal Maximum Palaeogeogr. Palaeoclimatol. Palaeoecol., 329: 10-21, 10.1016/j.palaeo.2012.02.002

Handley, L., Pearson, P.N., McMillan, I.K. and Pancost, R.D. (2008). Large terrestrial and marine carbon and hydrogen isotope excursions in a new Paleocene/Eocene boundary section from Tanzania. Earth and Planetary Science Letters 275: 17–25

Handley, L. Crouch, E.M. and Pancost, R.D. (2011). A New Zealand record of sea level rise and environmental change during the Paleocene-Eocene Thermal Maximum Palaeogeogr. Palaeoclimatol. Palaeoecol., 305: 185-200, 10.1016/j.palaeo.2011.03.001

Harrington, G. J. and Jaramillo, C. A. (2007). Paratropical floral extinction in the Late Palaeocene-Early Eocene, Palaeontology 46, 725– 738.

Hausner, V. H., Yoccoz, N. G. and Ims, R. A. (2003). Selecting indicator traits for monitoring land use impacts: Birds in northern coastal birch forests. Ecol. Appl. 13: 999–1012.

Haynes, J. R. (1982). Foraminifera. John Wiley & Sons, New York, NY, 433 p.

Hecht, A.D., Eslinger, E.V., Garmon, L.B. (1975). Experimental studies on the dissolution of planktonic foraminifera, in Dissolution of deep-sea carbonates. Spec. Publ., Cushman Found. Foraminiferal Res., 13, 56-69.

Hecht, A.D., Eslinger, E.V. and Garmon, L.B. (1975). Experimental studies on the dissolution of planktonic foraminifera. Cushman Foundation for Research, Special Publication, 13, 56 - 69.

Heinz, P., Ruepp, D. and Hemleben, C. (2004). Benthic foraminifera assemblages at great Meteor Seamount, Marine Biology, 144: 985-998.

Heinze, C., Meyer, S., Goris, N., Anderson, L., Steinfeldt, R., Chang, N., Le Quéré, C., Bakker, D.C.E. (2015). The ocean carbon sink: impacts, vulnerabilities and challenges. Earth Syst Dyn. 6(1):327–358. doi: 10.5194/esd-6-327

Hemleben, C., Spindler, M., and Anderson, O. R. (1989) Modern Planktonic Foraminifera: Springer Verlag, Berlin, 363 p.

Henehan, M. J., Evans, D., Shankle, M., Burke, J. E., Foster, G. L., Anagnostou, E., Chalk, T. B., Stewart, J. A., Alt, C. H. S., Durrant, J. and Hull, P. M. (2017). Size-dependent response of foraminiferal calcification to seawater carbonate chemistry, Biogeosciences, 14: 3287-3308

Henriksson, A. S., Widmark, Joen, G. V., Holbourn A. E., Thies, A. and Kuhnt, W. (1998). Coccoliths as test-building material for foraminifera (coccolithofera). Journal of Nannoplankton Research, 20(1): 15- 19.

Higgins, J. A. and Schrag, D.P. (2006). Beyond methane: towards a theory for the Paleocene-Eocene Thermal Maximum. Earth Planet. Sci. Lett. 245:523–37

Hohenegger, J. (2011). Large Foraminifera: Greenhouse Constructions and Gardeners in the Oceanic Microcosm. The Kagoshima University Museum, Kagoshima, Japan, 85 pp.

Holbourn, A., Henderson, A.S. and Macleod, N. (2013). Atlas of Benthic Foraminifera. Wiley-Blackwell. UK. 642P

Holbourn, A.E.L. and Kaminski, M.A. (1997). Lower Cretaceous deep-water benthic foraminifera of the Indian Ocean. Grzybowski Found . Spec. Pub. 4: I 72.

Hollis, C.J., Dickens, G.R., Field, B.D., Jones, C.M., Strong, C.P. (2005). The Paleocene–Eocene transition at Mead Stream, New Zealand: a southern Pacific record of early Cenozoic global change. Palaeogeography, Palaeoclimatology, Palaeoecology 215: 313–343.

Holzmann, M. and Pawlowski, J. (2017). An updated classification of rotaliid foraminifera based on ribosomal DNA phylogeny. Marine Micropaleontology 132, 18-34.

Hönisch, B., Ridgwell, A., Schmidt, D . N., Thomas, E., Gibbs, S. J., Sluijs, A,. Zeebe, R., Kump, L. ,Martindale, R. C., Greene, S. E., Kiessling, W., Ries, J., Zachos, J. C., Royer, D. L., Barker, S., Marchitto, T. M., Moyer, R., Pelejero, C., Ziveri, P., Foster, G. L. and Williams B. (2012).The geological record of ocean acidification. Science 335, 1058–1063

Hottinger, L. (2006). Illustrated glossary of terms used in foraminiferal research. Carnets de Géologie. Notebooks on Geology, Brest, Memoir 2006/02 (CG2006_M02), 126 p

Huber, M. and Caballero, R. (2011). The early Eocene equable climate problem revisited. Climate of the Past 7, 603–633.

Huber, M., Sloan, L. C., and Shellito, C. (2003). Early Paleogene oceans and climate: A fully coupled modeling approach using the NCAR CCSM, in: Causes and Consequences of globally warm climates in the early Paleogene, edited by: Wing, S., Gingerich, P., Schmitz, B., and Thomas, E. Geological Society of America Special Paper, Boulder, Colorado, 369, 25–47, doi:10.1130/0-8137-2369-8.25.

Huber, M. (2008). A hotter greenhouse? Science, 321, 353–354, doi:10.1126/science.1161170

Hyland, E. G., Sheldon, N. D. and Cotton, J. M. (2017). Constraining the early Eocene climatic optimum: A terrestrial interhemispheric comparison. Geological Society of America Bulletin, .B31493.1. 128 (10): 1–9:

Iakovleva, A. I., Brinkhuis, H. and Cavagnetto, C. (2001). Late Palaeocene–Early Eocene dinoflagellate cysts from the Turgay Strait, Kazakhstan; correlations across ancient seaways. Palaeogeography, Palaeoclimatology, Palaeoecology, 172, 243–268

Ilyina, T. and Zeebe, R. E. (2012). Detection and projection of carbonate dissolution in the water column and deep-sea sediments due to ocean acidification. Geophys. Res. Lett. 39: L06606,1-6. doi:10.1029/2012GL051272,

Intergovernmental Panel on Climate Change. (2018). An IPCC Special Report on the impacts of global warming of 1.5°C above pre-industrial levels and related global greenhouse gas emission pathways, in the context of strengthening the global response to the threat of climate change, sustainable development, and efforts to eradicate poverty. IPCC, Switzerland

IPCC Climate Change. (2013). The Physical Science Basis. Stocker,T.F., Qin, D., Plattner, G.-K., Tignor, M., Allen, S.K., Boschung, J., Nauels, A., Xia, Y., Bex V. and Midgley, P.M. (eds.). Cambridge University Press, Cambridge, United Kingdom and New York, NY, USA, 1535 p, doi:10.1017/CBO9781107415324

Itou, M., Ono, T., Oba, T. and Noriki, S. (2001). Isotopic composition and morphology of living Globorotalia scitula: a new proxy of sub-intermediate ocean carbonate chemistry? Mar. Micropaleontol. 42:189–210

Jennions, S. M., Thomas, E., Schmidt, D. N., Lunt, I. D., Ridgwell, A. (2015). Changes in benthic ecosystems and ocean circulation in the Southeast Atlantic across Eocene Thermal Maximum 2. Paleoceanography 30(8): 1059-1077.

Jepps, M.W. 1956. The Protozoa, Sarcodina. Oliver and Boyd, Edinburgh, 183pp.

John, E H., Wilson, J.D., Pearson, P. N. and Ridgwell, A. (2014). Temperature-dependent remineralization and carbon cycling in the warm Eocene oceans. Palaeogeography, Palaeoclimatology, Palaeoecology 413: 158-166.

Jorissen, F. J., Fontanier, C., and Thomas, E. (2007). Paleoceanographical proxies based on deep-sea benthic foraminiferal assemblage characteristics, in: Proxies in Late Cenozoic Paleoceanography: Pt. 2: Biological tracers and biomarkers, 1, Elsevier, Amsterdam, The Netherlands, 264–325

Jorissen, F.J. (1999). Benthic foraminiferal microhabitats below the sediment-water interface. En: Sen Gupta, B. (edited): Ecology of recent foraminifera, Kluwer Academic Publishers, chapter 10, 161-179.

Jorissen, F.J., de Stigter, H.C. and Widmark J.G.V. (1995). A conceptual model explaining benthic foraminiferal microhabitats. Marine Micropaleontology 26, 3–15.

Kaiho, K., Arinobu, T., Ishiwatari, R., Morgans, H.E.G., Okada, H., Takeda, N., Tazaki, K., Zhou, G., Kajiwara, Y., Matsumoto, R., Hirai, A., Niitsuma, N. and Wada, H (1996). Latest Paleocene benthic foraminiferal extinction and environmental changes at Tawanui, New Zealand. Paleoceanography 11:447–65

Kaiho, K. (1991). Global changes of Paleogene aerobic anaerobic benthic foraminifera and deep-sea circulation. Palaeogeogr, Palaeoclimatol., Palaeoecol. 83, 65–85.

Kaiho, K. (1994). Benthic foraminiferal dissolved-oxygen index and dissolved-oxygen levels in the modern ocean. Geology, 22(8): 719–722.

Kaiho, K. (1999a). Effect of organic carbon flux and dissolved oxygen on the benthic foraminiferal oxygen index (BFOI). Marine Micropaleontology, 37(1), 67–76.

Kaiho, K. (1999b). Evolution in the test size of deep-sea benthic foraminifera during the past 120 m.y. Marine Micropaleontology, 37(1): 53–65.

Kaiho, K., Takeda, K., Petrizzo, M.R. and Zachos, J.C. (2006). Anomalous shifts in tropical Pacific planktonic and benthic foraminiferal test size during the Paleocene-Eocene thermal maximum. Palaeogeogr. Palaeoclimatol. Palaeoecol. 237:456–64

Kaminski, M. A. (2004). The Year 2000 Classification of the Agglutinated Foraminifera. In: M. K. Bubik, Ma. (ed). Proceedings of the Sixth International Workshop on Agglutinated Foraminifera. Grzybowski Foundation Special Publication. 237-255.

Kaminski, M.A. and Gradstein, F.M. (2005). Atlas of Paleogene cosmopolitan deepwater agglutinated foraminifera. Grzybowski Foundation Special Publication, 10, 1–547.

Katz, M.E., Cramer, B.S., Franzese, A., Hönisch, B., Miller, K.G., Rosenthal, Y. and Wright, J.D. (2010). Traditional and emerging geochemical proxies in foraminifera. Journal of Foraminiferal Research 40, 165–192.

Katz, M.E., Pak, D.K., Dickens, G.R. and Miller, K. G. (1999). The source and fate of massive carbon input during the Latest Paleocene Thermal Maximum. Science 286:1531–33

Keating-Bitonti, C. R and Payne, J. L. (2017). Ecophenotypic responses of benthic foraminifera to oxygen availability along an oxygen gradient in the California Borderland. Mar Ecol.;38:e12430, 1-16. https://doi.org/ 10.1111/maec.12430

Keister, J.E., Bonnet, D., Chiba, S., Johnson, C.L., Mackas, D.L., and Escribano, R. (2012). Zooplankton population connections, community dynamics, and climate variability. ICES J. Mar. Sci., 69: 347-350

Kelly D. C., Zachos J. C., Bralower T. J., Schellenberg, S A. (2005). Enhanced terrestrial weathering/runoff and surface ocean carbonate production during the recovery stages of the Paleocene-Eocene Thermal Maximum. Paleoceanography 20:PA4023, 1-11

Kelly, D. C. (2002). Response of Antarctic (ODP Site 690) planktonic foraminifera to the Paleocene –Eocene thermal maximum: Faunal evidence for ocean/climate change, Paleoceanography, 17(4): 1071 doi:10.1029/2002PA000761.

Kelly, D. C., T. J. Bralower, and J. C. Zachos (1998). Evolutionary consequences of the latest Paleocene thermal maximum for tropical planktonic foraminifera, Palaeogeogr. Palaeoclimatol. Palaeoecol., 141, 139–161.

Kelly, D.C, Bralower, T.J, Zachos, J.C, Silva, I.P. and Thomas, E. (1996). Rapid diversification of planktonic foraminifera in the tropical Pacific (ODP Site 865) during the Late Paleocene Thermal Maximum. Geology 24:423–26

Kennett, J.P. and Stott, L.D. (1991). Abrupt deep-sea warming, palaeoceanographic changes and benthic extinctions at the end of the Palaeocene. Nature 353:225–29

Kent, D. V., Cramer, B. S., Lanci, L., Wang, D., Wright, J. D. and Van der Voo, R. (2003). A case for a comet impact trigger for the Paleocene/Eocene thermal maximum and carbon isotope excursion, Earth Planet. Sci. Lett., 211, 13 – 26.

Kiehl, J.T, Shields, C.A, Snyder, M. A, Zachos, J. C, Rothstein, M. (2018). Greenhouse and orbital-forced climate extremes during the early Eocene. Phil. Trans. R. Soc. A 376: 20170085. http://dx.doi.org/10.1098/rsta.2017.0085

Kitazato, H and Bernhard, M. J. (2014). Approaches to study living foraminifera: Collection, Maintenance and Experimentation, Springer Japan, 227p

Knox, R.W.O'B. (1996). Correlation of the early Paleogene in northwest Europe: an overview. In: Knox, R.W.O'B., Corfield, R., Dunay, R.E. (Eds.). Correlation of the Early Paleogene in Northwest Europe, Special Publication, Geological Society of London, 101: 1–11

Koch, P.L., Zachos, J.C and Gingerich, P. D. (1992). Correlation between isotope records in marine and continental carbon reservoirs near the Paleocene/Eocene boundary. Nature 358:319–22

Korty, R., Emanuel, K. A., and Scott, J. (2008). Tropical cyclone-induced upper-ocean mixing and climate: Application to equable climates, J. Climate, 21: 638–654, doi:10.1175/2007JCLI1659.1,

Kraus, M.J. and Riggins, S. (2007). Transient drying during the Palaeocene-Eocene Thermal Maximum (PETM): analysis of paleosols in the Bighorn Basin,Wyoming. Palaeogeogr. Palaeoclimatol. Palaeoecol. 245:444–61

Kroon, D., Zachos, J.C., and Leg 208 Scientific Party. (2007). Leg 208 synthesis: Cenozoic climate cycles and excursions. In Kroon, D., Zachos, J.C., and Richter, C. (Eds.), Proc. ODP, Sci. Results, 208: College Station, TX (Ocean Drilling Program), 1–55.

Kuhnt, T., Friedrich, O., Schmiedl, G., Milker, Y., Mackensen, A., Lückge, A. (2013). Relationship between pore density in benthic foraminifera and bottom-water oxygen content. Deep-Sea Res. I 76, 85–95. http://dx.doi.org/10.1016/j.dsr.2012.11.013.

Kuhnt, T., Schmiedl, G., Ehrmann, W., Hamann, Y., Hemleben, C. (2007). Deep-Sea Ecosystem Variability of the Aegean Sea during the Past 22 kyr as Revealed by Benthic Foraminifera. Marine Micropaleontology 64, 147-162

Kurtz, A.C, Kump, L.R, Arthur, M. A, Zachos. J. C, Paytan A. (2003). Early Cenozoic decoupling of the global carbon and sulfur cycles. Paleoceanography 18 (4): 1-11

Kvenvolden, K. A. (1993) Gas hydrates—geological perspective and global change. Rev. Geophys. 31, 173–187. (doi:10.1029/93RG00268)

Laffoley, D. and Baxter, J. M. (editors) (2016). Explaining ocean warming: Causes, scale, effects and consequences. Full report. Gland, Switzerland: IUCN. 456p.

Laskar, J., Robutel, P., Joutel F., Gastineau, M., Correia A. C. M. and Levrard, B. (2004) A long-term numerical solution for the insolation quantities of the Earth. Astron. Astrophys. 428, 261–285

Lavorel, S and Garnier, E. (2002). Predicting changes in community composition and ecosystem functioning from plant traits: revisiting the Holy Grail. Funct. Ecol. 16:545–556.

Lee, J. J. (1974). Towards understanding the niche of foraminifera. In: Hedley, R.H., and Adams, C.G. (eds), Foraminifera, Academic Press, New York 1, 207-260.

Lee, J.J. and Anderson O.R. (1991). Symbiosis in foraminifera: Biology of foraminifera, Academic Press, New York, 157-220

Leon-Rodriguez, L. and Dickens, G. R. (2010). Constraints on ocean acidification associated with rapid and massive carbon injections: The early Paleogene record at ocean drilling program site 1215, equatorial Pacific Ocean, Palaeogeogr. Palaeocl., 298, 409–420

Licari, L.N., Schumacher, S., Wenzhofer, F., Zabel, M. and Mackensen, A (2003). Communities and microhabitats of living benthic foraminifera from the tropical East Atlantic: impact of different productivity regimes. Journal of Foraminiferal Research, 33(1): 10-31,

Lipps, J. H. (1983). Biotic interactions in benthic foraminifera. In M. J. J. Tevez and P. L. McCall (Eds.), Biotic interactions in recent and fossil benthic communities. New York: Plenum. 331–376.

Littler, K., Röhl, U., Westerhold, T., and Zachos, J. C. (2014). A high resolution benthic stable-isotope record for the South Atlantic: Implications for orbital-scale changes in Late Paleocene–Early Eocene climate and carbon cycling. Palaeogeogr. Palaeocl., 401, 18–30

Loeblich, A.R., and Tappan, H. (1987). Foraminiferal Genera and Their Classification: New York Van Nostrand Reinhold Co. 2031p

Loeblich, A. R., and Tappan, H. (1992). Present status of foraminiferal classification. In "Studies in Benthic foraminifera. Proceedings of the Fourth Symposium on benthic

foraminifera : Proceedings of the fourth symposium on benthic foraminifera, Sendai, 1990, Tokai University Press. 93-102

Lourens, L.J., Sluijs, A., Kroon, D., Zachos, J.C., Thomas, E., Röhl, U., Bowles, J., and Raffi, I. (2005). Astronomical pacing of late Palaeocene to early Eocene global warming events: Nature, 435, 1083–1087, doi: 10.1038/ nature03814.

Lu, G. and Keller, G.1995b. Planktic foraminiferal turnovers in the subtropical Pacific during the late Paleocene to early Eocene. Journal of Foraminiferal Research 25, 97–116

Luciani, V., D'Onofrio, R., Dickens, G. R., and Wade, B. S. (2017). Planktic foraminiferal response to early Eocene carbon cycle perturbations in the southeast Atlantic Ocean (ODP Site 1263). Global and Planetary Change, 158, 119-133.

Luciani, V., Giusberti, L., Agnini, C., Backman, J., Fornaciari, E., and Rio, D. (2007) The Paleocene–Eocene Thermal Maximum as recorded by Tethyan planktonic foraminifera in the Forada section (northern Italy): Marine Micropaleontology. 64, 189–214.

Luciani, V., Giusberti, L., Agnini, C., Fornaciari, E., Rio, D., Spofforth, D. J. A. and Pälike H. (2010). Ecological and evolutionary response of Tethyan planktonic foraminifera to the middle Eocene climatic optimum (MECO) from the Alano section (NE Italy), PPalaeogeography, Palaeoclimatology, Palaeoecology, 292 (1-2), 82-95. doi:10.1016/j.palaeo.2010.03.029

Lunt, D.J., Huber, M., Baatsen, M.L.J., Caballero, R., DeConto, R., Donnadieu, Y., Evans, D., Feng, R., Foster, G., Gasson, E., von der Heydt, A.S., Hollis, C.J., Kirtland Turner, S., Korty, R.L., Kozdon, R., Krishnan, S., Ladant, J.-B., Langebroek, P., Lear, C.H., LeGrande, A.N., Littler, K., Markwick, P., Otto-Bliesner, B., Pearson, P., Poulsen, C., Salzmann, U., Shields, C., Snell, K., Starz, M., Super, J., Tabour, C., Tierney, J., Tourte, G.J.L., Upchurch, G.R., Wade, B., Wing, S.L., Winguth, A.M.E., Wright, N., Zachos, J.C. and Zeebe, R. (2017). The DeepMIP contribution to PMIP4: experimental design for model simulations of the EECO, PETM, and pre-PETM (version 1.0). Geosci. Model Dev., 10, 889–901

Luterbacher, H., Hardenbol, J. and Schmitz, B. (2000). Decision of the voting members of the International Subcommission on Paleogene Stratigraphy on the criterion for the recognition of the Paleocene/Eocene boundary. Newsl. Int. Subcomm. Paleogene Stratigr. 9:13

Lutze, G.F. (1980). Depth distribution of benthic foraminifera on the continental margin off NW Africa. Meteor Forschungsergebnisse, Deutsche Forschungsgemeinschaft, Reihe C Geologie und Geophysik, Gebrüder Bornträger, Berlin, Stuttgart, C32, 31-80

Lyle, M., and Wilson, P.A. (2006). Leg 199 synthesis: Evolution of the equatorial Pacific in the early Cenozoic. In Wilson, P.A., Lyle, M., and Firth, J.V. (Eds.), Proc. ODP, Sci. Results, 199. Ocean Drilling Program. College Station, TX, 1-39.

Lyle, M.W. and Wilson, P.A. (2002). Leg 199 Summary. Proceedings of the Ocean Drilling Program, Initial Reports 199. Ocean Drilling Program. College Station, TX, 1-87.

Ma, Z., Gray, E., Thomas, E., Murphy, B., Zachos, J. and Paytan A. (2014) Carbon sequestration during the Palaeocene– Eocene Thermal Maximum by an ancient biological pump. Nature Geoscience, 7, 382 – 388. doi: 10.1038/NGEO2139

Makarova, M., Wright, J. D., Miller, K. G., Babila, T. L., Rosenthal, Y. and Park, J. I. (2017). Hydrographic and ecologic implications of foraminiferal stable isotopic response across the U.S. mid-Atlantic continental shelf during the Paleocene-Eocene Thermal Maximum, Paleoceanography, 32, 56–73, doi:10.1002/2016PA00298

Mancin, N., Hayward, B. W., Trattenero, I., Cobianchi, M., and Lupi, C. (2013). Can the morphology of deep-sea benthic foraminifera reveal what caused their extinction during the mid-Pleistocene Climate Transition? Mar. Micropaleont., 104, 53–70.

Manners, H.R., Grimes, S.T., Sutton, P.A., Domingo, L., Leng, M.J., Twitchett, R.T., Hart, M.B., Dunkley Jones, T., Pancost, R.D., Duller, R., Lopez-Martinez, N. (2013). Magnitude and profile of organic carbon isotope records from the Paleocene–Eocene Thermal Maximum: evidence from northern Spain. Earth Planet. Sci. Lett. 377, 220–230.

Martin, J.H., Knauer, G.A., Karl, D.M. and Broenkow, W.W. (1987). Vertex: carbon cycling in the northeast Pacific Deep-Sea Research, 34. 267-285

Martini, E. (1971). Standard Tertiary and Quaternary calcareous nannoplankton zonation. In: A. Farinacci (ed.) Proceedings of the II Planktonic Conference, Roma 1970. Edizioni Tecnoscienza, Rome. 2. 739–785

Maslin, M., Owen, M., Betts, R., Day, S., Dunkley Jones, T. and Ridgwell, A. (2010). Gas hydrates: past and future geohazard? Phil. Trans. R. Soc. A 368, 2369–2393. (doi:10.1098/ rsta.2010.0065

McCarren, H., Thomas, E., Hasegawa, T., Röhl, U., and Zachos, J. C. (2008). Depth dependency of the Paleocene-Eocene carbon isotope excursion: Paired benthic and terrestrial biomarker records (Ocean Drilling Program Leg 208, Walvis Ridge), Geochem. Geophy. Geosy., 9, Q10008, https://doi.org/10.1029/2008GC002116

McClanahan, T. R., Muthiga, N. A., Kamukuru, A. T., Machano, H. and Kiambo, R. (1999). The effects of marine parks and fishing on the coral reefs of northern Tanzania. Biological Conservation 89:161-182.

McGill, B.J., Enquist, B.J., Weiher, E. and Westoby, M. (2006). Rebuilding community ecology from functional traits. Trends in Ecology and Evolution, 21, 178–185.

McInerney, F. A. and Wing S. L. (2011). The Paleocene-Eocene Thermal Maximum: A Perturbation of Carbon Cycle, Climate, and Biosphere with Implications for the Future. Annual Review of Earth and Planetary Sciences 39(1): 489-516.

McIntyre, S., Lavorel, S. and Tremont, R.M. (1995). Plant life-history attributes – their relationship to disturbance responses in herbaceous vegetation. Journal of Ecology, 83,31–44.

Meckler, A. N., Ren, H., Sigman, D. M., Gruber, N., Plessen, B., Schubert, C. J. and Haug, G. H. (2011) Deglacial nitrogen isotope changes in the Gulf of Mexico: Evidence from bulk sedimentary and foraminifera - bound nitrogen in Orca Basin sediments, Paleoceanography, 26, PA4216, 1-13. doi:10.1029/2011PA002156.

Meissner K. J., Bralower T. J., Alexander K., Dunkley Jones T., Sijp W. and Ward M. (2014) The Paleocene-Eocene Thermal Maximum: How much carbon is enough? Paleoceanography 29, 946–963

Molina, E., Arenillas, I. and Pardo, A. (1999). High resolution planktic foraminiferal biostratigraphy and correlation across the Palaeocene/Eocene boundary in the Tethys. Bulletin de la Société géologique de France 170 (4), 521–530.

Monechi, S., Angori, E. and Von Salis, K. (2000). Calcareous nannofossil turnover around the Paleocene/Eocene transition at Alamedilla (southern Spain). Bulletin de la Société géologique de France 171 (4), 477–489.

Moore Jr. T.C., Rabinowitz, P. D., Boersma, A., Borella, P. E., Chave, A. D., Duée, G., Jiang, M. J., Kleinert, K., Lever, A., Manivit, H., O'Connell, S., Richardson, S. H. and Shackleton,

N. J. (1984a). Initial Reports of the Deep Sea Drilling Project 74. U.S. Government Printing Office, Washington, D.C. 74: 237-306

Moore Jr, T .C., Rabinowitz, P.D., Borella, P.E., Shackleton, N.J. and Boersma, A. (1984c). History of the Walvis Ridge. Initial Reports of the Deep Sea Drilling Project. U.S. Government Printing Office, Washington, D.C. 74: 873-894

Moore, E. A and Kurtz, A. C. (2008). Black carbon in Paleocene-Eocene boundary sediments: a test of biomass combustion as the PETM trigger. Palaeogeogr. Palaeoclimatol. Palaeoecol. 267:147–52

Moore, E. A., and Kurtz, A. C. (2008), Black carbon in Paleocene-Eocene boundary sediments: A test of biomass combustion as the PETM trigger, Palaeogeogr. Palaeoclimatol. Palaeoecol., 267, 147 – 152, doi:10.1016/j.palaeo.2008.06.010.

Moore, T.C. (2005). Opal accumulation in the equatorial Pacific. Eos, Trans. Am. Geophys. Union, 86(52) (Suppl.):PP24A-05.

Moore, T.C., Backman, J., Raffi, I., Nigrini, C., Sanfilippo, A., Pälike, H., and Lyle, M. (2004). Paleogene tropical Pacific: clues to circulation, productivity, and plate motion. Paleoceanography, 19(3):PA3013. doi:10.1029/2003PA000998

Morsi, A. M., Speijer, R. P., Stassen, P., Steurbaut, E. (2011). Shallow marine ostracode turnover in response to environmental change during the Paleocene-Eocene thermal maximum in northwest Tunisia. Journal. Afr. Earth Sci. 59:243–68

Murphy, B. H., Farley, K.A, and Zachos, J. C. (2010). An extraterrestrial 3He-based timescale for the Paleocene-Eocene Thermal Maximum (PETM) from Walvis Ridge, IODP Site 1266. Geochim. Cosmochim. Acta 74:5098–108

Murray, J.W. (1991). Ecology and palaeoecology of benthic foraminifera. Longman, Harlow, 397p.

Murray, J.W. (2000). When does environmental variability become environmental change? The Proxy Record of benthic Formanifera. Environmental Micropaleontology, Volume 15 of Topics in Geobiology. Kluwer Academic/Plenum Publishers, New York, 7-37.

Naeem, S., Chapin, F. S., Costanza, R., Ehrlich, P. R., Golley, F. B., Hooper, D. U., Lawton, J. H., O'Neill, R. V., Mooney, H. A., Sala, O. E., Symstad, A. J. and Tilman, D. (1999).

Biodiversity and Ecosystem Functioning: Maintaining Natural Life Support Processes. Issues in Ecology. Ecological Society of America, Washington, 4: 11.

Nagy, J., Gradstein, F.M., Kaminski, M.A. and Holbourn, A.E. (1995) Foraminiferal morphogroups, paleoenvironments and new taxa from Jurassic to Cretaceous strata of Thakkhola, Nepal. In: Kaminski, M.A., Geroch, S. and Gasinski, M.A. (eds). Proceedings of the Fourth International Workshop on Agglutinated Foraminifera. Grzybowski Foundation Special Publication, 3, 181-209.

Nguyen, T.M.P., Petrizzo, M.R. and Speijer, R.P. (2009). Experimental dissolution of a fossil foraminiferal assemblage (Paleocene-Eocene Thermal Maximum, Dababiya, Egypt): Implications for paleoenvironmental reconstructions. Marine Micropaleontology, 73, 241-258.

Noel D. (1958). Etude de cocolithes du Jurassique et du Cretace inferieur. Publ. Serv. Carte Geol. Algerie, Bull. N.S., 20, 157 – 195 In Alfred *et al.,* 1967. Electron Micrographs of Limestones and their Nannofossils. Princeton University Press, 141p

Nomura, R. (1991). Paleoceanography of upper Maestrichtian to Eocene benthic foraminiferal assemblages at Sites 752, 753, and 754, Eastern Indian Ocean. Proc. ODP, Sci. Results. College Station, TX (Ocean Drilling Program), 121: 3–30.

Nomura, R. and Takata, H. (2005). Data report: Paleocene/Eocene benthic foraminifers, ODP Leg 199 Sites 1215, 1220, and 1221, equatorial central Pacific Ocean. In: Wilson, PA., Lyle, M., Firth, J. V. (eds.) Proceedings of the Ocean Drilling Program, Scientific Results, College Station, TX (Ocean Drilling Program), 199, 1-34

Nunes, F. and Norris, R. D. (2006). Abrupt reversal in ocean overturning during the Palaeocene/Eocene warm period. Nature 439, 60–63. (doi:10.1038/nature04386)

Nwojiji, C. N., Osterloff, P., Okoro, A. U. and Ndulue, G. (2014). Foraminiferal Stratigraphy and Paleoecological Interpretation of Sediments Penetrated by Kolmani River -1 Well, Gongola Basin, Nigeria. Journal of Geosciences and Geomatics, 2(3), 85-93.

O'Halloran, A.; Nicholas, C. J. and Goodhue, R. (2010). Changes in seasonality and productivity recorded at low latitudes in Tanzania during the PETM. American Geophysical Union, Fall Meeting 2010, abstract id. PP23B-1744

Ohtsuka, S., Suzaki, T., Horiguchi, T., Suzuki, N. and Not, F. (2015). Marine Protists: Diversity and Dynamics. Springer Japan, 648p

Okada, H. and Bukry, D. (1980). Supplementary modification and introduction of code numbers to the low-latitude coccolith biostratigraphic zonation (Bukry, 1973; 1975). Marine Micropaleontology, 5, 321–325.

Olff, H., Pegtel, D. M., Van Groenendanel, J. M. and Bakker, J. P. (1994). Germination strategies during grassland germination. Journal of Ecology 82(1): 69-77.

Olsson, R.K., Berggren, W.A., Hemleben, C.H., and Hubber, B.T.(eds) (1999). Atlas of Palaeocene Foraminifera: Smithsonian Contributions to Palaeobiology, 85:1-252.

Ortiz, S. and Kaminski, M. A. 2012. Record of deep-sea, benthic elongate-cylindrical foraminifera across the Eocene-Oligocene transition in the North Atlantic Ocean (ODP Hole 647A). Journal of Foraminiferal Research, 42: 345-36

Oschmann, W. (1998). Kimmeridge clay sedimentation- a new cyclic model. Palaeogeo., Palaeoclim., Palaeoeco. 65: 217 - 251

Pachauri, R.K. and Meyer, L. (2014). Climate Change 2014 Synthesis Report. Contribution of Working Groups I, II and III to the Fifth Assessment Report of the Intergovernmental Panel on Climate Change. Geneva, Switzerland, 151p

Padilla, D. K. and Allen, B. J. (2000). Paradigm lost reconsidering functional form and group hypotheses in marine ecology. Journal of Experimental Marine Biology and Ecology 250: 207-221.

Paganelli, D., Marchini, A. and Occhipinti-Ambrogi, A. (2012). Functional structure of marine benthic assemblages using Biological Traits Analysis (BTA): A study along the Emilia-Romagna coastline (Italy, North-West Adriatic Sea). Estuarine, Coastal and Shelf Science 96: 245-256.

Paganelli, D., Forni, G., Marchini, A., Mazziotti, C., Occhipinti-Ambrogi, A. (2011). Critical appraisal on the identification of reference conditions for the evaluation of ecological quality status along the Emilia-Romagna Coast (Italy) using M-AMBI. Marine Pollution Bulletin 62, 1725-1735.

Pagani, M., Pedentchouk, N. Huber, M., Sluijs, A., Schouten, S., Brinkhuis, H., Sinninghe, J.S., Damsté, Dickens, G.R., and the Expedition 302 Scientists (2006a). Arctic hydrology during global warming at the Paleocene/Eocene thermal maximum. Nature, 442: 671-675.

Pagani, M., Caldeira, K., Archer, D. and Zachos, J.C. (2006b). An ancient carbon mystery. Science, 314: 1556 - 1557

Pak, D. K., and K. G. Miller. (1992). Palaeocene to Eocene benthic foraminiferal isotopes and assemblages: Implications for deep water circulation, Paleoceanography, 7, 405-422.

Pälike, C., Delaney, M. L. and Zachos, J. C. (2014). Deep-sea redox across the Paleocene-Eocene Thermal Maximum, Geochem. Geophys. Geosyst., 15, 1038-1053 doi:10.1002/2013GC005074

Panchuk, K. Ridgwell, A. and Kump, L. R. (2008) Sedimentary response to Paleocene-Eocene Thermal Maximum carbon release; a model-data comparison Geology 36(4): 315-318

Pawłowska, J., Lejzerowicz, F., Esling, P., Szczucinski, W., Zajączkowski, M. and Pawlowski, J. (2013). Ancient DNA sheds new light on the Svalbard foraminiferal fossil record of the last millennium. Geobiology 12: 277–288

Pawlowski J. (2000): Introduction to the molecular systematics of foraminifera. Micropal. 46 (supplement1), 1–12

Payne, J. L., McClain, C. R., Boyer, A. G., Brown, J. H., Finnegan, S., Kowalewski, M., Wang, S. C. (2011). The evolutionary consequences of oxygenic photosynthesis: A body size perspective. Photosynthesis Research, 107(1): 37–57.

Paytan, A. and Kastner, M. (1996). Benthic Ba fluxes in the central equatorial Pacific: Implications for the oceanic Ba cycle, Earth Planet. Sci. Lett. 142, 439–450.

Pearson P. N. and Burgess C. E. (2008) Foraminifer test preservation and diagenesis: comparison of high latitude Eocene sites. Geol. Soc. (London, special publications). 303, 59–72

Pearson, P. N. and Berggren, W. A. (2005). Revised Tropical to Subtropical Paleogene Planktonic Foraminiferal Zonation. Journal of Foraminiferal Research 35, 279–298.

Pearson, P. N. (1993). A lineage phylogeny for the Paleogene planktonic foraminifera. Micropaleontology, 39, 193–232.

Pearson, P. N., Olsson, R. K., Huber, B. T., Hemleben, C. and Berggren, W. A. (eds).(2006). Atlas of Eocene planktonic foraminifera. Cushman Foundation Special Publication, 41, 514.

Pearson P. N. and Peeters, F. J. C., Ivanova, E., Conan, S. M.H., Brummer, G. J. A., Ganssen, G., Troelstra, S., van Weering, T., and van Hinte, J. E. (1999). Size analysis of planktic foraminifera from the Arabian Sea: Marine Micropaleontology. 36, 31–63.

Penman, D. E., Hönisch, B., Zeebe, R. E., Thomas, E. and Zachos, J. C. (2014). Rapid and sustained surface ocean acidificationduring the Paleocene-Eocene Thermal Maximum, Paleoceanography, 29,357–369, doi:10.1002/2014PA002621

Penman, D. E., Kirtland-Turner, S., Sexton, P. F., Norris, R. D., Dickson, A. J., Boulila, S; Ridgwell, A., Zeebe, R. E., Zachos, J. C., Cameron, A., Westerhold, T and Rohl, U. (2016). An abyssal carbonate compensation depth overshoot in the aftermath of the Palaeocene–Eocene Thermal Maximum. Nature Geoscience, 9, 575–580.

Peterse, F., J. van der Meer, S. Schouten, J. W. H. Weijers, N. Fierer, R. B. Jackson, J. H. Kim, and J. S. Sinninghe Damsté (2012), Revised calibration of the MBT-CBT paleotemperature proxy based on branched tetraether membrane lipids in surface soils, Geochim. Cosmochim. Acta, 96, 215–229, doi:10.1016/j.gca.2012.08.011.

Petrizzo, M. R., Huber, B. T., Wilson, P. A. and Macleod, K. G. (2008). Dissolution susceptibility of some Paleogene planktonic foraminifera from ODP site 1209 (Shatsky Rise, Pacific Ocean). Journal of Foraminiferal Research, v. 38, 4, 357–371

Petrizzo M. R. (2007). The onset of the Palaeocene–Eocene Thermal Maximum (PETM) at Sites 1209 and 1210 (Shatsky Rise, Pacific Ocean) as recorded by planktonic foraminifera. Marine Micropaleontology, 63 (3–4): 187–200

Petrizzo, M. R. (2006). The Palaeocene-Eocene transition in the subtropical Pacific Ocean (Shatsky Rise, Leg 198): Inference from planktonic foraminifera. International Conference Climate and Biota of the Early Paleogene, Bilbao, Volume of abstracts, 99.

Petrizzo, M. R., Jiménez Berrocoso, Á, Falzoni, F., Huber, B. T. and MacLeod, K.G. (2017). The Coniacian–Santonian sedimentary record in southern Tanzania (Ruvuma Basin, East Africa): Planktonic foraminiferal evolutionary, geochemical and palaeoceanographic patterns. Sedimentology 64, 252–285.

Pettit, L. R., Hart, M.B., Medina-Sánchez, A.N., Smart, C.W., Rodolfo-Metalpa, R., Hall-Spencer, J.M. and Prol-Ledesma, R.M. (2013). Benthic foraminifera show some resilience to

ocean acidification in the northern Gulf of California, Mexico. Mar Pollut. Bull. 73(2): 452-462.

Phipps, M. J., Reston, T. J. and Ranero, C. R. (2004). Contemporaneous mass extinctions, continental flood basalts, and 'impact signals': are mantle plume induced lithospheric gas explosions the causal link? Earth and Planetary Science Letters, 217, 263–284.

Pross, J., Contreras, L., Bijl, P.K., Greenwood, D.R., Bohaty, S., Schouten, S., Bendle, J.A., Röhl, U., Tauxe, L., Raine, J., Huck, C.E., van de Flierdt, T., Jamieson, S.S.R., Stickley, C.E., van de Schootbrugge, B., Escutia, C., Brinkhuis, H., Scientists, I.O.D.P.E. (2012). Persistent near-tropical warmth on the Antarctic continent during the early Eocene epoch. Nature, 488, 73–77.

Quillevere, F. and Norris, R. D. (2003). Ecological development of acarininids (planktonic Foraminifera) and hydrographic evolution of Paleocene surface waters. Special Paper - Geological Society of America. 369(Wing, S.L., Gingerich, P.D., Schmitz, B., Thomas, E (Eds.).:223-238.

Rabinowitz, P.D., and Simpson, E.S.W. (1984). Geophysical site survey results on the Walvis Ridge. In Moore, T.C., Jr., Rabinowitz, P.D., et al., Init. Repts. DSDP, 74: Washington (U.S. Government Printing Office), 795–825

Rad S, Basile-Doelsch I, Quesnel F and Dupuis C. (2009). Silicium isotopes as a proxy of weathering processes during the PETM. Geochim. Cosmochim. Acta 73:A1066 (Abstr.)

Raffi I., Backman J., Palike H. (2005). Changes in calcareous nannofossil assemblages across the Paleocene/Eocene transition from the Paleo-equatorial Pacific Ocean Palaeogeography, Palaeoclimatology, Palaeoecology, 226, 93-126

Ren, H., Studer, A.S., Serno, S., Sigman, D.M., Winckler, G., Anderson, R. F., Oleynik, S., Gersonde, R. and Haug, G. H. (2015) Glacial-to-interglacial changes in nitrate supply and consumption in the subarctic North Pacific from microfossil-bound N isotopes at two trophic levels. Paleoceanography 30:1217–1232

Ren. H., Sigman, D. M., Chen, M.T. and Kao, S.J. (2012). Elevated foraminifera-bound nitrogen isotopic composition during the last ice age in the South China Sea and its global and regional implications. Glob. Biogeochem. Cycles 26:GB1031, 1-11

Ridgwell, A. and Edwards, U. (2007). Geological carbon sinks. In Greenhouse gas sinks Reay, D., Hewitt, C. N., Smith, K. and Grace, J. (eds.), Wallingford, CT: CAB International, 74–97.

Riebesell, U., Bach, L. T., Bellerby, R. G. J., Bermudez Monsalve, J. R., Boxhammer, T., Czerny, J., Larsen, A., Ludwig, A. and Schulz, K. G. (2017). Competitive fitness of a predominant pelagic calcifier impaired by ocean acidification. Nature Geoscience 10, 19–23, doi:10.1038/ngeo2854

Robert, C. and Kennett, J. P. (1994) Antarctic subtropical humid episode at the Paleocene–Eocene boundary – clay mineral evidence. Geology, 22, 211–214

Rogner, H.H. (1997). An assessment of world hydrocarbon resources. Annual Review of Energy and the Environment, 22:217-262

Röhl, U., Bralower, T.J., Norris, R.D. and Wefer G. (2000). New chronology for the late Paleocene thermal maximum and its environmental implications. Geology; 28 (10): 927–930. doi: https://doi.org/10.1130/0091-7613(2000)28<927:NCFTLP>2.0.CO;2

Röhl, U., Westerhold, T., Bralower, T.J. and Zachos, J. C. (2007). On the duration of the Palaeocene-Eocene Thermal Maximum (PETM). Geochem. Geophys. Geosyst. 8:Q12002, 1-13

Rutherford, S., D'Hondt, S., and Prell, W. (1999). Environmental controls on the geographic distribution of zooplankton diversity. Nature, 400(6746), 749–753. https://doi.org/10.1038/23449

Sager, W. W., Neal, C. R., Sano, T. and Erba E. (2015). The Origin, Evolution, and Environmental Impact of Oceanic Large Igneous Provinces. Geological Society of America Special papers, 511p.

Schaller, M.F and Fung, M. K. (2018). The extraterrestrial impact evidence at the Palaeocene–Eocene boundary and sequence of environmental change on the continental shelf. Phil. Trans. R. Soc. A 376: 20170081, 1- 30. http://dx.doi.org/10.1098/rsta.2017.0081

Schiebel, R. and Hemleben, C. (2017). Planktic Foraminifers in the Modern Ocean. Springer-Verlag Berlin Heidelberg. 358p. doi 10.1007/978-3-662-50297-6_1

Schiebel, R., Smart, S.M., Jentzen, A., Jonkers, L., Morard, R., Meilland, J., Michel, E., Coxall, H.K., Hull, P.M., de Garidel-Thoron, T., Aze, T., Quillévéré, F., Ren, H., Sigman D.M.,

Vonhof, H.B., Martínez-García, A., Kučera, M., Bijma, J., Spero, H.J., Haug, G.H. (2018) Advances in planktonic foraminifer research: New perspectives for paleoceanography. Revue de micropaléontologie, 1 – 26.

Schiebel, R., Spielhagen, R. F., Garnier, J., Hagemann, J., Howa, H., Jentzen, A., MartínezGarcia, A., Meilland, J., Michel, E., Repschläger, J., Salter, I., Yamasaki, M., and Haug, G. (2017). Modern planktic foraminifers in the high-latitude ocean, Mar. Micropal., 136, 1–13

Schmidt, D. N., Thomas, E., Authier, E., Saunders, D. and Ridgwell, A. (2018) Strategies in times of crisis—insights into the benthic foraminiferal record of the Palaeocene–Eocene Thermal Maximum. Phil. Trans. R. Soc. A 376, 1-17, 20170328. http://dx.doi.org/10.1098/rsta.2017.0328

Schmidt, G. A. (2012) Climate sensitivity — how sensitive is Earth's climate to CO_2; past. PAGES News 20, 11

Schmiedl, G., de Bovee, F., Buscail, R. Charrie`re, B., Hemleben, C. and Medernach, L. (2000). Trophic control of benthic foraminiferal abundance and microhabitat in the bathyal Gulf of Lions, western Mediterranean Sea. Marine Micropaleontology, 40(3), 167-188

Schmiedl, G., Mitschele, A., Beck, S., Emeis, Kay-C. Hemleben, C., Schulz, H., Sperling, M. and Weldeab, S. (2003). Benthic foraminiferal record of ecosystem variability in the eastern Mediterranean Sea during times of sapropel S5 and S6 formation. Palaeogeography, Palaeoclimatology, Palaeoecology. 190, 139-164

Schmitz, B. and Pujalte, V. (2007).Abrupt increase in seasonal extreme precipitation at the Paleocene-Eocene boundary. Geology. 35, 215–218

Schneider, L. J., Bralower, T.J., Kump, L.R., Patzkowsky, M.E. (2013). Calcareous nannoplankton ecology and community change across the Paleocene-Eocene Thermal Maximum, Paleobiology, 39(4):628–647 doi: 10.1666/12050.

Schwab, D. (1976). Gametogenesis in *Allogromia laticollaris*. Journal of Foraminiferal Research 6, 251–257.

Scotese, C. R. (2010). The PALEOMAP Project PaleoAtlas for ArcGIS, Vol. 1: Cenozoic Paleogeographic and Plate Tectonic Reconstructions. Arlington, Tex.: PALEOMAP Project

Seears, H. (2011). Biogeography and phylogenetics of the planktonic foraminifera. PhD thesis, University of Nottingham, UK. 380p

Sen Gupta, B. K. (1999). Modern Foraminifera. Springer. 371p

Sen Gupta, B.K. and Machain-Castillo, M.L. (1993). Benthic foraminifera in oxygen-poor habitats. Marine Micropaleontology 20, 183–201.

Sexton, P. F., Wilson, P. A. and Pearson, P. N. (2006). Microstructural and geochemical perspectives on planktic foraminiferal preservation: ‘‘Glassy’’ versus ‘‘frosty’’, Geochem. Geophys. Geosyst., 7, Q12P19, 1-29, doi:10.1029/ 2006GC001291.

Shaffer, G., Huber, M., Rondanelli, R., and Pepke Pedersen, J. O. (2016). Deep time evidence for climate sensitivity increase with warming, Geophys. Res. Lett., 43, 6538–6545

Shellito, C. J., and Sloan, L. C. (2006). Reconstructing a lost Eocene paradise: Part I. Simulating the change in global floral distribution at the initial Eocene thermal maximum. Global Planet. Change, 50, 1–17

Shojaei, M. G., Gutow, L., Dannheim, J., Pehlke, H., and Brey, T. (2015). Functional diversity and traits assembly patterns of benthic macrofaunal communities in the Southern North Sea. In Towards an Interdisciplinary Approach in Earth System Science. Springer International Publishing, 183-195.

Si, W. and Aubry, M.P. (2018). Vital effects and ecologic adaptation of photosymbiont-bearing planktonic foraminifera during the Paleocene Eocene Thermal Maximum, implications for paleoclimate. Paleoceanography and Paleoclimatology, 33, 112–125. https:// doi.org/10.1002/2017PA003219

Sigman, D. M., DiFiore, P. J., Hain, M. P., Deutsch, C. and Karl D. M. (2009). Sinking organic matter spreads the nitrogen isotope signal of pelagic denitrification in the North Pacific. Geophys Res Lett 36:L08605, 1-5

Sluijs, A., Schouten, S., Donders, T. H., Schoon, P. L., Röhl, U., Reichart, G.J., Sangiorgi, F., Kim, J.H., Sinninghe Damsté, S. J. and Brinkhuis, H. (2014). Warming, euxinia and sea level rise during the Paleocene–Eocene Thermal Maximum on the Gulf Coastal Plain: implications for ocean oxygenation and nutrient cycling. Climate of the Past 10(4): 1421-1439.

Sluijs, A. and Brinkhuis, H. (2009). A dynamic climate and ecosystem state during the Paleocene- Eocene Thermal Maximum: Inferences from dinoflagellate cyst assemblages at the New Jersey Shelf. Biogeosciences 6, 1755–1781

Sluijs, A., Bowen, G., Brinkhuis, H., Lourens. L. and Thomas E. (2007a). The Palaeocene-Eocene Thermal Maximum super greenhouse: biotic and geochemical signatures, age models and mechanisms of global change. London: Geol. Soc. 323–49.

Sluijs, A., Brinkhuis, H., Schouten, S., Boharty, S. M., John, C. M., Zachos, J. C., Reichart, G.-J., Sinninghe Damsté, J. S., Crouch, E. M., and Dickens, G. R (2007b). Environmental precursors to rapid light carbon injection at the Palaeocene/Eocene boundary. Nature 450:1218–21

Smart, S. M., Ren, H., Fawcett, S. E., Schiebel, R., Conte, M., Rafter, P. A., Ellis, K. K. and Weigand M. A., Oleynik, S., Haug, G. H. and Sigman, D.M. (2018). Ground-truthing the planktic foraminifer-bound nitrogen isotope paleo-proxy in the Sargasso Sea. Geochimica et Cosmochimica Acta 235, 463–482

Speijer, R. P. (1994). Extinction and recovery patterns in benthic foraminiferal paleocommunities across the Cretaceous/Paleogene and Paleocene/Eocene boundaries. Geol. Ultraiectina,124:1–91.

Speijer, R. P., Scheibner, C., Stassen, P. and Morsi, A.M. M. (2012), Response of marine ecosystems to deep-time global warming: A synthesis of biotic patterns across the Paleocene-Eocene thermal maximum (PETM), Aust. J. Earth Sci., 150(1), 6–12.

Speijer, R.P. and Morsi, A.M.M. (2002). Ostracode turnover and sea-level changes associated with the Paleocene- Eocene Thermal Maximum. Geology 30:23–26

Speijer, R.P., Schmitz, B. and Luger, P. (2000). Stratigraphy of late Paleocene events in the Middle East: implications for low- to middle latitude successions and correlations. Journal of the Geological Society, London, 157: 37–47.

Stassen, P., Thomas, E. and Speijer, R. P. (2012). Restructuring outer neritic foraminiferal assemblages in the aftermath of the Palaeocene-Eocene thermal maximum. Journal of Micropalaeontology, 31: 89-93, http://dx.doi.org/10.1144/0262-821X11-026

Stassen, P., Thomas, E. and Speijer, R. P. (2015). Paleocene–Eocene Thermal Maximum environmental change in the New Jersey Coastal Plain: Benthic foraminiferal biotic events, Mar. Micropaleontol. 115, 1–23, doi:10.1016/j.marmicro.2014.12.001

Statzner B., Bis B., Doledec S. and Usseglio-Polatera P. (2001). Perspectives for biomonitoring at large spatial scales: a unified measure for the functional composition of invertebrate communities in European running waters. Basic and Applied Ecology, 2, 73–85

Statzner, B., Resh, V.H. and Roux, L.A. (1994). The synthesis of long-term ecological research in the context of concurrently developed ecological theory: design of research strategy for the Upper Rhone River and its flood plain. Freshwater Biology. 31, 253-263.

Steineck, P.L. and Thomas E. (1996). The latest Paleocene crisis in the deep sea: Ostracode succession at Maud Rise, Southern Ocean. Geology 24:583–86

Steurbaut, E., Magioncalda, R., Dupuis, C., Van Simaeys, S., Roche, E., Roche, M. (2003). Palynology, paleoenvironments, and organic carbon isotope evolution in lagoonal PaleoceneEocene boundary sections in North Belgium. 291–317.

Strain, D. (2015). Acidifying Conditions Could Bring Benefits and Problems for the Bay's Iconic Crustaceans. Sea Grant Maryland. https://www.mdsg.umd.edu/onthebay-blog/will-ocean-acidification-create-%E2%80%9Csuper-crabs%E2%80%9D-bay-maybe-not.

Straub, M., Tremblay, M.M., Sigman, D.M., Studer, A.S., Ren, H., Toggweiler, J.R., Haug, G.H. (2013). Changes in North Atlantic nitrogen fixation controlled by ocean circulation. Nature 501:200–203

Suess, E. (1980). Particulate organic carbon flux in the oceans – surface productivity and oxygen utilization. Nature, 288: 260-263.

Svensen, H., Planke, S., Malthe-Sorenssen, A., Jamtveit, B., Myklebust, R., Eidem, T.R. and Rey, S.S. (2004). Release of methane from a volcanic basin as a mechanism for initial Eocene global warming. Nature 429:542–45

Takeda, K. and Kaiho, K. (2007). Faunal turnovers in central Pacific benthic foraminifera during the Paleocene–Eocene thermal maximum. Palaeogeography, Palaeoclimatology, Palaeoecology 251(2): 175-197.

Thomas, E. (1998). Biogeography of the late Paleocene benthic foraminiferal extinction. In Aubry, M.-P., Lucas, S.G., and Berggren, W.A., (Eds.), Late Paleocene–Early Eocene Biotic and Climatic Events in the Marine and Terrestrial Records: New York (Columbia Univ. Press), 214–243.

Thomas, D. J., Zachos, J. C., Bralower, T. J., Thomas, E. and Bohaty, S. (2002). Warming the fuel for the fire: Evidence for the thermal dissociation of methane hydrate during the Paleocene–Eocene thermal maximum. Geology, 30, 1067–1070.

Thomas, E., Dickens, G. R., Fewless, T. and Bralower, T. J. (2003). Excess Barite Accumulation during the Paleocene/Eocene Thermal Maximum: Massive Input of Dissolved Barium from Seafloor Gas Hydrate Reservoirs. In: Wing, S., Gingerich, P., Schmitz, B., and Thomas, E., eds. Causes and Consequences of Globally Warm Climates of the Paleogene, GSA Special Paper, 369: 13-27

Thomas, E. (2003). Extinction and food at the seafloor: A high-resolution benthic foraminiferal record across the Initial Eocene Thermal Maximum, Southern Ocean Site 690, in: Causes and Consequences of Globally Warm Climates in the Early Paleogene, edited by: Wing, S. L., Gingerich, P. D., Schmitz, B., and Thomas, E., Geol. S. Am. S., Boulder, Colorado, The Geological Society of America, 369, 319–332.

Thomas, E. (2007). Cenozoic mass extinctions in the deep sea: What perturbs the largest habitat on Earth?, in: Large Ecosystem Perturbations: Causes and Consequences, edited by: Monechi, S., Coccioni, R., and Rampino, M., Geol. S. Am. S., Boulder, Colorado, The Geological Society of America, 424, 1–23.

Thomas, E. and Shackleton, N.J. (1996). The Paleocene-Eocene benthic foraminiferal extinction and stable isotope anomalies. In Correlation of the Early Paleogene in Northwest Europe Correlation of the Early Paleogene in Northwest Europe, Spec. Pub. 101, ed. RWOB Knox, R Corfield, RE Dunay, Washington, DC: Geol. Soc. 401–41.

Tierney, J. E., J. M. Russell, H. Eggermont, E. C. Hopmans, D. Verschuren, and J. S. Sinninghe Damsté .(2010). Environmental controls on branched tetraether lipid distributions in tropical East African lake sediments, Geochim. Cosmochim. Acta, 74, 4902–4918, doi:10.1016/ j.gca.2010.06.002

Tjalsma, R.C. and Lohmann, G.P. (1983). Paleocene–Eocene Bathyal and Abyssal Benthic Foraminifera from the Atlantic Ocean. Micropaleontology, Spec. Publ., 4:1–90.

Torfstein, A., Winckler, G. and Tripati, A. (2010). Productivity feedback did not terminate the Paleocene-Eocene -Thermal Maximum (PETM). Clim. Past Discuss. 5:2391–410

Törnroos, A., Bonsdorff, E., Bremner, J., Blomqvist, M., Josefson, A. B., Garcia, C. and Warzocha, J. (2015). Marine benthic ecological functioning over decreasing taxonomic richness. Journal of Sea Research 98: 49-56.

Townsend, C. R. and Hildrew, A. G. (1994). Species traits in relation to a habitat templet for river systems. Freshwater Biology 31:265–275.

Tremolada, F. and Bralower, T.J. (2004). Nannofossil assemblage fluctuations during the PaleoceneEocene Thermal Maximum at Sites 213 (Indian Ocean) and 401 (North Atlantic Ocean): palaeoceanographic implications. Marine Micropaleontology, 52(1-4): 107-116.

Tripati, A. K. and Elderfield, H. (2004). Abrupt hydrographic changes in the equatorial Pacific and subtropical Atlantic from foraminiferal Mg/Ca indicate greenhouse origin for the thermal maximum at the Paleocene–Eocene Boundary. Geochem. Geophys. Geosyst. 5, Q02006. (doi:10.1029/2003GC000631)

Turner, S. K. (2018) Constraints on the onset duration of the Paleocene–Eocene Thermal Maximum. Phil. Trans. R. Soc. A 376: 1-16. http://dx.doi.org/10.1098/rsta.2017.0082

Twitchett, R. J. (2006). The palaeoclimatology, palaeoecology and palaeoenvironmental analysis of mass extinction events: Palaeogeography, Palaeoclimatology, Palaeoecology, 232, 190–213, doi:10.1016/j.palaeo.2005.05.019

Tyler, E.H.M., Somerfield, P.J., Vanden Berghe, E., Bremner, J., Jackson, E and Langmead, O. (2012). Extensive gaps and biases in our knowledge of a well-known fauna: implications for integrating biological traits into macroecology. Global Ecology and Biogeography. 21:922–934. doi: 10.1111/j.1466-8238.2011.00726.

Wade, B.S., Berggren, W. A. and Olsson R. K. (2006). The biostratigraphy and paleobiology of Oligocene planktonic foraminifera from the equatorial Pacific Ocean (ODP Site 1218), Marine Micropaleontology. 167–179. doi:10.1016/j.marmicro.2006.08.005.

Wade, B.S., Berggren, W.A. and Olsson, R.K. (2007). The biostratigraphy and paleobiology of Oligocene planktonic foraminifera from the equatorial Pacific Ocean (ODP Site 1218). Mar. Micropaleontol. 62, 167–179.

Wade, B.S., Pearson, P.N., Berggren, W.A. and Pälike, H. (2011). Review and revision of Cenozoic tropical planktonic foraminiferal biostratigraphy and calibration to the geomagnetic polarity and astronomical time scale: Earth Science Reviews. 104, 111-142.

Wang, S. C and Marshall, C. R. (2016). Estimating times of extinction in the fossil record. Biol. Lett. 12, 1-5.

Webb, A., Leighton, L. R., Schellenberg, S. A., Landau, E. A. and Thomas E. (2009) Impact of the Paleocene-Eocene thermal maximum on deep-ocean microbenthic community structure: Using rank-abundance curves to quantify paleoecological response, Geology. 37, 783–786.

Westerhold, T., Röhl, U., Frederichs, T., Agnini, C., Raffi, I., Zachos, J. C., and Wilkens, R. H. (2017). Astronomical calibration of the Ypresian timescale: implications for seafloor spreading rates and the chaotic behavior of the solar system?, Clim. Past, 13, 1129-1152, https://doi.org/10.5194/cp-13-1129-2017.

Westerhold, T., Röhl, U., Laskar, J., Bowles, J., Raffi, I., Lourens, L. J., and Zachos, J. C. (2007). On the duration of magnetochrons C24r and C25n and the timing of early Eocene global warming events: Implications from the Ocean Drilling Program Leg 208 Walvis Ridge depth transect, Paleoceanography, 22, PA2201, https://doi.org/10.1029/2006PA001322,

Westerhold, T., U. Röhl, I. Raffi, E. Fornaciari, S. Monechi, V. Reale, J. Bowles, and H. F. Evans (2008). Astronomical calibration of the Paleocene time, Palaeogeogr. Palaeoclimatol. Palaeoecol., 257(4), 377–403, doi:10.1016/j.palaeo.2007.09.016.

Widmark, J.G.V. (1997). Deep-sea benthic foraminifera from Cretaceous-Tertiary boundary strata in the South Atlantic Ocean: taxonomy and paleoecology. Fossils Strata, 43:1–94.

Widmark, J.G.V. and Henriksson, A.S. (1995). The "orphaned" agglutinated foraminifera - *Gaudryina cribrosphaerellifera n.sp*. from the Upper Cretaceous (Maastrichtian), Central Pacific Ocean . In: S. Geroch et al. (Eds). Proc. 4th lnt. Workshop on Agglutinated foraminifera. Grzybowski Formd. Spec. Pub. 3: 293-300.

Williams, M., Haywood, A.M., Gregory, F.J. and Schmidt, D.N. (2007). Deep-time perspectives on climate change: marrying the signal from computer models and biological

proxies. London, Geological Society. (Micropalaeontological Society Special Publications). 589p.

Wing, S. L., Harrington, G. J., Smith, F. A., Bloch, J. I., Boyer, D. M and Freeman K. H. (2005). Transient floral change and rapid global warming at the Paleocene-Eocene boundary. Science, 310:993–96

Winguth, A. M. E. (2011). The Paleocene-Eocene Thermal Maximum: Feedbacks between Climate Change and Biogeochemical Cycles. Climate Change - Geophysical Foundations and Ecological Effects. J. Blanco and H. Kheradmand. Rijeka, InTech. 03: 43-64

Winguth, A., Thomas, E., and Winguth, C. (2012). Global decline in ocean ventilation, oxygenation and productivity during the Paleocene-Eocene Thermal Maximum - Implications for the benthic extinction. Geology, 40: 263-266

Zachos J, Pagani M, Sloan L, Thomas E and Billups K. (2001). Trends, rhythms, and aberrations in global climate 65 Ma to present. Science, 292:686–93

Zachos, J. C., Lohmann, K. C., Walker, J. C. G. and Wise, S.W. (1993). Abrupt climate and transient climates during the Palaeocene: A marine perspective. Journal of Geology, 101, 191-213

Zachos, J. C., M. W. Wara, S. M. Bohaty, M. L. Delaney, M. Rose-Petrizzo, A. Brill, T. J. Bralower, and I. Premoli –Silva. (2003). A transient rise in tropical sea surface temperature during the Paleocene-Eocene Thermal Maximum. Science, 302, 1551-1554.

Zachos, J. C., Kroon, D., Blum, P., Bowles, J., Gaillot, P., Hasegawa, T., Hathorne, E. C., Hodell, D. A., Kelly, D. C., Jung, J.H., Keller, S. M., Lee, Y. S., Leuschner, D. C., Liu, Z., Lohmann, K. C., Lourens, L., Monechi, S., Nicolo, M., Raffi, I., Riesselman, C., Röhl, U., Schellenberg, S. A., Schmidt, D., Sluijs, A., Thomas, D., Thomas, E. Vallius, H. (2004). Proc. ODP, Init. Reports. 208. Available from World Wide Web: http://www-odp.tamu.edu/publications/208_IR/208ir.htm.

Zachos, J. C., Röhl, U., Schellenberg, S. A., Sluijs, A., Hodell, D. A., Kelly, D. C., Thomas, E., Nicolo, M., Raffi, I., Lourens, L. J., Mccarren, H., and Kroon, D. (2005). Rapid acidification of the ocean during the Paleocene-Eocene Thermal Maximum, Science, 308, 1611–1615

Zachos, J.C., Dickens, G.R., and Zeebe, R.E. (2008). An early Cenozoic perspective on greenhouse warming and carbon-cycle dynamics. Nature. 451(17): 279-832008|doi:10.1038/nature.

Zeebe, R. and Zachos, J.C. (2013). Long-term legacy of massive carbon input to the Earth system: Anthropocene vs. Eocene. Phil. Trans. Royal Soc. A371: 29–31. http://dx.doi.org/10.1098/rsta.2012.0006

Zeebe, R., Ridgwell, A. and Zachos J.C. (2016). Anthropogenic carbon release rate unprecedented during past 66 million years. Nat. Geosci. 9, 1-5. doi: 10.1038/NGEO2681

Zeebe, R.E., and J.C. Zachos (2007). Reversed deep-sea carbonate ion basin-gradient during the Paleocene-Eocene Thermal Maximum. Paleoceanography PA3201 22 (3): 1-27, 10.1029/2006PA001395